



ISSN 2518-718X (Print)
ISSN 2663-4872 (Online)

BULLETIN

OF THE KARAGANDA UNIVERSITY

CHEMISTRY
Series

№ 1(101)/2021

ISSN 2663-4872 (Online)
ISSN-L 2518-718X (Print)
Индексі 74617
Индекс 74617

**ҚАРАҒАНДЫ
УНИВЕРСИТЕТІНІҢ
ХАБАРШЫСЫ**

ВЕСТНИК
КАРАГАНДИНСКОГО
УНИВЕРСИТЕТА

BULLETIN
OF THE KARAGANDA
UNIVERSITY

ХИМИЯ сериясы

Серия **ХИМИЯ**

CHEMISTRY Series

№ 1(101)/2021

Қаңтар–ақпан–наурыз
30 наурыз 2021 ж.

Январь–февраль–март
30 марта 2021 г.

January–February–March
March 30th, 2021

1996 жылдан бастап шығады
Издается с 1996 года
Founded in 1996

Жылына 4 рет шығады
Выходит 4 раза в год
Published 4 times a year

Қарағанды, 2021
Караганда, 2021
Karaganda, 2021

Main Editor

Doctor of Chemical sciences

M.Zh. Burkeev

Responsible secretary

Candidate of chem. sciences PhD

I.A. Pustolaikina

Editorial board

- Z.M. Muldakhmetov**, Academician of NAS RK, Doctor of chem. sciences, Institute of Organic Synthesis and Coal Chemistry of the Republic of Kazakhstan, Karaganda (Kazakhstan);
- S.M. Adekenov**, Academician of NAS RK, Doctor of chem. sciences, International Research and Production Holding «Phytochemistry», Karaganda (Kazakhstan);
- S.E. Kudaibergenov**, Doctor of chem. sciences, Institute of Polymer Materials and Technologies, Almaty (Kazakhstan);
- V. Khutoryanskiy**, Professor, University of Reading, Reading (United Kingdom);
- Fengyung Ma**, Professor, Xinjiang University, Urumqi (PRC);
- Xintai Su**, Professor, South China University of Technology, Guangzhou (PRC);
- R.R. Rakhimov**, Doctor of chem. sciences, Norfolk State University, Norfolk (USA);
- M.B. Batkibekova**, Academician of the Engineering Academy of the Kyrgyz Republic, Doctor of chem. sciences, Kyrgyz State Technical University named after I. Razzakov, Bishkek (Kyrgyzstan);
- S.A. Beznosyuk**, Doctor of phys.-math. sciences, Altai State University, Barnaul (Russia);
- B.F. Minaev**, Doctor of chem. sciences, Bohdan Khmelnytsky National University of Cherkasy, Cherkasy (Ukraine);
- N.U. Aliev**, Doctor of chem. sciences, Asfendiyarov Kazakh national medical University, Almaty (Kazakhstan);
- R.Sh. Erkasov**, Doctor of chem. sciences, L.N. Gumilyov Eurasian National University, Nur-Sultan (Kazakhstan);
- V.P. Malyshev**, Doctor of techn. sciences, Zh. Abishev Chemical-Metallurgical Institute, Karaganda (Kazakhstan);
- M.I. Baikenov**, Doctor of chem. sciences, Karagandy University of the name of acad. E.A. Buketov (Kazakhstan);
- L.K. Salkeeva**, Doctor of chem. sciences, Karagandy University of the name of acad. E.A. Buketov (Kazakhstan);
- Ye.M. Tazhbaev**, Doctor of chem. sciences, Karagandy University of the name of acad. E.A. Buketov (Kazakhstan);
- A.K. Tashenov**, Doctor of chem. sciences, L.N. Gumilyov Eurasian National University, Nur-Sultan (Kazakhstan);
- Xian Li**, Associated Professor, Huazhong University of Science and Technology, Wuhan (PRC);

Postal address: 28, University Str., Karaganda, 100024, Kazakhstan

Tel./fax: (7212) 34-19-40.

E-mail: vestnikku@gmail.com; ipustolaikina@gmail.com

Web-site: <http://chemistry-vestnik.ksu.kz>

Editors

Zh.T. Nurmukhanova, S.S. Balkeyeva

Computer layout

V.V. Butyaikin

Bulletin of the Karaganda University. Chemistry series.

ISSN 2663-4872 (Online). ISSN-L 2518-718X (Print).

Proprietary: NLC «Karagandy University of the name of academician E.A. Buketov».

Registered by the Ministry of Information and Social Development of the Republic of Kazakhstan. Rediscout certificate No. KZ27VPY00027382 dated 30.09.2020.

Signed in print 29.03.2021. Format 60×84 1/8. Offset paper. Volume 13,5 p.sh. Circulation 200 copies. Price upon request. Order № 27.

Printed in the Publishing house of NLC «Karagandy University of the name of acad. E.A. Buketov».
28, University Str., Karaganda, 100024, Kazakhstan. Tel.: (7212) 35-63-16. E-mail: izd_kargu@mail.ru

© Karagandy University of the name of acad. E.A. Buketov, 2021

CONTENTS

ORGANIC CHEMISTRY

- Nurkenov O.A., Fazylov S.D., Seilkhanov T.M., Nurmaganbetov Zh., Gazaliev A.M., Karipova G.Zh.* Synthesis and structure of thiourea derivatives of functionally substituted pyridines..... 4
- Salkeeva L.K., Muratbekova A.A., Minayeva E.V., Voitichek P., Tayshibekova E.K., Dostanova A.R., Tateeva A.B., Salkeeva A.K.* Phosphorylation of glycoluril derivatives with phosphorus pentachloride 12
- Sinitsyna A.A., Il'yasov S.G.* Synthesis of alkyl derivatives of 3,7,10-trioxo-2,4,6,8,9,11-hexaaza[3.3.3]propellane and evaluation of their biological activity 19
- Bhole R.P., Yogita Shinde, Bonde C.G., Wavhale R.D.* Vitamin Drug conjugate: a systematic review of pharmacological potential 27

PHYSICAL AND ANALYTICAL CHEMISTRY

- Shipunov B.P., Zakharova M.V.* Change in the volume of water crystallization as a result of exposure to a high-frequency electromagnetic field 53
- Tazhbayev Ye.M., Galiyeva A.R., Zhumagaliyeva T.S., Burkeyev M.Zh., Kazhmuratova A.T., Zhakupbekova E.Zh., Zhaparova L.Zh., Bakibayev A.A.* Synthesis and characterization of isoniazid immobilized polylactide-co-glycolide nanoparticles 61
- Bakibaev A.A., Panshina S.Yu., Ponomarenko O.V., Malkov V.S., Kotelnikov O.A., Tashenov A.K.* 1D and 2D NMR spectroscopy for identification of carbamide-containing biologically active compounds 71

CHEMICAL TECHNOLOGY

- Aitbekova D.E., Makenov D.K., Andreikov E.I., Tsaur A.G., Feng Yung Ma, Baikenova G.G., Tusipkhan A., Muratbekova A.A., Baikenov M.I.* Hydrogen distribution in primary coke oven tar and its fractions 82
- Pirniyazov K.K., Tikhonov V.E., Rashidova S.Sh.* Synthesis and properties of oligochitosan ascorbate from *Bombyx mori* 91
- Korolkov I.V., Ludzik K., Lisovskaya L.I., Zibert A.V., Yeszhanov A.B., Zdorovets M.V.* Modification of magnetic Fe₃O₄ nanoparticles for targeted delivery of payloads 99

ORGANIC CHEMISTRY

UDC 547.7/8:547.057

<https://doi.org/10.31489/2021Ch1/4-11>

O.A. Nurkenov^{1*}, S.D. Fazylov¹, T.M. Seilkhanov²,
Zh. Nurmaganbetov¹, A.M. Gazaliev¹, G.Zh. Karipova¹

¹*Institute of Organic Synthesis and Coal Chemistry of the Republic of Kazakhstan, Karaganda, Kazakhstan;*

²*Sh. Ualikhanov Kokshetau University, Kokshetau, Kazakhstan*

(*Corresponding author's e-mail: nurkenov_oral@mail.ru)

Synthesis and structure of thiourea derivatives of functionally substituted pyridines

The article presents data on the synthesis and study of the structure of thiourea derivatives of functionally substituted pyridines. New thiourea derivatives containing a pharmacologically active pyridine moiety in their structure were obtained. As the starting synton, 2-amino-5-bromopyridine, 2-amino-3-hydroxypyridine and 2-aminomethylpyridine were selected. It was shown that the interaction of 2-amino-5-bromopyridine, 2-amino-3-hydroxypyridine and 2-aminomethylpyridine with ethyl and phenylisothiocyanates in ethanol leads to the formation of the corresponding pyridine-containing thioureas. The synthesis of the initial isothiocyanates was carried out in situ from the corresponding acidic chlorides (benzoyl chloride and p-bromobenzoyl chloride) by heating them with potassium thiocyanate in acetone. The structure of the synthesized compounds was studied by ¹H and ¹³C NMR spectroscopy, as well as by the data of two-dimensional spectra of COSY (¹H-¹H) and HMQC (¹H-¹³C). The values of chemical shifts, multiplicity, and integrated intensity of ¹H and ¹³C signals in one-dimensional NMR spectra were determined. Using spectra in the formats COSY (¹H-¹H) and HMQC (¹H-¹³C), homo- and heteronuclear interactions were established, confirming the structure of the studied compounds.

Keywords: ethylisothiocyanates, phenylisothiocyanates, 2-amino-5-bromopyridine, 2-amino-3-hydroxypyridine, 2-aminomethylpyridine, thioureas, 2-aminopyridine, ¹H and ¹³C NMR spectra.

Introduction

It is known that the pyridine cycle is part of many vital organic compounds, which determines its one of the leading roles among heterocycles. Compounds including the pyridine ring are widely used in nature [1–5]. Pyridine derivatives have found various practical applications, for example, as pesticides, herbicides (dithiopyr, imazachine, nicosulfuron, ivinpicolinic acid) and drugs (isoniazid, phthivazide, nialamide, promedol, and many others) [2, 3]. A significant part of the biologically active derivatives of pyridine is aminopyridines [5]. An example is suprastin, which has an antihistamine effect and is used for treatment of allergic dermatoses. Another example is the triamine derivative of phenazopyridine, which is used as an analgesic at painful urination.

Currently, 2-aminopyridines are widely used as key building blocks in the search and synthesis of anti-HIV/antiviral [6–9], anti-tuberculosis [10–13], analgesic [14, 15] and anti-cancer drugs [16–18].

Experimental

¹H and ¹³C NMR spectra (DMSO-d₆) were recorded on a JNM-ECA Jeol 400 spectrometer (399.78 and 100.53 MHz respectively) relative to the signals of residual protons or carbon atoms of a deuterated solvent. The melting point of the substances was determined on an SMP10 digital instrument. The reaction progress

and the purity of the obtained compounds were monitored by thin layer chromatography on Silufol UV-254 plates in an isopropyl alcohol-ammonia-water system, 7:2:1. The plates showed iodine vapor.

1-(5-Bromopyridin-2-yl)-3-ethylthiourea (5). When stirring, 0.3 g (0.003 mol) of ethylisothiocyanate is added drop by drop to a solution of 0.5 g (0.003 mol) of 2-amino-5-bromopyridine in 10 ml of ethanol. When stirring, 0.3 g (0.003 mol) of ethylisothiocyanate is added drop by drop to a solution of 0.5 g (0.003 mol) of 2-amino-5-bromopyridine in 10 ml of ethanol. The reaction mixture was heated at 50–60 °C for 6 hours. The completion of the reaction was monitored by TLC. Next, the reaction mixture was cooled, the precipitate formed was filtered off and recrystallized from ethanol. Obtained 0.38 g (49 %) of substance 5 with m.p. 120–121 °C. ¹H NMR spectrum, δ, ppm (J, Hz): 1.15 t (2H, H-12,12,12, 3J 7.4), 3.57 q (2H, H-11,11, 3J 7.2), 7.10 d (1H, H-3, 3J 8.8), 7.91 dd (1H, H-4, 3J 11.6, 4J 2.8), 8.28 d (1H, H-6, 4J 2.8), 10.59 br.s (1H, H-7), 11.11 br. s (1H, H-11). ¹³C NMR spectrum, δ_c, ppm: 14.47 (C-12), 39.46 (C-11), 105.61 (C-5), 112.29 (C-3), 116.04 (C-6), 146.63 (C-4), 159.16 (C-2), 179.60 (C-8). Cross peaks of the COSY (¹H-¹H) NMR spectra, ppm: H12-H11 (1.15, 3.57 and 3.54, 1.15), H3-H4 (7.11, 7.92 and 7.92, 7.11). Cross peaks of the HMQC (¹H-¹³C) NMR spectra, ppm: H12-C12 (1.12, 14.36), H11-C11 (3.58, 9.67), H3-C3 (7.11, 112.30), H4-C4 (7.91, 146.50), H6-C6 (8.27, 116.05).

1-(5-Bromopyridin-2-yl)-3-phenylthiourea (6) was obtained analogously to compound 5 from 0.5 g (0.003 mol) of 2-amino-5-bromopyridine and 0.4 g (0.003 mol) of phenyl-isothiocyanate. Obtained 0.43 g (41 %) of substance 6 with m.p. 229–230 °C. ¹H NMR spectrum, δ, ppm (J, Hz): 7.16–7.24 m (2H, H-3,15), 7.35 t (2H, H-14,16, 3J 7.6), 7.64 d (2H, H-13,17, 3J 8.4), 8.00 dd (1H, H-4, 3J 9.2, 4J 2.8), 8.41 d (1H, H-6, 4J 2.4), 8.41 br. s (2H, H-7,11). ¹³C NMR spectrum, δ_c, ppm: 112.82 (C-5), 115.43 (C-3), 124.84 (C-13,17), 126.16 (C-15), 129.03 (C-14,16), 139.21 (C-12), 142.25 (C-4), 146.73 (C-6), 152.75 (C-2), 178.62 (C-8). Cross peaks of the COSY (¹H-¹H) NMR spectra, ppm: H15-H14,16 (7.18, 7.31 and 7.31, 7.18), H14,16-H13,17 (7.31, 7.63 and 7.63, 7.31), H3-H4 (7.21, 7.98 and 7.98, 7.21). Cross peaks of the HMQC (¹H-¹³C) NMR spectra, ppm: H3-C3 (7.17, 115.23), H15-C15 (7.25, 126.16), H14,16-C14,16 (7.34, 129.18), H13,17-C13,17 (7.67, 124.86), H4-C4 (8.02, 142.14) and H6-C6 (8.46, 146.76).

N-((5-Bromopyridin-2-yl)carbamothioyl)benzamide (7). While stirring on a magnetic stirrer, 0.11 g (0.0012 mol) of potassium thiocyanate was added to a solution of 0.17 g (0.0012 mol) of benzoyl chloride in 10 ml of acetone. It was stirred at reflux for 2 hours, and then filtered through a paper filter to a solution of 0.2 g (0.0012 mol) of 2-amino-5-bromopyridine in 10 ml of acetone. Then it was stirred at 30–40 °C for 3 hours. The solvent was distilled off. The residue was crystallized upon cooling with isopropanol. The product was recrystallized from isopropyl alcohol. Obtained 0.22 g (55 %) white powder with m.p. 159–160 °C. ¹H NMR spectrum, δ, ppm (J, Hz): 1.31–1.52 m (1H, H9ax), 1.53–1.61 m (3H, H8ax,10ax,9eq), 1.70–1.88 m (1H, H8eq), 2.18–2.40 m (1H, H10eq), 2.76–2.84 m (2H, H4ax,7ax), 2.96–2.98 m (1H, H7eq), 3.58–3.65 m (2H, H4eq, H-11), 4.58 br. s (1H, H1), 5.12–5.21 m (1H, H5), 7.18–7.22 m (3H, H14,15,16), 7.25–7.37 m (4H, H13,17,22,23), 8.40–8.50 (2H, H19,21). ¹³C NMR spectrum, δ_c, ppm: 19.43 (C9), 25.93 (C8), 26.96 (C10), 42.12 (C11), 42.14 (C4), 49.01 (C7), 70.49 (C5), 126.29 (C14,15,16), 127.58 (C15,21), 128.61 (C13,17,19,23), 134.60 (C13,17,22,23), 141.20 (C18), 141.22 (C12), 148.61 (C19,21). Cross peaks of the COSY (¹H-¹H) NMR spectra, ppm: H4ax-H5 (2.76, 5.16 and 5.16, 2.75), H13,17-H14,16 (7.34, 7.16 and 7.16, 7.34), H21,23-H22 (8.39, 7.34 и 7.34, 8.39). Cross peaks of the HMQC (¹H-¹³C) NMR spectra, ppm: H4ax-C4 (2.75, 42.19), H4eq-C4 (3.64, 42.19), H5-C5 (5.20, 70.38), H8ax-C8 (1.53, 25.86), H8eq-C8 (1.73, 25.86), H9ax-C9 (1.37, 19.54), H9eq-C9 (1.61, 19.54), H10eq-C10 (2.25, 26.85), H11-C11 (3.58, 42.12), H22-C22 (7.34, 134.83).

4-Bromo-N-((5-bromopyridin-2-yl)carbamothioyl)benzamide (8) was obtained analogously to compound 7. Obtained 0.2 g (40 %) white powder with m.p. 205–207 °C. ¹H NMR spectrum, δ, ppm (J, Hz): 7.73–7.85 m (4H, H-15,16,18,19), 8.10–8.54 m (3H, H-3,4,6), 11.97 br. s (2H, H-7,11). ¹³C NMR spectrum, δ_c, ppm: 115.93 (C-5), 117.54 (C-3), 127.74 (C-17), 131.24 (C-15,19), 132.09 (C-16,18), 138.59 (C-14), 141.23 (C-4), 149.45 (C-6), 150.70 (C-2), 167.80 (C-12), 178.43 (C-8). Cross peaks of the COSY (¹H-¹H) NMR spectra, ppm: H16,18-H15,19 (7.72, 7.83 and 7.83, 7.72). Cross peaks of the HMQC (¹H-¹³C) NMR spectra, ppm: H16,18-C16,18 (27.72, 132.17).

1-(3-Hydroxypyridin-2-yl)-3-phenylthiourea (9). 1.23 g (0.009 mol) of phenylisothiocyanate is added dropwise with stirring to a solution of 1g (0.009 mol) of 2-amino-3-hydroxypyridine in 10 ml of ethanol. The reaction mixture was heated at 50–60 °C for 6 hours. The completion of the reaction was monitored by TLC. Then the reaction mixture was cooled, the precipitate formed was filtered off and recrystallized from isopropanol. Obtained 0.9 g (41 %) of substance 9 with m.p. 258–259 °C. ¹H NMR spectrum, δ, ppm (J, Hz): 7.03–7.09 m (2H, H-5,15), 7.36 t (2H, H-14,16, 3J 7.6), 7.73 d (2H, H-13,17, 3J 8.7), 7.79 d (1H, H-4, 3J 8.2),

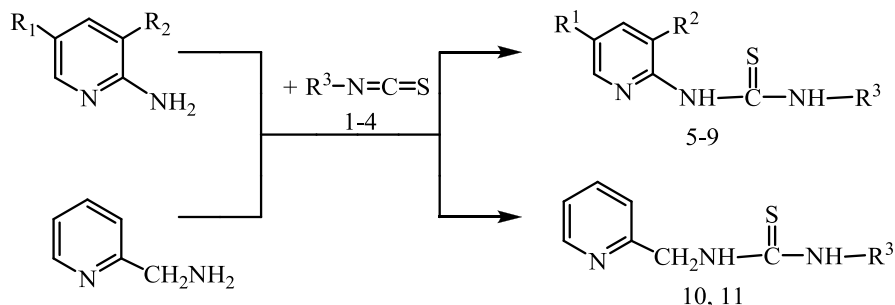
8.19 d (1H, H-6, 3J 5.0), 9.91 br. s (1H, H-10), 10.88 br. s (2H, H-7,11). ^{13}C NMR spectrum, δ_{C} , ppm: 115.64 (C-5), 116.97 (C-4), 118.15 (C-13,17), 122.81 (C-15), 128.89 (C-14,16), 138.02 (C-12), 139.57 (C-6), 144.26 (C-3), 157.04 (C-2), 159.94 (C-8). Cross peaks of the COSY (^1H - ^1H) NMR spectra, ppm: H15-H14,16 (7.03, 7.35 и 7.35, 7.03), H5-H6 (7.03, 8.17 and 8.17, 5.03), H5-H4 (7.05, 7.78 и 7.78, 7.05), H14,16-H13,17 (7.35, 7.72 and 7.72, 7.35). Cross peaks of the HMQC (^1H - ^{13}C) NMR spectra, ppm: H13,15-C13,15 (7.38, 117.59), H14,16-C14,16 (7.34, 129.51), H4-C4 (7.72, 118.80), H6-C6 (8.19, 139.58).

1-Ethyl-3-(pyridin-2-ylmethyl)thiourea (10). When stirring, 0.78 g (0.009 mol) of ethylisothiocyanate was added dropwise to a solution of 1 g (0.009 mol) of 2-aminomethylpyridine in 10 ml of ethanol. The reaction mixture was heated at 50–60 °C for 2 hours. The completion of the reaction was monitored by TLC. Then the reaction mixture was cooled, the precipitate formed was filtered off and recrystallized from isopropanol. Obtained 1.44 g (66 %) of substance with m.p. 66–67 °C. ^1H NMR spectrum, δ , ppm (J, Hz): 1.05 t (3H, H-13,13,13, 3J 7.6), 3.37 br. s (2H, H-12,12), 4.70 s (H, H-7,7), 7.20–7.26 m (2H, H-3,5), 7.68–7.73 m (2H, H-2,4), 7.83 br. s (1H, H-8), 8.43 br. s (1H, H-11). ^{13}C NMR spectrum, δ_{C} , ppm: 14.93 (C-13), 38.96 (C-12), 49.24 (C-7), 121.81 (C-5), 122.62 (C-3), 137.16 (C-4), 149.24 (C-2), 158.76 (C-6) and 182.91 (C-9). Cross peaks of the COSY (^1H - ^1H) NMR spectra, ppm: H13-H12 (1.05, 3.2 and 3.34, 1.04), H3,5-H2,4 (7.22, 7.72 and 7.69, 7.25). Cross peaks of the HMQC (^1H - ^{13}C) NMR spectra, ppm: H13-C13 (1.01, 13.37), H12-C12 (3.34, 38.97), H7-C7 (4.68, 49.06), H3,5-C3,5 (7.21, 121.84), H4-C4 (7.70, 137.25) and H2-C2 (8.45, 149.25).

1-Phenyl-3-(pyridin-2-ylmethyl)thiourea 11 was obtained analogously to compound 10 from 1 g (0.009 mol) of 2-aminomethylpyridine and 1.22 g (0.009 mol) of phenylisothiocyanate. Obtained 1.2 g (43 %) of substance 11 with m.p. 109–110 °C. ^1H NMR spectrum, δ , ppm (J, Hz): 4.80 d (2H, H-7,7, 3J 5.4), 7.09 d (1H, H-15, 3J 7.4), 7.25 t (1H, H-3, 3J 4.8), 7.28–7.34 m (3H, H-5,14,16), 7.47 d (2H, H-13,17, 3J 8.4), 7.74 dd (1H, H-4, 3J 7.6, 4J 1.2), 8.23 br. s (1H, H-8), 8.49 d (1H, H-2, 3J 4.8), 10.94 br. s (1H, H-11). ^{13}C NMR spectrum, δ_{C} , ppm: 49.46 (C-7), 121.99 (C-3), 122.73 (C-13,17), 123.75 (C-5), 124.84 (C-14,16), 129.19 (C-15), 137.24 (C-4), 139.77 (C-12), 149.27 (C-2), 158.08 (C-6), 181.33 (C-9). Cross peaks of the COSY (^1H - ^1H) NMR spectra, ppm: H7-H8 (4.78, 8.23 and 8.21, 4.80), H15-H14,16 (7.08, 7.30 and 7.30, 7.08), H14,16-H13,17 (7.26, 7.46 and 7.46, 7.26), H5-H4 (7.26, 7.72 and 7.72, 7.26), H7-H8 (4.78, 8.23 and 8.21, 4.80). Cross peaks of the HMQC (^1H - ^{13}C) NMR spectra, ppm: H7-C7 (4.79, 49.45), H5-C5 (7.28, 123.87), H4-C4 (7.72, 137.16), H2-C2 (8.53, 149.15).

Results and Discussion

In the present work, in order to obtain new thiourea compounds, we selected 2-amino-5-bromopyridine, 2-amino-3-hydroxypyridine, and 2-aminomethylpyridine as the initial synton. By the interaction of the above 2-aminopyridines with ethyl and phenylisothiocyanates in ethanol, their thiourea derivatives 5, 6 and 9–11 were synthesized. The syntheses of new acyl derivatives of thiourea 7, 8 were also studied. The synthesis of new compounds was carried out by the interaction of isothiocyanates 1–4 with 2-amino-5-bromopyridine, 2-amino-3-hydroxypyridine and 2-aminomethylpyridine. Isothiocyanates 1–4 were obtained by the interaction of potassium thiocyanate with the corresponding chlorides (benzoyl chloride and p-bromobenzoyl chloride) under in situ interaction conditions.



5: $\text{R}^1 = \text{Br}$, $\text{R}^2 = \text{H}$, $\text{R}^3 = \text{CH}_3\text{CH}_2$ -;

6: $\text{R}^1 = \text{Br}$, $\text{R}^2 = \text{H}$, $\text{R}^3 = \text{Ph}$;

7: $\text{R}^1 = \text{Br}$, $\text{R}^2 = \text{H}$, $\text{R}^3 = \text{PhC(O)}$ -;

8: $\text{R}^1 = \text{Br}$, $\text{R}^2 = \text{H}$, $\text{R}^3 = 4\text{-BrPhC(O)}$ -;

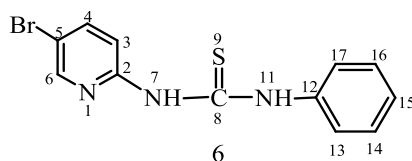
9: $\text{R}^1 = \text{H}$, $\text{R}^2 = \text{HO}$, $\text{R}^3 = \text{Ph}$;

10: $\text{R}^3 = \text{CH}_3\text{CH}_2$ -;

11: $\text{R}^3 = \text{Ph}$.

The obtained compounds 5–11 after recrystallization are white crystalline substances, soluble in most organic solvents, except saturated hydrocarbons. The structure of the synthesized compound 5–11 was proved by ^1H and ^{13}C NMR spectroscopy, as well as by the data of the two-dimensional spectrum of HMQC (^1H - ^{13}C).

The ^1H NMR spectrum of compound 6 is characterized by the presence of phenyl radical protons in the low-field part of the spectrum of signals. Symmetrically located methine protons H-14,16 and H-13,17 are manifested by a two-proton triplet at 7.35 (3J 7.6 Hz) and a two-proton doublet at 7.64 (3J 8.4 Hz) ppm respectively. The remaining phenyl proton H-15 was manifested together with the pyridine proton H-3 by a two-proton multiplet at 7.16–7.24 ppm. The pyridine protons H-4 and H-6 resonated with a single-proton doublet of doublets at 8.00 ppm with 3J 9.2 Hz and 4J 2.8 Hz and a doublet at 8.41 ppm with 4J 2.4 Hz respectively. In the weakest field of the spectrum at 10.94 ppm with a broadened two-proton singlet, thioamide protons H-7 and H-11 appeared.



In the carbon spectrum of compound 6, NMR signals of ^{13}C nuclei of the phenyl radical are observed at 124.84 (C-13,17), 126.16 (C-15), 129.03 ppm (C-14,16) and 139.21 ppm (C-12). The carbon atoms of the pyridine heterocycle give signals at 112.82 (C-5), 115.43 (C-3), 142.25 (C-4), 146.73 (C-6) and 152.75 (C-2) ppm. The most weak-field signal at 178.62 ppm refers to carbon at the sulfur atom C-8.

The structure of compound 6 was also confirmed by the methods of two-dimensional spectroscopy COSY (^1H - ^1H) and HMQC (^1H - ^{13}C), which allows one to establish spin-spin interactions of a homo- and heteronuclear nature. The observed correlations in the molecule are shown in Figures 1 and 2. In the spectra of the ^1H - ^1H COSY compound, spin-spin correlations are observed through three proton bonds of the neighboring methine groups H15-H14,16 (7.18, 7.31 and 7.31, 7.18) and H14,16-H13,17 (7.31, 7.63 and 7.63, 7.31) the phenyl fragment and neighboring methine protons H3-H4 (7.21, 7.98 and 7.98, 7.21) of the pyridine nucleus. Heteronuclear interactions of protons with carbon atoms through one bond were established using 1H-13C HMQC spectroscopy for the following pairs present in the compound: H3-C3 (7.17, 115.23), H15-C15 (7.25, 126.16), H14,16-C14,16 (7.34, 129.18), H13,17-C13,17 (7.67, 124.86), H4-C4 (8.02, 142.14) and H6-C6 (8.46, 146.76).

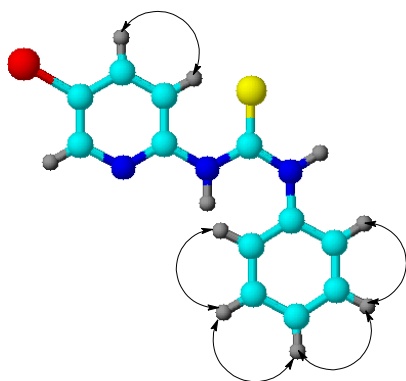


Figure 1. Correlation of COSY (^1H - ^1H) of compound 6

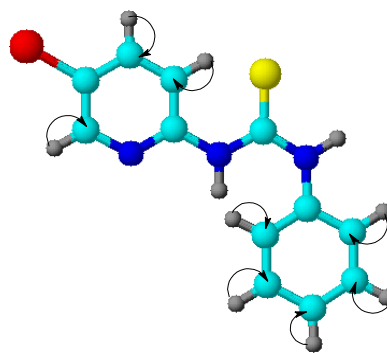
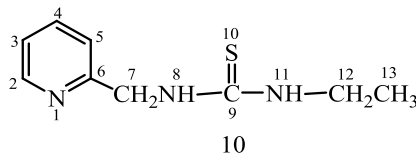


Figure 2. Correlation of HMQC (^1H - ^{13}C) of compound 6

The presence of additional aromatic fragments in compounds 7–9 increases the number of signals in the weak zone of the spectra. Signals indicating the presence of an N-ethyl fragment in the molecule are present in compound 1.

The NMR spectra of compounds 5, 7–9 contain signals characteristic of atoms of the pyridine nucleus and thioamide moiety. The presence of additional aromatic fragments in compounds 7–9 increases the number of signals in the weak region of the spectra. In compound 1, there are signals indicating the presence of an N-ethyl fragment in the molecule.

In the ^1H NMR spectrum of compound 10 in the high-field part of the spectrum, the N-ethyl protons H-13,13,13 and H-12,12 were manifested by a three-proton triplet at 1.05 ppm with $3J$ 7.6 Hz and an extended two-proton singlet at 3.37 ppm respectively. Methylene protons H-7,7 were resonated by a two-proton singlet at 4.70 ppm. The pyridine protons H-3,5 and H-2,4 were manifested by two-proton multiplets at 7.20–7.26 and 7.68–7.73 ppm respectively. In the most weak-field part of the spectrum at 7.83 and 8.43 ppm broadened single-proton singlets showed the thioamide protons H-8 and H-11 respectively.



In the carbon spectrum of compound 10, signals of the methyl and methylene groups of the N-ethyl radical appear at 14.93 (C-13) and 38.96 (C-12) ppm respectively. Signal at 49.24 ppm corresponds to methylene carbon atom C-7. The pyridine fragment is characterized by resonance at 121.81 (C-5), 122.62 (C-3), 137.16 (C-4) and 149.24 (C-2) ppm. The most weak-field signals at 158.76 and 182.91 ppm correspond to the quaternary carbon atom C-6 and the thiocarbonyl atom C-9 respectively.

The structure of compound 10 was also confirmed by the methods of two-dimensional spectroscopy COSY (^1H - ^1H) and HMQC (^1H - ^{13}C). The observed correlations in the molecule are shown in Figures 3 and 4. In the spectra of the ^1H - ^1H COSY compound, spin-spin correlations are observed through three bonds of protons of the neighboring methyl and methylene groups H13-H12 (1.05, 3.2 and 3.34, 1.04) of the N-ethyl fragment and methine protons H3,5-H2,4 (7.22, 7.72 and 7.69, 7.25) of the pyridine nucleus. Heteronuclear interactions of protons with carbon atoms through a single bond were established using ^1H - ^{13}C HMQC spectroscopy for the following pairs present in the compound: H13-C13 (1.01, 13.37), H12-C12 (3.34, 38.97), H7-C7 (4.68, 49.06), H3,5-C3,5 (7.21, 121.84), H4-C4 (7.70, 137.25) and H2-C2 (8.45, 149.25).

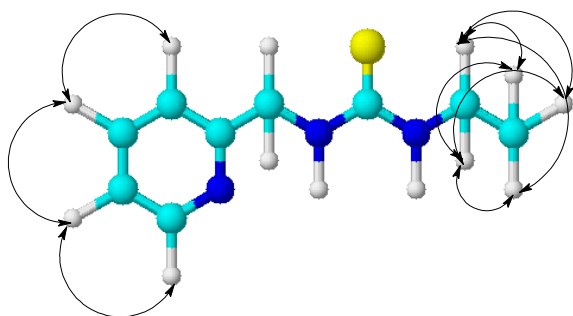


Figure 3. Correlations of COSY (^1H - ^1H) of compound 10

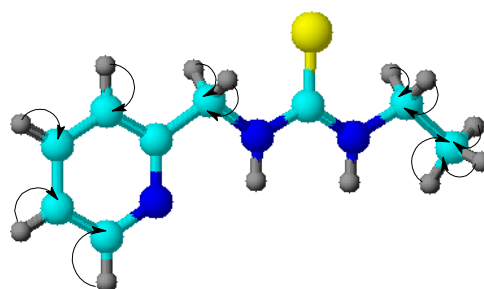


Figure 4. Correlation of HMQC (^1H - ^{13}C) of compound 10

Conclusions

Thus, a new derivatives of thiourea were synthesized at interaction of 2-aminopyridines (2-amino-5-bromopyridine, 2-amino-3-hydroxypyridine and 2-aminomethylpyridine) with ethyl- and phenylisothiocyanate. They were characterized; their structures being confirmed by NMR spectroscopy ^1H and ^{13}C , as well as data the two-dimensional spectra, COSY (^1H - ^1H) and HMQC (^1H - ^{13}C).

The study was performed with financial support from RK Ministry of Education and Science Committee (grant № AP08855567).

References

- 1 Государственная фармакопея СССР (Изд. X). — М.: Медицина, 1968.
- 2 Машковский М.Д. Лекарственные средства / М.Д. Машковский. — 15-е изд. — М.: Новая волна, 2007. — 1206 с.
- 3 Машковский М.Д. Лекарства XX века / М.Д. Машковский. — М.: Новая волна, 1998. — 320 с.

- 4 Беликов В.Г. Фармацевтическая химия: учеб. пос. / В.Г. Беликов. — М.: Высш. шк., 1985. — 552 с.
- 5 Bakirova R. Obtaining and Investigation of the beta-Cyclodextrin Inclusion Complex with Vitamin D-3 Oil Solution / R. Bakirova, A. Nukhuly, A. Iskineyeva, S. Fazylov, M. Burkeev, A. Mustafaeva, E. Minaeva, A. Sarsenbekova // *Scientifica*. — 2020. — Vol. 2020. — P. 1–8. — ID 6148939.
- 6 Yu T. Synthesis and fluorescence properties of 7-hydroxy-3-(2-pyridyl)coumarin derivatives / T. Yu, S. Yang, Y. Zhao // *Research on Chemical Intermediates*. — 2012. — Vol. 38. — P. 215–222.
- 7 Balasubramanian M. *Comprehensive Heterocyclic Chemistry II* / M. Balasubramanian, J.G. Keay, A.R. Katritzky // Pergamon Press. — 1996. — Vol. 5. — P. 245–300.
- 8 Klimesova V. New pyridine derivatives as potential antimicrobial agents / V. Klimesova, M. Svoboda, K. Waisser // *IL Farmaco*. — 1999. — Vol. 54. — P. 666–672.
- 9 Enyedy I.J. Pharmacophore-based discovery of substituted pyridines as novel dopamine transporter inhibitors / I.J. Enyedy, S. Sakamuri, W.A. Zaman // *Bioorganic & Medicinal Chemistry Letters*. — 2003. — V. 13. — P. 513–517.
- 10 Pillai A.D. Novel drug designing approach for dual inhibitors as anti-inflammatory agents: implication of pyridine template / A.D. Pillai, P.D. Rathod, P.X. Franklin // *Biochemical and Biophysical Research Communications*. — 2003. — Vol. 301. — P. 183–186.
- 11 Kim B.Y. Synthesis and biological activity of novel substituted pyridines and purines containing 2,4-thiazolidinedione / B.Y. Kim, J.B. Ahn, H.W. Lee // *European Journal of Medicinal Chemistry*. — 2004. — V. 39. — P. 433–447.
- 12 Lowe G. Cytotoxicity of (2,2':6',2"-terpyridine)platinum (II) complexes to *Leishmania donovani*, *Trypanosoma cruzi*, and *Trypanosoma brucei* / G. Lowe, A.S. Droz, T. Vilaivan // *Journal of Medicinal Chemistry*. — 1999. — Vol. 42. — P. 999–1006.
- 13 Bonse S. (2,2':6',2"-Terpyridine)platinum(II) complexes are irreversible inhibitors of *Trypanosoma cruzi* trypanothione reductase but not of human glutathione reductase / S. Bonse, J.M. Richards, S.A. Ross // *Journal of Medicinal Chemistry*. — 2000. — Vol. 43. — P. 4812–4821.
- 14 Zhao L.X. Synthesis, topoisomerase I inhibition and antitumor cytotoxicity of 2,2':6',2"-, 2,2':6',3"- and 2,2':6',4"-terpyridine derivatives / L.X. Zhao, T.S. Kim, S.H. Ahn // *Bioorganic & Medicinal Chemistry Letters*. — 2001. — Vol. 11. — P. 2659–2662.
- 15 Zhao L.X. Synthesis, topoisomerase I inhibition and structure-activity relationship study of 2,4,6-trisubstituted pyridine derivatives / L.X. Zhao, Y.S. Moon, A. Basnet // *Bioorganic & Medicinal Chemistry Letters*. — 2004. — Vol. 14. — P. 1333–1337.
- 16 O'Kennedy R. *Coumarins: Biology, Applications and Mode of Actions* / R. O'Kennedy, R.D. Thornes. — Chichester; New York: John Wiley & Sons, 1997.
- 17 Ahmed A. Cytotoxicity, antioxidant, and antimicrobial activities of novel 2-quinolone derivatives derived from coumarin / A. Ahmed, Al-Amiery, I.H. Redha // *Research on Chemical Intermediates*. — 2012. — Vol. 38. — P. 559–569.
- 18 Zhan W.H. The synthesis and characterization of novel coumarin-containing cyanine dyes via «Click» chemistry / W.H. Zhan, J.L. Hua, Y.H. Jin // *Research on Chemical Intermediates*. — 2008. — Vol. 34. — P. 229–239.

О.А. Нұркенов, С.Д. Фазылов, Т.М. Сейлханов,
Ж. Нұрмағанбетов, А.М. Ғазалиев, Г.Ж. Кәріпова

Функционалдық-орынбасылған пиридиндердің тиомочевинді туындыларының синтезі және құрылысы

Мақалада функционалдық-орынбасылған пиридиндердің тиомочевинді туындыларының синтезі және құрылысын зерттеу бойынша деректері келтірілген. Құрамында фармакологиялық белсенді пиридин тобы бар жаңа тиомочевинді туындылар алынды. Бастапқы синтон ретінде 2-амино-5-бромпиридин, 2-амино-3-гидроксипиридин және 2-аминометилпиридин таңдалды. 2-амин-5-бромпиридиннің, 2-амин-3-гидроксипиридиннің және 2-аминометилпиридиннің этанолдағы этил және фенилизотиоцианаттармен өзара әрекеттесуі тиісті пиридин бар тиомочевин түзілуіне әкеп соқтыратыны көрсетілген. Бастапқы изотиоцианаттардың синтезі ацетон ортасында роданисті калиймен *in situ* жағдайында тиісті хлорангидридтерден (бензоилхлорид және *n*-бромбензоилхлорид) қыздыру кезінде алынды. Синтезделген қосылыстардың құрылысы ЯМР ^1H - және ^{13}C -спектроскопия әдістерімен, сондай-ақ екі өлшемді COSY (^1H - ^1H) және НМҚС (1H-13C) спектрлерінің деректерімен зерттелді. Бір өлшемді ЯМР спектрлерінде ^1H және ^{13}C сигналдардың интегралдық қарқындылығы, мультиплеттілігі және химиялық ығысу мәндері анықталды. COSY (^1H - ^1H) және НМҚС (^1H - ^{13}C) форматтарында спектрлер көмегімен зерттелетін қосылыстардың құрылымын растайтын гомо- және гетероядролық өзара әрекеттесулері белгіленді.

Кілт сөздер: этилизотиоцианат, фенилизотиоцианат, 2-амино-5-бромпиридин, 2-амино-3-гидроксипиридин, 2-аминометилпиридин, тиомочевиндер, 2-аминопиридин, ЯМР ^1H -және ^{13}C -спектрлер.

О.А. Нуркенов, С.Д. Фазылов, Т.М. Сейлханов,
Ж. Нурмаганбетов, А.М. Газалиев, Г.Ж. Карипова

Синтез и строение тиомочевинных производных функционально-замещенных пиридинов

В статье приведены данные по синтезу и изучению строения тиомочевинных производных функционально-замещенных пиридинов. Получены новые тиомочевинные производные, содержащие в своей структуре фармакологически активную пиридиновую группировку. В качестве исходного синтона были выбраны 2-амино-5-бромпиридин, 2-амино-3-гидроксипиридин и 2-аминометилпиридин. Показано, что взаимодействие 2-амино-5-бромпиридина, 2-амино-3-гидроксипиридина и 2-аминометилпиридина с этил- и фенилизотиоцианатами в этаноле приводит к образованию соответствующих пиридинсодержащих тиомочевин. Синтез исходных изотиоцианатов был проведен *in situ* из соответствующих кислых хлоридов (бензоилхлорид и *n*-бромбензоилхлорид) путем нагревания их с тиоцианатом калия в ацетоне. Строение синтезированных соединений исследовано методами ^1H и ^{13}C ЯМР-спектроскопии, а также данными двумерных спектров COSY (^1H - ^1H) и HMQC (^1H - ^{13}C). С помощью спектров в форматах COSY (^1H - ^1H) и HMQC (^1H - ^{13}C) установлены гомо- и гетероядерные взаимодействия, подтверждающие структуру исследуемых соединений.

Ключевые слова: этилизотиоцианат, фенилизотиоцианат, 2-амино-5-бромпиридин, 2-амино-3-гидроксипиридин, 2-аминометилпиридин, тиомочевины, 2-аминопиридин, ^1H - и ^{13}C ЯМР-спектры.

References

- 1 *Hosudarstvennaia farmakopeia SSSR [The State Pharmacopoeia of the USSR]* (1968). (10th ed.). Moscow: Meditsina [in Russian].
- 2 Mashkovsky, M.D. (2007). *Lekarstvennye sredstva [Medicines]*. (15th ed.). Moscow: Novaia volna [in Russian].
- 3 Mashkovsky, M.D. (1998). *Lekarstva XX veka [Medications of the 20th century]*. Moscow: Novaia volna [in Russian].
- 4 Belikov, V.G. (1985). *Farmatsevticheskaia khimiia [Pharmaceutical chemistry]*. Moscow: Vysshiaia shkola [in Russian].
- 5 Bakirova, R., Nukhuly, A., Iskineyeva, A., Fazylov, S., Burkeev, M., & Mustafaeva, A., et al. (2020). Obtaining and Investigation of the beta-Cyclodextrin Inclusion Complex with Vitamin D-3 Oil Solution. *Scientifica*, 2020, 1–8. ID 6148939.
- 6 Yu, T., Yang, S., & Zhao, Y. (2012). Synthesis and fluorescence properties of 7-hydroxy-3-(2-pyridyl)coumarin derivatives. *Research on Chemical Intermediates*, 38, 215–222.
- 7 Balasubramanian, M., Keay, J.G., & Katritzky, A.R. (1996). *Comprehensive Heterocyclic Chemistry II*. Pergamon Press., 5, 245–300.
- 8 Klimesova, V., Svoboda, M., & Waisser, K. (1999). New pyridine derivatives as potential antimicrobial agents. *IL Farmaco.*, 54, 666–672.
- 9 Enyedy, I.J., Sakamuri, S., & Zaman, W.A. (2003). Pharmacophore-based discovery of substituted pyridines as novel dopamine transporter inhibitors. *Bioorganic & Medicinal Chemistry Letters*, 13, 513–517.
- 10 Pillai, A.D., Rathod, P.D., & Franklin, P.X. (2003). Novel drug designing approach for dual inhibitors as anti-inflammatory agents: implication of pyridine template. *Biochemical and Biophysical Research Communications*, 301, 183–186.
- 11 Kim, B.Y., Ahn, J.B., & Lee, H.W. (2004). Synthesis and biological activity of novel substituted pyridines and purines containing 2,4-thiazolidinedione. *European Journal of Medicinal Chemistry*, 39, 433–447.
- 12 Lowe, G., Droz, A.S., Vilaivan, T. (1999). Cytotoxicity of (2,2':6',2"-terpyridine)platinum (II) complexes to *Leishmania donovani*, *Trypanosoma cruzi*, and *Trypanosoma brucei*. *Journal of Medicinal Chemistry*, 42, 999–1006.
- 13 Bonse, S., Richards, J.M., & Ross, S.A. (2000). (2,2':6',2"-Terpyridine)platinum (II) complexes are irreversible inhibitors of *Trypanosoma cruzi* trypanothione reductase but not of human glutathione reductase. *Journal of Medicinal Chemistry*, 43, 4812–4821.
- 14 Zhao, L.X., Kim, T.S., & Ahn, S.H. (2001). Synthesis, topoisomerase I inhibition and antitumor cytotoxicity of 2,2':6',2"-, 2,2':6',3"- and 2,2':6',4"-terpyridine derivatives. *Bioorganic & Medicinal Chemistry Letters*, 11, 2659–2662.
- 15 Zhao, L.X., Moon, Y.S., & Basnet, A. (2004). Synthesis, topoisomerase I inhibition and structure-activity relationship study of 2,4,6-trisubstituted pyridine derivatives. *Bioorganic & Medicinal Chemistry Letters*, 14, 1333–1337.
- 16 O'Kennedy, R., & Thornes, R.D. (1997). *Coumarins: Biology, Applications and Mode of Actions*. Chichester; New York: John Wiley & Sons.
- 17 Ahmed, A., Al-Amiery, & Redha, I.H. (2012). Cytotoxicity, antioxidant, and antimicrobial activities of novel 2-quinolone derivatives derived from coumarin. *Research on Chemical Intermediates*, 38, 559–569.
- 18 Zhan, W.H., Hua, J.L., Jin, Y.H. The synthesis and characterization of novel coumarin-containing cyanine dyes via «Click» chemistry. *Research on Chemical Intermediates*, 34, 229–239.

Information about authors

Nurkenov, Oralgazy Aktaevich — Doctor of Chemical Sciences, Professor, Institute of Organic Synthesis and Coal Chemistry of the Republic of Kazakhstan, Karaganda, Kazakhstan; e-mail: nurkenov_oral@mail.ru, <https://orcid.org/0000-0003-1878-2787>

Fazylov, Serik Drakhmetovich — Academician of the National Academy of Sciences of the Republic of Kazakhstan, Doctor of Chemical Sciences, Professor, Institute of Organic Synthesis and Coal Chemistry of the Republic of Kazakhstan, Karaganda, Kazakhstan, e-mail: iosu8990@mail.ru, <https://orcid.org/0000-0002-4240-6450> (Contact person: +77078660841).

Seilkhanov, Tolegen Muratovich — Candidate of Chemical Sciences, Head of the laboratory of engineering profile NMR spectroscopy of Kokshetau State University named after Sh. Ualikhanov MES RK, Kokshetau, Kazakhstan, e-mail: tseilkhanov@mail.ru, <https://orcid.org/0000-0003-0079-4755>

Nurmaganbetov, Zhaneldy — Candidate of Chemical Sciences, Leading researcher of the Laboratory of synthesis of biologically active substances, Institute of Organic Synthesis and Coal Chemistry of the Republic of Kazakhstan, Karaganda, Kazakhstan, e-mail: nzhangeldy@yandex.ru. <https://orcid.org/0000-0002-0978-5663>

Gazaliev, Arstan Maulenovich — Academician of the National Academy of Sciences of the Republic of Kazakhstan, Doctor of Chemical Sciences Professor, Institute of Organic Synthesis and Coal Chemistry of the Republic of Kazakhstan, Karaganda, Kazakhstan, e-mail: iosu@mail.ru. <https://orcid.org/0000-0003-2161-0329>

Karipova, Gulzhanat Zhumazhanovna — Master of education, Researcher of the Laboratory of synthesis of biologically active substances, Institute of Organic Synthesis and Coal Chemistry of the Republic of Kazakhstan, Karaganda, Kazakhstan, e-mail: gulia_1708@mail.ru. <https://orcid.org/0000-0002-3896-6156>

L.K. Salkeeva^{1*}, A.A. Muratbekova¹, E.V. Minayeva¹, P. Voitichek²,
E.K. Tayshibekova¹, A.R. Dostanova¹, A.B. Tateeva¹, A.K. Salkeeva³

¹Karagandy University of the name of academician E.A. Buketov, Kazakhstan;

²Charles University, Prague, Czech Republic;

³Karaganda Technical University, Kazakhstan

(*Corresponding author's e-mail: lsalkeeva@mail.ru)

Phosphorylation of glycoluril derivatives with phosphorus pentachloride

The paper presents the research results on the synthesis and study of new organophosphorus derivatives of glycoluril, obtained on the basis of pentavalent phosphorus. New organoelement phosphorus derivatives synthesized on the basis of N-acyl-substituted glycoluril have been obtained. They are of considerable interest due to the presence of effective reaction centers. Tetraacetyl-substituted glycoluril — 2,4,6,8-tetraacetyl-2,4,6,8-tetraazabicyclo[3,3,0]octane-3,7-dione was chosen as the initial synthon. The use of unsubstituted glycoluril in the reaction of direct phosphorylation by the action of phosphorus trichloride or pentachloride is not possible due to the absence of active phosphorylation centers. It was experimentally shown that the reaction proceeds with prolonged heating for at least 48 hours in an argon. The initial acyl derivative of glycoluril and phosphorus pentachloride in the ratio of 1:6 and leads to the formation of diphosphonic complex of tetraacetyl glycoluril — dihexachlorophosphate 2,6-diacetyl-(4,8-diacetyl-2,4,6,8-tetraazabicyclo[3.3.0]octane-3,7-dione)-2,6-di(chloroethenyltrichlorophosphonium). The obtained compound is a white crystalline substance unstable in air. Decomposition of the diphosphonic complex was carried out using benzaldehyde and proceeds with the formation of the corresponding dichlorophosphate derivative, also unstable in air and rapidly decomposing at room temperature.

Keywords: glycoluril, bicyclic bisureas, phosphorus pentachloride, phosphorylation, N-acylation, phosphorus, bicyclic, synthesis.

Introduction

Currently the synthesis of 2,4,6,8-tetraazabicyclo[3.3.0]octane-3,7-dione (glycoluril) derivatives and the study its properties remain one of the rapidly developing areas of modern chemistry of heterocyclic compounds. This substance is a representative of the bicyclic bisureas class. Glycolurils find wide application in various areas of industry: in particular, resins containing glycoluril are used for the manufacture of paints and coatings; in the pulp and paper industry, the application of glycoluril is also known as an intermediate product in the synthesis of antioxidants, detergents, disinfectants and bleaching agents [1–3].

All these properties of glycoluril make it a promising object among the researchers as this class of compounds possesses with many undiscovered potential properties. The first reports on the interaction of glycoluril and acetic anhydride with the formation of N-acetyl-substituted glycoluril derivatives date back to the beginning of the last century [4–8]. Despite the diversity of the N-acetyl-substituted bicyclic bisureas series, it was noted the N-acylation of glycoluril was limited by the synthesis of N,N-di- and N,N,N,N-tetraacetylated derivatives. It is obvious the possibilities of the glycoluril acylation reaction are larger and varied.

It is known N-substituted glycolurils have a wide spectrum of biological activity. Previously it was reported about the neuroleptic, antidepressant and psychostimulating activity of glycoluril and its derivatives. This property is the main reason that arouses a great interest in the syntheses of the new group compounds capable to show various activities.

Organic phosphorus compounds are also used in a different areas of human life and the synthesis of new organophosphorus derivatives with various biological activity continues to be a priority.

Experimental

Equipment. NMR spectra were recorded by a JeolECX-400 spectrometer for NMR (400 MHz) relatively TMS, for ³¹P NMR (162 MHz) versus an external standard (85 % H₃PO₄) and for ¹³C NMR (100 MHz) versus an internal standard — TMS in DMSO-solutions. d₆, CDCl₃, D₂O. IR spectra were recorded with the FSM-1201 Fourier spectrometer from 450 cm⁻¹ to 4000 cm⁻¹ in KBr pellets. NMR spectra were recorded in

the medium of argon. Mass spectra were recorded by a MicroTOF instrument (ESI-TOFMS), Bruker. Melting points were determined by the MP50 MeltingPointSystem.

The reactions procedure and the compounds identity were monitored by thin layer chromatography on standard Silufol UV-254 plates in the benzene: ethyl alcohol = 6:1 system. The plates were detected with iodine vapor and a UV lamp.

Synthesis of 2,4,6,8-tetraacetyl-2,4,6,8-tetraazabicyclo[3,3,0]octane-3,7-dione (1)

153.0 g (1.5 mol) of acetic anhydride and 1 ml (0.01–0.02 mol) of 56 % perchloric acid were added to the 35.0 g (0.25 mol) of glycoluril with stirring. The mixture was heated until self-heating began. After complete homogenization, 20.0 g (0.2 mol) of sodium acetate was added to the reaction mixture and was boiled for an hour. The reaction mixture was cooled, the precipitated crystals were filtered off and washed with acetic anhydride and dried. Yield is 65.7 g (89 %), m.p. 244 °C. IR spectrum (ν , cm^{-1}): 1695 (C=O), 1780 (COCH₃). ¹H NMR spectrum (400 MHz, DMSO), δ , ppm: 2.34 s (12H, COCH₃), 6.33 s (2H, CH). ¹³C NMR spectrum (CDCl₃): 59.95 (CH), 148.65 (CO), 167.57 (COCH₃). Found, %: C 46.93, H 4.78, N 18.28. C₁₂H₁₄N₄O₆. Calculated, %: C 46.45, H 4.52, N 18.06.

Synthesis of hexachlorophosphate of 2,6-di(4,8-diacetyl-2,4,6,8-tetraazabicyclo[3.3.0]octane-3,7-dione)-2-hloroethenyltrichlorophosphonium (2)

2.0 g (0.0064 mol) of tetraacetyl glycoluril in chloroform was added to 21.5 g (0.103 mol) of phosphorus pentachloride in chloroform and in argon, then was heated for 48 hours with stirring. In an inert atmosphere, the solvent was distilled off, the crystals decomposing in air were filtered off then dried in a vacuum. Yield is 3.97 g (56 %), ³¹P NMR spectrum (162 MHz, CDCl₃): δ , ppm.: 2.67 (PCl₃⁺), -97.03 (PCl₆⁻).

Synthesis of 2,6-di(2-chloroethynyl)-4,8-diacetyl-2,4,6,8-tetraazabicyclo[3.3.0]octane-3,7-dione diphosphonic acid (3)

3.8 g (0.035 mol) of benzaldehyde was added to the suspension of 3.97 g (0.0035 mol) 2 and dry toluene in an argon. After complete dissolution, the mixture was heated at 80–90 °C for 3 hours. The solvent and low-boiling fractions were distilled off in a vacuum and the residue decomposed in air was recrystallized with dichloromethane. Yield is 1.0 g (48 %). ¹H NMR spectrum (400 MHz, CDCl₃), δ , ppm: 2.46 s (6H, 2(COCH₃)), 3.71–3.79 m (2H, 2C = CH), 5.70 s (2H, CHCH). ³¹P NMR spectrum (162 MHz, CDCl₃), δ , ppm: 5.29.

Results and discussion

A detailed analysis of the literature data shows the lack of related reports on the study in particular, the phosphorylation of glycoluril and its derivatives. Previously there was a possibility of effective using glycoluril phosphorus derivatives according to the classical scheme of the Arbuzov reaction, i.e. by the interaction of bisacetyl brom derivatives of glycoluril — 1,4-bis(bromoacetyl)tetra-hydroimidazo[4,5-d]-imidazole-2,5(1H, 3H)dione with triethylphosphate [9]. As a result of the reaction, {(2,5-dioxohexahydroimidazo[4,5-d]imidazole-1,4-diyl)-bis(2-oxoethane-2,1-diyl)}-bis(diethylphosphonate) was obtained as a non-distillable oil acid hydrolysis of which gave the corresponding {(2,5-dioxohexahydroimidazo[4,5-d]imidazole-1,4-diyl)-bis(2-oxoethane-2,1-diyl)}bisphosphonic acid.

Despite the wide range of possibilities for the chemical modification of trivalent phosphorus derivatives, pentavalent phosphorus derivatives continue to attract the attention of organic chemists as important synthons in the creating of new biologically active compounds.

The most promising reagent in the synthesis of trivalent phosphorus derivatives is undoubtedly phosphorus pentachloride. For the first time, the reaction of phosphorus pentachloride with methylene compounds was described in the nineteenth century.

Subsequently, various derivatives of styrenes, dienes, unsymmetrical ethylenes and acetylenes, ethers and esters of enols, as well as enamides were subjected to phosphorylation with phosphorus pentachloride. Most of these reactions were carried out at room temperature [10–12].

Continuing research in this direction, we attempted to synthesize for the first time a new organophosphorus compounds based on acylated derivatives of glycoluril. 2,4,6,8-Tetraacetyl-2,4,6,8-tetraazabicyclo[3,3,0]octane-3,7-dione was chosen as an object in the phosphorylation reaction 1. The use of unsubstituted glycoluril in the reaction of direct phosphorylation by the action of phosphorus trichloride or pentachloride is not possible due to the absence of active centers for phosphorylation.

The reaction proceeds on heating for 48 hours in an argon atmosphere in a dry chloroform medium, in the ratio 1:6. The reaction resulted in diphosphonic complex tetraacetyl glycoluril — dihexachlorophos-

phorate 2,6-di-(4,8-diacetyl-2,4,6,8-tetraazabicyclo[3.3.0]octane-3,7-dione) — 2,6-di(chloroethenyltrichlorophosphonium) 2 according to the following scheme:

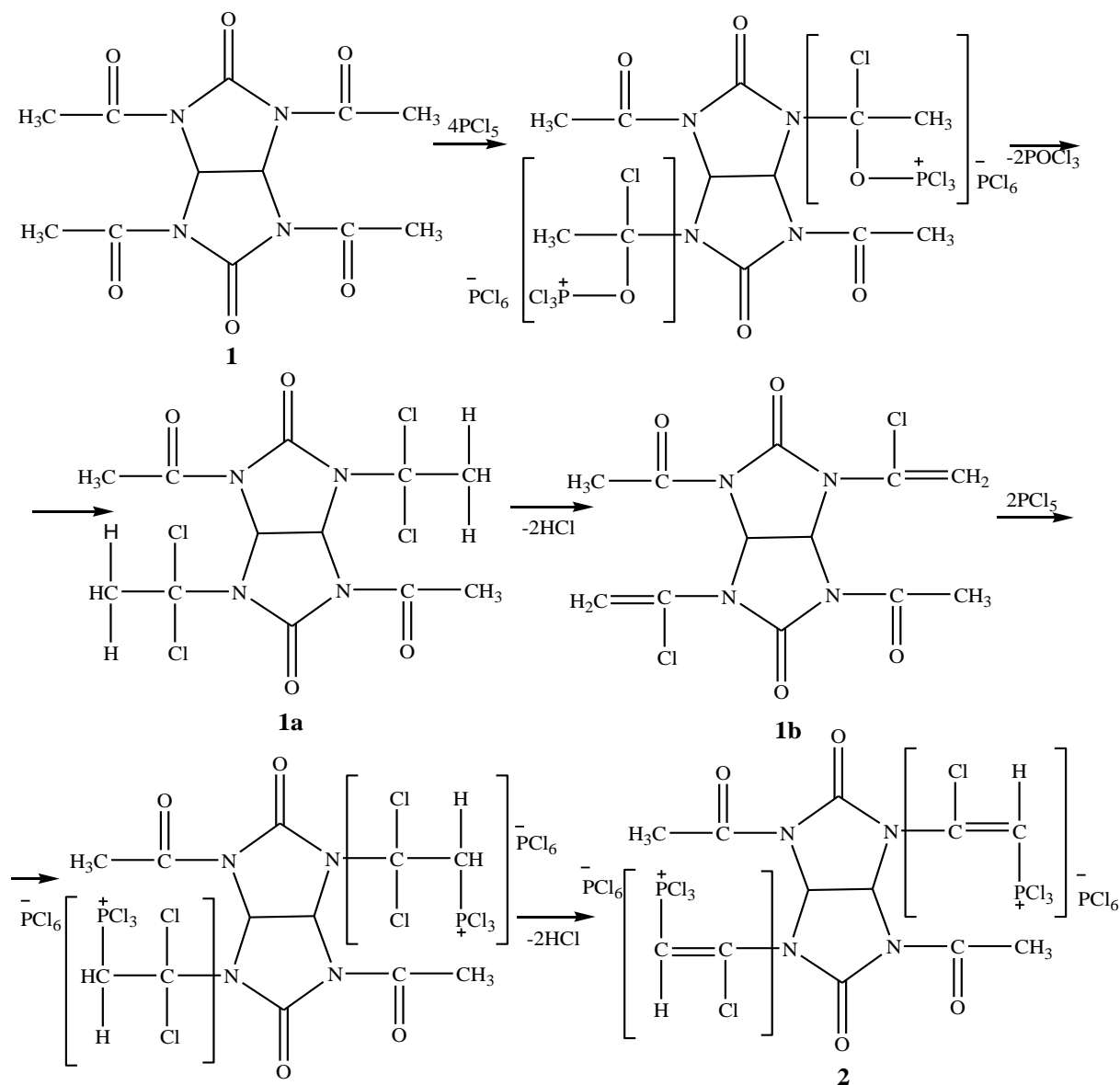


Figure 1. Phosphorylation of 2,4,6,8-tetraacetyl-2,4,6,8-tetraazabicyclo[3,3,0]octane-3,7-dione

The product is a white crystalline substance unstable in air.

Obviously, the reaction proceeds through the stage of phosphorus pentachloride addition to the oxygen atom of the acetyl group, and the resulting adduct gradually decomposes to intermediate 1a, which is dehydrochlorinated under the reaction conditions to unsaturated chlorine derivative 1b. Further, product 1b is phosphorylated with phosphorus pentachloride forming the final product 2.

The structure of compound 2 was proved by spectral data. In particular the ³¹P NMR spectrum contains signals 2.67 (PCl₃⁺) and -97.03 (PCl₆⁻). Structure 2 shows that phosphorylation of 1 proceeds with the participation of two acetyl groups. The decomposition of the diphosphonic complex 2 was carried out using benzaldehyde and proceeds according to the following scheme:

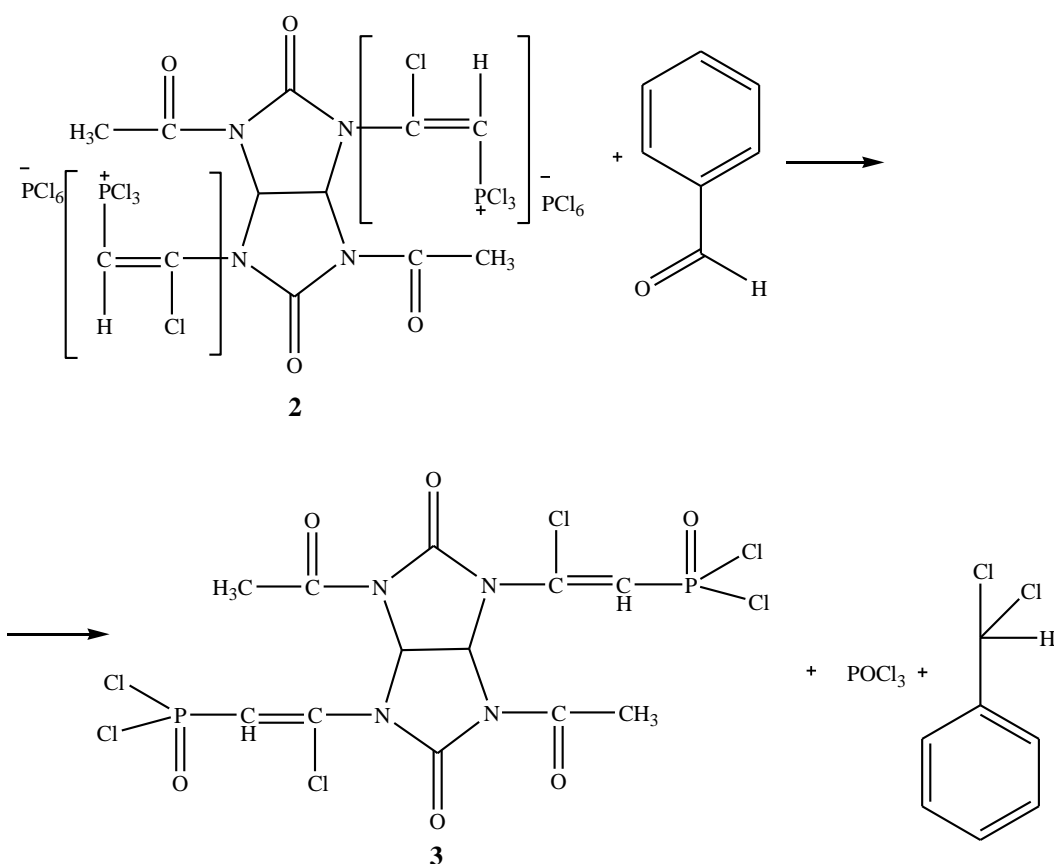


Figure 2. Decomposition of the diphosphonic complex with benzaldehyde

The structure of compound 3 was proved by spectral data. The ^1H NMR spectrum contains a signal of 2.46 ppm corresponding to the presence of six protons of two CH_3CO groups, a multiplet signal in the region of 3.71–3.79 ppm, corresponding to signals of two protons of $\text{C}=\text{CH}$ groups, and a singlet in the region of 5.70 ppm., which characterizes the signal of protons of CHCH groups; in the ^{31}P NMR spectrum there is a signal of 5.29 ppm corresponding to the vibrations of the phosphorus atom.

Conclusion

The corresponding acylated derivatives of the bicyclic bisureas class i.e. glycoluril have been obtained according to the reaction of phosphorylation with phosphorus pentachloride for the first time. It was shown the reaction proceeds on heating for 48 hours in the argon and in dry chloroform with a sixfold excess of PCl_5 . The reaction leads to the formation of diphosphonic complex of tetraacetyl-glycoluril – dihexachlorophosphate 2,6-di-(4,8-diacetyl-2,4,6,8-tetraazabicyclo[3.3.0]octane-3,7-dione)-2,6-di-(chloroethynyltrichlorophosphonium). This compound is a white crystalline substance unstable in air, the decomposition of which under the action of benzaldehyde leads to the corresponding 2,6-di-(2-chloroethynyl)-4,8-diacetyl-2,4,6,8-tetraazabicyclo[3.3.0]octane-3,7-dione diphosphonic acid.

References

- 1 Bakibaev A.A. Synthetic anticonvulsants, antihypoxics, and inducers of the liver monooxygenase system based on amides and ureas. XVI. Studies of the antihypoxic properties of bicyclic bis-ureas / A.A. Bakibaev, V.K. Gorshkova, A.Yu. Yagovkin // *Pharm. Chem. J.* — 1994. — No. 8. — P. 547. <https://doi.org/10.1007/BF02219026>
- 2 Salkeeva L.K. Effect of Glycoluril and Its Derivatives on the Flame Resistance and Physicomechanical Properties of Rubber / L.K. Salkeeva, A.A. Bakibaev, G.T. Khasanova // *Russian Journal of Applied Chemistry.* — 2016. — Vol. 89, No. 1. — P. 132–139.
- 3 Grillon E. Isolation and X-ray structure of the intermediate dihydroxyimidazolidine (DHI) in the synthesis of glycoluril from glyoxal and urea / E. Grillon, R. Gallo, M. Pierrot, J. Boileau // *Tetrahedron Lett.* — 1988. — Vol. 29, No. 9. — P. 1015–1016. [https://doi.org/10.1016/0040-4039\(88\)85322-X](https://doi.org/10.1016/0040-4039(88)85322-X)

- 4 Jarvo E.R. Amino acids and peptides as asymmetric organocatalysts / E.R. Jarvo, S.J. Miller // *Tetrahedron Lett.* — 2002. — № 58. — P. 2481–2495. [https://doi.org/10.1016/S0040-4020\(02\)00122-9](https://doi.org/10.1016/S0040-4020(02)00122-9)
- 5 Christoffers J. Enantioselective Construction of Quaternary Stereocenters / J. Christoffers, A. Mann // *Chem. Int. Ed.* — 2001. — No. 40. — P. 4591–4597.
- 6 Krause N. Recent advances in catalytic enantioselective Michael additions / N. Krause, A. Hoffmann-Roder // *Synthesis.* — 2001. — P. 171–196.
- 7 Sibi M.P. Enantioselective conjugate additions / M.P. Sibi, S. Manyem // *Tetrahedron.* — 2000. — No. 56. — P. 8033–8061. [https://doi.org/10.1016/S0040-4020\(00\)00618-9](https://doi.org/10.1016/S0040-4020(00)00618-9)
- 8 Leonard J. Control of Asymmetry Through Conjugate Addition Reactions / J. Leonard, E. Diez-Barra, S. Merino // *Eur. J. Org. Chem.* — 1998. — P. 2051–2061.
- 9 Бакибаев А.А. Тетраацетилгликолурил и некоторые его производные: синтез, свойства и применение / А.А. Бакибаев, Н.Ф. Хоанг, В.С. Мальков, С.И. Горбин, С.Ю. Паньшина // *Изв. высш. учеб. зав.* — 2019. — Т. 62, No. 9. — С. 4–19. <https://doi.org/10.6060/ivkkt.20196209.5924>
- 10 Salkeeva L.K. New Phosphorylated Glycoluril Derivatives / L.K. Salkeeva, E.K. Taishibekova, A.A. Bakibaev, E.V. Minaeva, L.M. Sugralina, A.K. Salkeeva et al. // *Russ. J. Gen. Chem.* — 2017. — Vol. 87, No. 3. — P. 442. <https://doi.org/10.1134/S1070363217030124>
- 11 Пудовик А.Н. Реакции галоидангидридов кислот фосфора с непредельными соединениями / А.Н. Пудовик, В.К. Хайруллин // *Успехи химии.* — 1968. — Т. 37. — С. 745–777. <https://doi.org/10.1070/RC1968v037n05ABEH001638>
- 12 Промоненков В.К. Способы получения и свойства соединений с непредельными радикалами при атоме фосфора / В.К. Промоненков, С.З. Ивин // *Успехи химии.* — 1968. — Т. 37. — С. 1577–1599. <https://doi.org/10.1070/RC1968v037n09ABEH001699>
- 13 Kosolapoff G.M. Addition Reactions in Phospho-organic Syntheses. I. The Addition of Phosphorus Pentachloride to Olefins / G.M. Kosolapoff, W.F. Huber // *J. Am. Chem. Soc.* — 1946. — Vol. 68. — P. 2540–2541. <https://doi.org/10.1021/ja01216a034>

Л.К. Сэлкеева, А.А. Мұратбекова, Е.В. Минаева, П. Войтичек,
Е.К. Тайшыбекова, А.Р. Достанова, А.Б. Тәтеева, А.К. Сэлкеева

Гликолурил туындыларын фосфордың пентахлоридімен фосфорлау

Мақалада бесвалентті фосфор негізінде алынған гликолурилдің жаңа фосфорорганикалық туындыларын алу және олардың құрамын зерттеу бойынша жасалған ғылыми жұмыстың нәтижелері келтірілген. Тиімді реакция орталықтарының болуы себебінен өте жоғары қызығушылық тудыратын N-ацил алмасқан гликолурил негізінде синтезделген фосфордың жаңа элементорганикалық туындылары алынған. Алғашқы синтон ретінде тетраацетил алмасқан гликолурил — 2,4,6,8-тетраацетил-2,4,6,8-тетраазабицикло[3,3,0]октан-3,7-дион алынды, себебі, үш немесе бесхлорлы фосфор әсерімен тікелей реакциясында алмаспаған гликолурилді қолдану фосфорлаудың белсенді орталықтары болмағандықтан мүмкін болмайды. Эксперимент нәтижесінде реакция өте ұзақ, 48 сағаттан аз емес уақыт аралығында, аргон атмосферасында алғашқы гликолурилдің ацил туындысы мен бесхлорлы фосфордың 1:6 қатынасында қыздыру арқылы іске асатыны көрсетілді. Реакция нәтижесінде ауада тұрақсыз, ақ кристалды зат болатын тетраацетилгликолурилдің — дигексахлорофосфат 2,6-ди-(4,8-диацетил-2,4,6,8-тетраазабицикло[3.3.0]октан-3,7-дион)-2,6-ди(хлорэте-нилтрихлорфосфония) дифосфоноды комплексі алынды. Дифосфоноды комплекстің ыдырауы бензальдегидті пайдалана отырып және ауада тұрақсыз болатын, бөлме температурасында тез ыдырайтын, сәйкес дихлорфосфатты туындының түзілуімен жүреді.

Кілт сөздер: гликолурил, бисмочевина, фосфорпентахлориді, фосфорлау, N-ацилдеу, фосфор, бициклді, синтез.

Л.К. Салькеева, А.А. Муратбекова, Е.В. Минаева, П. Войтичек,
Е.К. Тайшыбекова, А.Р. Достанова, А.Б. Татеева, А.К. Салькеева

Фосфорилирование производных гликолурила пентахлоридом фосфора

В статье представлены результаты научных исследований по синтезу и исследованию строения новых фосфорорганических производных гликолурила, полученных на основе пятивалентного фосфора. Синтезированы новые элементоорганические производные фосфора на основе N-ацилзамещенных гликолурилов, представляющих значительный интерес благодаря наличию эффективных реакционных центров. В качестве исходного синтона был выбран тетраацетилзамещенный гликолурил — 2,4,6,8-тетраацетил-2,4,6,8-тетраазабицикло[3,3,0]октан-3,7-дион, так как использование незамещенного гликолурила в реакции прямого фосфорилирования действием трех- или пятихлористого фосфора не представляется возможным из-за отсутствия активных центров фосфорилирования. Экспериментально было показано, что реакция протекает при длительном нагревании в течение не менее 48 ч

в атмосфере аргона исходного ацилпроизводного гликолурила и пятихлористого фосфора в соотношении 1:6 и приводит к образованию дифосфонового комплекса тетраацетилгликолурила — дигексахлорофосфат 2,6-ди-(4,8-диацетил-2,4,6,8-тетраазабицикло[3.3.0]октан-3,7-дион)-2,6-ди(хлорэтилтрихлорфосфония), представляющего собой неустойчивое на воздухе белое кристаллическое вещество. Разложение дифосфонового комплекса было проведено с использованием бензальдегида и протекало с образованием соответствующего дихлорфосфатного производного, так же неустойчивого на воздухе и быстро разлагающегося при комнатной температуре.

Ключевые слова: гликолурил, бисмочевина, пентахлорид фосфора, фосфорилирование, N-ацилирование, фосфор, бициклические, синтез.

References

- 1 Bakibaev, A.A., Gorshkova, V.K., & Yagovkin, A.Yu. (1994). Synthetic anticonvulsants, antihypoxics, and inducers of the liver monoxygenase system based on amides and ureas. XVI. Studies of the antihypoxic properties of bicyclic bis-ureas. *Pharm. Chem. J.*, 8, 547. <https://doi.org/10.1007/BF02219026>
- 2 Salkeeva, L.K., Bakibaev, A.A., & Khasenova, G.T. (2016). Effect of Glycoluril and Its Derivatives on the Flame Resistance and Physicomechanical Properties of Rubber. *Russian Journal of Applied Chemistry*, 89, 1, 132–139.
- 3 Grillon, E., Gallo, R., Pierrot, M., & Boileau, J. (1988). Isolation and X-ray structure of the intermediate dihydroxyimidazolidine(DHI) in the synthesis of glycoluril from glyoxal and urea. *Tetrahedron Lett.*, 29, 9, 1015–1016. [https://doi.org/10.1016/0040-4039\(88\)85322-X](https://doi.org/10.1016/0040-4039(88)85322-X)
- 4 Jarvo, E. R., & Miller, S.J. (2002). Amino acids and peptides as asymmetric organocatalysts. *Tetrahedron Lett.*, 58, 2481–2495. DOI: 10.1016/S0040-4020(02)00122-9
- 5 Christoffers, J., & Mann, A. (2001). Enantioselective Construction of Quaternary Stereocenters. *Chem. Int. Ed.*, 40, 4591–4597. [https://doi.org/10.1002/1521-3773\(20011217\)40:24<4591:aid-anie4591>3.0.co;2-v](https://doi.org/10.1002/1521-3773(20011217)40:24<4591:aid-anie4591>3.0.co;2-v)
- 6 Krause, N., & Hoffmann-Roder, A. (2001). Recent advances in catalytic enantioselective Michael additions. *Synthesis*, 171–196.
- 7 Sibi, M.P., & Manyem, S. (2000). Enantioselective conjugate additions. *Tetrahedron Lett.*, 56, 8033–8061. [https://doi.org/10.1016/S0040-4020\(00\)00618-9](https://doi.org/10.1016/S0040-4020(00)00618-9)
- 8 Leonard, J., Diez-Barra, E., & Merino, S. (1998). Control of Asymmetry Through Conjugate Addition Reactions. *Eur. J. Org. Chem.*, 2051–2061.
- 9 Bakibaev, A.A., Hoang, N.P., Malkov, V.S., Gorbin, S.I., & Panshina, S.Yu. (2019). Tetraacetilhlkoluril i nekotorye eho proizvodnye: sintez, svoystva i primeneniye [Tetraacetyl glycoluril and its derivatives: synthesis, properties and application]. *Izvestiya vysshikh uchebnykh zavedenii — Russian journal of chemistry and chemical technology*, 62, 9, 4–19. <https://doi.org/10.6060/ivkkt.20196209.5924> [in Russian].
- 10 Salkeeva, L.K., Taishibekova, E.K., Bakibaev, A.A., Minaeva, E.V., Sugralina, L.M., & Salkeeva, A.K. et al. (2017). New Phosphorylated Glycoluril Derivatives. *Russ. J. Gen. Chem.*, 87, 3, 442. <https://doi.org/10.1134/S1070363217030124>
- 11 Pudovik, A.N., & Khairullin, V.K. (1968). Reaktsii haloidanhidridov kislot fosfora s nepredelnymi soedineniyami [Reactions of phosphorus acid halides with unsaturated compounds]. *Uspekhi khimii — Advances in chemistry*, 37, 745–777. <https://doi.org/10.1070/RC1968v037n05ABEH001638> [in Russian].
- 12 Promonenkov, V.K., & Ivin, S.Z. (1968). Sposoby polucheniia i svoystva soedinenii s nepredelnymi radikalami pri atome fosfora [Production methods and properties of compounds with unsaturated radicals at the phosphorus atom]. *Uspekhi khimii — Advances in chemistry*, 37, 1577–1599 [in Russian]. <https://doi.org/10.1070/RC1968v037n09ABEH001699>
- 13 Kosolapoff, G. M., & Huber, W.F. (1946). Addition Reactions in Phospho-organic Syntheses. The Addition of Phosphorus Pentachloride to Olefins. *J. Am. Chem. Soc.*, 68, 2540–2541. <https://doi.org/10.1021/ja01216a034>

Information about authors:

Salkeeva, Lyazat Karishovna — Doctor of Chemical Sciences, Professor of the Organic Chemistry and Polymers Department, Karagandy University of the name of Academician E.A. Buketov, Kazakhstan, Karagandy, 100024, Universitetskaya str., 28. E-mail: lsalkeeva@mail.ru; <https://orcid.org/0000-0003-4207-916X>

Muratbekova, Aigul Akizhanovna — Candidate of Chemical Sciences, Associate Professor of the Chemical Technology and Petrochemistry Department, Karagandy University of the name of Academician E.A. Buketov, Kazakhstan, Karagandy, 100024, Universitetskaya str., 28. E-mail: aigulmuratbekova@mail.ru; <https://orcid.org/0000-0002-2156-9306>

Minayeva, Yelena Viktorovna — Candidate of Chemical Sciences, Associate Professor of the Organic Chemistry and Polymers Department, Karagandy University of the name of Academician E.A. Buketov, Kazakhstan, Karagandy, 100024, Universitetskaya str., 28. E-mail: yelenaminayeva@yandex.ru; <https://orcid.org/0000-0001-9382-5965>

Vojtíšek, Pavel — Associate Professor RNDr., CSc. Charles University of Prague, Czech Republic, Prague, 400 96, Pasteurova 1. E-mail: pavojt@natur.cuni.cz; <https://orcid.org/0000-0002-4685-9238>

Tateeva, Alma Baymaganbetovna — Candidate of Chemical Sciences, Associate Professor of the Chemical Technology and Petrochemistry Department, Karagandy University of the name of Academician E.A. Buketov, Kazakhstan, Karagandy, 100024, Universitetskaya str., 28. E-mail: almatateeva@mail.ru; <https://orcid.org/0000-0002-4538-9457>

Salkeeva, Ayzhan Karishovna — Associate Professor of the Physics Department, Karagandy Polytechnic University, Kazakhstan, Karagandy, 100027, Nursultana Nazarbaeva str., 56. E-mail: asalkeeva58@mail.ru; <https://orcid.org/0000-0002-2277-7959>

Tayshibekova, Ekaterina Karimovna — PhD, Lecturer at the Organic Chemistry and Polymers Department, Karagandy University of the name of Academician E.A. Buketov, Kazakhstan, Karagandy, 100024, Universitetskaya str., 28. E-mail: ekaterina_teishi@mail.ru; <https://orcid.org/0000-0001-5557-9177>

Dostanova, Aida Ruslanovna — 2nd year master's student. Karagandy University of the name of Academician E.A. Buketov, Kazakhstan, Karagandy, 100024, Universitetskaya str., 28. E-mail: Dostanova1997@mail.ru; <https://orcid.org/0000-0002-7460-9682>

A.A. Sinitsyna*, S.G. Il'yasov

*Institute for Problems of Chemical and Energetic Technologies,
Siberian Branch of the Russian Academy of Sciences (IPCET SB RAS), Biysk, Russia
(*Corresponding author's e-mail: nastya.sinitsyna.1994@mail.ru)*

Synthesis of alkyl derivatives of 3,7,10-trioxo-2,4,6,8,9,11-hexaaza[3.3.3]propellane and evaluation of their biological activity

Today 3,7,10-trioxo-2,4,6,8,9,11-hexaaza[3.3.3]propellane (THAP) has not yet received widespread research attention due to the complexity of the synthesis. This work is devoted to the development of a method for the THAP derivatives synthesis, as well as to the study of their biological activity in comparison with alkyl-substituted glycolurils (subject of comparison). THAP was *N*-alkylated to furnish novel hexaalkyl derivatives of THAP with methyl, ethyl and propyl substituents. The conditions for obtaining the maximum yield of the target product were optimized on the base of methyl derivative. The reaction proceeded in DMSO/KOH at 75–80 °C for 13 hours in a moderate yield of 56 %. The ethyl and propyl derivatives of THAP were synthesized under the same conditions. The biological activity of the obtained THAP alkyl derivatives and glycoluril alkyl derivatives was evaluated against *Sporosarcina ureae*, *Bacillus pumilus*, *Salmonella typhimurium* and *Staphylococcus aureus* bacteria and influenza A virus. All the samples were found to exhibit antibacterial activity against *Staphylococcus aureus*. It was shown that 2,4,6,8,9,11-hexapropyl-THAP, di-*tert*-butyl-diphenyl-, di-*tert*-butyl-dibenzyl-, di-*tert*-butyl-dimethyl- and di-isopropyl-dibenzylglycoluril, have exhibited also toxicity to living cells besides antiviral activity.

Keywords: propellane, azapropellane, THAP, glycoluril, *N*-alkylation, biological activity, influenza virus, *Sporosarcina ureae*, *Bacillus pumilus*, *Salmonella typhimurium*, *Staphylococcus aureus*

Introduction

Propellanes are molecules with a central single (ethane) bond and three bridged rings (carbon or heteroatomic) [1]. They are found in natural resources [2–3] and are widely applied in polymeric materials, medicines, pesticides and so on [4–6]. Zalkow et al. [7] were the first to isolate sesquiterpene modephene from the poisonous plant *Isocoma Wrightii* in 1978. It was the first compound with a [3.3.3]propellane skeleton discovered in natural products [3.3.3]. Due to their structure, modephene and its derivatives exhibit a variety of biological activity [8, 9] and its toxicity can passivate certain biological enzymes and selectively inhibit anti-proliferation of some cancer cells. Thus, propellanes have been in focus of many chemists and biologists over a few last decades.

Among propellanes, heterocyclic compounds, especially those with nitrogen atoms (azapropellanes), are of considerable interest, since they can be easily be functionalized.

Research on the synthesis of azapropellanes was carried out by Ashkenazi et al. [10]. Shin and co-workers managed to have synthesized propellane bearing five nitrogen atoms through the glycoluril derivative in three stages in 2014 [11].

Lee, Zhang and co-workers developed a synthetic method for 3,7,10-trioxo-2,4,6,8,9,11-hexaaza[3.3.3]propellane (Fig. 1) [12–13].

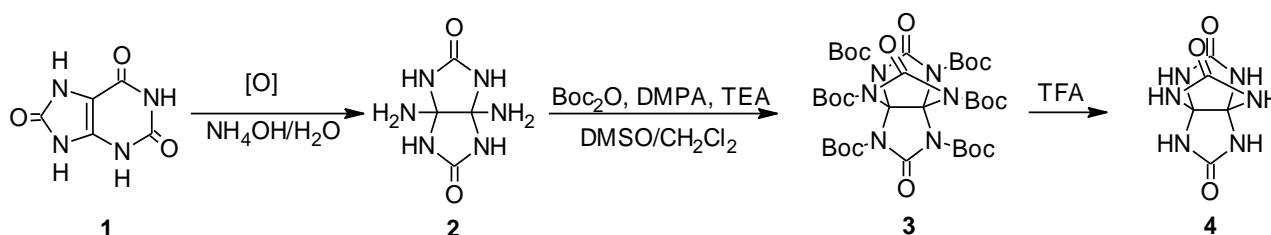


Figure 1. A synthetic protocol for 3,7,10-trioxo-2,4,6,8,9,11-hexaaza[3.3.3]propellane

Evaluation of biological activity

To determine the antibacterial activity, two-fold dilution of experimental preparations (volume 100 μ l) was made in the cells of a 96-well culture plate with a U-shaped bottom on MPB medium (mesopotamia broth). 100 μ l of an overnight culture diluted to a concentration of 10⁶ cells/ml was added to each well. Incubation took place at 37 °C for 40 hours. Determination of optical density in relation to control (growth of bacterial culture without preparation) was performed.

To examine the antiviral activity *in vitro*, two methods were used:

- 1) the inhibition of the virus-induced cytopathic effect was determined visually under a microscope [17];
- 2) by changing the absorption of the vital dye by cells — neutral red [17, 18].

For this purpose, a 96-well plate was seeded with a MDCK (dog, kidney, cell monolayer) cell line, with a seed dose of 2×10^4 cell per well. After 90 % of the monolayer was formed (20-h incubation at 37 °C under 5 % CO₂), the influenza A/California/ 07/09 (H1N1pdm09) virus strain was inserted at a dose of 100 TCID₅₀ per well. This dose is equivalent to the multiplicity of infection at 0.001 of infection particles per cell. 30 minutes after infection, the test sample contained in the culture medium was placed in the wells and incubated at 37 °C under 5 % CO₂ for 72 h. After that, neutral red (0.34 % final concentration) was added into each well, the cells were washed in 1.5 h, and a solution (0.1 M NH₄H₂PO₄ and 96 % ethanol in equal volumes) was added for the stain extraction, and the optical density of the liberated stain was measured at a wavelength of 490 nm. The antiviral activity of the compound was estimated as a dose (concentration) of the test drug, which 50 % inhibits the viral reproduction or IC₅₀. Although IC₅₀ was estimated by the two methods (determination of virus-induced cytopathic effect and incubation with neutral red), here we presented data obtained only with neutral red as more objective.

To assess the toxicity of the compounds, the 96-well plate was seeded with a MDCK cell culture with a seed dose of 2×10^4 cells per well. After a 20-hour incubation at 37 °C in an atmosphere of 5 % CO₂, the compounds dissolved in a MEM medium (Gibco) containing 5 % fetal bovine serum were introduced. Three days after incubation, the inhibition percentage of cell proliferation was evaluated using neutral red, as described above. The toxicity of the compounds was estimated as a dose (concentration) of the test drug at which 50 % cells are died (CD₅₀).

The therapeutic index or index of selectivity (IS) was determined as the ratio of CD₅₀ to IC₅₀.

*Results and Discussion**Synthesis of alkyl derivatives of 3,7,10-trioxo-2,4,6,8,9,11-hexaaza[3.3.3]propellane*

It would be logical to apply the glycoluril alkylation methods to THAP since it molecule is characterized by the presence of three imidazolidinone rings and has a structure similar to glycoluril. We have earlier developed a synthetic method for tetrasubstituted glycolurils with mono- and heterofunctional substituents in an acetonitrile/KOH medium [14, 15]. The method incorporates the alkyl groups into the partially substituted glycoluril and uses a low-boiling solvent to simplify the isolation of reaction products.

The alkylation reaction of 3,7,10-trioxo-2,4,6,8,9,11-hexaaza[3.3.3]propellane was carried out under conditions similar to the alkylation of glycoluril. In this case, the yield of hexaaryl derivatives of THAP was found low and reached only 6–8 % in acetonitrile medium.

That is why we investigated the effects of different solvents (DMSO, DMF, ethanol, 1,4-dioxane and methylene chloride), reaction temperature and bases on the target product yield by an example of the **5c** synthesis (Table 1).

Table 1

Selection of synthesis conditions for 2,4,6,8,9,11-hexamethyl-2,4,6,8,9,11-hexaaza[3.3.3]propellane 5c

Exp.	Solvent	Base	Reaction temperature, °C	Yield, %	Exp.	Solvent	Base	Reaction temperature, °C	Yield, %
1	DMSO	KOH	80	24	6	DMSO	K ₂ CO ₃	80	–
2	DMF	KOH	80	11	7	DMF	K ₂ CO ₃	80	–
3	Ethanol	KOH	70	–	8	Ethanol	K ₂ CO ₃	70	–
4	1,4-Dioxane	KOH	80	–	9	1,4-Dioxane	K ₂ CO ₃	80	–
5	Methylene chloride	KOH	40	–	10	Methylene chloride	K ₂ CO ₃	40	–

Note. «→» THAP was quantitatively isolated back; no reaction has occurred.

As can be seen from Table 1, the N-alkylation reaction took place only at 80 °C and only in the two solvents such as DMSO and DMF. It is also evident that the yield of the target product **5c** in DMSO is almost 2 times more than that in DMF. The superbasic medium DMSO / KOH was selected for further research based on these preliminary results (Table 1). The results of the THAP alkylation with methyl iodide in the superbasic medium as a function of the reaction temperature and time are given in Figure 3.

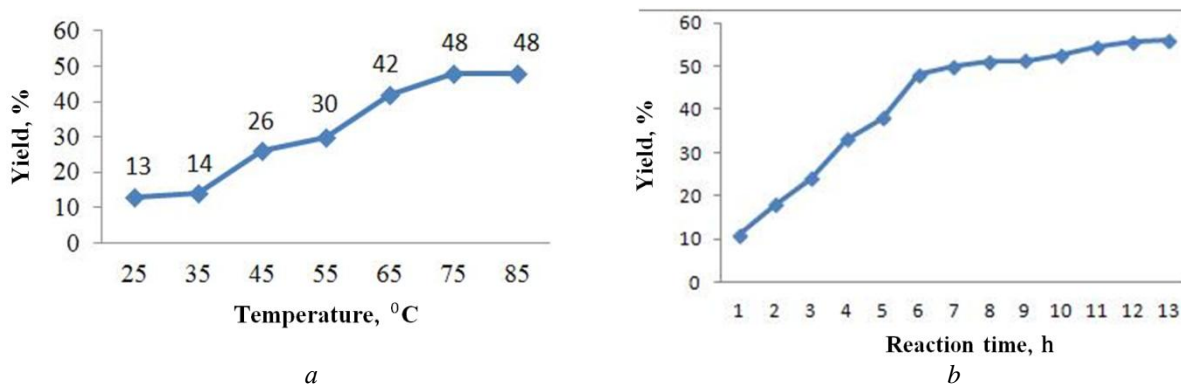


Figure 3. Dependence of the **5c** yield: (a) on the reaction temperature (reaction time 6 hours) and (b) on the reaction time (temperature 75 °C)

Figure 3a shows that an increase in the reaction temperature from 25 °C to 85 °C led to a smooth raising in the content of product **5c** from 12 % to 48 %. An increase of the alkylation time from 6 to 8 hours (3b) showed a slight growing in the yield of product **5c** to 51 %. When the reaction time was extended to 13 h, the yield of product **5c** got higher insignificantly and was 56 %. The slowdown in the formation of reaction product **5c** in 13 hours can be explained by the emerging of competing reactions due to the prolonged residence of the reagents in the superbasic medium at high temperature.

We sequentially have obtained THAP hexa-derivatives with methyl (**5c**), ethyl (**5d**) and propyl (**5e**) substituents (Fig. 4).

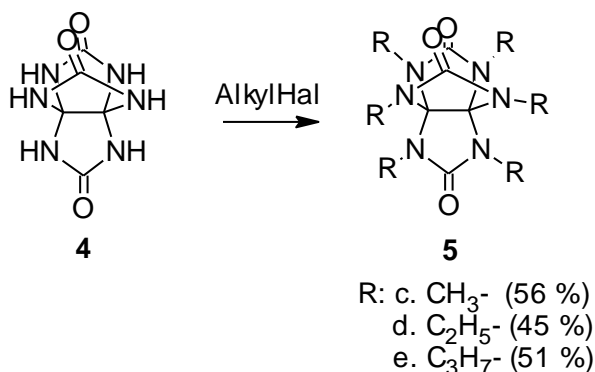


Figure 4. Synthesis of alkyl derivatives of 3,7,10-trioxo-2,4,6,8,9,11-hexaaza[3.3.3]propellane

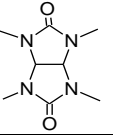
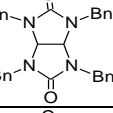
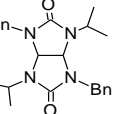
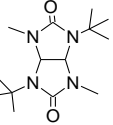
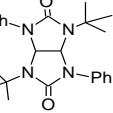
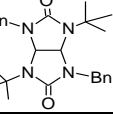
An attempted of isopropyl and *tert*-butyl groups incorporation into THAP did not lead to the expected result. This is probably due to the steric factor of the radicals.

Biological activity

The tetrasubstituted glycolurils synthesized previously [14, 15] and the new THAP derivatives were evaluated *in vitro* against some bacteria (*Sporosarcina ureae*, *Bacillus pumilus*, *Salmonella typhimurium* and *Staphylococcus aureus*) and influenza A virus. Tables 2 and 3 summarize the biological activity evaluation results.

Table 2

Evaluation of antibacterial activity of the THAP hexaaza- derivatives and tetrasubstituted glycolurils

Compound	<i>Sporosarcina ureae</i>	<i>Bacillus pumilus</i>	<i>Salmonella typhimurium</i>	<i>Staphylococcus aureus</i>
5c	$1,3 \cdot 10^{-2}$	$2,6 \cdot 10^{-2}$	$1,3 \cdot 10^{-2}$	$1,3 \cdot 10^{-2}$
5d	$4,2 \cdot 10^{-3}$	$8,4 \cdot 10^{-3}$	$4,2 \cdot 10^{-3}$	$4,2 \cdot 10^{-3}$
5e	$5,9 \cdot 10^{-3}$	no	no	$2,9 \cdot 10^{-3}$
6a	 $4,6 \cdot 10^{-2}$	$9,2 \cdot 10^{-2}$	$9,2 \cdot 10^{-2}$	$4,6 \cdot 10^{-2}$
6b	 $2,0 \cdot 10^{-3}$	no	no	$8,0 \cdot 10^{-3}$
6c	 $1,2 \cdot 10^{-3}$	no	$9,8 \cdot 10^{-3}$	$4,6 \cdot 10^{-3}$
6d	 $1,8 \cdot 10^{-2}$	$1,8 \cdot 10^{-2}$	$1,8 \cdot 10^{-2}$	$8,8 \cdot 10^{-3}$
6e	 $4,2 \cdot 10^{-3}$	no	no	$4,2 \cdot 10^{-3}$
6f	 no	no	no	$7,0 \cdot 10^{-3}$

Sporosarcina ureae are spore-forming bacteria and ammonifying microorganisms that decompose urea. They are used in agriculture for nitrogen enrichment of the soil. *Bacillus pumilus* are phytopathogenic bacteria affecting agricultural crops (flax, pumpkin, corn, beet, oranges, apricots, marrow-type pumpkin, etc.) and thus cause significant economic damage to agricultural and processing companies. *Salmonella typhimurium* is a salmonellosis causal agent. *Staphylococcus aureus* (opportunistic pathogenic bacterium) initiates skin diseases (furuncles), respiratory diseases (angina, pneumonia), nervous system and sensory organ diseases (otitis media, conjunctivitis, cerebral fever), digestive system diseases (stomatitis, acute food poisoning) and etc.

All the test samples were found to inhibit the growth of *Staphylococcus aureus* at low concentrations. In contrast, suppression of the reproduction of *Sporosarcina ureae* is an undesirable effect as they are used in agriculture.

Table 3

Evaluation of antiviral activity of the THAP hexaaza derivatives and tetrasubstituted glycolurils

Sample	CD ₅₀ toxicity (the lowest dilution at which 50 % cells survive)	IC ₅₀ antiviral activity (the highest dilution which protects 50 % cells from virus)	Therapeutic index IS (ratio of toxic dose to the efficient)
5c	$6.6 \cdot 10^{-3}$	no	no
5d	$2.1 \cdot 10^{-3}$	no	no
5e	$3.7 \cdot 10^{-4}$	$2.9 \cdot 10^{-4}$	1.28
6a	$5.7 \cdot 10^{-3}$	no	no
6b	$5.0 \cdot 10^{-4}$	no	no
6c	$5.8 \cdot 10^{-4}$	$4.6 \cdot 10^{-4}$	1.26
6d	$4.4 \cdot 10^{-3}$	$2.8 \cdot 10^{-3}$	1.57
6e	$2.1 \cdot 10^{-3}$	$1.7 \cdot 10^{-3}$	1.24
6f	$3.5 \cdot 10^{-3}$	$2.8 \cdot 10^{-3}$	1.25

As can be seen from Table 3, only **5e** propyl derivative of THAP exhibited an antiviral activity, while the methyl and ethyl derivatives did not. It was found that compound **5e** at a concentration of $2.9 \cdot 10^{-4}$ g/ml is able to protect 50 % of cells from influenza virus. Tetrasubstituted glycolurils **6c-e** were also active at low concentrations. Further studies of the antiviral activity of these compounds were unreasonable because they had a high toxicity and a low therapeutic index. Samples **6a** and **6b** did not exert the antiviral activity. Note that sample **6a** has found its application as a day-time sedative and is marketed as Mebicar [16]. Therefore, the biological activity of the resultant hexaalkyl derivatives of THAP should be further examined.

Conclusions

New hexaalkyl derivatives of THAP with methyl, ethyl and propyl substituents were synthesized. The conditions for the maximum product yield were selected using the example of a methyl derivative: the reaction proceeded in DMSO/KOH at 85 °C for 13 hours with a 56 % yield. The biological activity of the obtained compounds and of earlier synthesized model compounds (tetrasubstituted glycolurils) against influenza A virus was evaluated. The biological activity against the *Staphylococcus aureus* bacterium was exhibited by all of the test compounds, while the antiviral activity was exhibited by 2,4,6,8,9,11-hexapropyl-THAP, di-*tert*-butyl-dibenzyl-, di-*tert*-butyl-diphenyl-, di-*tert*-butyl-dimethyl- and di-isopropyl-dibenzylglycoluril. However, these compounds proved to be toxic to living cells.

This work was performed using instruments provided by the Biysk Regional Center for Shared Use of Scientific Equipment of the SB RAS (IPCET SB RAS, Biysk). The reported study was funded by RFBR, project number 19-33-90060.

References

- 1 Aizawa N. Instant low-temperature cross-linking of poly(N-vinylcarbazole) for solution-processed multilayer blue phosphorescent organic light-emitting devices / N. Aizawa, Y.-J. Pu, T. Chiba, // *J. Adv. Mater.* — 2014. — Vol. 26. — P. 7543–7546.
- 2 Schmidt A.W. Occurrence, biogenesis, and synthesis of biologically active carbazole alkaloids / A.W. Schmidt, K.R. Reddy, H.-J. Knölker // *J. Chem. Rev.* — 2012. — Vol. 112. — P. 3193–3328.
- 3 Kotha S. Synthesis of propellanes containing a bicyclo[2.2.2]octene unit, via, the Diels-Alder reaction and ring-closing metathesis as key steps / S. Kotha, S. Pulletikurti // *J. RSC Advances.* — 2018. — Vol. 8, No. 27. — P. 14906–14915.
- 4 Huisgen R. Synthese von heterocyclen mit 1,4-dipolaren cycloadditionen // *J. Zeit. Chem.* — 2015. — Vol. 8, No. 8. — P. 290–298.
- 5 Naoki O. Synthesis and properties of tribenzocarbazoles via an acid-promoted retro (2+2)-cycloaddition of azapropellanes / O. Naoki, Y. Yousuke, T. Hiroshi // *J. Org. Chem.* — 2018. — Vol. 26, No. 8 — P. 7994–8002.
- 6 Torres Gómez H. Synthesis of 3-aza[4.4.3]propellanes with high σ_1 receptor affinity / H. Torres Gómez, C. Daniliuc, D. Schepmann // *J. Bioorg. Med. Chem.* — 2018. — Vol. 26, No. 8. — P. 1705–1712.
- 7 Zalkov L.H. Modhephene: a sesquiterpenoid carbocyclic [3.3.3]propellane. X-Ray crystal structure of the corresponding diol / L.H. Zalkov, R.N. Harris, D.V. Derveer // *J. Chem. Soc. Chem. Commun.* — 1978. — P. 420–421.
- 8 Beyrati M. One-pot, sequential four-component synthesis of novel heterocyclic [3.3.3]propellane derivatives at room temperature / M. Beyrati, A. Hasaninejad, // *J. RSC Adv.* — 2018. — Vol. 8, No. 26. — P. 14171–14176.
- 9 Tian X. Dichrocephones A and B, two cytotoxic sesquiterpenoids with the unique [3.3.3] propellane nucleus skeleton from *Dichrocephala benthamii* / X. Tian, L. Li, Y. Hu // *J. RSC Advances.* — 2013. — Vol. 3, No. 21. — P. 7880–7883.
- 10 Ashkenazi P. Propellanes: XCVIII. Treading of anti, anti[20.3.3]propellane-24,27-diol by sebacic acid / P. Ashkenazi, A.L. Gutman, D. Ginsburg // *Tetrahedron.* — 1988. — Vol. 44. — P. 6875–6880.
- 11 Shin M. Synthesis of novel 2,4,6,8,10-pentaaza[3.3.3]propellane derivatives / Shin, M., M.H. Kim, T. Ha, J. Jeon, K.-H. Chung, J.S. Kim, Y. GyuKim // *Tetrahedron.* — 2014. — Vol. 70, No. 8. — P. 1617–1620.
- 12 Lee B. Synthesis of 2,4,6,8,9,11-hexaaza[3.3.3]propellanes as a new molecular skeleton for explosives / B. Lee, M. Shin, Y. Seo, M.H. Kim, H.R. Lee, J.S. Kim, K.-H. Chung, D. Yoo, Y.G. Kim // *Tetrahedron.* — 2018. — Vol. 74, No. 1 — P. 130–134.
- 13 Zhang J. Synthesis, structure characterizations, and theoretical studies of novel tricyclic multiple(urea) molecules / J. Zhang, Y. Liu, F. Bi, J. Zhou, B. Wang // *Journal of Molecular Structure.* — 2017. — Vol. 1141. — P. 268–275.
- 14 Sinitsyna A.A. A search for synthetic routes to tetrabenzylglycoluril / A.A. Sinitsyna, S.G. Il'yasov, M.V. Chikina, I.V. Eltsov, A.A. Nefedov // *Chemical Papers.* — 2020. — Vol. 74. — P. 1019–1025. <https://doi.org/10.1007/s11696-019-00941-4>
- 15 Sinitsyna A.A. N-alkylation reaction in the synthesis of tetrasubstituted glycolurils / A.A. Sinitsyna, S.G. Il'yasov // *J. Sib. Fed. Univ. Chem.* — 2020. — Vol. 13, No. 1. — P. 40–45. <https://doi.org/10.17516/1998-2836-0164>
- 16 Chegaev K.Yu. New functional glycoluril derivatives / K.Yu. Chegaev, A.N. Kravchenko, O.V. Lebedev, Y.A. Strelenko // *J. Mendeleev Commun.* — 2001. — Vol. 11. — P. 32–33. <https://doi.org/10.1070/mc2001v011n01abeh001357>
- 17 Sidwell R.W. Use of disposable micro tissue culture plates for antiviral and interferon induction studies / R.W. Sidwell, J.H. Huffman // *Appl. Microbiol.* — 1971. — Vol. 22. — P. 797–801.
- 18 Finter N.B. Dye uptake methods for assessing viral cytopathogenicity and their application to interferon assays // *J. Gen. Virol.* — 1969. — Vol. 5. — P. 419–427.

А.А. Сеницына, С.Г. Ильясов

3,7,10-триоксо-2,4,6,8,9,11-гексааза[3.3.3]пропелланның алкил туындыларын синтездеу және олардың биологиялық белсенділігін зерттеу

Жұмыс 3,7,10-триоксо-2,4,6,8,9,11-гексааза[3.3.3]пропелланның алкил туындыларын синтездеу әдісін жасауға және алынған заттардың алкилалмасқан гликолурилдермен (зерттеу объектісі) салыстырғанда биологиялық белсенділігін зерттеуге арналған. Бұл бағыт синтездің күрделілігі себебінен зерттеушілердің назарынан тыс қалған. ТНАР-ты N-алкилдеу әдісі арқылы гексаалкил-туындыларының метилді, этилді және пропилді гексаалкил туындыларымен жаңа қосылыстары синтезделді. Метил туындысы мысалында негізгі өнімнің максималды шығымы болатындай тиімді жағдайлары жасалды. Реакция ДМСО/КОН ортасында 75–80 °С температурада 13 сағат бойы жүреді, реакция шығымы 56 %. ТНАР этилді және пропилді туындылары тура осындай жағдайда синтезделген. ТНАР-тың және гликолурилдың алынған алкилтуындыларының *Sporosarcina ureae*, *Bacillus pumilus*, *Salmonella typhimurium* u *Staphylococcus aureus* бактерияларына және А тұмауының вирусына қатысты биологиялық белсенділігі зерттелген. Барлық үлгілер *Staphylococcus aureus* қарсы бактериалды белсенділік көрсететіні анықталған. 2,4,6,8,9,11-гексапропил-ТНАР, ди-*трет*-бутил-дифенил-, ди-*трет*-бутил-добензил-, ди-*трет*-бутил-диметил-, ди-изопропил-добензилгликолурил қосылыстарының вирусқақарсы белсенділіктен басқа тірі жасушалар үшін уытты болатыны байқалған.

Кілт сөздер: пропеллан, азапропеллан, ТНАР, гликолурил, N-алкилдеу, биологиялық белсенділік, тұмау вирусы, *Sporosarcina ureae*, *Bacillus pumilus*, *Salmonella typhimurium*, *Staphylococcus aureus*.

А.А. Сеницына, С.Г. Ильясов

Синтез алкилпроизводных 3,7,10-триоксо-2,4,6,8,9,11-гексааза[3.3.3]пропеллана и изучение их биологической активности

Работа посвящена разработке метода синтеза производных 3,7,10-триоксо-2,4,6,8,9,11-гексааза[3.3.3]пропеллана (ТНАР), который ещё не получил широкого внимания исследователей ввиду сложности синтеза, а также изучению биологической активности синтезированных соединений в сравнении с алкилзамещенными гликолурилами (объектом сравнения). Методом N-алкилирования ТНАР были синтезированы новые гексаалкилпроизводные ТНАР с метильными, этильными и пропиловыми заместителями. На примере метильного производного были оптимизированы условия получения максимального выхода целевого продукта. Реакция протекает в среде ДМСО/КОН при температуре 75–80 °С в течение 13 ч с умеренным выходом 56 %. Этильные и пропиловые производные ТНАР синтезированы в аналогичных условиях. Изучена биологическая активность полученных алкилпроизводных ТНАР и алкилпроизводных гликолурила в отношении бактерий *Sporosarcina ureae*, *Bacillus pumilus*, *Salmonella typhimurium* и *Staphylococcus aureus*, а также вируса гриппа А. Установлено, что все образцы проявляют антибактериальную активность против *Staphylococcus aureus*. Было показано, что, наряду с проявленной противовирусной активностью, у соединений 2,4,6,8,9,11-гексапропил-ТНАР, ди-*трет*-бутил-дифенил-, ди-*трет*-бутил-добензил-, ди-*трет*-бутил-диметил-, ди-изопропил-добензилгликолурил также обнаружена токсичность для живых клеток.

Ключевые слова: пропеллан, азапропеллан, ТНАР, гликолурил, N-алкилирование, биологическая активность, вирус гриппа, *Sporosarcina ureae*, *Bacillus pumilus*, *Salmonella typhimurium*, *Staphylococcus aureus*.

References

- 1 Aizawa, N., Pu, Y.-J., & Chiba, T. (2014). Instant low-temperature cross-linking of poly(N-vinylcarbazole) for solution-processed multilayer blue phosphorescent organic light-emitting devices. *J. Adv. Mater.*, 26, 7543–7546.
- 2 Schmidt, A.W., Reddy, K.R., Knölker, H.-J. (2012). Occurrence, biogenesis, and synthesis of biologically active carbazole alkaloids. *J. Chem. Rev.*, 112, 3193–3328.
- 3 Kotha, S., & Pulletikurti, S. (2015). Synthesis of propellanes containing a bicyclo[2.2.2]octene unit, via, the Diels-Alder reaction and ring-closing metathesis as key steps. *J. RSC Advances*, 8, 27, 14906–14915.
- 4 Huisgen, R. (2015). Synthese von heterocyclen mit 1,4-dipolaren cycloadditionen. *J. Zeit. Chem.*, 83, 290–298.
- 5 Naoki, O., Yousuke, Y., & Hiroshi, T. (2018). Synthesis and properties of tribenzocarbazoles via an acid-promoted retro (2+2)-cycloaddition of azapropellanes. *J. Org. Chem.*, 26, 8, 7994–8002.

- 6 Torres Gómez, H., Daniliuc, C., & Schepmann, D. (2018). Synthesis of 3-aza[4.4.3]propellanes with high σ_1 receptor affinity. *J. Bioorg. Med. Chem.*, 26, 8, 1705–1712.
- 7 Zalkov, L.H., Harris, R.N., & Derveer, D.V. (1978). Modhephene: a sesquiterpenoid carbocyclic [3.3.3]propellane. X-Ray crystal structure of the corresponding diol. *J. Chem. Soc. Chem. Commun.*, 420–421.
- 8 Beyrati, M., & Hasaninejad, A. (2018). One-pot, sequential four-component synthesis of novel heterocyclic[3.3.3]propellane derivatives at room temperature. *J. RSC Adv.*, 8, 26, 14171–14176.
- 9 Tian, X., Li, L., & Hu, Y. (2013). Dichrocephones A and B, two cytotoxic sesquiterpenoids with the unique [3.3.3]propellane nucleus skeleton from *Dichrocephala benthamii*. *J. RSC Advances.*, 3, 21, 7880–7883.
- 10 Ashkenazi, P., Gutman, A.L., & Ginsburg, D. (1988). Propellanes: XCVIII. Treading of anti, anti[20.3.3]propellane-24,27-diol by sebacic acid. *Tetrahedron*, 44, 6875–6880.
- 11 Shin, M., Kim, M.H., Ha, T., Jeon, J., Chung, K.-H., & Kim, J.S. et al. (2014). Synthesis of novel 2,4,6,8,10-pentaza[3.3.3]propellane derivatives. *Tetrahedron*, 70, 8, 1617–1620.
- 12 Lee, B., Shin, M., Seo, Y., Kim, M.H., Lee, H.R., & Kim, J.S. et al. (2018). Synthesis of 2,4,6,8,9,11-hexaaza[3.3.3]propellanes as a new molecular skeleton for explosives. *Tetrahedron*, 74, 1, 130–134.
- 13 Zhang, J., Liu, Y., Bi, F., Zhou, J., & Wang, B. (2017). Synthesis, structure characterizations, and theoretical studies of novel tricyclic multiple(urea) molecules. *Journal of Molecular Structure*, 1141, 268–275.
- 14 Sinitsyna, A.A., Il'yasov, S.G., Chikina, M.V., Eltsov, I.V., & Nefedov, A.A. (2020). A search for synthetic routes to tetrabenzylglycoluril. *Chemical Papers*, 74, 1019–1025.
- 15 Sinitsyna, A.A., & Il'yasov, S.G. (2020). N-alkylation reaction in the synthesis of tetrasubstituted glycolurils. *J. Sib. Fed. Univ. Chem.*, 13, 1, 40–45.
- 16 Chegaev, K.Yu., Kravchenko, A.N., Lebedev, O.V., & Strelenko, Y.A. (2001). New functional glycoluril derivatives. *J. Mendeleev Commun.*, 11, 32–33.
- 17 Sidwell, R.W., & Huffman, J.H. (1971.) Use of disposable micro tissue culture plates for antiviral and interferon induction studies. *Appl. Microbiol.*, 22, 797–801.
- 18 Finter, N.B. (1969). Dye uptake methods for assessing viral cytopathogenicity and their application to interferon assays. *J. Gen. Virol.*, 5, 419–427.

Information about authors

Sinitsyna, Anastasia Aleksandrovna — Junior Research Scientist at the Laboratory of High-Energy Compounds Synthesis, Institute for Problems of Chemical and Energetic Technologies, Siberian Branch of the Russian Academy of Sciences (IPCET SB RAS), Sotsialisticheskaya st., 1, 659322, Biysk, Russia; e-mail: nastya.sinitsyna.1994@mail.ru; <https://orcid.org/0000-0003-3850-3132>

Il'yasov, Sergey Gavrilovich — Dr. (Chem.), Deputy Director for Research, Head of Laboratory, Laboratory of High-Energy Compounds Synthesis, Institute for Problems of Chemical and Energetic Technologies, Siberian Branch of the Russian Academy of Sciences (IPCET SB RAS), Sotsialisticheskaya st., 1, 659322, Biysk, Russia; e-mail: ilysov@ipcet.ru; <https://orcid.org/0000-0002-7853-6118>

R.P. Bhole^{1*}, Yogita Shinde¹, C.G. Bonde², R.D. Wavhale¹

¹*Dr. D.Y. Patil Institute of Pharmaceutical Sciences and Research, Pimpri, Pune, Maharashtra, India;*

²*SVKM's, NMIMS School of Pharmacy, Shirpur, Dist: Dhule, India*

(*Corresponding author's e-mail: ritesh.bhole@dypvp.edu.in)

Vitamin Drug conjugate: a systematic review of pharmacological potential

Cancer is a chronic disease which can cause death. In traditional chemotherapy cytotoxic drugs are used to kill proliferating cancer cells. The cytotoxic agent exhibits less specificity, less biological activity, causes systemic toxicity and undesirable side effects. Each year, about 1.8 million of the population are infected and die due to tuberculosis infection. An increase of drug resistance during the tuberculosis treatment is a significant concern. So, it is necessary to develop a new approach or therapies to resolve drug resistance, drug selectivity in tuberculosis infection and the reduction of the side effects of cytotoxic agents and anti-tubercular drugs. This review describes the newly emerging concept of «vitamin drug conjugate». Vitamin-drug conjugate is a specifically carried drug toward the target site, is one of the promising ways to treat chronic diseases like cancer and tuberculosis and enhance the therapeutic outcome. The purpose of this review is to explore vitamin as a targeting moiety for new anticancer and anti-tubercular drug to overcome challenges, such as non-selectivity, systemic toxicity and multidrug resistance. This approach is beneficial in the treatment of life-threatening disease like cancer, tuberculosis and also in many viral infections.

Keywords: Cancer, Tuberculosis, Vitamin-Drug conjugate, Vitamin B12 conjugate, Folic acid conjugate, Biotin conjugate, Vitamin-E conjugate, Lipid drug conjugate.

Content

List of abbreviations

Review Plan

Introduction

- 1 Vitamin-Drug conjugate
2. Folic acid-drug conjugate
3. Biotin Drug conjugate
4. Vit-E-drug conjugate
5. Vitamin-C Conjugate
6. Lipid-Drug conjugate
7. Polymer drug conjugate

Conclusions

List of abbreviations

WHO: World Health Organization

FRA: Folate Receptor Alpha

B₁₂-Co-III-CN-M: Heterodinuclear derivative

MCF7: Human Breast cells

A2780: Human Ovary Cancer Cells

B12-Co-III-CN-Pt-II: Vitamin B₁₂-Platinum conjugate

N₄PY: Pentadentate Nitrogen ligand

N₄PY-S-S-FA: Redox sensitive cleavable linker

FRP: Folate Receptor Positive

AG: Arabinogalactan

FR-AG-GFCG-MTX: Folate receptor Arabinogalactan endosomal cleavable peptide of methotrexate

MTX: Methotrexate

GFLG: Endosomal cleavable peptide

PLGA-PEG-FOL: Polylactideco-glycolide-polyethylene glycol-folate

SKOV₃: Folate receptor positive malignant cells

PEG: Polyethylene glycol

PA-PEG-DSPE: Lipopolymer
mPEG-DTP-DSPE: Lipopolymer
FA: Folic acid
PLGA: Polylactic –Co-glycolic acid
FU: 5-Fluorouracil
GG-NP: Guar gum loaded nanoparticles
MTX-FR-GGNP: Guar gum loaded methotrexate folic acid conjugated NP's
G₅-MTX: Pentadentate dendrimer-MTX adduct
5BT-1214: New generation taxoid
TPG5: α -Tocophenyl polyethylene glycol succinate
 γ -T₃-Tocotrienol
CoQ₁₀: Ubiquinol
CoQ₁₀H₂-PEG5000-Vit E: Ubiquinol-Polyethylene glycol-Vit- E Conjugate
SiRNA: Small interfering RNA
RNAi: RNA interference
TPGS: α -Tocopheryl polyethylene glycol succinate
Aa-Su-Saq: Ascorbyl succinic-Saquinavir conjugate
CYP3A4: Cytochrome P₄₅₀ metabolizing enzyme
MTX-PGA: Methotrexate-poly(glycerol adipate)
ATRA-g-PBEA: Docetaxel loaded trans-retinoic acid with poly- β -amino ester
HPMA: N-(2-Hydroxypropyl) methyl acrylamide
MA-Gly-Gly-NHN-Dex: Dexamethasone containing monomer

Review Plan

Inclusion and Exclusion Criteria: The present review is focused on vitamin drug conjugate, its synthetic methodology and its pharmacological screening.

The review data are based on the publication of the last 15 years and in English. Only articles in the relevant area were searched and analyzed from the sources like Scopus, Web of Science along with other online scientific search engines. The keywords used for the search were, 'Vitamin Drug Conjugate', 'anticancer activity', 'anti-tubercular activity', 'pharmacological screening', etc. The resultant data are described in this article. No statistical methods were used in this review.

Introduction

Cancer is an abnormal growth of the cells which tends to proliferate in an uncontrolled way and in some cases to metastasize [1]. There are many methods treating cancer, the most commonly applied one is chemotherapy, but the problem associated with that is non-selectivity in treatment. Severe, often life-threatening, side effects arise in cytotoxic chemotherapy because of the toxicity to susceptible normal cells as the treatment is not selective for tumor cells [2]. In the case of traditional chemotherapy, the most challenging step is to deliver a cytotoxic agent which kills proliferating cancer cells. [3]. The limitation of the used cytotoxic agents, such as doxorubicin, cisplatin, paclitaxel etc., is that these drugs cannot differentiate between tumor cells and normal healthy cells. In other words, non-specificity leads to systemic toxicity causing undesirable adverse effects like hair fall, kidney damage, lung and bone marrow [4, 5]. Thereby it is challenging to deliver the anticancer drug to the tumor site. Thus, by this reason there is a need in urgent requirement to develop a targeted drug delivery system for the selective action of drugs toward the growing cancerous cells with minimum side effects. [5]. It is expected that marked medicines specifically taken up by target cells, can significantly improve the effectiveness of cancer therapy. In recent years, drugs containing different targeting ligands like polysaccharides, folate and peptides are tested to increase antitumor activity [6–10].

In order to eliminate such toxicities the methods have been developed under which the therapeutic agent is targeted by conjugation to a tumor-cell-specific small-molecule linker, thereby minimizing exposure to healthy cells and related side toxicity [11]. Delivering of the therapeutic agent with no affinity for normal cells but a strong affinity for abnormal cells with a targeting ligand is the best approach to improve safety and effectiveness of the drug. There are many advantages of targeted medications over their non-targeted equivalents. Besides, the targeted drugs can specifically distribute their medicinal payloads into the cancer cell, thus preventing non-specific absorption and related normal cell toxicity [12, 13]. In order to achieve effective tumor-targeting drug delivery, it should consist of tumor recognizing moiety and chemotherapeutic

agent which directly connected through a linker. As a result conjugate acting 'prodrug' is formed which upon incorporated in cancer cell readily undergoes to splitting and regenerate the activity of cytotoxic agent [14].

All living cells need vitamins for survival and whereas the main physiological characteristic of cancer cell is an increased appetite for crucial vitamins because of their fast growth [15, 16]. Thus, the receptor involved for the absorption of vitamins will be overexpressed on the surface of cancer cells. Crucial vitamins like Folic acid, biotin, Vitamin B12, and riboflavin are required for tumors rapid growth. One of the approaches is to combine the drugs with vitamins that detect tumor-associated antigens, which raise the sensitivity of cancerous cells to ligand-targeted therapeutics and decrease the exposure of healthy cells to drugs [2]. Recently, it is observed that the folate receptors are more overexpressed in the cancer cells in comparison to normal healthy cells. So, it is accepted that folate receptors may act as excellent biomarkers [16–20]. Folate receptor alpha (FRA) is overexpressed on the surface of multiple types of tumors, including cancer of the pancreas, liver, breast and ovary. Folate can bound to anticancer drugs. The best approach is targeting the FRA-positive tumor cells with several therapeutic probes using folic acid conjugates. Folate conjugates can achieve cancer-specific drug delivery with minimal toxicity [21–23]. Biotin acts as a growth promoter especially in the tumor, as compared to normal cells. Recently it has been reported that biotin receptors are also more overexpressed in the cancer cells like breast, lung, renal, ovarian in contrast to folate as well as vit. B12 receptors [15, 16]. Combination of the anticancer drug with any particular vitamin gives vitamin-anticancer drug conjugate. Conjugation of anticancer agents with vitamin, has proven a novel prodrug approach, improving specificity with minimum side effects. The conjugation scaffold can improve potency as well as bioavailability of cytotoxic agents. The vitamin drug conjugate provides a high dose of a cytotoxic drug to the targeted cancer cell, so the essential vitamins like biotin, vitamin B12, folic acid, riboflavin may act as targeting moiety towards cancer cells. Most commonly, vitamin B12 and folic acid suggested as a targeting agent to tumor cell. Vitamin drug conjugate like folic acid -drug conjugate, Vit.B12–drug conjugate, biotin -drug conjugate and Vit.E–drug conjugate, as well as vitamin C–drug conjugate are listed in this review.

Other than cancer, tuberculosis is also one of the chronic illness, so there is an urgent need to find an effective treatment against chronic tuberculosis infection. Mycobacterium tuberculosis is the pathogen agent causing the infectious disease tuberculosis. Tuberculosis is one of the terrible human diseases which infects about 9 million of the population, including 1.5 million deaths in 2013 as per the WHO survey [24]. Drugs used for the treatment of TB are categorized into two groups; first-line drug and second-line drugs. The most commonly used first-line drugs for the treatment of tuberculosis are Isoniazid, Rifampicin, Ethambutol and pyrazinamide [25]. These drugs develop multidrug resistance because of the lengthy period of treatment, mostly 12–18 months or more [26]. Thereby there is a need of searching for a new anti-tubercular agent or other supportive therapy [27]. Vitamins also play a crucial role to prevent the spread of this chronic illness. Any bacteria like mycobacterium tuberculosis needs essential vitamins like biotin, thiamin to fulfil their requirement and to initiate their infection. Vitamin C, for instance, has antimycobacterial property. Vitamins act as a promising agent to change life cycle as well as the biology of mycobacterium tuberculosis and helps to stop the spread of infection [27]. Lipid drug conjugate improving the bioavailability of the anti-tubercular drug by incorporation of short lipid chain is discussed in this review. Limitations associated with the anti-tubercular drugs like Isoniazid, Rifampicin, Ethambutol and pyrazinamide is lipophilicity issue resulting poor blood-brain barrier penetration. Lipid-antitubercular drug conjugate is also a new approach having potential to enhance efficacy, bioavailability, with reduction in drug resistance.

Vitamin drug conjugate is the novel term that provides selective delivery of cytotoxic agent towards cancer cells with desirable therapeutic effect. This review focuses on the requirements that must be met to achieve the necessary therapeutic efficacy with minimal side effects during the design of vitamin drug conjugate. This review also emphasises on various vitamin drug conjugate reported to date with its synthetic methodology and pharmacological evaluation. Vitamin drug conjugates like folic acid drug conjugate, vitamin B12, biotin, vitamin E, vitamin C–conjugates are listed in this review. All these conjugates were studied to find out the best fit conjugate in terms of its clinical applicability.

1 Vitamin-Drug conjugate

Vitamin-Drug conjugate is considered as a targeted drug delivery system for tumors. It generally consists of the drug connected directly or through a linker to the targeted moiety to form an active pharmacological object, i.e the 'vitamin-Drug conjugate' (Fig. 1). The benefits of vitamin drug conjugate are nontoxic and

it must be stable in circulation and do not harm to normal cells. Upon entry of this conjugate into the cancer cells, it should effectively release the anticancer drug without losing biological activity [5, 28].



Figure 1 Vitamin-drug conjugate

1.1 Vitamin B12- drug conjugate [30].

1.1.1 Vit-B₁₂-metal conjugate

The cancer cells need vitamin B12 and more cellular uptake, so it can be concluded that on conjugation with vit. B12 increases tumor selectivity and enhance therapeutic outcomes. This type of conjugate consists of an anticancer drug with tumor imaging metal-containing compound [31]. A variety of vitamin B12 metal analogues are identified to date, but some provide a promising proof of concept promoting the use of cobalamins in targeted chemotherapy and diagnosis as metal-based medicine and imaging drug carriers [31, 32]. There are number of studies on platinum and other metal-based anticancer agents, but on other hand the clinically established anticancer drug cisplatin has some disadvantages, like low bioavailability, water-solubility, lack of tumor selectivity and undesirable side effects proved. In spite of its harmfulness the platinum complex was clinically approved and accepted because of its pharmacological activity with less side effects [31, 33–34].

Platinum

Cisplatin is also platinum-based drug with anticancer activity. However there are some disadvantages of this drug, such as nephrotoxicity, neurotoxicity, phototoxicity, nausea etc. Alberto et al. developed a method to overcome the problem associated with anticancer drug cisplatin and its side effects. Conjugation of cisplatin with cobalamine (vit B12) increases tumor selectivity and enhance the clinical output [31, 35, 36]. Metal containing scaffolds is attached to the nitrogen atom to the cyano group on vit B12, producing a derivative (B12-Co-III-CN-M) where vitamin is functioning as a ligand. A further step is vitamin B12 converted to its cofactor (either methylcobalamine or adenosylcobalamin) required for reduction of Co (III) to Co (II) by removing bioactive molecule Vit.B12 Co III. CN is mixed with metal. The formed cyano metal fragment (CN-M) release directly inside the cell. This cyanocobalamine metal conjugate (Figure 2) considered as prodrug, which shows the clinical endpoint [31, 36].

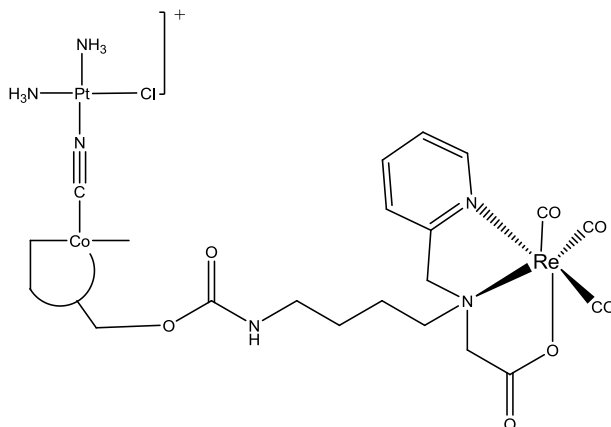


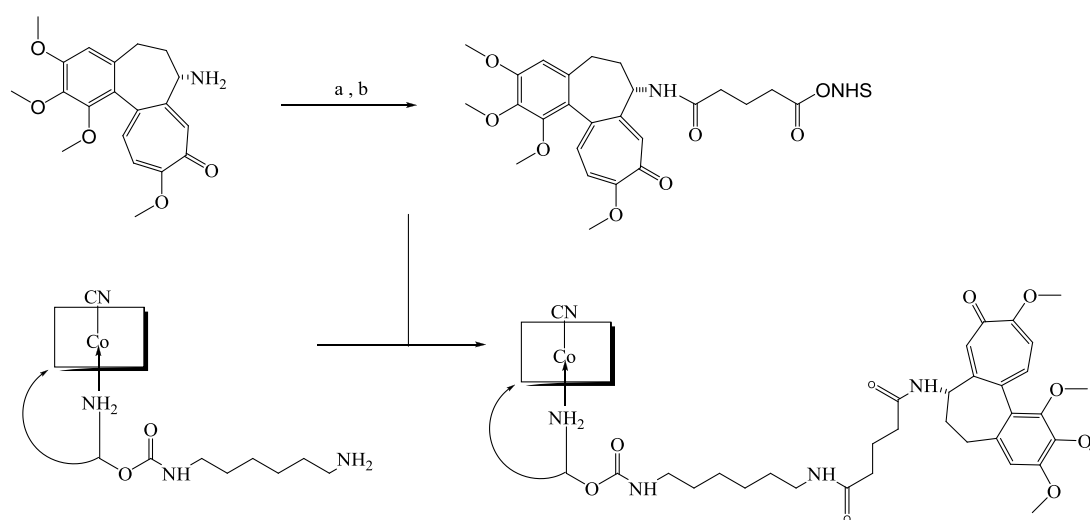
Figure 2. Vitamin B12-Platinum Conjugate

In vitro cytotoxicity experimental investigation on adenocarcinoma of human breast cells (MCF7) and adenocarcinoma of cells of human ovary (A2780) demonstrated that differentiated Pt (II)-Cyano complexes exhibited antitumor action equivalent to that seen in cisplatin, suggesting that (B12-CoIII-CN-PtII) analogue should be considered as an active drug because they have an affinity to generate Pt-II containing antitumor drug quickly in the body effectively. Unfortunately, this theory was not compatible with the data that the original analogues were less carcinogenic than cisplatin [31, 37].

1.1.2 Colchicine- Cobalamins conjugate

Colchicine functions as a spindle toxin with a mode of action close to that of taxanes, and it also acts as a cytotoxic agent. Colchicine inhibits the polymerization of tubulin and prevents cancer cell proliferation at metaphase in mitosis. But colchicine has not proven effective for cancer therapy to date because of its overbearing toxic effects that cause undesirable side effects at endovenously medication [38–40]. Using the cobalamin leads to selective delivery of colchicine to tumor cells, the side effects associated with colchicine can decrease drastically [38].

Joshua et al., developed colchicine-cobalamin conjugate (Fig. 3). By substitution at the C7 position of colchicine by p-alkoxy-acetophenone and bonded with cobalamin via hydrazone, which has acid sensitive nature. Malignant cells are more likely prone to cellular absorption of this scaffold. Upon interaction of this scaffold with cancer cells occurs hydrolysis of the acid liable hydrazone linker inside the lysosome. Colchicine behaves as a powerful antineoplastic agent, helps to balance the microtubule as well as shows cellular apoptosis. This scaffold is highly stable at pH 7 and in the cellular medium, is more susceptible to hydrolysis at pH 4.5, having a half-life of 138 min. This scaffold display LC50 values in nanomolar across the variety of cancer cell such as brain, breast and melanoma in cellular medium. The increase of the drug's bioavailability by overcoming the undesirable side effects associated with tubulin can be achieved by adding colchicine to cobalamin. The in vitro cytotoxicity of this bioconjugate is equivalent to that of existing chemotherapy medications such as paclitaxel and docetaxel. However, bioconjugate is highly soluble in water and considerably inexpensive than paclitaxel or docetaxel [38, 41–43].



(a) Glutaric anhydride in DMSO : (b) EDCI , NHS in DMSO (34% yield, 3 steps)

Figure 3. Synthesis of colchicine cobalamine conjugate

2 Folic acid-drug conjugate

Folic acid is one of the essential vitamins, and folate receptors act as a target for the cancer treatment [44]. The folate receptors are recently emerged as a promising theragnostic target due to their great functional flexibility in multiple solid tumors [45]. The major problem is the delivery of anticancer drug due to non-selectivity, which result in toxicity because having an inability to distinguish between cancer and normal healthy cells. This problem can be resolved by conjugating anticancer drug with folic acid. Folic acid acts as a targeting ligand to deliver many therapeutic agents towards growing tumors tissues. Folic is used as a tar-

get because it easy conjugate with therapeutic, as well as diagnostic agent and also shows a high affinity towards the folate receptor. Most important that folate receptor is limitly distributed in the normal cell, but overexpressed in cancer cells [46]. This foremost approach involves linking FA to the anticancer drug forming small molecule drug compound to get effectual clinical output. Folate conjugate attached to folate receptor by means of endocytosis process, which is overexpressed in cancer cells and attached drug shows its therapeutic output after cellular administration. [44].

2.1 Folic acid- Bleomycin conjugate

Most challenging step in cancer therapy is to deliver anticancer drug due to their non-selectivity and systemic toxicity [47]. Bleomycin acts as an anticancer antibiotic. The problem associated with bleomycin is short half-life, less clinical output and more undesirable side effect. Due to this problem, there is limited use of bleomycin as a therapeutic agent in cancer therapy [48].

Geersing et al., developed a method which shows that bleomycin imitates conjugate of folic acid (Fig. 4) where folic acid conjugate with pentadentate nitrogen ligand(N4Py) through a cleavable di-sulphide linker. This conjugate exhibits promising efficacy and selective delivery of the anticancer drug in cancer cells which are overexpressed toward folate receptor. This conjugate also increases potency as well as selectivity of cytotoxic anticancer agent. A significant effect was seen by the MTS assay conducted in KB cells on N4Py-S-S-FA metabolic function after 48 h, which is enhanced after 72 hours. Pentadentate iron ligand conjugated with folic acid can induce selective apoptosis of FR (+) cancerous cells in contrast with a minimum effect observed for FR (-) cells. Enhanced efficacy is observed after a duration of 72 hrs due to the existence of a disulphide bond-containing cleavable linker moiety. These observations demonstrate the strength of therapeutics targeted by ligands, with strong potency and improved selectivity relative to compounds without targeted moiety [47, 49–51].

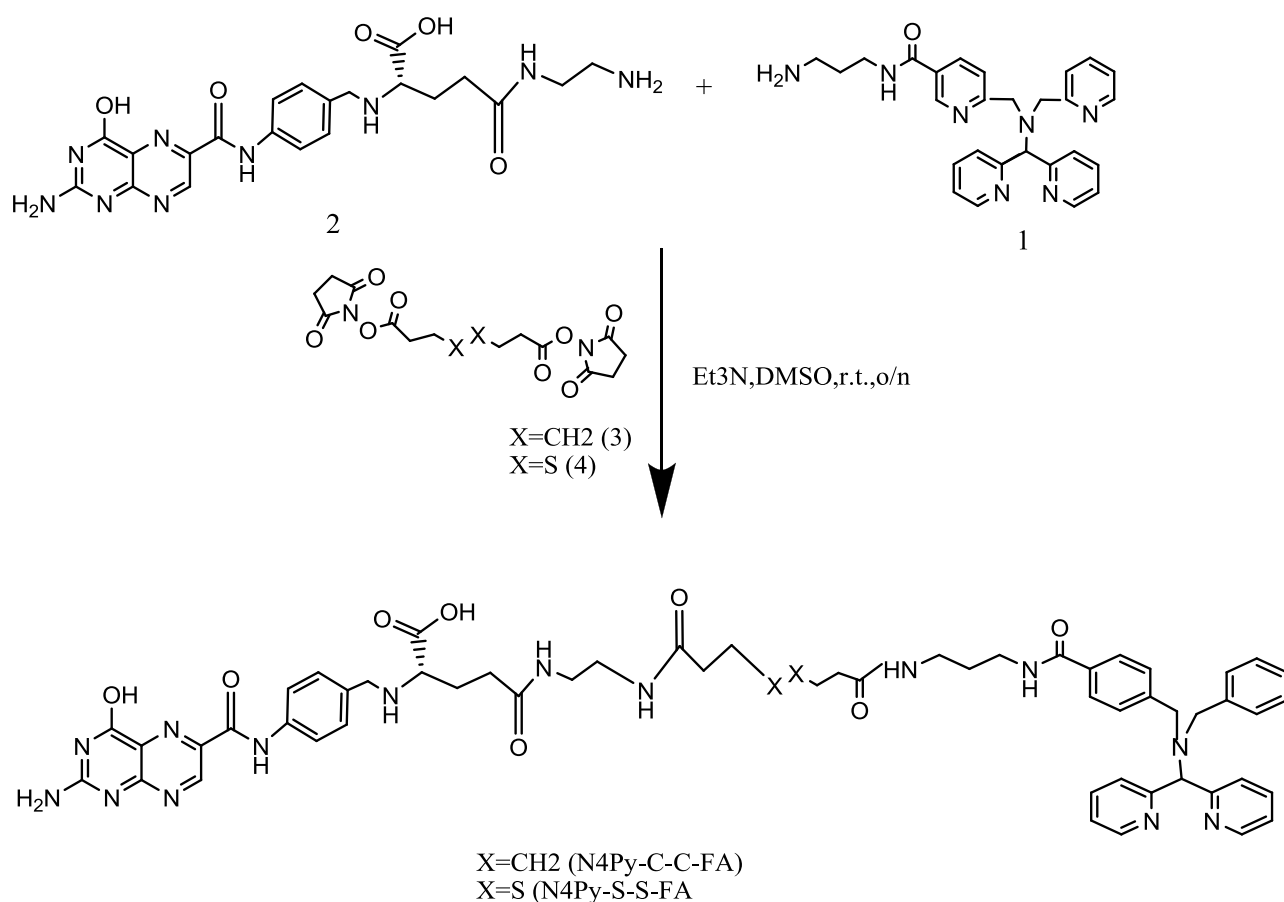


Figure 4. Synthesis of N4Py-C-C-FA and N4Py-S-S-FA

2.2 Arabinogalactan-folic acid-methotrexate conjugate

Folic acid exhibits a high affinity toward the folate receptor (FR). We proposed a new selective delivery mechanism based on the naturally occurring polymer AG for anticancer drugs and characterized their ability to detect, penetrate and kill tumor cells with overexpression of folate receptor [52].

Pinhasi et al., developed a method, in this FR-AG-GFLG-MTX (Folate receptor Arabinogalactan endosomal cleavable peptide of methotrexate) (Figure5) is the conjugate which delivers a cytotoxic agent in FR overexpressing cells. In this conjugate, folic acid and methotrexate are bond to arabinogalactan (AG) via endosomal cleavable peptide (GFLG). The formed conjugate FR-AG-GFLG-MTX shows 6.3-fold increase in the cytotoxic activity. This research produces a new FA bound anticancer agent conjugate to deliver methotrexate to the overexpressed cancer cells in FR [40–42]. An important potential benefit of this drug delivery mechanism is that it exhibits effective therapy for malignant cells and multidrug-resistant tumor cells [52, 55].

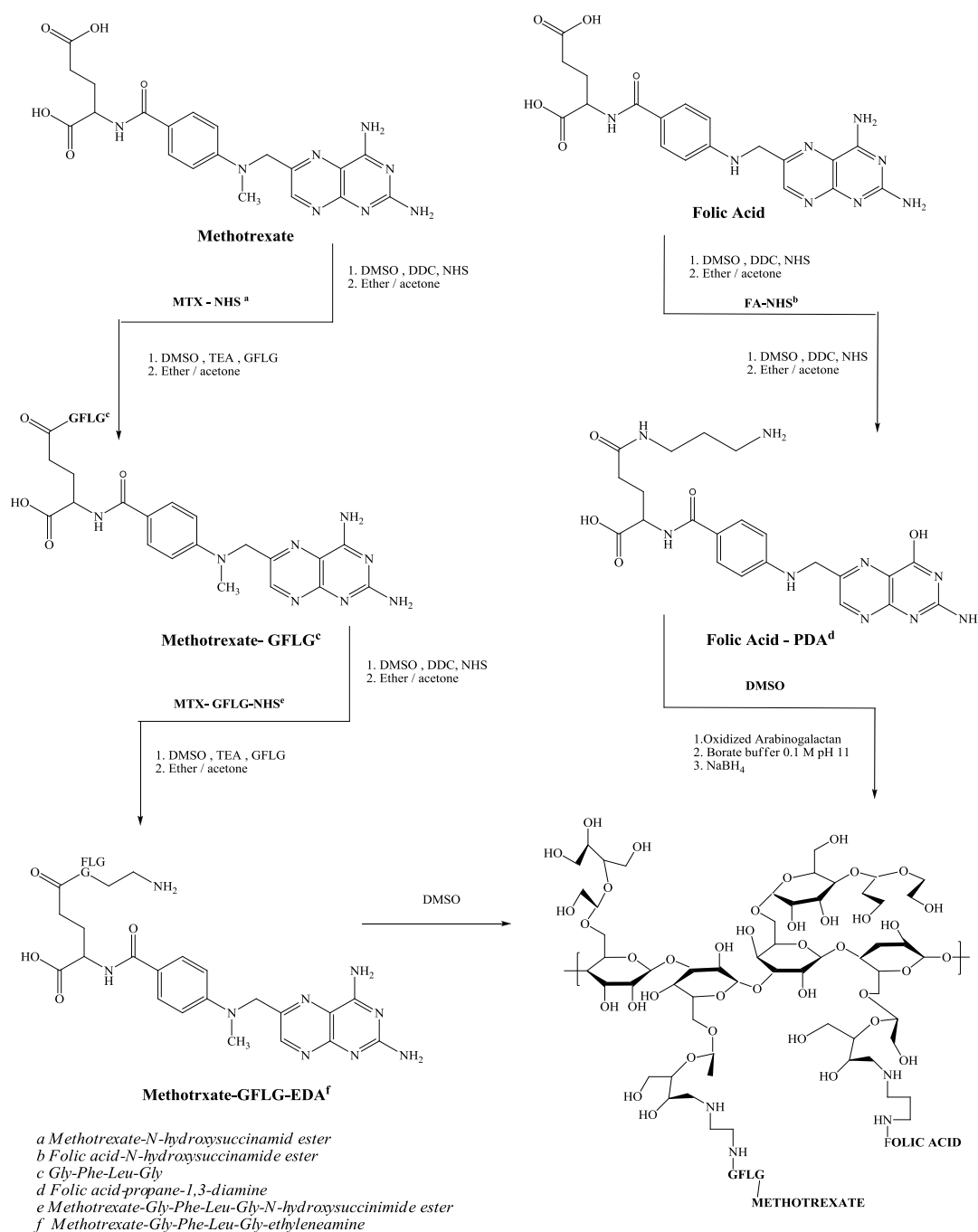


Figure 5. Synthetic scheme of FA-AG-GFLG-MTX Conjugate

2.3 Docetaxel loaded -PLGA-PEG Folate conjugated nanoparticles

Nanoparticulate formulations incorporating anticancer drugs have recently gained much interest due to their accumulation the tumor cells [56, 57]. Esmaeilli et al., reported a method, in which Docetaxel nanoparticles were developed for folate receptor-targeted cancer therapeutics using poly(lactide-co-glycolide)-polyethylene glycol-folate (PLGA-PEG-FOL) conjugate (Fig. 6). The FOL-coupled di-block co-polymer was obtained by the reaction of active Folic acid with the co-polymer of the PLGA-PEG-NH₂ di-block, where the folate ligands were supposed to be revealed on the micellar layer. The docetaxel loaded folate conjugate was formed by an emulsification process, with an overall size of 200 nm in diameter.

In contrast with the non-targeted nanoparticles, the folate targeted ones exhibited a higher degree of intracellular absorption via Folate receptor-mediated endocytosis process, which plays an essential role in the absorption of nanoparticles in Folate receptor-positive malignant cells (SKOV3). These studies indicate Docetaxel loaded-folate targeted nanoparticles are a highly beneficial drug delivery system for the tumor cells that are folate receptor-positive and which contribute to increased cytotoxicity [56, 58–60].

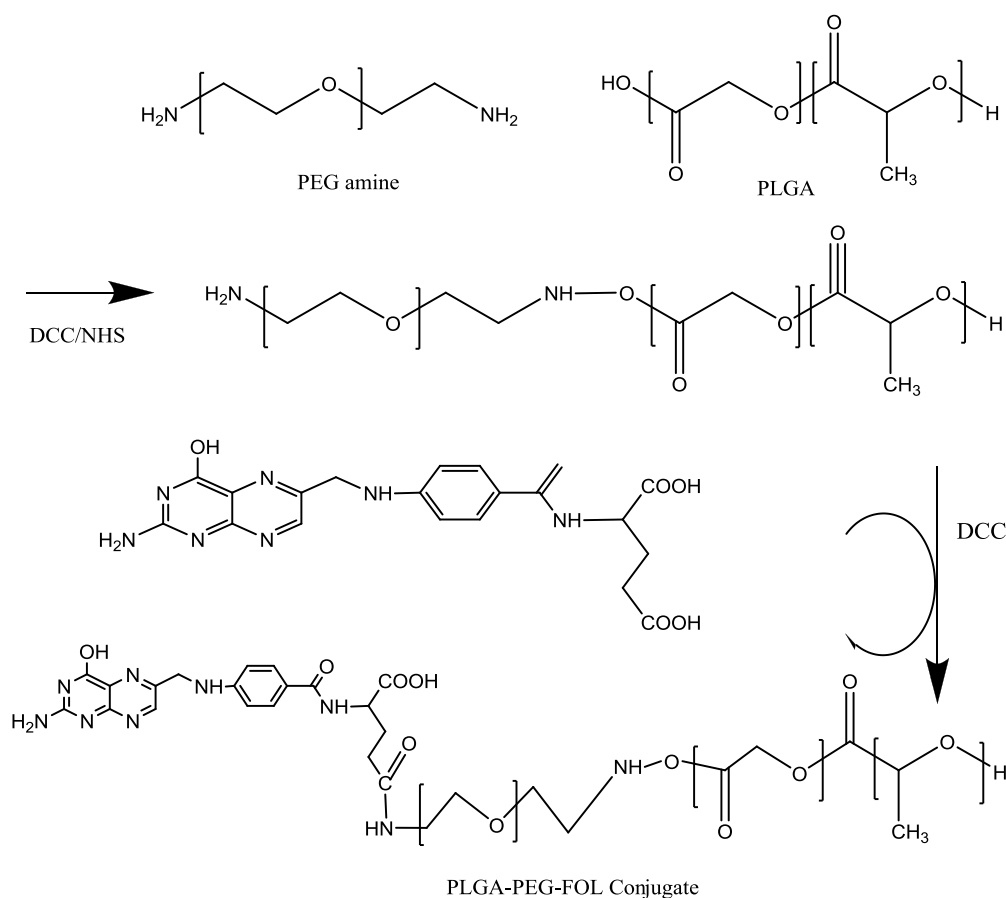


Figure 6. Synthetic scheme of PLGA-PEG-FOL conjugate

2.4 Folic acid-PEG conjugate

Folate bond polyethylene glycol (PEG) liposome are obtained for effective cancer therapy because they have an affinity to accumulate into the tumors due to increased permeability [61, 62]. Folic acid phospholipid conjugation (Fig. 7) is the best approach to transfer chemotherapeutic agent to folate receptor (FR) expressing tumor. In this case is used polyethylene glycol (PEG) liposome with folate linked to the outer end of phospholipid attached PEG molecule. It seems to be a suitable way for liposome deposition in tumor and binding of liposome to FR on cancer cells and release anticancer drug via receptor-mediated endocytosis process. [61, 63]. In vitro studies demonstrate that increase in the antitumor activity of liposomal agents occurs via folate targeting in the FR expressing malignant cells [61, 64, 65].

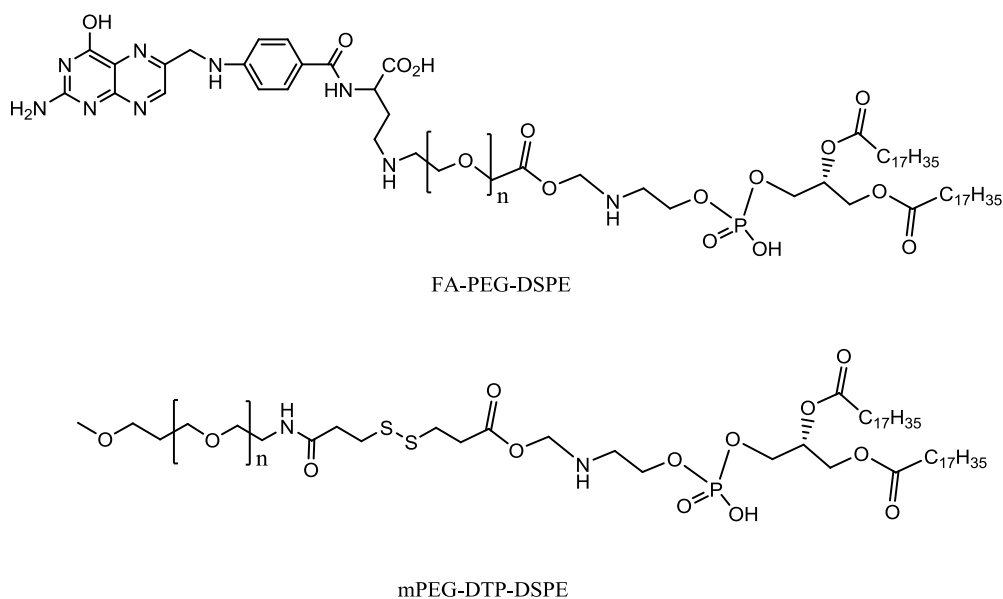
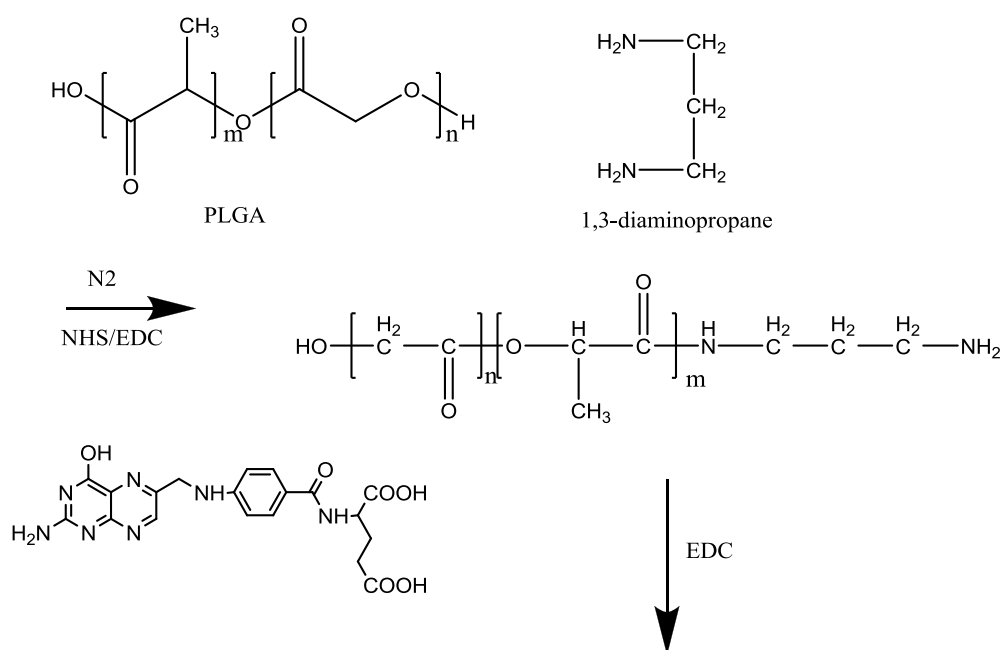
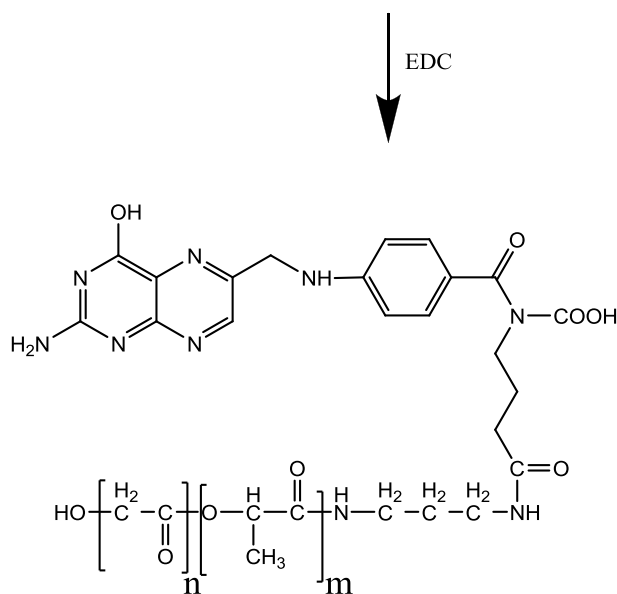


Figure 7. Folate-PEG Conjugate

2.5 Folic acid-5-fluorouracil conjugated nanoparticles

Wanget al., developed a method in which folic acid (FA) shows the low target efficiency, low conjugation ratios at loading as a carrier in PLGA drug delivery system. They used 1,3-diaminopropane as a crosslinker in FA conjugated PLGA system to reach high conjugation ratio of 46.7 % (mol/mol). The prepared PLGA (Polylactic-co-glycolic acid) [66, 67] was used to encapsulated drug 5-fluorouracil (5-FU) into nanoparticles on HT-29, cancer cells were observed to be 5–69 $\mu\text{g/ml}$ in-vitro. In the experiment the value IC₅₀ is smaller for 5-FU and 5-FU loaded PLGA nanoparticles which is 22.9 and 14.17 $\mu\text{g/mL}$, respectively. The fluorescent microscopy image showed that targeting nanoparticles have a high affinity for cancer cells and nanoparticles with FA. This is more significant amount taken up by cancer cells of HT-29 than the pure drug and untreated nanoparticles. 1,3 di-aminopropane forms a new polymer by facilitating conjugation of FA to PLGA. This FU loaded PLGA-1,3-diaminopropane folic acid nanoparticles (Fig. 8) are one of the efficient approaches to transfer the drug to tumor cells [66, 68, 69].





PLGA 1,3-diaminopropane folic acid

Figure 8. Synthetic scheme of PLGA-1,3 diaminopropane-folic acid

2.6 Guar gum loaded methotrexate-folic acid conjugated nanoparticles

Prepared nanoparticles have excellent properties for drug delivery, such as small size, including the use of biodegradable polymers, and advantages over other innovative drug delivery systems and provide protection, increased stability. Nanoparticles can easily accumulate into the tumor cells due to their small size and provide effective cancer treatment [70–72].

This nanoparticles are developed to target colon cancer. Sharma et al. developed guar gum nanoparticles (GG-NP) with methotrexate (MTX) loaded folic acid. Emulsion cross-linking methods are used to prepare the MTX charged folic acid biocompatible guar gum nanoparticles. The formed conjugate MTX-FR-GGNP shows promising release anticancer drug methotrexate to overexpressed folate receptor and treating colorectal carcinoma. This formulation has dual benefits tend to release the drug in the colon and case of carcinoma [70, 73, 74].

2.7 Methotrexate-dendrimer-folic acid conjugate

Thomas et al., demonstrated that conjugating Folic acid and methotrexate with 5th generation dendrimer [75–77] increases the therapeutic index of Methotrexate (MTX) comparing with methotrexate administered alone [75, 78, 79]. Batch to batch discrepancies in the number of methotrexate (MTX) and folic acid molecules associated with each dendrimer, mainly while scale up processing resulted in differing the therapeutic action of conjugated batches [80, 81].

The biological differences might arise from the enzymatic activity of serum esterase enzyme and result in differences in bioavailability of selected conjugate because methotrexate is bonded through an ester bond [75, 78]. In this study, they attempted a new methodology to generate specialized G5-MTX_n adduct via a selective synthesis process by linking MTX to the pentavalent dendrimer using an esterase-stable amide coupling. Synthesized G5-MTX adduct bind to the folic acid receptor via pentavalent coupling that displays 4300-fold more significant activity than free MTX, it was demonstrated by the results of surface plasmon resonance linking studies. This adducts resist enzyme dihydrofolate reductase and also promote cytotoxic effect in FR-expressing KB cells lines via the FR-specific cellular interaction process and by coupling of MTX with pentavalent dendrimer, which plays a significant role as an anticancer agent and also a targeting molecule. The G5-MTX_n adduct acts as a promising FR-selective, cytotoxic agent for the treatment of cancer [75, 78, 79, 82].

3 Biotin Drug conjugate

Biotin is one of the essential vitamins and acts as a promising targeting agent. Vitamin drug conjugate is an approach to deliver a high dose of the targeted drug to cancer cells [83]. Biotin is an essential vitamin and is transported through sodium-dependent multivitamin transporter, which is more expressed in many cancers cell lines like colon, breast, lung cancer cell line. Biotin shows overexpression in folate receptor, so growing tumors more need for biotin than normal cells.

It is reported that the conjugation of biotin with many organic molecules and protein shows selective delivery of a cytotoxic agent to cancer cells [84].

3.1 Biotin-taxoid conjugate

Yang et al., developed conjugate in which biotin is combined with new generation taxoids 5BT-1214 [83]. The approach of this invention is simple for tumour-targeted drug delivery system. The use of biotin 5BT-1214 conjugate (Fig. 9) exploits the biotin receptor's upregulation on the cancer cells. The invented process involved the drug delivery via endocytosis mediated by vitamin receptor [16, 83].

The testing result of biotin 5BT-1214 fluorescence conjugate showed the biotin drug conjugate easily incorporate into tumor cell and shows reduced toxicity against normal cells and also shows well systematic stability. Therefore it is one of the best novel targeted drug delivery system for tumor cells [83]. The findings suggest that only the biocompatible biotin-dendrimer adduct may be a successful nano-platform towards cancer treatment and cancer detection [85].

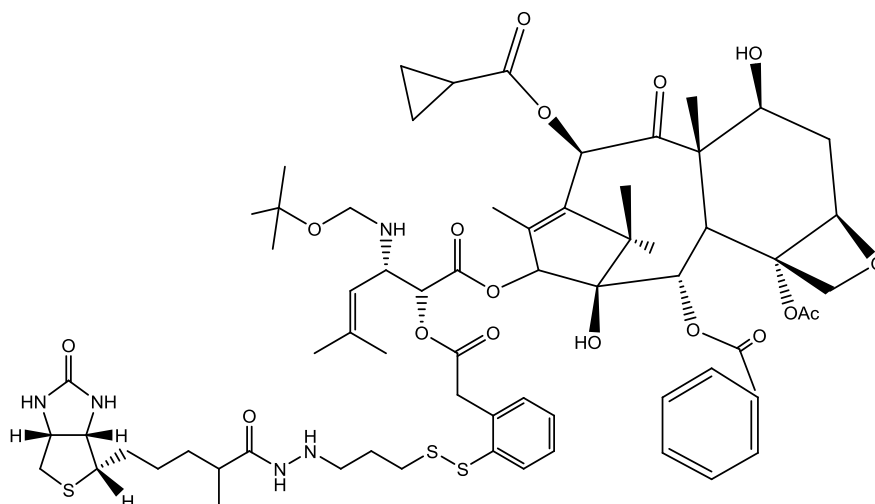


Figure 9. Chemical structure of Biotin-SBT-1214 conjugate

3.2 Gemcitabine-Coumarin-Biotin conjugate

Maiti et al., developed target-specific anticancer prodrug moiety Gemcitabine-Coumarin-biotin conjugate (Fig. 10) to treat various cancers [16, 86]. In this method, they proposed the formulation, development, spectroscopic analysis, and in vitro biological evaluation of Gemcitabine-coumarin-biotin conjugate. This conjugate is a multipurpose molecule mainly consisting of a splittable disulphide bond with a thiol group, fluorescent coumarin moiety, therapeutic action given by gemcitabine and biotin is serve as a cancer-targeting component. Breakdown of the disulphide bond occurs when a free thiol group are added, which is exceptionally high in cancerous cells and also release of therapeutic agent gemcitabine, as well as concurrently rise in fluorescence intensity [86, 87].

Confocal microscopic studies demonstrate that instead of W138 cells, this scaffold is selectively absorbed by A549 cells. Fluorescence-based colocalization experiments utilizing specific lysosome and endoplasmic reticulum additives indicate that splitting of thiol-containing disulphide bond of the conjugate can occur in the lysosome by receptor-mediated endocytosis process. This is latest approach with a therapeutic and diagnostic tool that provides both therapeutic benefit, and drug absorption at the cellular level is effectively controlled by fluorescence imaging [86, 88, 89].

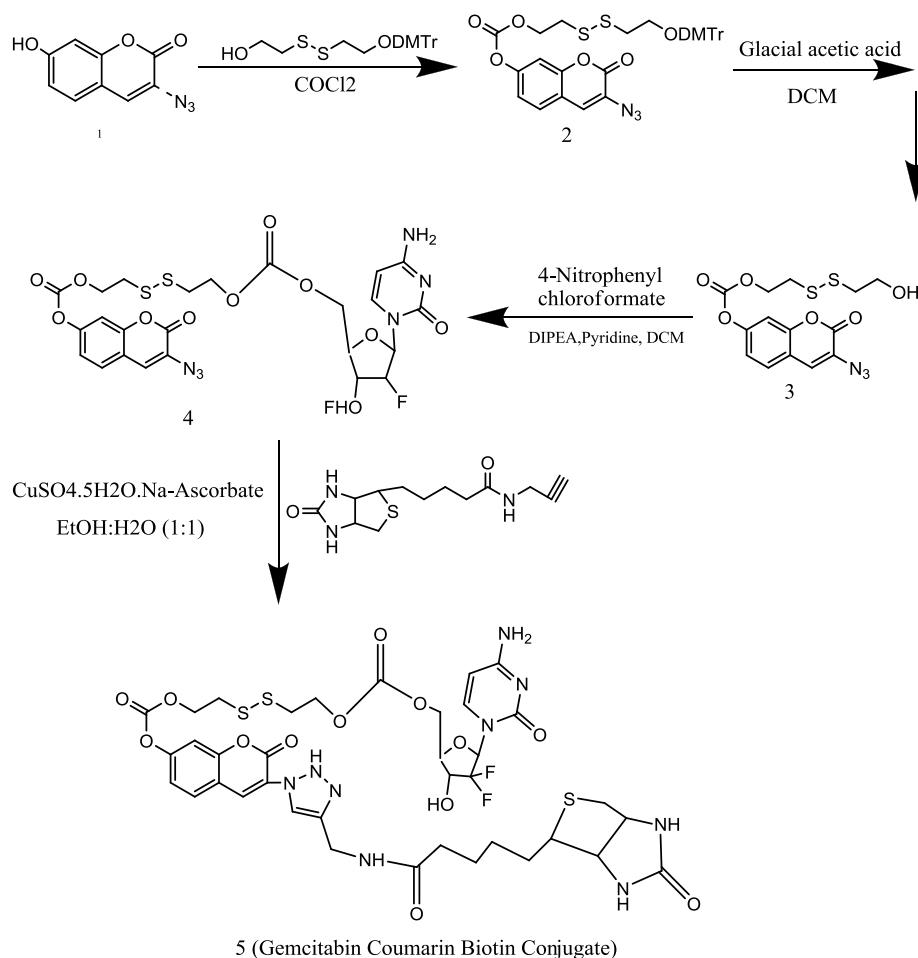


Figure 10. Synthetic scheme of Gemcitabin Coumarin Biotin Conjugate

4 Vit-E-drug conjugate

Vitamin-E and α -tocopherol analogues have a pro-apoptotic property and can kill cancerous cells, also helps in the prevention of cancer without any undesirable effects [90]. Vitamin-E and tocopherol analogues are used in drug delivery system because of their many excellent advantages like drug solubility, biocompatibility and antitumor activity. Upon esterification of vitamin-E succinate, the formation of non-ionic amphiphile known as α -Tocopheryl polyethylene glycol succinate (TPGS) shows the ability to cluster formation behaviour with other organic molecules. Hence it is helpful to develop many drug formulations which show properties like increase bioavailability and targetability of many anticancer drugs [91].

4.1 Gemcitabine-Vit E Conjugate

The main aim of this study is to test in vitro anticancer activity of gemcitabine conjugate to the tocotrienol isomer of vitamin-E (Fig. 11) against pancreatic tumor cells [92, 93]. Abu-Fayyad et al., reported that the free tocotrienol isomer of vit E shows the anticancer activity of gemcitabine. By using ¹H NMR and mass spectrometry analysis technique, the conjugate was identified and tested for deamination sensitivity. The anticancer activity of gemcitabine was studied in vitro for pancreatic cancer cells BX-PC3 and PNAC-1 in which [92, 94].

γ -T3 conjugation of gemcitabine studied in vitro for enzymatic deamination showed that it was least affected comparing with free and conjugated gemcitabine in solution by deamination deactivation reaction. In vitro cytotoxicity studies indicate that an increase of anticancer activity by entrapping gemcitabine lipid conjugate into a nano-emulsion compared to a free drug is observed. It was concluded that for effective delivery of gemcitabine, conjugation with γ -T3 isomer is one of the feasible options [92, 93, 95].

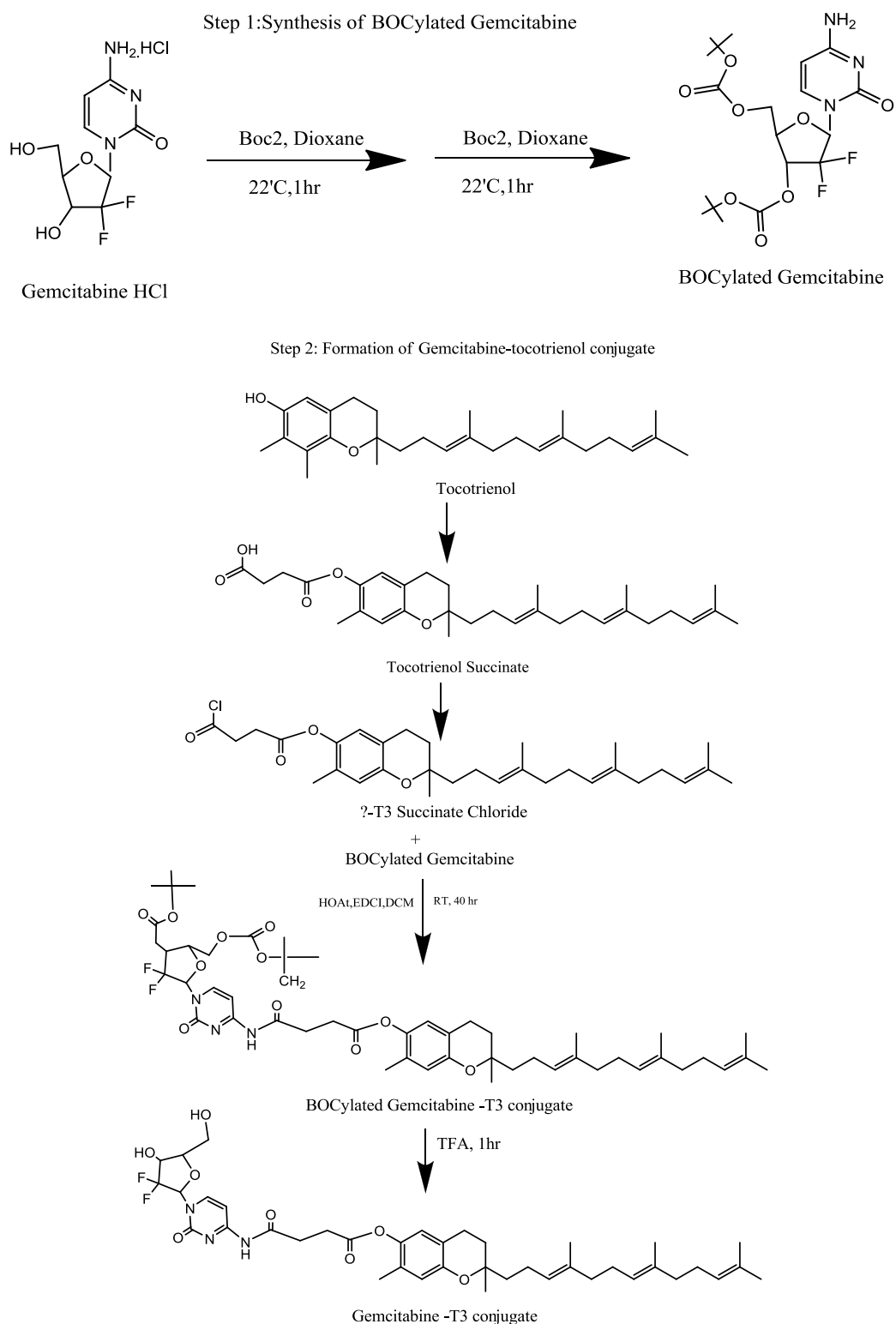


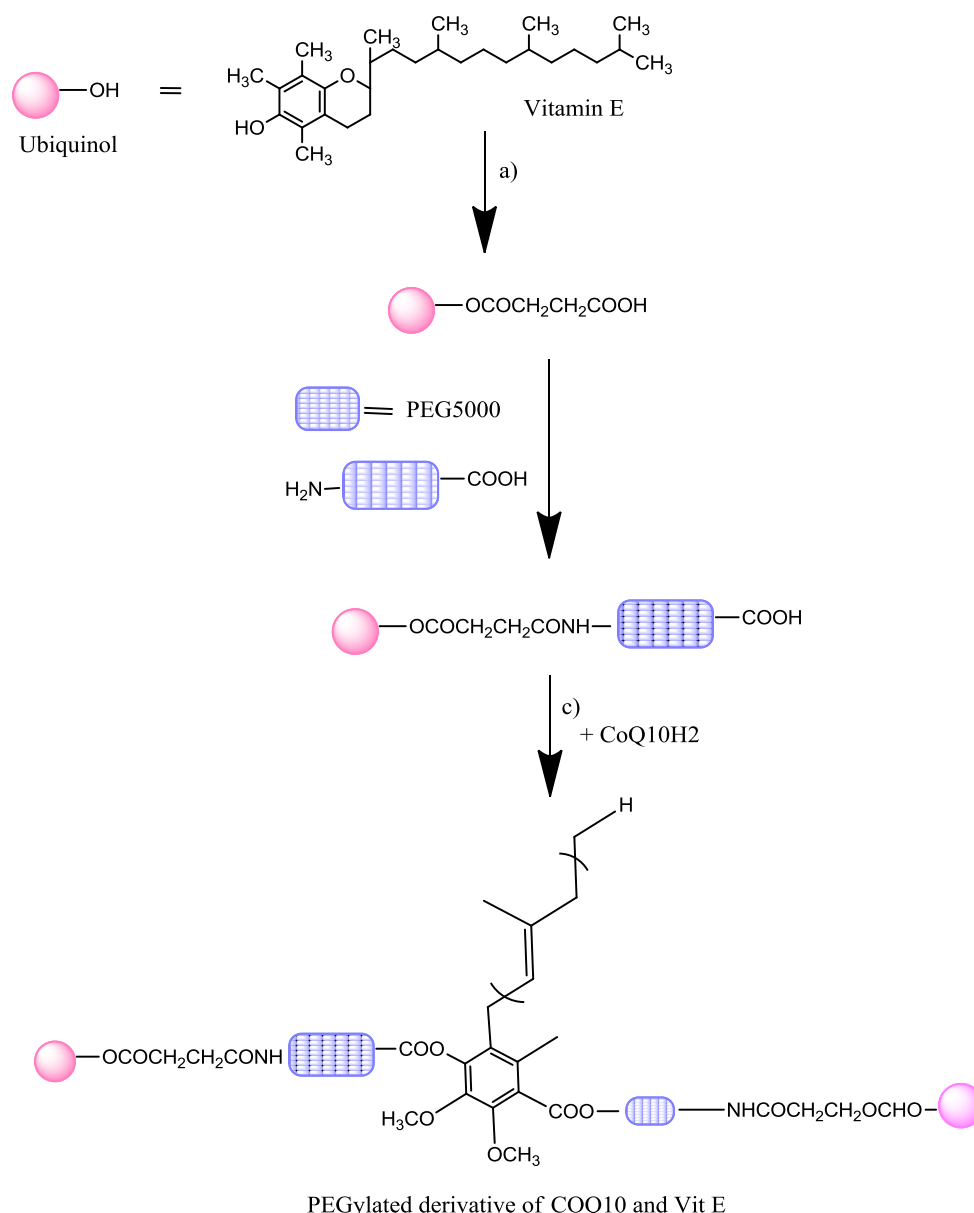
Figure 11. Synthetic scheme of Gemcitabine Vitamin E (Tocotrienol) Conjugate

4.2 Ubiquinol-Polyethylene glycol-Vit E conjugate

Both Ubiquinol and vit E have medicinal value but drawback associated with the Ubiquinol and Vit E, shows low bioavailability, potential toxicity because they have less soluble in aqueous media [96, 97]. Cateniet al., developed a method to overcome the challenge associated with vitamin-E and Ubiquinol. The objective of the present study is to improve the bioavailability of ubiquinol and vit E; the mixed conjugate of Ubiquinol-Polyethylene Glycol-Vitamin E (Fig. 12) was synthesized and characterized. By spectroscopic

methods such as ^1H NMR and mass spectroscopy, the synthesized mix conjugate of PEG was characterized. The in vitro release of the conjugate was calculated and evaluation of ubiquinol and vit E also carried out in different pH conditions in human plasma. The obtained result indicates that at pH 7.4, occurs more release of ubiquinol and vit E from PEG conjugate in plasma within 24 hrs. The evaluation of antioxidant activity carried out by DPPH assay and obtained results show that there is no effect on antioxidant activity of ubiquinol and vit-E after esterification with PEG.

The novel CoQ10H2-PEG5000-Vitamin E combined conjugate was obtained and observed an enhancement in water solubility of CoQ10, Vitamin E is predicted by this conjugate. The increase of the beneficial effects and reducing the undesirable side effects of the parent products are observed. [96, 98, 99].

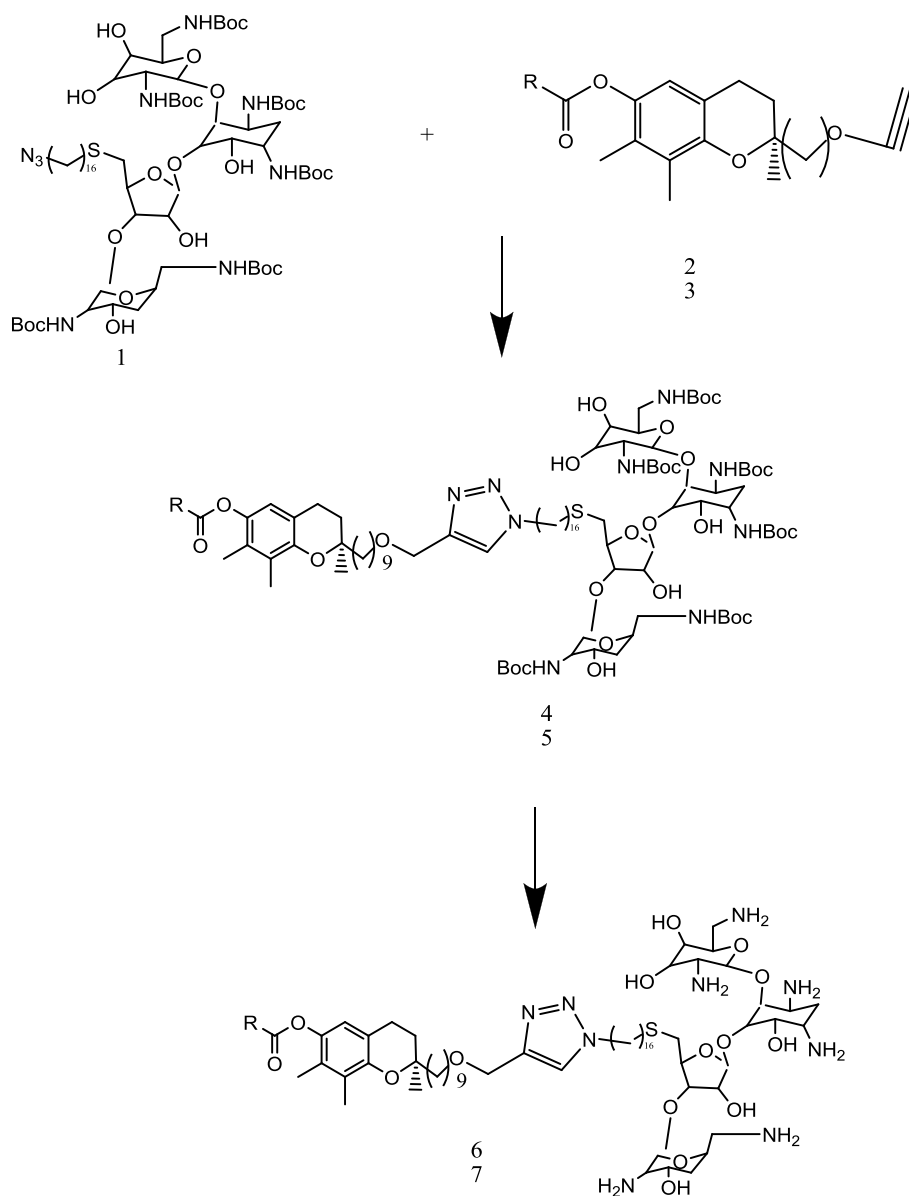


a) Succinic anhydride, Toluene Et₃N, 85°C, 9 H; b) Et₃N, DCC, HOBT, dry CH₂Cl₂, Room temperature, 24h; c) DCC, DMAP, dry CH₂Cl₂, Room temperature, under nitrogen 24h.

Figure 12. Synthetic scheme of PEGylated Ubiquinol-Vit E conjugate

4.3 Vit-E-neomycin conjugate

Vit E conjugated neomycin derivative (Fig. 13) is a novel approach to deliver siRNA (small interfering RNSs) to liver cells. In this approach the neomycin derivative exhibited RNAi (RNA interference) activity in liver cancer cell [100, 101].



Scheme 1. Synthesis of the prodrug derivatives 6 & 7. Reagents and conditions : (a) Cu powder, t-BuOH-water, 80°C, 4h, 89-97%, (b) Triisopropylsilane, TFA-CH₂Cl₂, rt, 1h, 79-92%

Figure 13. Synthetic scheme of Vit-E-neomycin conjugate

4.4 Docetaxel loaded Vitamin-E TPGS micelle with cetuximab:

Kutty et al., and Feng et al., developed docetaxel loaded vitamin E TPGS micelle to treat triple-negative breast cancer. For the selective delivery of docetaxel as a design anticancer drug for the treatment of triple-negative breast cancer (TNBC), produced a Cetuximab-conjugated vitamin E TPGS micelles. Hormone progesterone receptor (PR), estrogen receptor (ER) and epidermal growth factor receptor 2 (HER2) [102, 103] are not expressed, therefore their treatment more challenging than positive breast cancer. In docetaxel loaded vitamin E TPGS micelle cetuximab behaves like as targeting ligand. Vitamin E TPGS micelle is designed

with small particle size, have more drug loading capacity, also shows excellent drug release pattern. Micelles are characterized by surface appearance, charge. [102, 104].

TNBC cell lines like MDA MB468, MDA MB 231 and HCC 38 cell line with the expression of epidermal growth factor receptor 2 at a high frequency are used. Moderate and low frequencies are used to check in vitro, anticancer activity, as well as cellular absorption of docetaxel, loaded Vit.E TPGS micelles with cetuximab in contrast to a free drug-like Taxotere. The evaluated IC50 value indicates that the therapeutic agent's concentration can kill 50 % of malignant cells in desired time, like 24 hrs. By comparing the free drug Taxotere, the IC50 value for the micelle is obtained. Thus it was found that docetaxel loaded vitamin E TPGS micelle exhibits a 205.6 and 223.8 fold increase in anticancer activity in TNBC compared to free drug Taxotere [102, 105].

5 Vitamin-C Conjugate

5.1 Vitamin C-Saquinavir conjugate (Ascorbyl-succinic-saquinavir)

Luo et al., and Wang et al., developed the ascorbyl-succinic-saquinavir (Aa-Su-Saq) conjugate (Figure 14). It was synthesized and evaluated to target sodium-dependent vitamin-C transporter (SVCT) in order to improve the oral absorption of prodrug saquinavir. The affinity of Aa-Su-Saq regarding efflux pump p-glycoprotein (p-gp) and recognition by SVCT of Aa-Su-Saq have also been studied [106, 108].

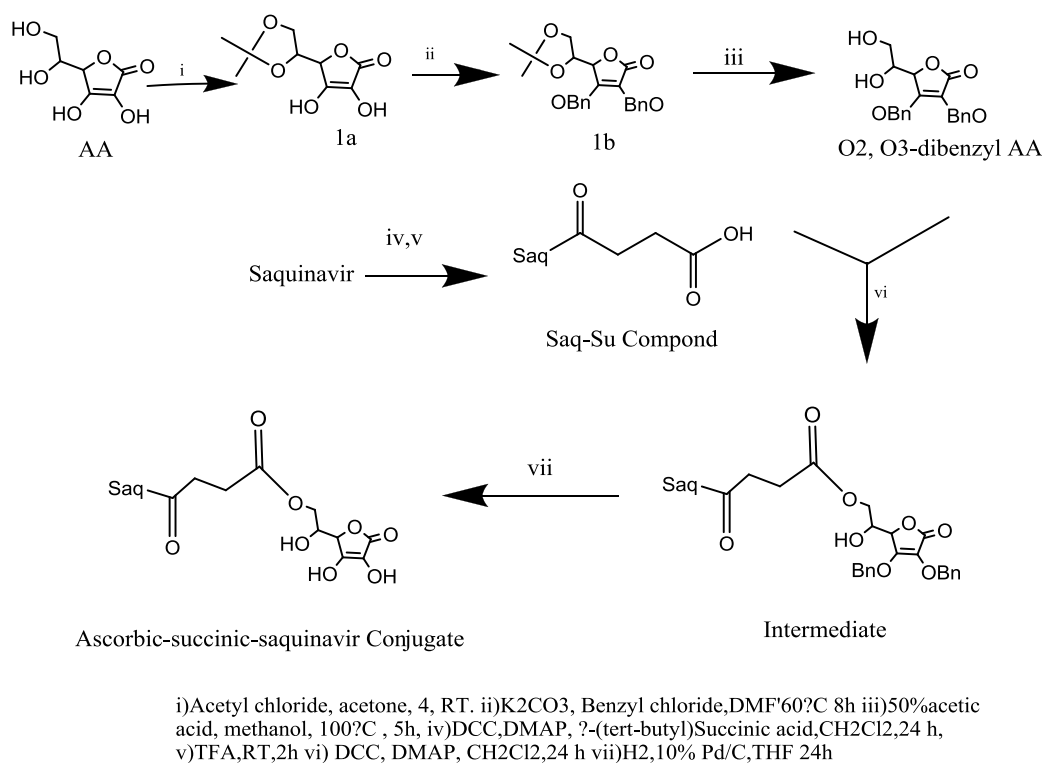


Figure 14. Synthetic scheme of Ascorbic-succinic-saquinavir Conjugate

Polarized MDCK-MDR1 and CaCO-2 cells were taken to determine transepithelial permeability, and rat liver microsomes were used to study the metabolic stability of Aa-Su-Saq. Aa-Su-Saq is stable in DPBS and CaCO-2 cells, having a half-cell life of 9.65 and 5.73 h. In MDCK-MDR1 cells, saquinavir absorption increased by 2.7 and 1.9-fold at the conc. 50 μM Saq and Aa-Su-Saq. In MDCK-MDR1 and CaCO-2 cells, cellular accumulation of AA was decreased by 50–70 % compared to control in the presence of 200 μM of Aa-Su-Saq. In the presence of 5 μM ascorbic acid, the uptake of AA-Su-Saq was decreased by about 27 % to 34 %, and absorptive permeability was increased about 4.5-fold. The efflux index was lowered about 13–15-fold in polarized MDCK-MDR and CaCO-2 cells. Aa-Su-Saq not only free from cytotoxicity but also shows an increase in metabolic stability because it shows less affinity toward CYP3A4 [106, 107, 109].

6 Lipid-Drug conjugate

6.1 Stearoyl chloride-Isoniazid conjugate

Isoniazid is the first line anti-tubercular drug in the treatment of tuberculosis. However, there is some limitation associated with its hydrophilic nature, therefore exhibits low permeability and have less affinity to cross blood-brain barrier, which results in the low therapeutic output. This problem can be solved by incorporating hydrophobic moiety of the covalently linked lipid-drug conjugate of Isoniazid with a small lipid chain of stearoyl chloride (Fig. 15). Using the method of cold high-pressure homogenization also improves the bioavailability of Isoniazid; lipid-drug conjugate nanoparticles were produced by using an aqueous surfactant. The physicochemical analytical methods like transmission electron microscopy, differential scanning calorimetry, X-ray diffraction method were applied to characterize nanoparticles. In vitro, drug release studies conclude that at pH of 7.4, in phosphate buffer solution shows sustained drug release up to 72 hrs. Higuchi model of diffusion is an attractive one to study the drug release profile of nanoparticle.

This lipid drug conjugate is effective in mycobacterium tuberculosis infection by intracellular trafficking into endosomal and lysosomal vesicles and colocalization with intracellular protein like CD63, LAMP-2, EEA1 and Rab11. These nanoparticles exhibit affinity to improve effective intracellular absorption of water-soluble drug Isoniazid [110, 111].

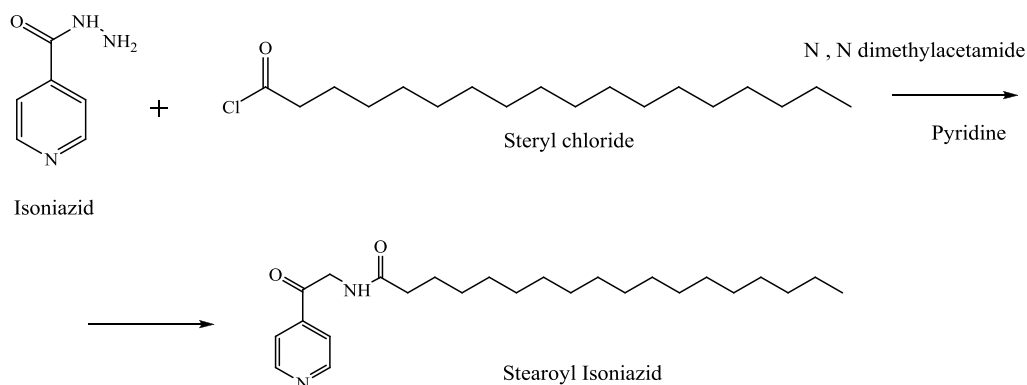


Figure 15. Synthesis of Isoniazid- Stearoyl chloride conjugate

Other approaches for the treatment of cancer and other diseases

7 Polymer drug conjugate

Cancer is considered as chronic illness which responsible for the elevated mortality rate in the world. The effective treatment for the cancer illness is the administration of the chemotherapeutic agent, even though its clinical status is not acceptable. The use of antitumor agent is minimal because it may cause serious complication. Therefore, to protect the normal cells from the severe side effects associated with a chemotherapeutic agent, «Polymer–Drug conjugate» is synthesized.

«Polymer–Drug conjugate» is a drug carrier system that consists of three components like a molecular targeting moiety, solubilizing moiety and active ingredient. Polymer-Drug conjugate in which the active drug is incorporated into the polymeric material. Polymer-Drug conjugate is also regarded as polymeric prodrug [112–114].

7.1 Methotrexate-Poly(glycerol-adipate) conjugate

Polymer drug conjugate is specially designed and intended for cancer therapy. The present study mentions the first polymer-antitumor drug conjugate obtained by combination of poly(glycerol adipate) with antitumor agent Methotrexate (Fig. 16). By using carbodiimide mediated reaction, MTX-PGA complex was developed with the reproducible result and with different high MTX molar concentration; the MTX-PGA adduct is self-build into size nanoparticles. The size of the nanoparticles depends on medium pH and the quantity of methotrexate. The change of particle size of NPs resulted in stearic hindrance and build bulkiness within nanoparticles centre and separation of the free functional group of the active agent.

MTX-PGA nanoparticles exhibit stability at ionic strength equivalent to 0.15M HCl, in the medium having pH 5–9. They also show chemical stability at pH 7.4 in case of hydrolysis for 30 days, even though it

undergoes enzymatic degradation and release of free drug in unchanged form. In comparison with MTX-PEA NP, earlier reported studies indicated that by conjugating MTX with serum albumin exhibits > 300 times less potent than pure MTX. But MTX-PEA nanoparticles are slightly potent than free MTX in 791T. Along with the studies on enzymatic degradation, these results show that a linker moiety is not a necessary element with a useful biodegradable polymer. Therefore, these quickly produced PGA drug conjugates without a linker moiety can be a practical new approach for polymer-drug conjugate growth [115].

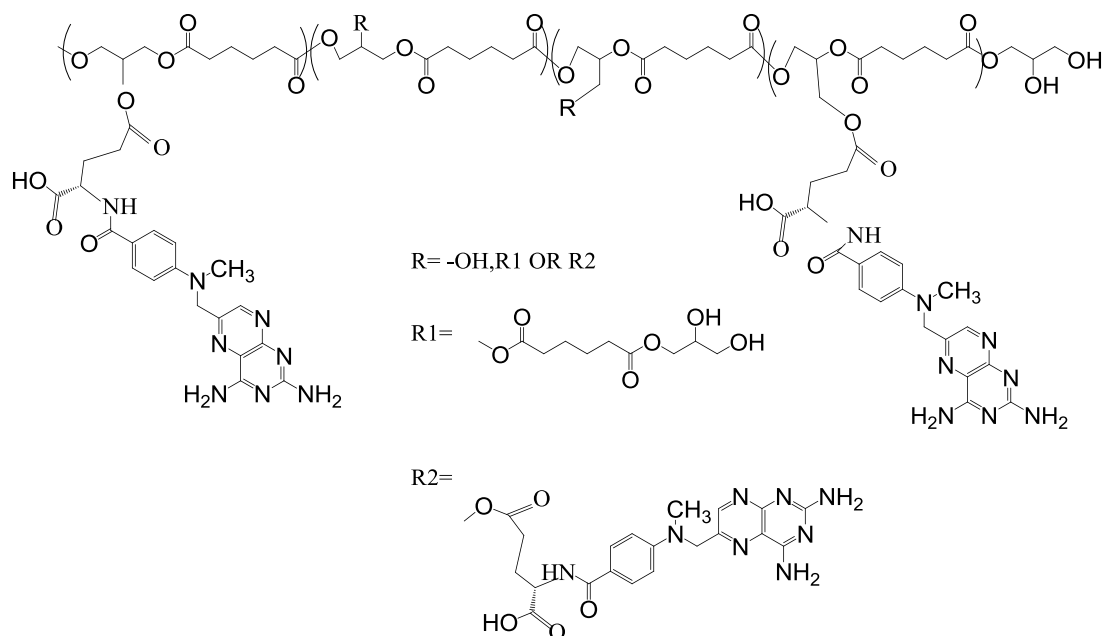


Figure 16. Methotrexate-Poly(glycerol adipate) conjugate

7.2 Docetaxel loaded polymeric nanoparticles

In this study, the drug is conjugated with a polymer producing polymeric nanoparticles to overcome obstacles associated with chemotherapy.

Docetaxel loaded trans-retinoic acid with poly- β -amino ester (ATRA-g-PBEA) nanoparticles is produced by encapsulation. Docetaxel is conjugated with trans-retinoic acid (ATRA) with poly- β -amino ester by the solvent displacement method. Using Zeta-sizer, the size and zeta potential of nanoparticles were measured and the morphology of nanoparticles was evaluated at pH 7.4, and 5.8. with the transmission electron microscopy. The in-vitro drug release study was studied. The cytotoxicity, anti-angiogenic effect and blood compatibility of this controlled release nanoparticles, also studied. The DTX loaded ATRA-g-DBAC nanoparticles show more cytotoxicity and better anti-angiogenic effect compared to free all trans-retinoic acid and docetaxel in chemotherapy. ATRA-g-PBAE nanoparticles are an attractive controlled released system compared to chemotherapy [116].

7.3 HPMA co-polymer-Dexamethasone conjugate

Liu et al., and Quan et al., developed pH-sensitive conjugate of N-(2-Hydroxypropyl) methyl acrylamide (HPMA) containing Dexamethasone polymeric conjugate is able to strengthen the therapy of rheumatoid arthritis. Reversible addition-fragmentation transfer (RAFT) polymerization technique is used to create an unique pH-sensitive and cross-linked Dexamethasone-containing monomer (MA-Gly-Gly-NHN=Dex) with HPMA. The scaffold of Dex-HPMA co-polymer conjugate was studied as well as its biological effectiveness was also tested on rodents with adjuvant-induced arthritis (AIA). Polymeric Dexamethasone conjugate was obtained with poly-dispersity index and with controlled molecular weight. Dexamethasone containing monomer (MA-Gly-Gly-NHN=Dex) regulates feed-in proportion ration Dexamethasone material.

The molecular weight of polymeric Dexamethasone conjugate is 34KDa and PDI is 1.34. at in vivo and in vitro assessment. The release of Dexamethasone from conjugate is caused due to low pH; it is demonstrated by in vitro drug release tests. Polymeric Dexamethasone conjugate has a significant and lengthy anti-inflammatory effect and joint safety. These properties are revealed by the tests such as, endpoint bone miner-

al density and histology grading. Conjugate of Dexamethasone–HPMA co-polymer is obtained with a very well structure is effective against rheumatoid arthritis. In the treatment of rheumatoid arthritis, it also has a specific therapeutic potential [117].

Conclusions

Chemotherapy is the golden method to treat a chronic disease like cancer, but there is some complication associated with chemotherapeutic agents causing undesirable side effects with systemic toxicity to the normal cells. Therefore, to avoid this problem, a new approach called «vitamin-drug conjugate» is developed. Many research studies reported various vitamin-drug conjugate like folic acid conjugate, Vitamin B12 conjugate, vitamin-C conjugate, vitamin-E conjugate, Biotin drug conjugate etc. In the case of Lipid drug conjugate, many drugs cannot cross the blood-brain barrier due to their hydrophilic nature. Thus, this problem can be solved by combining hydrophilic drug with short-chain of lipid resulting in new adduct is known as «Lipid-Drug conjugate».

The review describes vitamin drug conjugate which is the newly emerged concept for targeted drug delivery to the cancer cells with achieving desirable clinical output. The recent studies revealed that cancer cells are more overexpressed to vitamins than normal cells, so using the method receptor-mediated endocytosis system can deliver a cytotoxic agent to the cancer cells and may not harm any normal cells. To strengthen this concept, many approaches were studied like conjugation with metals, conjugation with gums and conjugation with vitamins etc. Metal drug conjugate is the clinically approved method as it can deliver both therapeutic and diagnostic agents to the cancer cells with a fewer side effect.

Vit.B12 conjugate, in this cobalamin, is covalently bound to the anticancer drug and produce high biological activity. Therefore the conjugation of drug with vitamin exhibits high efficacy and low systemic toxicity. In folic acid conjugate, folate receptor is highly overexpressed on cancer cells compared to normal cells. Thus selective drug delivery of cytotoxic agent toward malignant cells can be achieved by binding with folic acid. That is why it is one of the promising methods that have the potential to treat a variety of cancers in future. α -Tocopherol polyethene glycol succinate is an ester form of vitamin E succinate that shows excellent properties like increase selectivity as well as bioavailability of anticancer drugs. Another preparations like biotin conjugate, Vitamin-C conjugate and vitamin-A conjugate also proved to be useful in cancer therapy and reducing the toxicity. The folic acid drug conjugate was found to be most active and pharmacologically effective amongst all the other conjugates for the treatment of cancer.

Few challenges may arise associated with vitamin drug conjugate, as a synthesis of the conjugate in cobalamin drug conjugate and biotin drug conjugate. Vitamin B12- metal conjugate shows accumulation in non-targeted organs and leads to a severe undesirable side effect. Thus, it is necessary to design such conjugate that shows increased uptake and selectivity toward tumor in order to avoid accumulation in organs.

Tuberculosis infection treatment drugs develop multidrug resistance due to the more extended treatment period. This problem can be resolved using vitamin as a target molecule to stop the spread of tuberculosis infection. In addition to anti-tubercular therapy, the newer drug is conjugating with vitamins like vitamin-C and vitamin-D are useful and one of the novel approaches against tuberculosis infection in the future.

In future vitamin drug conjugate is an attractive approach of targeted preparation delivery to the many life-threatening disease like cancer, tuberculosis etc.

The summary of these methods and its advantage are shown in the Table.

T a b l e

Vitamin drug Conjugates

Sr. No	Vitamin Drug Conjugate	Advantages
1	2	3
1	Vitamin B12-Metaldrug conjugate	<ul style="list-style-type: none"> – Vitamin B12-Metal conjugate can overcome the problems associated with anti-cancer agents. – The increase in tumor selectivity and enhance clinical output by conjugating metal with cobalamin. – In vitro cytotoxicity experiments carried out on adenocarcinoma cells of human ovary and human breast cells demonstrated that Pt-II Cyano complex exhibit anti-tumor activity and quickly release antitumor drug in the body.

1	2	3
2	Colchicine- cobalamin conjugate	<ul style="list-style-type: none"> – This scaffold is effective against variety of cancers like brain, breast and melanoma. – Colchicine-cobalamin conjugate is one feasible option to resolve the problem associated with tubulin targeted anticancer drug.
3	Folic acid-Bleomycin conjugate	<ul style="list-style-type: none"> – This conjugate increase potency as well as selectivity of anticancer agents into tumor cells which over expressed toward folate receptor.
4	Arabinogalactan-folic acid-methotrexate conjugate	<ul style="list-style-type: none"> – Folate targeted arabinogalactan linked methotrexate adduct shows 6–3-fold increase in cytotoxic activity as well selective delivery of antitumor agent into the cancerous cells.
5	Guar gum loaded methotrexate-folic acid conjugated nanoparticles	<ul style="list-style-type: none"> – These nanoparticles were designed to target colon cancer. – Guar gum loaded methotrexate-folic acid nanoparticles play dual function, it provides robust treatment against the colorectal carcinoma and also show efficacy in case of another carcinoma.
6	Methotrexate-dendrimer-folic acid conjugate	<ul style="list-style-type: none"> – The coupling of methotrexates with 5th generation dendrimer result in increase of methotrexate therapeutic index comparing to free methotrexate. – This conjugate is not affected by serum esterase enzyme activity because it synthesized by esterase stable amide coupling, so this adduct exhibits 4300-fold greater biological activity in contrast with free methotrexate.
7	Docetaxel loaded -PLGA-PEG Folate conjugated nanoparticles	<ul style="list-style-type: none"> – Folate targeted docetaxel loaded NPs shows displayed a higher degree of intracellular absorption in Folate receptor-positive malignant cells (SKOV3).
8	Folic acid-PEG conjugate	<ul style="list-style-type: none"> – It is novel approach to deliver anticancer agent to cancerous cells by conjugating folic acid to phospholipid. – Via folate targeted drug delivery system can be increased anticancer activity of liposomal active agent in FR expressing cancerous cells.
9	Folic acid-5-fluorouracil conjugated nanoparticles	<ul style="list-style-type: none"> – 5-FU conjugated nanoparticles have high affinity toward malignant cells HT-29 compared to pure drug and display the excellent anticancer activity in the 5-HT cells, it is demonstrated by florescent microscopy.
10	Biotin-Taxoid conjugate	<ul style="list-style-type: none"> – Biotin conjugated with taxoid 5BT-1214, this scaffold is easily integrated into tumor cells and reduce the cytotoxicity of the normal healthy cells. So, it is novel approach and targeted drug delivery of cytotoxic agent to the tumor cells.
11	Gemcitabine-Coumarin-biotin conjugate	<ul style="list-style-type: none"> – This conjugate is multipurpose molecule, which selectively absorbed by the cancerous cells A549 instead of W138 cells. – This multipurpose scaffold provides both therapeutic benefit and also drug absorption at the cellular level in malignant tumors.
12	Ubiquinol-Polyethylene glycol-Vit E conjugate	<ul style="list-style-type: none"> – Ubiquinol-PEG-Vit.E conjugate resolved the problem associated with ubiquinol and vit.E like poor bioavailability, potential toxicity. – In vitro study carried out at different pH conditions in human plasma obtained results revealed that at pH 7.4 there is more release of ubiquinol and Vitamin-E from PEG conjugate in plasma within 24hrs.
13	Gemcitabine-vitamin-E conjugate	<ul style="list-style-type: none"> – In-vitro studies demonstrate that by conjugating gemcitabine with vit.E which is least affected by deamination deactivation reaction compared to free drug. – In-vitro cytotoxicity studies revealed that increase of anticancer activity by entrapping gemcitabine in lipid conjugate compared to free drug is observed.
14	Docetaxel loaded vit-E TPGS micelle with cetuximab	<ul style="list-style-type: none"> – DTX-loaded vit-E TPGS micelle have small particle size, have high drug loading capacity and excellent drug release pattern. – The TNBC cell lines like MDA-MB468, MDA MB 231 and HCC 38 cell line have been used to check in vitro activity and was found that docetaxel loaded vitamin-E TPGS micelle shows 205.6 and 223.8-fold increase in anticancer activity in TNBC cell line compared to free drug Taxotere.
15	Vitamin-C — Saquinavir conjugate (Aa-Suc-Saq)	<ul style="list-style-type: none"> – In MDCK-MDR1 cells the absorption permeability of saquinavir is increased about 4–5-fold from Aa-Suc-Saq conjugate. – Aa-Suc-Saq conjugate is free from cytotoxicity and show excellent metabolic stability because it shows less affinity toward CYP314.
16	Stearoyl chloride -Isoniazid conjugate	<ul style="list-style-type: none"> – Isoniazid-stearoyl chloride conjugate is effective in tuberculosis infection, by intracellular transfer into endosomal and lysosomal vesicles. – The addition of hydrophilic drug isoniazid to short lipid chain stearoyl chloride result into increase of Isoniazid's bioavailability.

References

- 1 <https://www.medicinenet.com/cancer/defination.com>
- 2 Allen, T.M. (2002). Ligand-targeted therapeutics in anticancer therapy. *Nature Reviews Cancer*, 2(10), 750–763. <https://doi.org/10.1038/nrc903>
- 3 Chari, R.V.J. (1998). Targeted delivery of chemotherapeutics: Tumor-activated prodrug therapy. *Advanced Drug Delivery Reviews*, 31(1), 89–104. [https://doi.org/10.1016/S0169-409X\(97\)00095-1](https://doi.org/10.1016/S0169-409X(97)00095-1)
- 4 Ojima, I., Geng, X., Wu, X., Qu, C., Borella, C.P., & Xie, H. et al. (2002). Tumor-Specific Novel Taxoid–Monoclonal Antibody Conjugates. *Journal of Medicinal Chemistry*, 45(26), 5620–5623. <https://doi.org/10.1021/jm025540g>
- 5 Jaracz, S., Chen, J., Kuznetsova, L. V., & Ojima, I. (2005). Recent advances in tumor-targeting anticancer drug conjugates. *Bioorganic & Medicinal Chemistry*, 13(17), 5043–5054. <https://doi.org/10.1016/j.bmc.2005.04.084>
- 6 Yan, Y., Dong, Y., Yue, S., Qiu, X., Sun, H., & Zhong, Z. (2019). Dually Active Targeting Nanomedicines Based on a Direct Conjugate of Two Purely Natural Ligands for Potent Chemotherapy of Ovarian Tumors. *ACS Applied Materials & Interfaces*, 11(50), 46548–46557. <https://doi.org/10.1021/acsami.9b17223>
- 7 Zhong, Y., Meng, F., Deng, C., & Zhong, Z. (2014). Ligand-Directed Active Tumor-Targeting Polymeric Nanoparticles for Cancer Chemotherapy. *Biomacromolecules*, 15(6), 1955–1969. <https://doi.org/10.1021/bm5003009>
- 8 Zagami, R., Rapozzi, V., Piperno, A., Scala, A., Triolo, C., & Trapani, M. et al. (2019). Folate-Decorated Amphiphilic Cyclodextrins as Cell-Targeted Nanophototherapeutics. *Biomacromolecules*, 20(7), 2530–2544. <https://doi.org/10.1021/acs.biomac.9b00306>
- 9 Sun, H., Dong, Y., Feijen, J., & Zhong, Z. (2018). Peptide-decorated polymeric nanomedicines for precision cancer therapy. *Journal of Controlled Release*, 290, 11–27. <https://doi.org/10.1016/j.jconrel.2018.09.029>
- 10 Jiang, Z., Guan, J., Qian, J., & Zhan, C. (2019). Peptide ligand-mediated targeted drug delivery of nanomedicines. *Biomaterials Science*, 7(2), 461–471. <https://doi.org/10.1039/C8BM01340C>
- 11 Srinivasarao, M., Galliford, C.V., & Low, P.S. (2015). Principles in the design of ligand-targeted cancer therapeutics and imaging agents. *Nature Reviews Drug Discovery*, 14(3), 203–219. <https://doi.org/10.1038/nrd4519>
- 12 Srinivasarao, M., & Low, P.S. (2017, September 12). *Ligand-Targeted Drug Delivery* (world) [Review-article]. American Chemical Society. <https://doi.org/10.1021/acs.chemrev.7b00013>
- 13 Muro, S. (2012). Challenges in design and characterization of ligand-targeted drug delivery systems. *Journal of Controlled Release*, 164(2), 125–137. <https://doi.org/10.1016/j.jconrel.2012.05.052>
- 14 Ojima, I. (2008). Guided Molecular Missiles for Tumor-Targeting Chemotherapy — Case Studies Using the Second-Generation Taxoids as Warheads. *Accounts of Chemical Research*, 41(1), 108–119. <https://doi.org/10.1021/ar700093f>
- 15 Russell-Jones, G., McTavish, K., McEwan, J., Rice, J., & Nowotnik, D. (2004). Vitamin-mediated targeting as a potential mechanism to increase drug uptake by tumours. *Journal of Inorganic Biochemistry*, 98(10), 1625–1633. <https://doi.org/10.1016/j.jinorgbio.2004.07.009>
- 16 Chen, S., Zhao, X., Chen, J., Chen, J., Kuznetsova, L., Wong, S.S., & Ojima, I. (2010). Mechanism-Based Tumor-Targeting Drug Delivery System. Validation of Efficient Vitamin Receptor-Mediated Endocytosis and Drug Release. *Bioconjugate Chemistry*, 21(5), 979–987. <https://doi.org/10.1021/bc9005656>
- 17 Leamon, C.P., & Reddy, J.A. (2004). Folate-targeted chemotherapy. *Advanced Drug Delivery Reviews*, 56(8), 1127–1141. <https://doi.org/10.1016/j.addr.2004.01.008>
- 18 Lu, Y., & Low, P.S. (2002). Folate-mediated delivery of macromolecular anticancer therapeutic agents. *Advanced Drug Delivery Reviews*, 54(5), 675–693. [https://doi.org/10.1016/S0169-409X\(02\)00042-X](https://doi.org/10.1016/S0169-409X(02)00042-X)
- 19 Reddy, J.A., Westrick, E., Vlahov, I., Howard, S.J., Santhapuram, H.K., & Leamon, C.P. (2006). Folate receptor specific antitumor activity of folate–mitomycin conjugates. *Cancer Chemotherapy and Pharmacology*, 58(2), 229–236. <https://doi.org/10.1007/s00280-005-0151-z>
- 20 Leamon, C.P., Reddy, J.A., Vlahov, I.R., Vetzal, M., Parker, N., Nicoson, J.S., Xu, L.-C., & Westrick, E. (2005). Synthesis and Biological Evaluation of EC72: A New Folate-Targeted Chemotherapeutic. *Bioconjugate Chemistry*, 16(4), 803–811. <https://doi.org/10.1021/bc049709b>
- 21 Shi, H., Guo, J., Li, C., & Wang, Z. (2015). A current review of folate receptor alpha as a potential tumor target in non-small-cell lung cancer. *Drug Design, Development and Therapy*, 9, 4989–4996. <https://doi.org/10.2147/DDDT.S90670>
- 22 Zhao, X., Li, H., & Lee, R.J. (2008). Targeted drug delivery via folate receptors. *Expert Opinion on Drug Delivery*, 5(3), 309–319. <https://doi.org/10.1517/17425247.5.3.309>
- 23 Low, Philip Stewart, & Kularatne, S.A. (2009). Folate-targeted therapeutic and imaging agents for cancer. *Current Opinion in Chemical Biology*, 13(3), 256–262. <https://doi.org/10.1016/j.cbpa.2009.03.022>
- 24 Lambert, N., Abdalla, A.E., Duan, X., & Xie, J. (2017). Emerging drugs and drug targets against tuberculosis. *Journal of Drug Targeting*, 25(4), 296–306. <https://doi.org/10.1080/1061186X.2016.1258705>
- 25 Riccardi, G., Pasca, M.R., & Buroni, S. (2009). Mycobacterium tuberculosis: Drug resistance and future perspectives. *Future Microbiology*, 4(5), 597–614. <https://doi.org/10.2217/fmb.09.20>
- 26 Tyagi. (n.d.). *Role of Vitamins B, C, and D in the fight against tuberculosis*. Retrieved January 18, 2021, from <https://www.ijmyco.org/article.asp?issn=2212-5531; year=2017; volume=6; issue=4; spage=328; epage=332; aulast=Tyagi>
- 27 Tomioka, H. (2006). Current Status of Some Antituberculosis Drugs and the Development of new Antituberculous Agents with Special Reference to their In Vitro and In Vivo Antimicrobial Activities. *Current Pharmaceutical Design*, 12(31), 4047–4070. <https://doi.org/10.2174/138161206778743646>
- 28 Ojima, I., Zuniga, E.S., Berger, W.T., & Seitz, J.D. (2011). Tumor-targeting drug delivery of new-generation taxoids. *Future Medicinal Chemistry*, 4(1), 33–50. <https://doi.org/10.4155/fmc.11.167>

- 29 Collins, D.A., & Hogenkamp, H.P. (2009). *Cobalamin conjugates useful as antitumor agents* (United States Patent No. US20090060837A1). <https://patents.google.com/patent/US20090060837A1/en>
- 30 Weinschenker, N.M., West, F.G., Araneo, B.A., & Li, W. (2007). *Cobalamin conjugates for antitumor therapy* (United States Patent No. US7232805B2). <https://patents.google.com/patent/US7232805B2/en>
- 31 Pettenuzzo, A., Pigot, R., & Ronconi, L. (2017). Vitamin B12–Metal Conjugates for Targeted Chemotherapy and Diagnosis: Current Status and Future Prospects. *European Journal of Inorganic Chemistry*, 2017(12), 1625–1638. <https://doi.org/10.1002/ejic.201601217>
- 32 Krall, N., Scheuermann, J., & Neri, D. (2013). Small Targeted Cytotoxics: Current State and Promises from DNA-Encoded Chemical Libraries. *Angewandte Chemie International Edition*, 52(5), 1384–1402. <https://doi.org/10.1002/anie.201204631>
- 33 Boulikas, T., Pantos, A., Bellis, E., & Christofis, P. (n.d.). *Designing platinum compounds in cancer: Structures and mechanisms*, 48.
- 34 Akepec, M.A., Galanski, M., Arion, V.B., Hartinger, C.G., & Keppler, B.K. (2007). Antitumour metal compounds: More than theme and variations. *Dalton Transactions*, 2, 183–194. <https://doi.org/10.1039/B712656P>
- 35 Kelland, L. (2007). The resurgence of platinum-based cancer chemotherapy. *Nature Reviews Cancer*, 7(8), 573–584. <https://doi.org/10.1038/nrc2167>
- 36 Mundwiler, S., Spingler, B., Kurz, P., Kunze, S., & Alberto, R. (2005). Cyanide-Bridged Vitamin B12–Cisplatin Conjugates. *Chemistry — A European Journal*, 11(14), 4089–4095. <https://doi.org/10.1002/chem.200500117>
- 37 Ruiz-Sánchez, P., König, C., Ferrari, S., & Alberto, R. (2011). Vitamin B12 as a carrier for targeted platinum delivery: In vitro cytotoxicity and mechanistic studies. *JBIC Journal of Biological Inorganic Chemistry*, 16(1), 33–44. <https://doi.org/10.1007/s00775-010-0697-z>
- 38 Bagnato, J.D., Eilers, A.L., Horton, R.A., & Grissom, C.B. (2004). Synthesis and Characterization of a Cobalamin–Colchicine Conjugate as a Novel Tumor-Targeted Cytotoxin. *The Journal of Organic Chemistry*, 69(26), 8987–8996. <https://doi.org/10.1021/jo049953w>
- 39 Kubler, P.A. (2000). Fatal colchicine toxicity. *Medical Journal of Australia*, 172(10), 498–499.
- 40 Iacobuzio-Donahue, C.A., Lee, E.L., Abraham, S.C., Yardley, J.H., & Wu, T.-T. (2001). Colchicine Toxicity: Distinct Morphologic Findings in Gastrointestinal Biopsies. *The American Journal of Surgical Pathology*, 25(8), 1067–1073.
- 41 Kratz, F., Beyer, U., & Schutte, M.T. (1999). Drug-Polymer Conjugates Containing Acid-Cleavable Bonds. *Critical Reviews & Trade; in Therapeutic Drug Carrier Systems*, 16(3). <https://doi.org/10.1615/CritRevTherDrugCarrierSyst.v16.i3.10>
- 42 Baker, M.A., Gray, B.D., Ohlsson-Wilhelm, B.M., Carpenter, D.C., & Muirhead, K.A. (1996). Zyn-Linked colchicines: Controlled-release lipophilic prodrugs with enhanced antitumor efficacy. *Journal of Controlled Release*, 40(1), 89–100. [https://doi.org/10.1016/0168-3659\(95\)00177-8](https://doi.org/10.1016/0168-3659(95)00177-8)
- 43 Mons, S., Veretout, F., Carlier, M.-F., Erk, I., Lepault, J., & Trudel, E. et al. (2000). The interaction between lipid derivatives of colchicine and tubulin: Consequences of the interaction of the alkaloid with lipid membranes. *Biochimica et Biophysica Acta (BBA) — Biomembranes*, 1468(1), 381–395. [https://doi.org/10.1016/S0005-2736\(00\)00279-0](https://doi.org/10.1016/S0005-2736(00)00279-0)
- 44 Vlahov, I.R., & Leamon, C.P. (2012). Engineering Folate–Drug Conjugates to Target Cancer: From Chemistry to Clinic. *Bioconjugate Chemistry*, 23(7), 1357–1369. <https://doi.org/10.1021/bc2005522>
- 45 Farran, B., Montenegro, R.C., Kasa, P., Pavitra, E., Huh, Y. S., & Han, Y.-K. et al. (2020). Folate-conjugated nanovehicles: Strategies for cancer therapy. *Materials Science and Engineering: C*, 107, 110341. <https://doi.org/10.1016/j.msec.2019.110341>
- 46 Low, P.S., Henne, W.A., & Doornweerd, D.D. (2008). Discovery and Development of Folic-Acid-Based Receptor Targeting for Imaging and Therapy of Cancer and Inflammatory Diseases. *Accounts of Chemical Research*, 41(1), 120–129. <https://doi.org/10.1021/ar7000815>
- 47 Geersing, A., de Vries, R.H., Jansen, G., Rots, M.G., & Roelfes, G. (2019). Folic acid conjugates of a bleomycin mimic for selective targeting of folate receptor positive cancer cells. *Bioorganic & Medicinal Chemistry Letters*, 29(15), 1922–1927. <https://doi.org/10.1016/j.bmcl.2019.05.047>
- 48 Chiani, M., Norouziyan, D., Shokrgozar, M.A., Azadmanesh, K., Najmafshar, A., Mehrabi, M.R., & Akbarzadeh, A. (2018). Folic acid conjugated nanoliposomes as promising carriers for targeted delivery of bleomycin. *Artificial Cells, Nanomedicine, and Biotechnology*, 46(4), 757–763. <https://doi.org/10.1080/21691401.2017.1337029>
- 49 Blum, R.H., Carter, S.K., & Agre, K. (1973). A clinical review of bleomycin — A new antineoplastic agent. *Cancer*, 31(4), 903–914. [https://doi.org/10.1002/1097-0142\(197304\)31:4<903::AID-CNCR2820310422>3.0.CO;2-N](https://doi.org/10.1002/1097-0142(197304)31:4<903::AID-CNCR2820310422>3.0.CO;2-N)
- 50 Chung, K.N., Saikawa, Y., Paik, T.H., Dixon, K.H., Mulligan, T., Cowan, K.H., & Elwood, P.C. (1993). Stable transfectants of human MCF-7 breast cancer cells with increased levels of the human folate receptor exhibit an increased sensitivity to antifolates. *The Journal of Clinical Investigation*, 91(4), 1289–1294. <https://doi.org/10.1172/JCI116327>
- 51 Lee, M.H., Sessler, J.L., & Kim, J.S. (2015). Disulfide-Based Multifunctional Conjugates for Targeted Theranostic Drug Delivery. *Accounts of Chemical Research*, 48(11), 2935–2946. <https://doi.org/10.1021/acs.accounts.5b00406>
- 52 Pinhassi, R.I., Assaraf, Y.G., Farber, S., Stark, M., Ickowicz, D., & Drori, S. et al. (2010). Arabinogalactan–Folic Acid–Drug Conjugate for Targeted Delivery and Target-Activated Release of Anticancer Drugs to Folate Receptor-Overexpressing Cells. *Biomacromolecules*, 11(1), 294–303. <https://doi.org/10.1021/bm900853z>
- 53 Ickowicz, D.E., Farber, S., Sionov, E., Kagan, S., Hoffman, A., Polacheck, I., & Domb, A.J. (2014). Activity, Reduced Toxicity, and Scale-Up Synthesis of Amphotericin B-Conjugated Polysaccharide. *Biomacromolecules*, 15(6), 2079–2089. <https://doi.org/10.1021/bm5002125>
- 54 Duncan, R. (2003). The dawning era of polymer therapeutics. *Nature Reviews Drug Discovery*, 2(5), 347–360. <https://doi.org/10.1038/nrd1088>
- 55 Assaraf, Y.G. (2006). The role of multidrug resistance efflux transporters in antifolate resistance and folate homeostasis. *Drug Resistance Updates*, 9(4), 227–246. <https://doi.org/10.1016/j.drug.2006.09.001>

- 56 Esmaeili, F., Ghahremani, M.H., Ostad, S.N., Atyabi, F., Seyedabadi, M., & Malekshahi, M. R. et al. (2008). Folate-receptor-targeted delivery of docetaxel nanoparticles prepared by PLGA-PEG-folate conjugate. *Journal of Drug Targeting*, 16(5), 415–423. <https://doi.org/10.1080/10611860802088630>
- 57 Kwon, G.S., & Okano, T. (1996). Polymeric micelles as new drug carriers. *Advanced Drug Delivery Reviews*, 21(2), 107–116. [https://doi.org/10.1016/S0169-409X\(96\)00401-2](https://doi.org/10.1016/S0169-409X(96)00401-2)
- 58 Guo, W., Lee, T., Sudimack, J., & Lee, R.J. (2000). Receptor-Specific Delivery of Liposomes Via Folate-Peg-Chol. *Journal of Liposome Research*, 10(2–3), 179–195. <https://doi.org/10.3109/08982100009029385>
- 59 Yoo, H.S., & Park, T.G. (2001). Biodegradable polymeric micelles composed of doxorubicin conjugated PLGA-PEG block co-polymer. *Journal of Controlled Release*, 70(1), 63–70. [https://doi.org/10.1016/S0168-3659\(00\)00340-0](https://doi.org/10.1016/S0168-3659(00)00340-0)
- 60 Yoo, H.S., & Park, T.G. (2004). Folate-receptor-targeted delivery of doxorubicin nano-aggregates stabilized by doxorubicin-PEG-folate conjugate. *Journal of Controlled Release*, 100(2), 247–256. <https://doi.org/10.1016/j.jconrel.2004.08.017>
- 61 Gabizon, A., Shmeeda, H., Horowitz, A. T., & Zalipsky, S. (2004). Tumor cell targeting of liposome-entrapped drugs with phospholipid-anchored folic acid-PEG conjugates. *Advanced Drug Delivery Reviews*, 56(8), 1177–1192. <https://doi.org/10.1016/j.addr.2004.01.011>
- 62 H, M. (2001). The enhanced permeability and retention (EPR) effect in tumor vasculature: The key role of tumor-selective macromolecular drug targeting. *Advances in Enzyme Regulation*, 41, 189–207. [https://doi.org/10.1016/s0065-2571\(00\)00013-3](https://doi.org/10.1016/s0065-2571(00)00013-3)
- 63 Jain, R.K. (2001). Delivery of molecular medicine to solid tumors: Lessons from in vivo imaging of gene expression and function. *Journal of Controlled Release*, 74(1), 7–25. [https://doi.org/10.1016/S0168-3659\(01\)00306-6](https://doi.org/10.1016/S0168-3659(01)00306-6)
- 64 Gabizon, A., Horowitz, A.T., Goren, D., Tzemach, D., Mandelbaum-Shavit, F., Qazen, M.M., & Zalipsky, S. (1999). Targeting Folate Receptor with Folate Linked to Extremities of Poly(ethylene glycol)-Grafted Liposomes: In Vitro Studies. *Bioconjugate Chemistry*, 10(2), 289–298. <https://doi.org/10.1021/bc9801124>
- 65 Gabizon, A., Horowitz, A.T., Goren, D., Tzemach, D., Shmeeda, H., & Zalipsky, S. (2003). In Vivo Fate of Folate-Targeted Polyethylene-Glycol Liposomes in Tumor-Bearing Mice. *Clinical Cancer Research*, 9(17), 6551–6559.
- 66 Wang, Y., Li, P., Chen, L., Gao, W., Zeng, F., & Kong, L.X. (2015). Targeted delivery of 5-fluorouracil to HT-29 cells using high efficient folic acid-conjugated nanoparticles. *Drug Delivery*, 22(2), 191–198. <https://doi.org/10.3109/10717544.2013.875603>
- 67 Chen, Y.-S., Alany, R.G., Young, S.A., Green, C.R., & Rupenthal, I.D. (2011). In vitro release characteristics and cellular uptake of poly(D,L-lactic-co-glycolic acid) nanoparticles for topical delivery of antisense oligodeoxynucleotides. *Drug Delivery*, 18(7), 493–501. <https://doi.org/10.3109/10717544.2011.589088>
- 68 Anfi, L., Guanti, G., & Riva, R. (1999). Synthesis of asymmetricized 2-benzyl-1,3-diaminopropane by a chemoenzymatic route: A tool for combinatorially developing peptidomimetics. *Tetrahedron: Asymmetry*, 10(18), 3571–3592. [https://doi.org/10.1016/S0957-4166\(99\)00371-7](https://doi.org/10.1016/S0957-4166(99)00371-7)
- 69 Gupta, Y., Jain, A., Jain, P., & Jain, S.K. (2007). Design and development of folate appended liposomes for enhanced delivery of 5-FU to tumor cells. *Journal of Drug Targeting*, 15(3), 231–240. <https://doi.org/10.1080/10611860701289719>
- 70 Sharma, M., Malik, R., Verma, A., Dwivedi, P., Banoth, G.S., & Pandey, N. et al. (2013). Folic Acid Conjugated Guar Gum Nanoparticles for Targeting Methotrexate to Colon Cancer. *Journal of Biomedical Nanotechnology*, 9(1), 96–106. <https://doi.org/10.1166/jbn.2013.1474>
- 71 Praetorius, N.P., & Mandal, T.K. (2007). Engineered Nanoparticles in Cancer Therapy. *Recent Patents on Drug Delivery & Formulation*, 1(1), 37–51. <https://doi.org/10.2174/187221107779814104>
- 72 Soppimath, K.S., Aminabhavi, T.M., Kulkarni, A.R., & Rudzinski, W.E. (2001). Biodegradable polymeric nanoparticles as drug delivery devices. *Journal of Controlled Release*, 70(1), 1–20. [https://doi.org/10.1016/S0168-3659\(00\)00339-4](https://doi.org/10.1016/S0168-3659(00)00339-4)
- 73 Chourasia, M.K., & Jain, S.K. (2004a). Polysaccharides for Colon Targeted Drug Delivery. *Drug Delivery*, 11(2), 129–148. <https://doi.org/10.1080/10717540490280778>
- 74 Chourasia, M.K., & Jain, S.K. (2004b). Potential of Guar Gum Microspheres for Target Specific Drug Release to Colon. *Journal of Drug Targeting*, 12(7), 435–442. <https://doi.org/10.1080/1061186040006604>
- 75 Thomas, T.P., Huang, B., Choi, S.K., Silpe, J.E., Kotlyar, A., & Desai, A.M. et al. (2012). Polyvalent Dendrimer-Methotrexate as a Folate Receptor-Targeted Cancer Therapeutic. *Molecular Pharmaceutics*, 9(9), 2669–2676. <https://doi.org/10.1021/mp3002232>
- 76 Nanjwade, B.K., Bechra, H.M., Derkar, G K., Manvi, F.V., & Nanjwade, V.K. (2009). Dendrimers: Emerging polymers for drug-delivery systems. *European Journal of Pharmaceutical Sciences*, 38(3), 185–196. <https://doi.org/10.1016/j.ejps.2009.07.008>
- 77 Quintana, A., Raczka, E., Piehler, L., Lee, I., Myc, A., & Majoros, I. et al. (2002). Design and Function of a Dendrimer-Based Therapeutic Nanodevice Targeted to Tumor Cells Through the Folate Receptor. *Pharmaceutical Research*, 19(9), 1310–1316. <https://doi.org/10.1023/A:1020398624602>
- 78 Majoros, I.J., Thomas, T.P., Mehta, C.B., & Baker, J.R. (2005). Poly(amidoamine) Dendrimer-Based Multifunctional Engineered Nanodevice for Cancer Therapy. *Journal of Medicinal Chemistry*, 48(19), 5892–5899. <https://doi.org/10.1021/jm0401863>
- 79 Majoros, I.J., Williams, C.R., Becker, A., & Baker, J.R. (2009). Methotrexate delivery via folate targeted dendrimer-based nanotherapeutic platform. *WIREs Nanomedicine and Nanobiotechnology*, 1(5), 502–510. <https://doi.org/10.1002/wnan.37>
- 80 Mullen, D.G., Fang, M., Desai, A., Baker, J.R., Orr, B.G., & Banaszak Holl, M.M. (2010). A Quantitative Assessment of Nanoparticle-Ligand Distributions: Implications for Targeted Drug and Imaging Delivery in Dendrimer Conjugates. *ACS Nano*, 4(2), 657–670. <https://doi.org/10.1021/nn900999c>
- 81 Gillies, E.R., & Fréchet, J.M.J. (2005). Dendrimers and dendritic polymers in drug delivery. *Drug Discovery Today*, 10(1), 35–43. [https://doi.org/10.1016/S1359-6446\(04\)03276-3](https://doi.org/10.1016/S1359-6446(04)03276-3)
- 82 Zhang, Y., Thomas, T.P., Desai, A., Zong, H., Leroueil, P.R., Majoros, I.J., & Baker, J.R. (2010). Targeted Dendrimeric Anticancer Prodrug: A Methotrexate-Folic Acid-Poly(amidoamine) Conjugate and a Novel, Rapid, «One Pot» Synthetic Approach. *Bioconjugate Chemistry*, 21(3), 489–495. <https://doi.org/10.1021/bc9003958>
- 83 Tripodo, G., Mandracchia, D., Collina, S., Rui, M., & Rossi, D. (2014). New Perspectives in Cancer Therapy: The Biotin-Antitumor Molecule Conjugates. *Open Access*, 8.

- 84 Maiti, Santanu, & Paira, P. (2018). Biotin conjugated organic molecules and proteins for cancer therapy: A review. *European Journal of Medicinal Chemistry*, 145, 206–223. <https://doi.org/10.1016/j.ejmech.2018.01.001>
- 85 Yang, W., Cheng, Y., Xu, T., Wang, X., & Wen, L. (2009). Targeting cancer cells with biotin–dendrimer conjugates. *European Journal of Medicinal Chemistry*, 44(2), 862–868. <https://doi.org/10.1016/j.ejmech.2008.04.021>
- 86 Maiti, Sukhendu, Park, N., Han, J.H., Jeon, H.M., Lee, J.H., Bhuniya, S., Kang, C., & Kim, J.S. (2013). Gemcitabine–Coumarin–Biotin Conjugates: A Target Specific Theranostic Anticancer Prodrug. *Journal of the American Chemical Society*, 135(11), 4567–4572. <https://doi.org/10.1021/ja401350x>
- 87 Lee, M.H., Kim, J.Y., Han, J.H., Bhuniya, S., Sessler, J.L., Kang, C., & Kim, J.S. (2012). Direct fluorescence monitoring of the delivery and cellular uptake of a cancer-targeted RGD peptide-appended naphthalimide theraagnostic prodrug. *Journal of the American Chemical Society*, 134(30), 12668–12674.
- 88 Cordero, F.M., Bonanno, P., Chioccioli, M., Gratteri, P., Robina, I., Moreno Vargas, A. J., & Brandi, A. (2011). Diversity-oriented syntheses of 7-substituted lentiniginosines. *Tetrahedron*, 67(49), 9555–9564. <https://doi.org/10.1016/j.tet.2011.10.008>
- 89 Gregory, J.D. (2002, May 1). *The Stability of N-Ethylmaleimide and its Reaction with Sulfhydryl Groups* (world). American Chemical Society. <https://doi.org/10.1021/ja01619a073>
- 90 Neuzil, J., Weber, T., Gellert, N., & Weber, C. (2001). Selective cancer cell killing by α -tocopheryl succinate. *British Journal of Cancer*, 84(1), 87–89. <https://doi.org/10.1054/bjoc.2000.1559>
- 91 Rathod, S., Bahadur, P., & Tiwari, S. (2021). Nanocarriers based on vitamin E-TPGS: Design principle and molecular insights into improving the efficacy of anticancer drugs. *International Journal of Pharmaceutics*, 592, 120045. <https://doi.org/10.1016/j.ijpharm.2020.120045>
- 92 Abu-Fayyad, A., & Nazzal, S. (2017). Gemcitabine-vitamin E conjugates: Synthesis, characterization, entrapment into nano-emulsions, and in-vitro deamination and antitumor activity. *International Journal of Pharmaceutics*, 528(1), 463–470. <https://doi.org/10.1016/j.ijpharm.2017.06.031>
- 93 Andersson, R., Aho, U., Nilsson, B.I., Peters, G.J., Pastor-Anglada, M., Rasch, W., & Sandvold, M.L. (2009). Gemcitabine chemoresistance in pancreatic cancer: Molecular mechanisms and potential solutions. *Scandinavian Journal of Gastroenterology*, 44(7), 782–786. <https://doi.org/10.1080/00365520902745039>
- 94 Abu-Fayyad, A., Behery, F., Sallam, A.A., Alqahtani, S., Ebrahim, H., & El Sayed, K.A. et al. (2015). PEGylated γ -tocotrienol isomer of vitamin E: Synthesis, characterization, in vitro cytotoxicity, and oral bioavailability. *European Journal of Pharmaceutics and Biopharmaceutics*, 96, 185–195. <https://doi.org/10.1016/j.ejpb.2015.07.022>
- 95 Lansakara-P., D.S.P., Rodriguez, B.L., & Cui, Z. (2012). Synthesis and in vitro evaluation of novel lipophilic monophosphorylated gemcitabine derivatives and their nanoparticles. *International Journal of Pharmaceutics*, 429(1), 123–134. <https://doi.org/10.1016/j.ijpharm.2012.03.014>
- 96 Cateni, F., Zacchigna, M., & Procida, G. (2020). Synthesis and controlled drug delivery studies of a novel Ubiquinol-Polyethylene glycol-Vitamin E adduct. *Bioorganic Chemistry*, 105, 104329. <https://doi.org/10.1016/j.bioorg.2020.104329>
- 97 Bhagavan, H.N., & Chopra, R.K. (2006). Coenzyme Q10: Absorption, tissue uptake, metabolism and pharmacokinetics. *Free Radical Research*, 40(5), 445–453. <https://doi.org/10.1080/10715760600617843>
- 98 James, A.M., Smith, R.A.J., & Murphy, M.P. (2004). Antioxidant and prooxidant properties of mitochondrial Coenzyme Q. *Archives of Biochemistry and Biophysics*, 423(1), 47–56. <https://doi.org/10.1016/j.abb.2003.12.025>
- 99 Cervellati, R., & Greco, E. (2016). In vitro Antioxidant Activity of Ubiquinone and Ubiquinol, Compared to Vitamin E. *Helvetica Chimica Acta*, 99(1), 41–45. <https://doi.org/10.1002/hlca.201500124>
- 100 Iwata, R., Nakayama, F., Hirochi, S., Sato, K., Piao, W., & Nishina, K. et al. (2015). Synthesis and properties of vitamin E analog-conjugated neomycin for delivery of RNAi drugs to liver cells. *Bioorganic & Medicinal Chemistry Letters*, 25(4), 815–819. <https://doi.org/10.1016/j.bmcl.2014.12.079>
- 101 Desigaux, L., Sainlos, M., Lambert, O., Chevre, R., Letrou-Bonneval, E., & Vigneron, J.-P. et al. (2007). Self-assembled lamellar complexes of siRNA with lipidic aminoglycoside derivatives promote efficient siRNA delivery and interference. *Proceedings of the National Academy of Sciences*, 104(42), 16534–16539. <https://doi.org/10.1073/pnas.0707431104>
- 102 Kutty, R.V., & Feng, S.-S. (2013). Cetuximab conjugated vitamin E TPGS micelles for targeted delivery of docetaxel for treatment of triple negative breast cancers. *Biomaterials*, 34(38), 10160–10171. <https://doi.org/10.1016/j.biomaterials.2013.09.043>
- 103 Nguyen, P., Taghian, A., Katz, M., Niemierko, A., Raad, R., & Boon, W. et al. (2008). Breast Cancer Subtype Approximated by Estrogen Receptor, Progesterone Receptor, and HER-2 Is Associated With Local and Distant Recurrence After Breast-Conserving Therapy. *Journal of Clinical Oncology: Official Journal of the American Society of Clinical Oncology*, 26, 2373–2378. <https://doi.org/10.1200/JCO.2007.14.4287>
- 104 Muthu, M.S., Avinash Kulkarni, S., Liu, Y., & Feng, S.-S. (2012). Development of docetaxel-loaded vitamin E TPGS micelles: Formulation optimization, effects on brain cancer cells and biodistribution in rats. *Nanomedicine*, 7(3), 353–364. <https://doi.org/10.2217/nnm.11.111>
- 105 Wong, C., & Chen, S. (2012). The development, application and limitations of breast cancer cell lines to study tamoxifen and aromatase inhibitor resistance. *The Journal of Steroid Biochemistry and Molecular Biology*, 131(3), 83–92. <https://doi.org/10.1016/j.jsbmb.2011.12.005>
- 106 Luo, S., Wang, Z., Patel, M., Khurana, V., Zhu, X., Pal, D., & Mitra, Ashim. K. (2011). Targeting SVCT for enhanced drug absorption: Synthesis and in vitro evaluation of a novel vitamin C conjugated prodrug of saquinavir. *International Journal of Pharmaceutics*, 414(1), 77–85. <https://doi.org/10.1016/j.ijpharm.2011.05.001>
- 107 Boyer, J.C., Campbell, C.E., Sigurdson, W.J., & Kuo, S.-M. (2005). Polarized localization of vitamin C transporters, SVCT1 and SVCT2, in epithelial cells. *Biochemical and Biophysical Research Communications*, 334(1), 150–156. <https://doi.org/10.1016/j.bbrc.2005.06.069>
- 108 Varma, M.V.S., Ashokraj, Y., Dey, C.S., & Panchagnula, R. (2003). P-glycoprotein inhibitors and their screening: A perspective from bioavailability enhancement. *Pharmacological Research*, 48(4), 347–359. [https://doi.org/10.1016/S1043-6618\(03\)00158-0](https://doi.org/10.1016/S1043-6618(03)00158-0)

- 109 Luo, S., Wang, Z., Kansara, V., Pal, D., & Mitra, Ashim, K. (2008). Activity of a sodium-dependent vitamin C transporter (SVCT) in MDCK-MDR1 cells and mechanism of ascorbate uptake. *International Journal of Pharmaceutics*, 358(1), 168–176. <https://doi.org/10.1016/j.ijpharm.2008.03.002>
- 110 Pandit, S., Roy, S., Pillai, J., & Banerjee, S. (2020). Formulation and Intracellular Trafficking of Lipid–Drug Conjugate Nanoparticles Containing a Hydrophilic Anti-tubercular Drug for Improved Intracellular Delivery to Human Macrophages. *ACS Omega*, 5(9), 4433–4448. <https://doi.org/10.1021/acsomega.9b03523>
- 111 Thalla, M., Gangasani, J., Saha, P., Ponneganti, S., Borkar, R.M., & Naidu, V. et al. (2020). Synthesis, Characterizations, and Use of O-Stearoyl Mannose Ligand-Engineered Lipid Nanoarchitectonics for Alveolar Macrophage Targeting. *ASSAY and Drug Development Technologies*. <https://doi.org/10.1089/adt.2020.999>
- 112 Alven, S., Nqoro, X., Buyana, B., & Aderibigbe, B.A. (2020). Polymer-Drug Conjugate, a Potential Therapeutic to Combat Breast and Lung Cancer. *Pharmaceutics*, 12(5), 406. <https://doi.org/10.3390/pharmaceutics12050406>
- 113 Elvira, C., Gallardo, A., Roman, J., & Cifuentes, A. (2005). Covalent Polymer-Drug Conjugates. *Molecules*, 10(1), 114–125. <https://doi.org/10.3390/10010114>
- 114 Kakde, D., Jain, D., Shrivastava, V., Kakde, R., & Patil, A.T. (n.d.). Cancer Therapeutics- Opportunities, Challenges and Advances in Drug Delivery. *Journal of Applied Pharmaceutical Science*, 10.
- 115 Suksiriworapong, J., Taresco, V., Ivanov, D.P., Styliari, I.D., Sakchaisri, K., Junyaprasert, V.B., & Garnett, M.C. (2018). Synthesis and properties of a biodegradable polymer-drug conjugate: Methotrexate-poly(glycerol adipate). *Colloids and Surfaces B: Biointerfaces*, 167, 115–125. <https://doi.org/10.1016/j.colsurfb.2018.03.048>
- 116 Karimi, N., Soleiman-Beigi, M., & Fattahi, A. (2020). Co-delivery of all-trans-retinoic acid and docetaxel in drug conjugated polymeric nanoparticles: Improving controlled release and anticancer effect. *Materials Today Communications*, 25, 101280. <https://doi.org/10.1016/j.mtcomm.2020.101280>
- 117 Liu, X.-M., Quan, L.-D., Tian, J., Alnouti, Y., Fu, K., Thiele, G.M., & Wang, D. (2008). Synthesis and Evaluation of a Well-defined HPMA Copolymer–Dexamethasone Conjugate for Effective Treatment of Rheumatoid Arthritis. *Pharmaceutical Research*, 25(12), 2910–2919. <https://doi.org/10.1007/s11095-008-9683-3>

Р.П. Бхоле, Йогита Шинде, Ч.Г. Бонде, Р.Д. Вавхейл

Дәруменді дәрілік конъюгат: фармакологиялық потенциалын жүйелі түрде талдау

Қатерлі ісік өлімге әкелуі мүмкін созылмалы ауру болып табылады. Дәстүрлі химиотерапияда цитотоксикалық препараттар көбейіп бара жатқан қатерлі ісік жасушаларын жою үшін қолданылады. Цитоуытты агенттің талғамдығы төмен болады, биологиялық белсенділік танытпайды, жүйелік уыттылық пен жағымсыз әсер етеді. Жыл сайын халықтың 1,8 миллионға жуығы туберкулез инфекциясын жұқтырып, соның салдарынан қайтыс болады. Туберкулезді емдеу кезінде дәрілік затқа төзімділіктің жоғарылауы маңызды мәселе болып табылады. Сонымен, дәріге тұрақтылықты, туберкулез инфекциясындағы дәрілік селективтілікті және цитоуытты агент пен туберкулезге қарсы препараттардың жанама әсерлерін азайтуды шешудің жаңа әдісін немесе терапиясын жасау өте өзекті мәселе. Бұл шолу мақалада жаңадан пайда болған «дәрумен–дәрілік конъюгаты» тұжырымдамасы сипатталған. Дәрумен–дәрілік конъюгат — бұл мақсатты орынға қарай арнайы жеткізілетін препарат, қатерлі ісік және туберкулез сияқты созылмалы ауруларды емдеудің және терапевтік нәтижелерді жақсартудың перспективалы әдістерінің бірі. Жұмыстың мақсаты — жаңа қатерлі ісікке және туберкулезге қарсы препараттың құрамына кіретін дәруменнің әсерін зерттеуге, селективті емес, жүйелік уыттылық және көп дәрілікке төзімділік сияқты қиындықтарды жеңуге бағытталған. Бұл тәсіл өмірге қауіп төндіретін қатерлі ісік, туберкулез сияқты ауруларды емдеуде және көптеген вирустық инфекцияларда тиімді.

Кілт сөздер: қатерлі ісік, туберкулез, дәрумен–дәрілік конъюгаты, В12 дәрумені конъюгаты, фолий қышқылының конъюгаты, биотин конъюгаты, Е дәрумені конъюгаты, липидті дәрі конъюгаты.

Р.П. Бхоле, Йогита Шинде, Ч.Г. Бонде, Р.Д. Вавхейл

Конъюгат витамин – лекарственный препарат: систематический обзор фармакологического потенциала

Рак является хроническим заболеванием, которое может привести к смерти. В традиционной химиотерапии цитотоксические препараты используются для уничтожения пролиферирующих раковых клеток. Цитотоксический агент обладает меньшей специфичностью и биологической активностью, также вызывает системную токсичность и нежелательные побочные эффекты. Ежегодно около 1,8 миллиона человек заражаются и умирают от туберкулезной инфекции. Повышение лекарственной устойчивости во время лечения туберкулеза вызывает серьезную озабоченность. Таким образом, необходимо разработать новый подход или методы лечения для устранения лекарственной устойчивости, лекарствен-

ной селективности при туберкулезной инфекции и уменьшения побочных эффектов цитотоксических агентов и противотуберкулезных препаратов. В данной обзорной статье описано недавно появившееся понятие «витаминно-лекарственный конъюгат». Конъюгат витамин–лекарство — препарат, который специально доставляется к месту назначения, и один из многообещающих способов лечения хронических заболеваний, таких как рак и туберкулез, и улучшения терапевтического результата. Цель работы — изучить витамин как целевую составляющую для нового противоопухолевого и противотуберкулезного препарата при преодолении таких проблем, как неселективность, системная токсичность и множественная лекарственная устойчивость. Этот подход полезен и при лечении опасных для жизни заболеваний, таких как вирусные инфекции.

Ключевые слова: рак, туберкулез, конъюгат витамин – лекарство, конъюгат витамина B12, конъюгат фолиевой кислоты, конъюгат биотина, конъюгат витамина E, конъюгат липид – лекарственный препарат.

Information about authors

Bhole, Ritesh Prakash — PhD, Associate Professor, Dr. D.Y. Patil Institute of Pharmaceutical Sciences and Research, Sant Tukaram Nagar, Pimpri, Pune-411018, India; email ritesh.bhole@dypvp.edu.in; <https://orcid.org/0000-0003-4088-7470>

Bonde, Chandrakant Ghansham — PhD, Professor, SPTM, NMIMS, School of Pharmacy, Shirpur, Dist: Dhule, India. Email: chandrakant.bonde@nmims.edu; <https://orcid.org/0000-0001-5712-1119>

Shinde, Yogita — M. Pharm, Research Scholar, Dr. D.Y. Patil Institute of Pharmaceutical Sciences and Research, Sant Tukaram Nagar, Pimpri, Pune-411018, India; email: shindeyogita48@gmail.com.

Wavhale, Ravindra — PhD, Assistant Professor, Dr. D.Y. Patil Institute of Pharmaceutical Sciences and Research, Sant Tukaram Nagar, Pimpri, Pune-411018; ravindra.wavhale@dypvp.edu.in, <https://orcid.org/0000-0003-1614-9742>

PHYSICAL AND ANALYTICAL CHEMISTRY

UDC 544.03; 538.12

<https://doi.org/10.31489/2021Ch1/53-60>

B.P. Shipunov*, M.V. Zakharova

Altai State University, Barnaul, Russia

(*Corresponding author's e-mail: sbp@mc.asu.ru)

Change in the volume of water crystallization as a result of exposure to a high-frequency electromagnetic field

The influence of a high-frequency electromagnetic field on the process of water crystallization has been studied. Water irradiated by a field at 30–200 MHz was kept from 0 to 21 days, then it was frozen. Volumes of ice at crystallization were compared for water irradiated and unirradiated by the field. Values located more or less symmetrically near zero; 2) values with a predominantly positive shift, and 3) values for which the shift is mostly negative. Positive shift was noted when combining 200 MHz and the exposure time up to 11 days. The maximum effect of relative volume increase almost two times was observed at 200 MHz and one day exposure time. The maximum compression of ice approximately three times compared to the unirradiated sample occurred twice: after field effect at 90 MHz and exposure time of 11 days, and at 140 MHz and exposure time of 21 days. The similarity of time dependence at 170 MHz with the dependence of thermal effect of glucose dissolution found in early works was noted. The data obtained confirm that field effect results in both strengthening and loosening of water structure.

Keywords: electromagnetic field, water structure, ice structure, defects in ice structure, frequency of field effect, post-effect changes in water structure, loosening of water structure, strengthening of water structure.

Introduction

The effect of physical fields on water and water-containing systems is of interest not only from an academic standpoint, but also from a practical point of view, since water is one of the most common substances on the earth's surface and is a part of living objects. Interest in liquid water, to which the presence of internal structure is attributed, is due not only to the presence of physical anomalies, but also to a crucial role in biological processes. Magnetic field as well as mechanical (ultrasonic), electrical and electromagnetic ones prevail among the factors of influence. There is a wide variability of influencing factors taking into account the diverse frequency range and field strength. The effect of magnetic field on water and aqueous solution properties are most often presented in literature [1–4]. One of the important issues is to explain the nature of changes in structural organization of water and water solutions due to field effect. Some models assume the presence of monomolecular water and polymolecular formations, which was expressed many years ago by Samoilov, and then by other researchers [5]. We studied crystallization processes when a magnetic field is applied to answer the question about the strengthening or loosening of the structural organization of water [6, 7]. O.M. Rosenthal and his team investigated the kinetics of ice crystal nucleation and growth. It was found that the share of fine-crystalline ice increases, while the dispersion of their size distribution decreases simultaneously in the 3 kE constant magnetic field [6]. O.M. Rosenthal as well as V.S. Dukhanin [3] believed, that the effect of magnetic field loosens the structure of water and promotes the formation of a skeletal rather than a close-packed ice structure. It was shown in [8], that the volume of ice increases by about 1.4 % under the influence of magnetic field.

In turn, electromagnetic fields have a very significant effect on the properties of water and aqueous solutions, which is manifested in changes of pH, electrical conductivity, redox potential, oxygen solubility [9], as well as in changes of the substances reactivity and of the crystalline hydrates thermodynamics [10, 11].

Although the term «water structure» is criticized and perhaps deservedly is applied to liquids, many properties of liquid water can be explained only by the presence of internal structural organization. D. Eisenberg and V. Kautsmann did not find the term «water structure» controversial, including it in the title of their monograph [12]. Zatssepina [13] agrees with them, using the term «structure» as well. However, this term is hardly applicable to dynamic systems, to which liquid water should be attributed. The majority of authors, describing the structural organization of liquid water, refer to the structure of ice, as noted in later reviews [14].

All models mention the nonideal structure of both ice and water to one degree or another. In this regard, it can be expected that structural defects of liquid water will influence the process of its crystallization and affect the properties of ice. There are many methods to study the structural organization of liquid water, such as IR, UV, NMR spectroscopy, dielcometry, etc. However, it is the structure that can be reliably studied directly or indirectly by transferring water to a crystalline state.

Naturally, the question of how the electromagnetic high-frequency field affects the process of water crystallization and the volume of ice was of great interest in order to find out if the water structure is strengthened or loosened due to the field effect.

Experimental

Water preparation. The field impact did not fundamentally differ from the methods used in earlier works. The cell is described in [15]. The experiment was conducted at 30–200 MHz frequency; the exposure time was 90 minutes. A G4–119A generator was used as the source of high-frequency signal. The difference was that the water after field exposure was kept in a closed container for a certain time (from 0 to 21 days), and then it was used in the experiment. This was due to the fact that a complex relationship between frequency and exposure time was found after the field effect [11]. Since we used common equipment, the main attention was paid to the crystallization process which allowed us to obtain the primary experimental data. To increase the reliability of the estimation parameter, it was necessary to determine the ice core size as accurately as possible. For this purpose, the crystallization was implemented in a narrow polypropylene tube with an inner diameter of 5 mm and a length of 125 mm. The tubes were precisely measured in length using a micrometer, sealed on the burner, checked for tightness, and calibrated in length again. The main problem was to organize the process of ice crystal growth so that it starts from the top of the tube, not from the bottom. Since we used a freezing chamber of the refrigerator as a cryochamber, we measured the temperature of mixture of water and glycerin in glasses and studied the temperature field; afterwards we chose a homogeneous area of $10 \times 15 \text{ cm}^2$, where the temperature differed by no more than 1 K. The cassette for tubes was made of PVC foam. It was $10 \times 15 \text{ cm}^2$ in area and 3 cm thick, in which holes were made equal to the diameter of the tubes. The selection of conditions involved changing the distance between the lower edge of the tube and the cooling surface.

If the distance was not optimal, either swelling occurred in the lower part of the tube followed by its destruction, or water was squeezed out and flowed downward with a distortion of the cylindrical shape, or the shape of the ice core deviated from the cylindrical one. The temperature during the experiment was $-2 \text{ }^\circ\text{C}$. The choice of temperature was based on preliminary experiments to obtain the correct core. This was also an important parameter, since the crystallization temperature determined the cooling rate and, consequently, the rate of crystal growth. Each tube was marked individually, and the dimensions were taken into account when calculating the relative change in the core length. Water was poured into the tubes with a thin needle. The control of homogeneity and volume (including the absence of bubbles) was monitored visually in front of the window. The tubes were filled on a level with the upper edge, placed in the cassette holder and put into a cryochamber. The core was measured every other day. Ordinary distilled water was frozen concurrently with the field-exposed water. Each tube was measured exactly before the experiment. After crystallization, we measured its length with a protruding core and determined how much the core was above the edge of the tube, or below it. The measurement was more complicated when the core was below the edge of the tube. In this case, the tube was shone through and the length of the ice column was determined by the shadow contour.

The mean and the confidence interval were determined using five parallel measurements. To quantify the effect of field and time exposure, we determined $\Delta l = l - l_0$, where l is the core above the edge of the tube

for the affected sample and l_0 is the same for the unaffected water. To reduce the effect of error mean square, we estimated the relative effect $\delta l = \Delta l / l_0$. The exposure time was chosen using the data obtained in [11], which indicated that the most significant changes took place within about 20 days. The scale of exposure time after the field effect was as follows: 0 (immediately after the field), 1, 3, 6, 9, 11, and 21 days. Compared with work [11], we increased the number of frequencies of the field effect, making a series of 30, 60, 90, 110, 140, 170, and 200 MHz.

Based on measurements and calculation of the relative change in the core length, the dependences of the relative size of the ice core on the frequency and exposure time of water after the field effect were constructed.

Results and Discussion

Figures 1 and 2 show the dependences of the relative change in the length of the ice core at different exposure time for all frequencies used in the experiment. To simplify the analysis, we present the dependences in two figures.

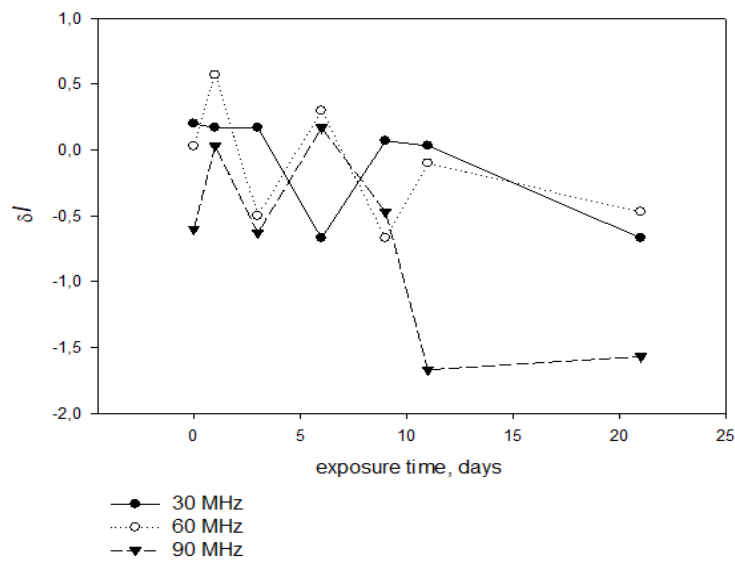


Figure 1. Dependence of the relative change in the length of the ice core on the exposure time after the field effect at given frequencies

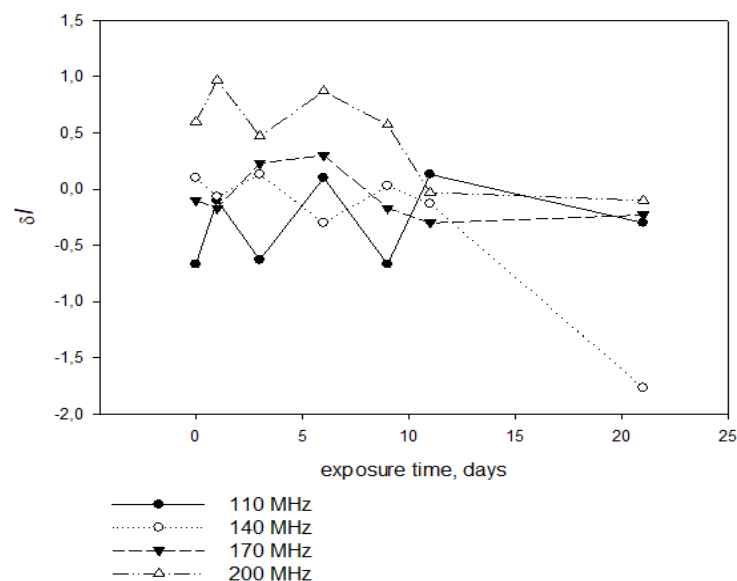


Figure 2. Dependence of the relative change in the length of the ice core on the exposure time after the field effect at given frequencies

As can be seen from the data presented in Figures 1 and 2, there are three groups of frequencies can be distinguished: 1) values located more or less symmetrically near zero; 2) values with a predominantly positive shift, and 3) values for which the shift is mostly negative. Frequencies 30, 60 and 140 MHz are included in the first group, frequencies 170 and 200 MHz are included in the second group, the remaining frequencies are included in the third group. Although this is not a completely deterministic feature, the individuality of the frequency factor is clearly visible. The specific nature of time dependence can also be noted. For example, the dependences on the exposure time are antiphase both for absolute values and δl in the frequency range of 30 and 60 MHz. At the same time, beats are observed for up to nine days at 90 MHz, and then a sharp shift to the negative region with a large δl takes place. The higher frequencies show a significant difference of δl dependence on the exposure time after the field effect. High positive values are observed at 200 MHz and noticeable negative ones at 110 MHz; beats close to zero are found at 170 MHz, and all curves are close to zero on the 21st day.

The frequency of 140 MHz stands apart; it showed an abnormally negative δl after 21 days of exposure. Figure 3 shows the time dependence of the core length at 170 MHz.

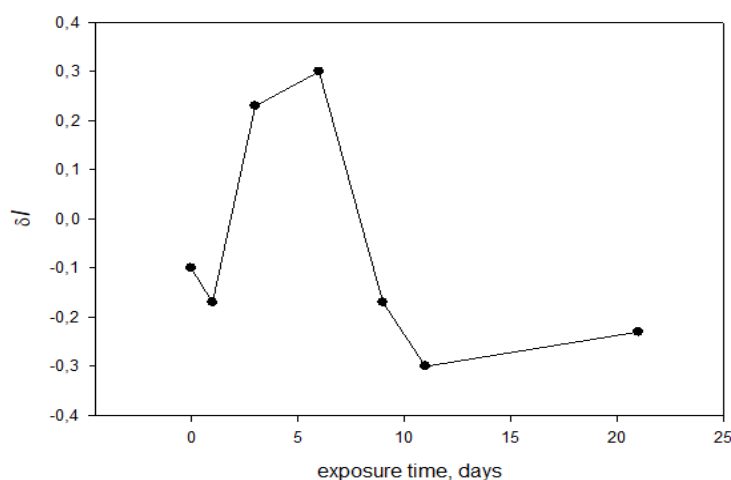


Figure 3. Dependence of the relative change in the length of the ice core on the exposure time after the field effect at 170 MHz

Comparison of the dependence form with the data given in [11] shows a sufficiently clear coincidence of the curve up to 21 days. It shows that certain changes in the structural organization of the water network are manifested in the same way in different processes. In this case, these are the hydration processes during the dissolution of glucose and the process of solvent crystallization (water).

When analyzing the exposure time for different frequencies presented in Figures 4 and 5, it should be noted the multidirectional influence of the frequency factor at short exposure time, which was observed in Figures 1 and 2. Nevertheless, an unidirectional effect of the 200 MHz field is clearly visible: an exposure from 0 to 6 days leads to close values of the relative core size. There is a similarity of dependences for 0 and 3-day exposure for all frequencies. If the exposure time is longer (9–21 days), the frequency dependence is more individual, though the location relative to the zero line is similar: most values are located in the negative area.

The models, detailed in [13], can be used to explain. First of all, it should be noted that water molecules in a liquid state have several types of motion: vibrational, rotational and translational. In addition, proton transfer along structural defects also occurs. These motions have significantly different transformation time. Taking this into account, it is possible to exclude fast processes and leave only slow ones, coincident or close to the frequencies of external influence. These include the rotation of a water molecule in the surrounding field of other molecules, which may coincide with the frequency of the field effect. Consideration of rotational processes and their peculiarity is associated with the fact that usually the ice I is not an ideal structure. It has D and L defects, the relaxation of which is caused by the rotation of individual molecules. The structural organization of water at 300 K is polymorphic according to modern models, i.e. consists of domains of $(\text{H}_2\text{O})_n$ type.

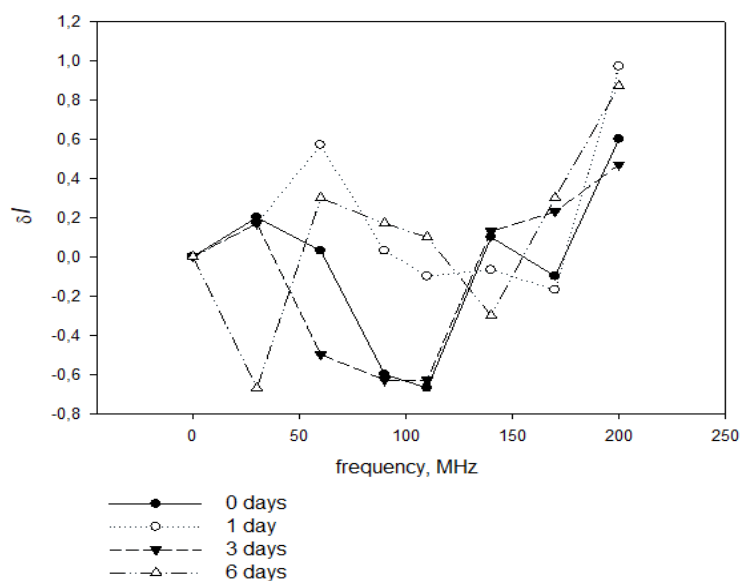


Figure 4. Dependence of the relative change in the length of ice core on the frequency of field effect for different exposure times

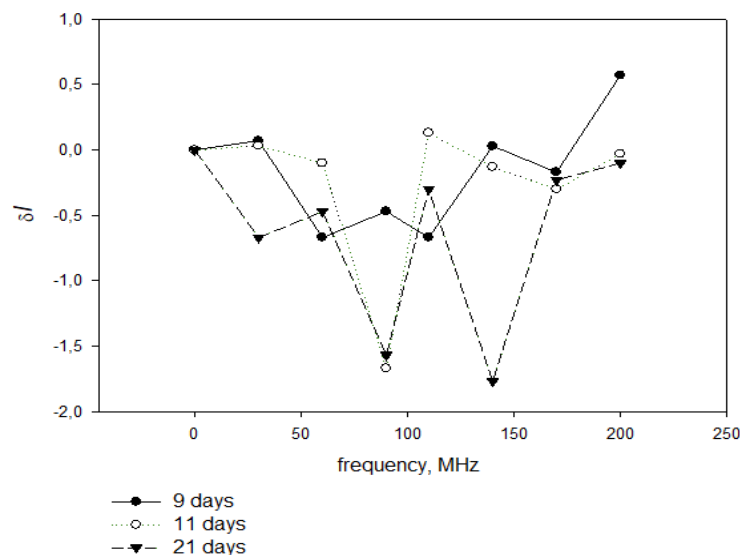


Figure 5. Dependence of the relative change in the length of the ice core on the frequency of the field effect for different exposure times

Taking into account this fact that, it can be assumed that for each domain group there is the resonance frequency of oscillation under the effect of an external electromagnetic field. This may lead to a redistribution of the ratio of the amount of monomolecular water (or the corresponding structural domain) and the polymolecular domain with a certain n . In turn, such a reconstruction either promotes the «healing» of defects in the ice structure, or stimulates their generation. Oscillation of the field effect in time can be associated with the fact that crystallization does not occur instantaneously, but takes a certain period of time, including the metastable state of supercooling. During this time, the relaxation of water structure to the closest energy state can occur either with a large or smaller number of defects. Thus, it follows that when the defects are «healed» and water does not tend to include single molecules in the cluster cavities, the volume of ice increases in comparison with unaffected water. If the number of defects increases, the structure becomes denser and shrinks.

Conclusion

It is shown that the effect of an electromagnetic field of 30–200 MHz on water subsequently causes a change in the crystallization volume of ice. The effect of changing the crystallization volume depends both on the frequency of field action and the time of water exposition after the field action before crystallization. Both increase and decrease in the ice volume as compared to the unaffected sample were found. The maximum effect of volume increase was observed for the frequency of 200 MHz and exposure time of 1 day. The maximum ice compression occurred after the field effect at a frequency of 90 MHz and exposure time of 11 days as well as, at 140 MHz and exposure time of 21 days. It is considered as both loosening and strengthening of water net structure.

References

- 1 Классен В.И. Омагничивание водных систем / В.И. Классен. — 2-е изд., перераб. и доп. — М.: Химия, 1982. — 296 с.
- 2 Мокроусов Г.М. Физико-химические процессы в магнитном поле / Г.М. Мокроусов, Н.П. Горленко. — Томск: Изд-во ТГУ, 1988. — 128 с.
- 3 Духанин В.С. Исследование влияния магнитного поля на гидратацию ионов в растворах электролитов и на скорость некоторых химических реакций: автореф. дис. ... канд. хим. наук: 02.00.04 — «Физическая химия» / В.С. Духанин. — М., 1973. — 21 с.
- 4 Кокшаров С.А. Оценка эффекта магнитной обработки растворов по данным термохимии растворения электролитов / С.А. Кокшаров, В.В. Иванов // Журн. общ. хим. — 1997. — Т. 67, Вып. 1. — С. 17–21.
- 5 Галаницкий А.А. О влиянии магнитного, электромагнитного и ультразвукового полей на физико-химические свойства водных растворов / А.А. Галаницкий // Вопросы теории и практики магнитной обработки воды и водных систем. — Новочеркасск, 1975. — С. 22–28.
- 6 Розенталь О.М. Кристаллизация воды в магнитном поле / О.М. Розенталь, Л.А. Бантыш, Ф.Е. Четин, В.В. Антипенков // Электронная обработка материалов. — 1976. — Вып. 5. — С. 50–52.
- 7 Бантыш Л.А. Особенности фазовых переходов вода–лед и вода–пар при действии постоянного магнитного поля / Л.А. Бантыш // Электронная обработка материалов. — 1977. — Вып. 5. — С. 63, 64.
- 8 Шипунов Б.П. Изменение объема воды и водных растворов под воздействием постоянного магнитного поля и пониженной температуры / Б.П. Шипунов, К.В. Селиков // Изв. АлтГУ. — 2005. — Вып. 3. — С. 94–101.
- 9 Шипунов Б.П. Влияние ВЧ поля на растворимость кислорода в воде и ее физико-химические свойства / Б.П. Шипунов, М.В. Жидько // Химия и химическая технология: материалы I Междунар. Рос.-Каз. конф. — Томск: Изд-во Том. политехн. ун-та, 2011. — С. 77–79.
- 10 Shipunov B.P. Change in the heat of D-glucose dissolution in water exposed to electromagnetic field / B.P. Shipunov, A.V. Ryabykh // Vestn. Karagand. un-ta. Ser. Khimiya. — 2020. — № 1(97). — С. 83–89.
- 11 Шипунов Б.П. Влияние ВЧ поля на термодинамическую устойчивость кристаллогидратов хлорида кобальта / Б.П. Шипунов, Ю.М. Чашева // Изв. вузов. Физика. — 2014. — Т. 57, Вып. 7/2. — С. 202–204.
- 12 Эйзенберг Д. Структура и свойства воды / Д. Эйзенберг, В. Кауцман. — Л.: Гидрометеиздат, 1975. — 280 с.
- 13 Зацепина Г.Н. Свойства и структура воды / Г.Н. Зацепина. — М.: Изд-во Моск. ун-та, 1974. — 168 с.
- 14 Саркисов Г.Н. Структурные модели воды / Г.Н. Саркисов // Успехи физ. наук. — 2006. — Т. 176, Вып. 8. — С. 833–845.
- 15 Stas' I.E. The Stripping Voltammetry In High Frequency Electromagnetic Field / I.E. Stas', B.P. Shipunov, T.S. Ivonina // Electroanalysis. — 2005. — Vol. 17, Iss. 5. — P. 794–799.
- 16 Корольков Д.В. Теоретическая химия / Д.В. Корольков, Т.А. Скоробогатов. — 2-изд., перераб. и доп. — СПб.: Изд. СПб. ун-та. — 2005. — С. 485–493.

Б.П. Шипунов, М.В. Захарова

Жоғарыжиілікті электромагниттік өрістің әсерінен судың кристалдану көлемінің өзгеруі

Судың кристалдану процесіне жоғарыжиілікті электромагниттік өрістің әсері зерттелді. 30-дан 200 МГц дейінгі жиіліктегі далалық өңдеуде ұшыраған су жабық ыдыста 0-ден 21 күнге дейін сақталды, содан кейін мұздатылды. Далалық өңделмеген судың кристалдануы кезіндегі мұздың көлемі далалық өңдеуден кейін судың кристалдануы кезіндегі мұздың көлемімен салыстырылды. Жиіліктердің 3 тобы бар: олар үшін шамалар сәулеленбеген судан алынған мұздың мәндеріне қатысты симметриялы түрде азды-көпті нөлге жақын орналасқан, олар үшін оң ауысу басым және ауысым негізінен теріс. Оң жақтылық 200 МГц жиілігінде және экспозиция уақыты 11 күнге дейін байқалды. Көлемнің салыстырмалы ұлғайуының максималды әсері шамамен 2 есе, 200 МГц жиілікте байқалды, 1 тәулікке экспозициямен, мұздың максималды сығылуы, сәулеленбеген сынамамен салыстырғанда шамамен

3 есе, 90 МГц жиіліктеге өріс әсерінен кейін 11 тәулік ұстау уақыты кезінде және 140 МГц жиілігі үшін 21 тәулік ұстау уақыты кезінде далалық әсер ету орын алды. 170 МГц жиіліктегі экспозиция уақытына тәуелділіктің ерте жұмыстарда алынған глюкозаның еруі жылудық әсеріне тәуелділігі ұқсастығы атап өтілді. Алынған мәліметтер далалық әрекеттің нәтижесінде су құрылымының күшеюі де, көпсығуы да болатынын растайды.

Кілт сөздер: электромагниттік өріс, су құрылымы, мұз құрылымы, мұз құрылымындағы ақаулар, өрістің әсер ету жиілігі, сәулеленуден кейінгі су құрылымындағы өзгерістер, су құрылымын босату, су құрылымын нығайту.

Б.П. Шипунов, М.В. Захарова

Изменение объёма кристаллизации воды в результате воздействия высокочастотного электромагнитного поля

Изучено влияние высокочастотного электромагнитного поля на процесс кристаллизации воды. Вода, подвергшаяся полевой обработке частотой в диапазоне от 30 до 200 МГц, выдерживалась от 0 до 21 дня, затем замораживалась. Объём льда при кристаллизации необработанной полем воды сравнивался с объёмом льда при кристаллизации воды после полевой обработки. Выделено 3 группы частот полевого воздействия: 1) те, для которых значения располагаются вблизи нулевого значения; 2) те, у которых превалирует положительный сдвиг и 3) те, у которых смещение, в основном, имеет знак минус. Положительное смещение отмечено при сочетании 200 МГц, и время выдержки — до 11 суток. Максимальный эффект относительного увеличения объёма, почти в 2 раза, наблюдался для частоты 200 МГц, при выдержке 1 сутки, максимальное сжатие льда, примерно в 3 раза, по сравнению с необлучённым образцом, происходило после полевого воздействия на частоте 90 МГц при времени выдержки 11 суток, и для частоты 140 МГц при времени выдержки — 21 сутки. Отмечено сходство зависимости от времени выдержки для частоты 170 МГц с зависимостью теплового эффекта растворения глюкозы, полученное в ранних работах. Результаты подтверждают, что при полевом воздействии происходит как упрочнение, так и разрыхление структуры воды.

Ключевые слова: электромагнитное поле, структура воды, структура льда, дефекты в структуре льда, частота полевого воздействия, изменения в структуре воды после облучения, разрыхление структуры воды, укрепление структуры воды.

References

- 1 Klassen, V.I. (1982). *Omahnichivanie vodnykh sistem [Magnetization of water systems]*. Moscow: Khimiia [in Russian].
- 2 Mokrousov, G.M., & Gorlenko, N.P. (1988). *Fiziko-khimicheskie protsessy v mahnitnom pole [Physicochemical processes in a magnetic field]*. Tomsk: TSU Publ. [in Russian].
- 3 Duhanin, V.S. (1973). Issledovanie vliianiia mahnitnoho polia na hidratatsiiu ionov v rastvorakh elektrolitov i na skorost nekotorykh khimicheskikh reaktsii [Study of the effect of a magnetic field on the hydration of ions in electrolyte solutions and on the rate of some chemical reactions]. *Candidate's thesis*. Moscow [in Russian].
- 4 Koksharov, S.A., & Ivanov, V.V. (1997). Otsenka effekta mahnitnoi obrabotki rastvorov po dannym termokhimii rastvorenniia elektrolitov [Evaluation of the effect of magnetic treatment of solutions according to thermochemistry data of dissolution of electrolytes]. *Zhurnal obshchei khimii — Russian Journal of General Chemistry*, 69, 129, 17–21 [in Russian].
- 5 Galanitsky, A.A. (1975). O vliianii mahnitnoho, elektromahnitnoho i ultrazvukovoho polei na fiziko-khimicheskie svoistva vodnykh rastvorov [On the influence of magnetic, electromagnetic and ultrasonic fields on the physicochemical properties of aqueous solutions]. *Voprosy teorii i praktiki mahnitnoi obrabotki vody i vodnykh sistem — Questions of theory and practice of magnetic treatment of water and water systems*. Novocherkassk [in Russian].
- 6 Rozental, O.M., Bantysh, L.A., Chetin, F.Ye., & Antipenkov, V.V. (1976). Kristallizatsiia vody v mahnitnom pole [Crystallization of water in a magnetic field]. *Elektronnaia obrabotka materialov — Surface Engineering and Applied Electrochemistry*, 5, 50–52 [in Russian].
- 7 Bantysh, L.A. (1977). Osobennosti fazovykh perekhodov voda–led i voda–par pri deistvii postoiannoho mahnitnoho polia [Features of phase transitions water-ice and water-steam under the action of a constant magnetic field]. *Elektronnaia obrabotka materialov — Surface Engineering and Applied Electrochemistry*, 5, 63–64 [in Russian].
- 8 Shipunov, B.P., & Selikov, K.V. (2005). Izmenenie obema vody i vodnykh rastvorov pod vozdeistviem postoiannoho mahnitnoho polia i ponizhennoi temperatury [Change in the volume of water and aqueous solutions under the influence of a constant magnetic field and low temperature]. *Izvestiia Altayskogo gosudarstvennogo universiteta — Izvestiia of Altai State University Journal*, 3(37), 94–101 [in Russian].
- 9 Shipunov, B.P., & Zhid'ko, M.V. (2011). Vliianie VCH polia na rastvorimost kislорода v vode i ee fiziko-khimicheskie svoistva [The HF field influence on oxygen solubility in water and its physicochemical properties]. *Proceedings from Chemistry and chemical technology: I Mezhdunarodnaia Rossiisko-Kazakhstanskaia konferentsiia — I International Russian-Kazakhstan conference*. (p. 77–79). Tomsk: Publ. of Tomsk polytechnical University [in Russian].

10 Shipunov, B.P., & Ryabykh, A.V. (2020). Change in the heat of D-glucose dissolution in water exposed to electromagnetic field. *Bulletin of the Karaganda university. Chemistry series*, 1(97), 83–89.

11 Shipunov, B.P., & Chashevaya, Yu.V. (2014). Vliianie vysokochastotnykh polei na termodinamicheskuiu stabilnost kristallogidratov khlorida kobalta [The effect of high-frequency fields on the thermodynamic stability of cobalt chloride crystal hydrates]. *Izvestiia vuzov. Seriya fizika i khimiia materialov — Russian journal of physics*, 57, 7/2, 202–204 [in Russian].

12 Eyzenberg, D., & Kautsman, V. (1975). *Struktura i svoistva vody [The structure and properties of water]*. Leningrad: Hidrometeoizdat [in Russian].

13 Zatsepina, G.N. (1974). *Svoistva i struktura vody [Properties and structure of water]*. Moscow: Publ. of Moscow University [in Russian].

14 Sarkisov, G.N. (2006). Strukturnye modeli vody [Structural models of water]. *Uspekhi fizicheskikh nauk — Physics-Uspekhi (Advances in Physical Sciences)*, 176, 8, 833–845 [in Russian].

15 Stas', I.E., Shipunov, B.P., & Ivonina, T.S. (2005). The Stripping Voltammetry in High Frequency Electromagnetic Field. *Electroanalysis*, 17, 5, 794–799.

16 Korol'kov, D.V., & Skorobogatov, T.A. (2005). *Teoreticheskaia khimiia [Theoretical Chemistry]*. Saint Petersburg: Saint Petersburg University Press [in Russian].

Information about authors

Shipunov, Boris Pavlovich — PhD in Chemistry, Associate Professor, Department of Physical and Inorganic Chemistry, Altai State University, Lenin av, 61, Barnaul, Russia. E-mail: sbp@mc.asu.ru/
<https://orcid.org/0000-0002-2387-0848>

Zakharova, Maria Vadimovna — Fifth year student, Department of Physical and Inorganic Chemistry, Altai State University, Lenin av, 61, Barnaul, Russia. E-mail: mascha-1998@bk.ru

Ye.M. Tazhbayev¹, A.R. Galiyeva^{1*}, T.S. Zhumagaliyeva¹, M.Zh. Burkeyev¹,
A.T. Kazhmuratova¹, E.Zh. Zhakupbekova¹, L.Zh. Zhaparova¹, A.A. Bakibayev²

¹Karagandy University of the name of academician E.A. Buketov, Kazakhstan;

²Tomsk State University, Russia

(*Corresponding author's e-mail: aldana_karaganda@mail.ru)

Synthesis and characterization of isoniazid immobilized polylactide-co-glycolide nanoparticles

This article considers some aspects of synthesis and characterization of polylactide-co-glycolide nanoparticles immobilized with the antituberculous drug isoniazid. The influence of some synthesis parameters of nanoparticles (the ratio of drug substance: polymer and surfactant concentration) on properties of the obtained nanosomal drug form of isoniazid has been studied. Optimal conditions for obtaining the nanoparticles with the best physicochemical parameters such as: particle size, polydispersity, conversion, etc. have been found. These nanoparticles can be used as drug carriers. The results revealed that a polymer: drug ratio of 1:1 and the use of 3 % Twin 80 are necessary to obtain stable emulsions of nanoparticles of polylactide-co-glycolide with satisfactory characteristics. Average size of the obtained particles was 196.4 nm, and the polydispersity value was 0.323. The aggregation stability of nanoparticles during 4 hours at temperatures of 4°C and 20°C has been evaluated. The morphology of the obtained nanoparticles has been studied. Analysis of nanoparticles was characterized by various instrumental methods including gas chromatography and thermogravimetry techniques. The resulting nanoparticles of polylactide-co-glycolide immobilized with isoniazid are stable in time and can prolong the action of the drug. *In vitro* release of isoniazid from polylactide-co-glycolide nanoparticles has been studied.

Keywords: nanoparticles, polylactide-co-glycolide, isoniazid, antituberculous drug, immobilization, polymers.

Introduction

Tuberculosis (TB) is one of the top 10 reasons of death worldwide; and the leading cause of death from a single infectious agent (ranking above HIV/AIDS) [1]. Isoniazid (INH) is an important first-line antituberculosis drug (anti-TB) and is used in combination with other anti-TB drugs (Fig. 1, a). The anti-TB drugs are encapsulated in polymer-based nanoparticles (NPs) in order to achieve the best therapeutic effect.

One of the promising polymer carriers is polylactide-co-glycolide (PLGA), which has low toxicity, excellent biological compatibility, and characterized by the absence of inflammation in contact with living organisms (Fig. 1, b). All listed characteristics combined with the controlled mechanical properties, makes PLGA the best polymer for the creation of prolonged systems [2].

PLGA NPs are extremely common in nanosystems, and have been used to encapsulate some anti-TB drugs (Table 1). Examples, such as liposomes/niosomes, polymeric NPs, microspheres composed of different polymers (PLGA, alginate, gelatin and SLNs) have been extensively described in various reviews as reported by Costa et al. 2016 [3].

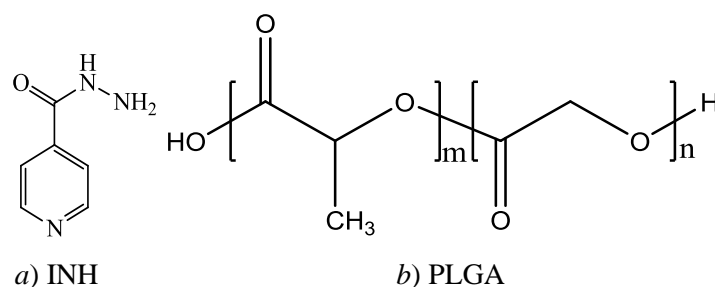


Figure 1. Structural formula of isoniazid and polylactide-co-glycolide

Polymeric NPs of anti-TB drugs

NP	Size	Drug(s)	Loading efficiency	Method for producing polymeric NPs	Ref.
PLGA	121–184 nm	Rifampicin (RIF)	38 %–42 %	Lactose-PLGA-NPs were prepared by the solvent displacement method	[4]
PLGA	186–290 nm	RIF, INH, Pyrazinamide (PZA)	RIF: 57 % INH: 66 % PZA: 68 %	Drug-loaded NPs were prepared by the multiple emulsion technique	[5]
PLGA	180–400 nm	RIF, INH, PZA	RIF: 54 % INH: 64 % PZA: 67 %	Wheat germ agglutinin-coated PLGA-NPs were prepared by a two-step carbodiimide procedure	[6]
PLGA	200–400 nm	RIF, D-cycloserine	N/A	Drug-loaded NPs were prepared using a technologically available production method	[7]
PLGA	200–250 nm	RIF	40–53 %	NPs were produced by homogenization under pressure followed by solvent evaporation	[8]

The entrapment of the therapeutic agents in biodegradable polymeric nano-systems is designed to enhance targeted entry, slow-release, and retention of the antibiotics in the cells for longer periods. It has to not only achieve an improved minimum inhibitory concentration, but also reduce dose frequency. Thus, it supposed to improve patient compliance and reduce systemic side effects associated with conventional free anti-TB drugs [9]. In this regard, in order to increase the therapeutic effect of the anti-TB drug INH, we studied the possibility of binding this drug to PLGA NPs.

Experimental

Preparation of INH loaded PLGA NP

PLGA (the copolymer of lactide-co-glycolide (50:50), molecular weight 24,000 to 38,000) and INH was purchased from Sigma Aldrich. PLGANPs immobilized with INH were prepared using the same method as in [10]. Briefly, INH and PLGA (drug/polymer: 1:1–1:5 by weight), D-mannite (1–5 %), Twin 80 (1–7 %) and Dimethylsulfoxide (DMSO) are sequentially loaded into a three-necked flask equipped with a stirrer, a backflow condenser and a thermometer at temperatures of 293–298 K. The mixture is stirred and heated up to 323–333 K for 15–20 min until the solid phase is completely dissolved; then cooled down to room temperature for 20–30 min. The above-mentioned product is a transparent homogeneous liquid of light yellow color. The resulting suspension volume was regulated to 10 mL, and NPs were washed three times with deionized water and collected by centrifugation at 14000 rpm for 15 min (Eppendorf, Hamburg, Germany).

Determination of the size of particles, their polydispersity, and morphology

Particle size and polydispersity of NPs were determined using a dynamic light scattering (DLS) on Malvern Zetasizer Nano S90 (Malvern Instruments Ltd., Malvern, UK). For all measurements, each sample was diluted to the appropriate concentration with deionized water. Each size analysis lasted for 120 s and was performed at 25 °C with an angle detection of 90°. The surface morphology of PLGA NPs was analyzed via atomic-force microscope (JSPM-5400 Scanning Probe Microscope «JEOL», Japan).

Encapsulation efficacy (EE%) within PLGA NPs

The amount of INH encapsulated within PLGA NPs was determined by measuring the amount of non-encapsulated INH in the aqueous solution recovered after ultracentrifugation and washing of the particles. Encapsulation efficacy was determined by UV spectrophotometer at a wave length of $\lambda_{\max} = 262$ nm. The EE was calculated using the following formula:

$$\text{Encapsulation efficiency (EE\%)} = \frac{\text{Mass of the total Drug} - \text{Mass of free Drug}}{\text{Mass of total Drug}} \times 100 \%$$

In vitro study of drug release from PLGA NPs

The *in vitro* release of INH from PLGA NPs was determined by dialysis in a phosphate-buffered saline (pH 7.4) at 310 K. Liquid samples were placed in a prepared dialysis tube using a pipette. The tube, sealed with clamps, were placed in dialysis vessels with 250 mL of buffer solution, closed with a lid, and stirred on

a magnetic stirrer at 200 rpm. Dialysate samples (3 mL each) were collected periodically. The amount of drug released was recorded on a UV spectrophotometer (Promecolab) at a wavelength of $\lambda_{\max} = 262$ nm for the drug, against a pure buffer solution.

Results and Discussion

The direct introduction of the drug into the reaction medium helps to increase the drug content in the NPs during the synthesizing drug loaded-NPs. However there is a question about the stability of the drug in the reaction, its compatibility with the components of the system, etc. [11]. In order to identify this effect, excerpts were conducted in the presence of the drug and without it. Drug-free PLGA-NPs (empty NPs) were prepared by the same procedure omitting the drug. In reactions with the drug INH was used. PLGA was used as a polymer carrier, and Twin-80 was used as a stabilizer. Characterization of polymers with and without drug is shown below (Table 2).

Table 2

Characteristics of empty and INH immobilized PLGANPs

Polymer	Average particle size, nm	Polydispersity index	Intensity, %
PLGA NPs	338.7±36.4	0.268±0.02	98.7±2.25
PLGA-INH-NPs	272.2±26.7	0.431±0.07	93.1±1.27

The lower value of the size of immobilized NPs seems to be related to the compactization of structures caused by the presence of INH.

In continuation of our research, we have made attempts to immobilize the anti-TB drug INH in PLGA NPs and have selected optimal conditions for the synthesis of NPs with satisfactory characteristics. According to the method proposed in Ref. [10], PLGANPs immobilized by INH with the use of different polymer/drug ratio and surfactant concentrations were obtained. The physicochemical characteristics of polymer NPs were determined using DLS. The investigations results of the effect of PLGA/INH ratio (Table 3, section I) and Twin-80 (Table 3, section II) concentrations on particle size and PDI are given in the Table 3.

Table 3

Physicochemical characteristics of the obtained PLGA-INH-NPs

PLGA/INH ratio	Concentration of Twin-80 (%)	Average particle size (nm)	Polydispersity index	Intensity, %	Encapsulation efficiency (%)
I					
1:1	1	272.2±26.7	0.431±0.07	93.1±1.27	49.4±1.91
1:2		387.3±56.8	0.420±0.07	74.7±17.34	53.5±0.95
2:1		341.8±43.3	0.419±0.13	94.6±4.93	62.6±0.63
5:1		373.8±16.6	0.472±0.07	90.7±6.91	63.5±2.72
II					
1:1	1	272.2±26.7	0.431±0.07	93.1±1.27	49.4±1.91
	1.5	248.6±18.8	0.485±0.09	94.1±2.03	64.9±0.44
	3	196.4±19.5	0.323±0.06	95.6±2.83	75.7±3.48
	7	220.1±24.3	0.364±0.08	88.8±3.80	65.0±1.66

It was found that PLGA-INH-NP with satisfactory characteristics are formed at a ratio of polymer/drug 1:1 and using 3 % Twin-80 to obtain stable emulsions. Thus, the average size of the prepared particles was 196.4 nm, the value of polydispersity was 0.323, and encapsulation efficiency was equal to 75,7 %.

For detailed study of morphology of the prepared PLGA NPs immobilized with INH, we took polymer images on a scanning microscope (Fig. 2).

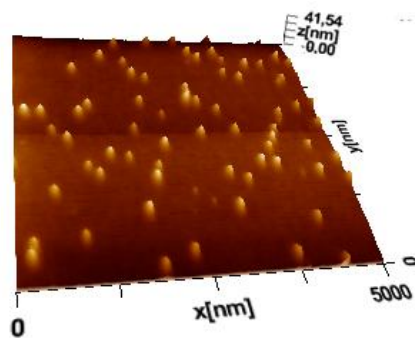


Figure 2. Microphotographs of scanning probe microscopy of PLGA-INH-NPs

All samples prepared for the atomic-force microscope study had a similar topography as presented in Figure 2. The scale at the top right corner of the image is the Z scale depicting the features that are protruding on the surface. The line scan of the image showed a relatively smooth surface on top of the particle [9]. A small standard deviation was obtained illustrating an overall smooth morphology of the particles. Thus, it is shown that using different ratios of INH and PLGA, as well as Twin 80, NPs of spherical shape with a controlled diameter can be obtained.

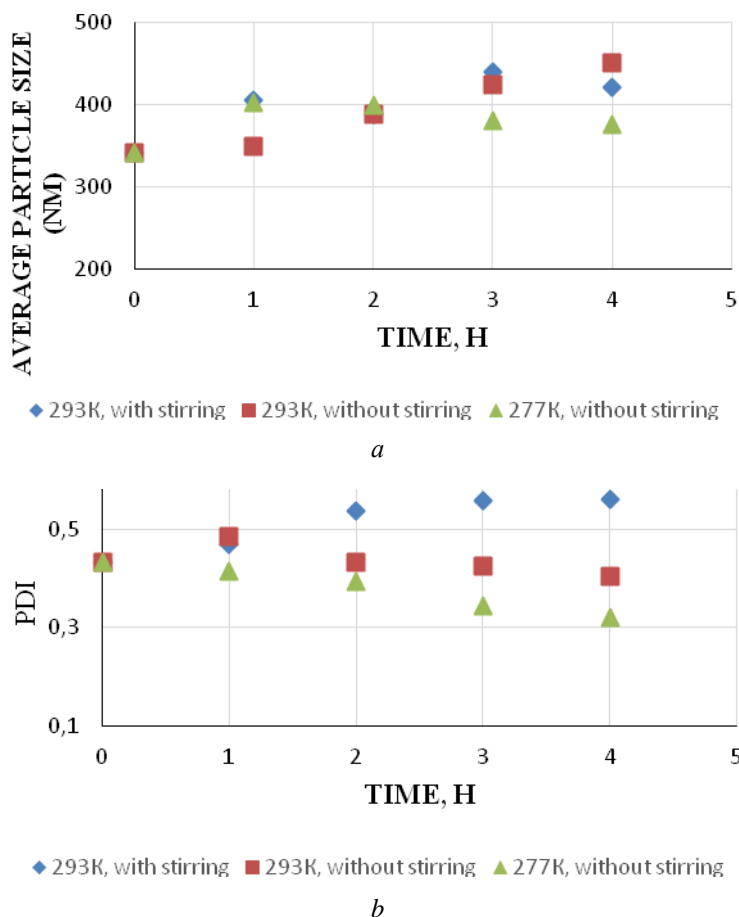


Figure 3. Size (a) and polydispersity index (b) of PLGA-INH-NP within 4 hours

The use of developed PLGANPs in further studies and in practice, suggests that the NPs' suspension must be stable for some time [12]., NPs' aggregation stability therefore was studied during 4 hours at temperatures of 277 K and 293 K. NPs' sizes in the suspension were determined both with and without stirring, preceding the determination of NPs' sizes. The results presented in Figure 3 demonstrate that in the specified time interval, the particle size practically does not change (as evidenced by both average NPs size and polydispersity index, which should have increased with the appearance of larger fractions and aggregates).

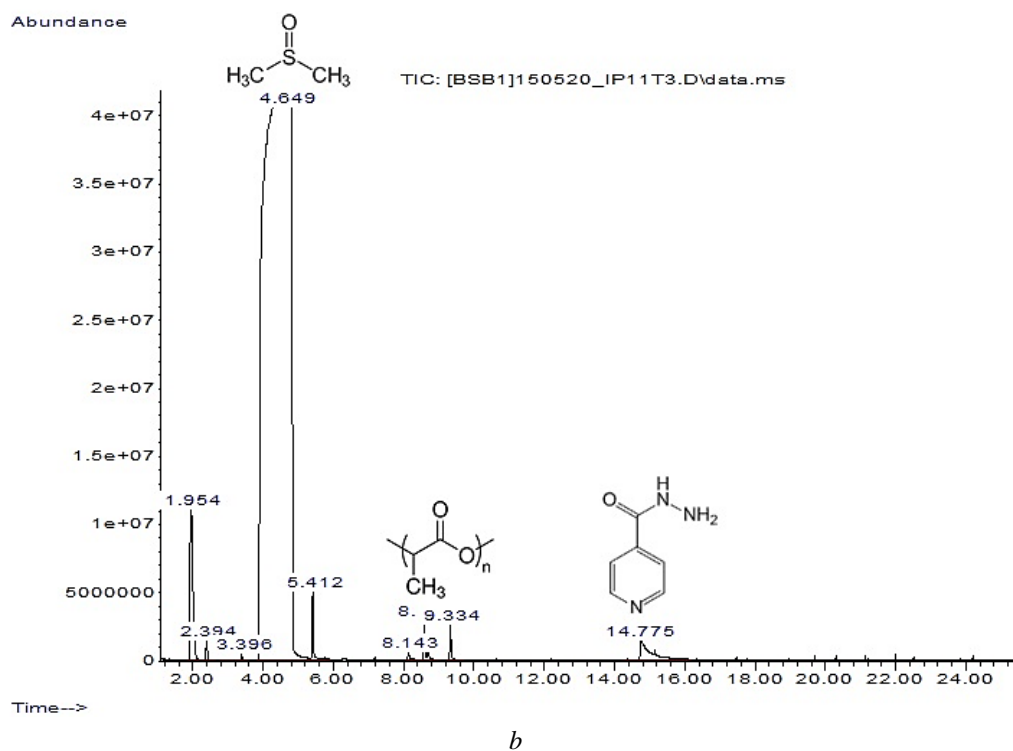
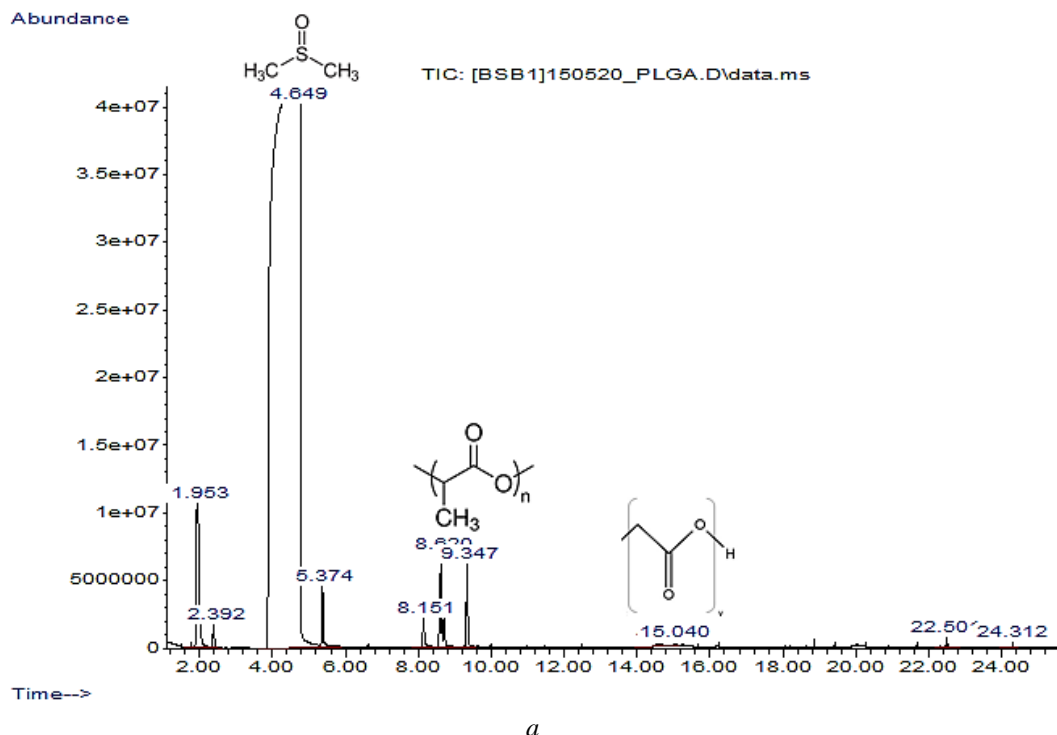


Figure 4. Mass spectra of empty (*a*) and immobilized with INH (*b*) PLGANPs

Empty and immobilized with anti-TB drug PLGANPs were analyzed by gas chromatography and thermogravimetry techniques. The results of analysis using gas chromatograph with mass-selective detector of the polymer with and without drug are given in Figure 4.

As it can be seen from mass spectra of PLGA NPs, polymers have a wide molecular weight distribution. In both spectra the main compounds are DMSO (94 %), water (2.66 %) and Poly(D-lactide) (0.3–0.78 %). In addition to the main peaks, one additional peak corresponds to INH (1.22 %). This suggests that a drug did not change the chemical nature as a result of immobilizing INH in the NPs, this information corroborated with thermogravimetric analysis (TGA) results.

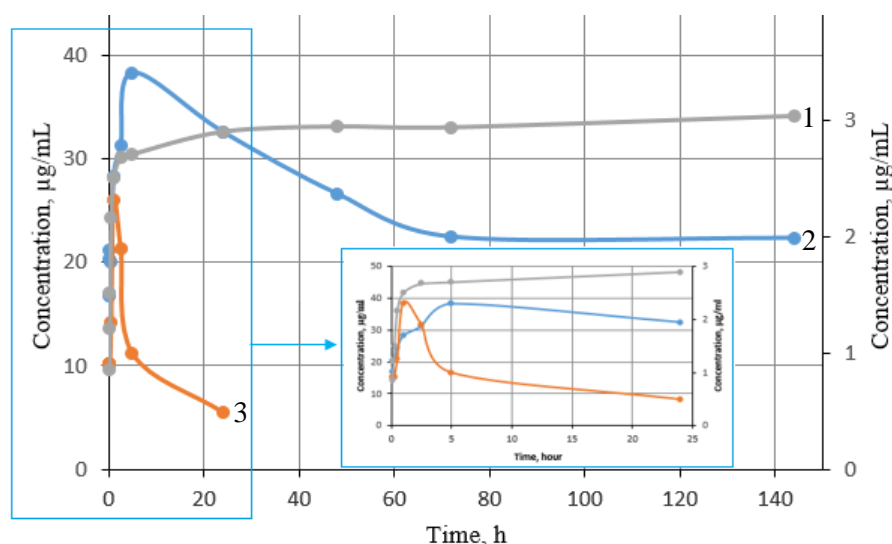


Figure 7. Dependence of INH release rate on time of the samples PLGA-INH-NPs at INH/PLGA ratio: 1:5 (1), 1:1 Twin-80 3 % (2); and INH (3)

The drug in the conventional dosage form (free INH) provides a single and short-term release of the drug. The drug was released from the dosage form in 5 hours, and the concentration is exponentially reduced until the next dose. Prolonged-release pharmaceutical forms also have a high rate of release in the first 5 hours, although less significant than conventional dosage forms. The drug concentration in blood cannot remain at the same level for long, so it starts decreasing gradually. Drug systems with controlled release eliminate leaps in blood concentration levels of the drug. They maintain a constant therapeutic concentration over a long period of time and result in a stable pharmacological effect [14]. The data presented in Figure 7 show that the release was prolonged for a long time. This property of release kinetics of INH can be used for long-term chemotherapy.

Conclusions

Thus, the work shows the possibility of including the drug into polymer-carriers directly at the stage of the synthesis of polymeric NPs. The obtained NPs have satisfactory physicochemical characteristics, as evidenced by DLS data. When the obtained NPs were diluted with water, a stable opalescent suspension was formed. The possibility of dilution with water can be used to regulate the dosage of the drug depending on the individual characteristics of the patient. The obtained results should be used for the creation of the drugs with prolonged effect. The data obtained using physicochemical methods of analysis (gas chromatograph and thermogravimetry) reveal that some drugs are immobilized in the matrix of PLGA NPs.

References

- 1 Site of World health organization [Electronic resource]. Access mode: https://www.who.int/tb/publications/global_report/TB20_Exec_Sum_20201022.pdf
- 2 Кедик С.А. Полимеры для систем доставки лекарственных веществ пролонгированного действия (обзор). Полимеры и сополимеры молочной и гликолевой кислот / С.А. Кедик, Е.С. Жаворонок, И.П. Седишев, А.В. Панов, В.В. Суслов, Е.А. Петрова и др. // Фармацевтическая технология. — 2013. — № 2 (3). — С. 18–35.
- 3 Costa A. The formulation of nanomedicines for treating tuberculosis / A. Costa, M. Pinheiro, J. Magalhães // *Advanced Drug Delivery Reviews*. — 2016. — Vol. 102. — P. 102–115.
- 4 Jain S.K. Lactose-conjugated PLGA nanoparticles for enhanced delivery of rifampicin to the lung for effective treatment of pulmonary tuberculosis / S.K. Jain, Y. Gupta, L. Ramalingam, A. Jain, A. Jain, P. Khare et al. // *Journal of Pharmaceutical Science and Technology*. — 2010. — Vol. 64. — P. 278–287.
- 5 Pandey R. Poly (DL-lactide-co-glycolide) nanoparticle-based inhalable sustained drug delivery system for experimental tuberculosis / R. Pandey, A. Sharma, A. Zahoor, S. Sharma, G.K. Khuller, B. Prasad // *Journal of Antimicrobial Chemotherapy*. — 2003. — Vol. 52. — P. 981–986.
- 6 Sharma A. Lectin-functionalized poly (lactide-co-glycolide) nanoparticles as oral/aerosolized antitubercular drug carriers for treatment of tuberculosis / A. Sharma, S. Sharma, G.K. Khuller // *Journal of Antimicrobial Chemotherapy*. — 2004. — Vol. 54. — P. 761–766.

7 Патент РФ № 2327459. Россия. Лекарственное средство противомикробного действия, способ получения лекарственного препарата направленного действия, содержащего наночастицы / Северин Е.С., Крюков Л.Н., Воронцов Е.А., Кузнецов С.Л., Помазкова Т.А. Оpubл. 27.06.2008.

8 Максименко О.О. Влияние технологических параметров на физико-химические свойства полилактидных наночастиц, содержащих рифампицин / О.О. Максименко, Л.В. Ванчугова, Е.В. Шипуло, Г.А. Шандрюк, Г.Н. Бондаренко, С.Э. Гельперина и др. // Хим.-фарм. журн. — 2010. — Т. 44, № 3. — С. 42–47.

9 Kalombo L. Spray-Dried, Nanoencapsulated, Multi-Drug Anti-Tuberculosis Therapy Aimed at Once Weekly Administration for the Duration of Treatment / L. Kalombo, Y. Lemmer, B. Semete-Makokotlela, B. Ramalapa, T. Nkuna, L. Booysen // Nanomaterials. — 2019. — Vol. 9, No. 1167. — P. 1–14.

10 Патент РФ № 2318513. Россия. Лекарственное средство на основе D-циклосерина, препарат пролонгированного действия, содержащий наночастицы, способ его получения / Северин Е.С., Крюков Л.Н., Зыкова И.Е., Барсегян Г.Г., Воронцов Е.А., Кузнецов С.Л. и др. Оpubл. 10.03.2008.

11 Жапарова Л.Ж. Изучение совместимости некоторых противотуберкулезных препаратов с системой радикальной полимеризации / Л.Ж. Жапарова, Е.М. Тажбаев, М.Ж. Буркеев, С.И. Али, А.М. Ван Херк // Вестн. Караганд. ун-та. Сер. Химия. — 2010. — № 4 (60). — С. 36–39.

12 Балабаньян В.Ю. Фармакологические и фармацевтические аспекты создания наноразмерных форм факторов роста нервной ткани феназепам и паклитаксела: дис. ... д-ра фарм. наук: 14.03.06 — «Фармакология, клиническая фармакология» / Вадим Юрьевич Балабаньян. — М., 2015. — 248 с.

13 Dinarvand R. Poly lactide-co-glycolide nanoparticles for controlled delivery of anticancer agents / R. Dinarvand, N. Sepehri, S. Manoochehri // International Journal of Nanomedicine. — 2011. — No. 6. — P. 877–895.

14 Филатова Е.В. Лекарственные системы противоопухолевого действия на основе микросфер из поли-3-оксибутирата: дис. ... канд. биол. наук: 03.01.04 — «Биохимия» / Елена Викторовна Филатова. — М., 2019. — 166 с.

Е.М. Тажбаев, А.Р. Галиева, Т.С. Жұмағалиева, М.Ж. Бүркеев,
А.Т. Қажмұратова, Э.Ж. Жакупбекова, Л.Ж. Жапарова, А.А. Бакибаев

Изониазидпен иммобилизацияланған полилактид-со-гликолид нанобөлшектерін синтездеу және зерттеу

Туберкулезге қарсы препарат изониазидпен иммобилизацияланған полилактид-со-гликолид нанобөлшектерін синтездеу және зерттеудің кейбір аспектілері қарастырылған. Нанобөлшектерді синтездеудің кейбір параметрлерінің (дәрілік зат қатынасы: полимер және ББЗ концентрациясы) алынатын изониазидтің наносомалық дәрілік түрінің қасиеттеріне әсері зерттелді. Дәрілік заттарды тасымалдаушы ретінде пайдалану үшін үздік физико-химиялық параметрлері болатын нанобөлшектерді алудың оңтайлы шарттары (бөлшектер мөлшері, полидисперстілігі, конверсия және т.б.) анықталды. Полилактид-со-гликолид нанобөлшектерінің тұрақты эмульсияларын алу үшін полимер / дәрілік қатынасы 1:1 және 3 % Твин-80 қолдану қажет екендігі анықталды. Алынған бөлшектердің орташа мөлшері 196,4 нм, ал полидисперстілік мәні 0,233 құрады. Нанобөлшектердің тұрақтылығы 4 °C және 20 °C температурада 4 сағат бойы зерттелді. Алынған нанобөлшектердің морфологиясы зерттелді. Алынған полилактид-со-гликолидтің нанобөлшектері газды хроматография және термogravиметрия әдісімен тексерілген. Изониазидпен иммобилизацияланған полилактид-со-гликолидтің нанобөлшектері уақыт бойынша тұрақты және дәрілік заттың әсерін ұзарта алады. Изониазидтің полилактид-со-гликолидті нанобөлшектерден *in vitro* босап шығуы зерттелді.

Кілт сөздер: нанобөлшектер, полилактид-со-гликолид, изониазид, иммобилизация, полимерлер.

Е.М. Тажбаев, А.Р. Галиева, Т.С. Жумағалиева, М.Ж. Буркеев,
А.Т. Кажмуратова, Э.Ж. Жакупбекова, Л.Ж. Жапарова, А.А. Бакибаев

Синтез и характеристика наночастиц полилактид-со-гликолида, иммобилизованных изониазидом

Рассмотрены некоторые аспекты синтеза и характеристики наночастиц полилактид-со-гликолида, иммобилизованных противотуберкулезным препаратом изониазидом. Изучено влияние некоторых параметров синтеза наночастиц (соотношение лекарственное вещество : полимер и концентрация ПАВ) на свойства получаемой наносомальной лекарственной формы изониазидом. Найден оптимальные условия для получения наночастиц с наилучшими физико-химическими показателями (размера частиц, полидисперсности, конверсии и т.д.) для применения в качестве носителей лекарственных препаратов. Установлено, что для получения устойчивых эмульсий наночастиц полилактид-со-гликолида с удовлетворительными характеристиками необходимо соотношение полимер : лекарственное вещество 1:1 и использование 3 % Твин-80. Средний размер полученных частиц составил 196,4 нм, а значение полидисперсности — 0,233. Изучена агрегационная устойчивость наночастиц различного состава в те-

чение 4-х ч при температурах 4 и 20 °С. Исследована морфология полученных наночастиц. Наночастицы полилактид-со-гликолида изучались методами газовой хроматографии и термогравиметрии. В ходе анализа выявлено, что наночастицы полилактид-со-гликолида, иммобилизованные изониазидом, стабильны во времени и способны пролонгировать действие лекарства. Кроме того, исследовано *in vitro* высвобождение изониазида из наночастиц полилактид-со-гликолида.

Ключевые слова: наночастицы, полилактид-со-гликоид, изониазид, иммобилизация, полимеры.

References

- 1 Site of World health organization. [www.who.int Retrieved from https://www.who.int/tb/publications/global_report/TB20_Exec_Sum_20201022.pdf](https://www.who.int/tb/publications/global_report/TB20_Exec_Sum_20201022.pdf)
- 2 Kedik, S.A., Zhavoronok, E.S., Sedishev, I.P., Panov, A.B., Suslov, V.V., & Petrova, E.A. (2013). Polimery dlia dostavki lekarstvennykh veshchestv prolonhirovanogo deistviia (obzor). Polimery i sopolimery molochnoi i hlikolevoi kislot [Polymers for prolonged drug delivery systems (review). Polymers and copolymers of lactic and glycolic acids]. *Farmatsevticheskaia tekhnolohiia — Pharmaceutical Technology*, 2(3), 18–35 [in Russian].
- 3 Costa, A., Pinheiro, M., & Magalhães, J. (2016). The formulation of nanomedicines for treating tuberculosis. *Advanced Drug Delivery Reviews*, 102, 102–115.
- 4 Jain, S.K., Gupta, Y., Ramalingam, L., Jain, A., Jain, A., & Khare, P., et al. (2010). Lactose-conjugated PLGA nanoparticles for enhanced delivery of rifampicin to the lung for effective treatment of pulmonary tuberculosis. *Journal of Pharmaceutical Science and Technology*, 64, 278–287.
- 5 Pandey, R., Sharma, A., Zahoor, A., Sharma, S., Khuller, G.K., & Prasad, B. (2003). Poly (DL-lactide-co-glycolide) nanoparticle-based inhalable sustained drug delivery system for experimental tuberculosis. *Journal of Antimicrobial Chemotherapy*, 52, 981–986.
- 6 Sharma, A., Sharma, S., & Khuller, G.K. (2004). Lectin-functionalized poly(lactide-co-glycolide) nanoparticles as oral/aerosolized antitubercular drug carriers for treatment of tuberculosis. *Journal of Antimicrobial Chemotherapy*, 54, 761–766.
- 7 Severin, E.S., Krukov, L.N., Vorontsov, E.A., Kuznetsov, S.L., & Pomazkova, T.A. (2008). Lekarstvennoe sredstvo protivomikrobnogo deistviia, sposob polucheniia lekarstvennogo preparata napravlennoho deistviia, sodержashcheho nanochastitsy [Antimicrobial action drug, method of obtaining a targeted Drug containing nanoparticles]. *Patent of the Russian Federation No. 2327459*. Russia [in Russian].
- 8 Maksimenko, O.O., Vanchugova, L.V., Shipulo, E.V., Shandryuk, G.A., Bondarenko, G.N., & Gelperina, S.E. et al. (2010). Vliianie tekhnolohicheskikh parametrov na fiziko-khimicheskie svoistva polilaktidnykh nanochastits, sodержashchikh rifampitsin [Effect of technological parameters on the physical and chemical properties of polylactide nanoparticles containing rifampicin] *Khimiko-farmatsevticheskii zhurnal — Chemico-pharmaceutical Journal*, 44, 3, 42–47 [in Russian].
- 9 Kalombo, L., Lemmer, Y., Semete-Makokotlela, B., Ramalapa, B., Nkuna T., & Booyesen L. (2019). Spray-Dried, Nanoencapsulated, Multi-Drug Anti-Tuberculosis Therapy Aimed at Once Weekly Administration for the Duration of Treatment. *Nanomaterials*, 9, 1167, 1–14.
- 10 Severin, E.S., Krukov, L.N., Zykova, I.E., Barsegyan, G.G., Vorontcov, E.A., & Kuznetcov, S.L., et al. (2008). Lekarstvennoe sredstvo na osnove D-tsikloserina, preparat prolonhirovanogo deistviia, sodержashchii nanochastitsy, sposob eho polucheniia [Drug based on D-cycloserine, a prolonged-action drug containing nanoparticles, method of its production]. *Patent of the Russian Federation № 2318513*. Russia [in Russian].
- 11 Zhaparova, L.Zh., Tazhbaev, E.M., Burkeev, M.Zh., Ali, S.I., & Van Herck, A.M. (2010). Izuchenie sovместimosti nekotorykh protivotuberkuleznykh preparatov s sistemoi radikalnoi polimerizatsii [The study of compatibility of some antituberculosis drugs]. *Vestnik Karahandinskoho universiteta. Serii Khimiia — Bulletin of the Karaganda University. Chemistry Series*, 4(60), 36–39 [in Russian].
- 12 Balabanyan, V.Yu. (2015). Farmakolohicheskie i farmatsevticheskie aspekty sozdaniia nanorazmernykh form faktorov rosta nervnoi tkani fenazepama i paklitaksela [Pharmacological and pharmaceutical aspects of the creation of nanoscale forms of neural tissue growth factors phenazepam and paclitaxel]. *Doctor's thesis*. Moscow [in Russian].
- 13 Dinarvand, R., Sepehri, N., Manoochehri, S. (2011). Polylactide-co-glycolide nanoparticles for controlled delivery of anti-cancer agents. *International Journal of Nanomedicine*, 6, 877–895
- 14 Philatova, E.V. (2019). Lekarstvennye sistemy protivopukholevogo deistviia na osnove mikrosfer iz poli-3-oksibutirata [Drug systems of antitumor action on the basis of poly-3-oxybutyrate microspheres]. *Candidate's thesis*. Moscow [in Russian].

Information about authors

Bakibayev, Abdigali Abdimanapovich — Doctor of Chemical Sciences, Professor, Leading Researcher of the Laboratory of Organic Synthesis, National Research Tomsk State University, Lenin str., 36, 634050, Tomsk, Russia; e-mail: bakibaev@mail.ru; <https://orcid.org/0000-0002-3335-3166>

Burkeyev, Meyram Zhunusovich — Full Professor, Doctor of Chemical Sciences, Karagandy University of the name of academician E.A. Buketov, Universitetskaya street, 28, 100028, Karaganda, Kazakhstan; e-mail: m_burkeev@mail.ru. <https://orcid.org/0000-0001-8084-4825>

Galiyeva, Aldana Rymzhanovna (*corresponding author*) — 2nd year PhD student, Department of organic chemistry and polymers, Karagandy University of the name of academician E.A. Buketov, Universitetskaya street, 28, 100028, Karaganda, Kazakhstan.; e-mail: aldana_karaganda@mail.ru; <https://orcid.org/0000-0002-8551-6297>

Kazhmuratova, Akerke Temirgaliyevna — Candidate of chemical sciences, Assoc. Professor, Karagandy University of the name of academician E.A. Buketov, Universitetskaya street, 28, 100028, Karaganda, Kazakhstan; e-mail: kazhmuratova@mail.ru; <https://orcid.org/0000-0003-4044-8419>

Tazhbayev, Yerkeblan Muratovich — Full Professor, Doctor of Chemical Sciences, Karagandy University of the name of academician E.A. Buketov, Universitetskaya street, 28, 100028, Karaganda, Kazakhstan; e-mail: tazhbayev@mail.ru; <https://orcid.org/0000-0003-4828-2521>

Zhakupbekova, Elmira Zhumataevna — Candidate of chemical sciences, Assoc. Professor, Karagandy University of the name of academician E.A. Buketov, Universitetskaya street, 28, 100028, Karaganda, Kazakhstan; e-mail: elmira_zhakupbek@mail.ru; <https://orcid.org/0000-0003-4384-9859>

Zhumagaliyeva, Tolkyn Sergazyevna — Candidate of chemical sciences, Assoc. Professor, Karagandy University of the name of academician E.A. Buketov, Universitetskaya street, 28, 100028, Karaganda, Kazakhstan; e-mail: zhumagalieva79@mail.ru; <https://orcid.org/0000-0003-1765-752X>

Zhaparova, Lyazzat Zhanybekovna — PhD, Karagandy University of the name of academician E.A. Buketov, Universitetskaya street, 28, 100028, Karaganda, Kazakhstan; e-mail: lyazzh@mail.ru, <https://orcid.org/0000-0003-1894-0255>

A.A. Bakibaev¹, S.Yu. Panshina^{1,2*}, O.V. Ponomarenko³,
V.S. Malkov¹, O.A. Kotelnikov¹, A.K. Tashenov³

¹National Research Tomsk State University, Tomsk, Russia;

²National Research Tomsk Polytechnic University, Tomsk, Russia;

³L.N. Gumilyov Eurasian National University, Nur-Sultan, Kazakhstan;

(*Corresponding author's e-mail: janim_svetatusik@mail.ru)

1D and 2D NMR spectroscopy for identification of carbamide-containing biologically active compounds

Urea (carbamide) is the main end product of amino acids' metabolism in mammals. Extensive research in the field of urea chemistry has contributed to the creation of many biologically active and other compounds based on the carbamide fragment NH–CO–NH. The substituting groups of urea directly affect its properties and characteristics which are reflected in the NMR spectral data and this circumstance can be the basis for the identification of urea derivatives. In this work, chemical shifts in the NMR spectra of urea and its acyclic structure, barbituric series, imidazolidinone series and bicyclic structure derivatives were studied and identified. A system analysis was carried out to determine the effect of the type of substituents on the positions of signals of the NH–CO–NH fragment in the NMR spectra. The possibility of 2D NMR spectroscopy using to simplify the identification procedure for complex mixtures was shown in the paper. The combined use of 1D and 2D NMR spectroscopy is convenient and informative to establish the structure of biologically active compounds. These methods make it possible to determine the presence and type of impurities, as well as to establish the destruction processes leading to the corresponding impurities.

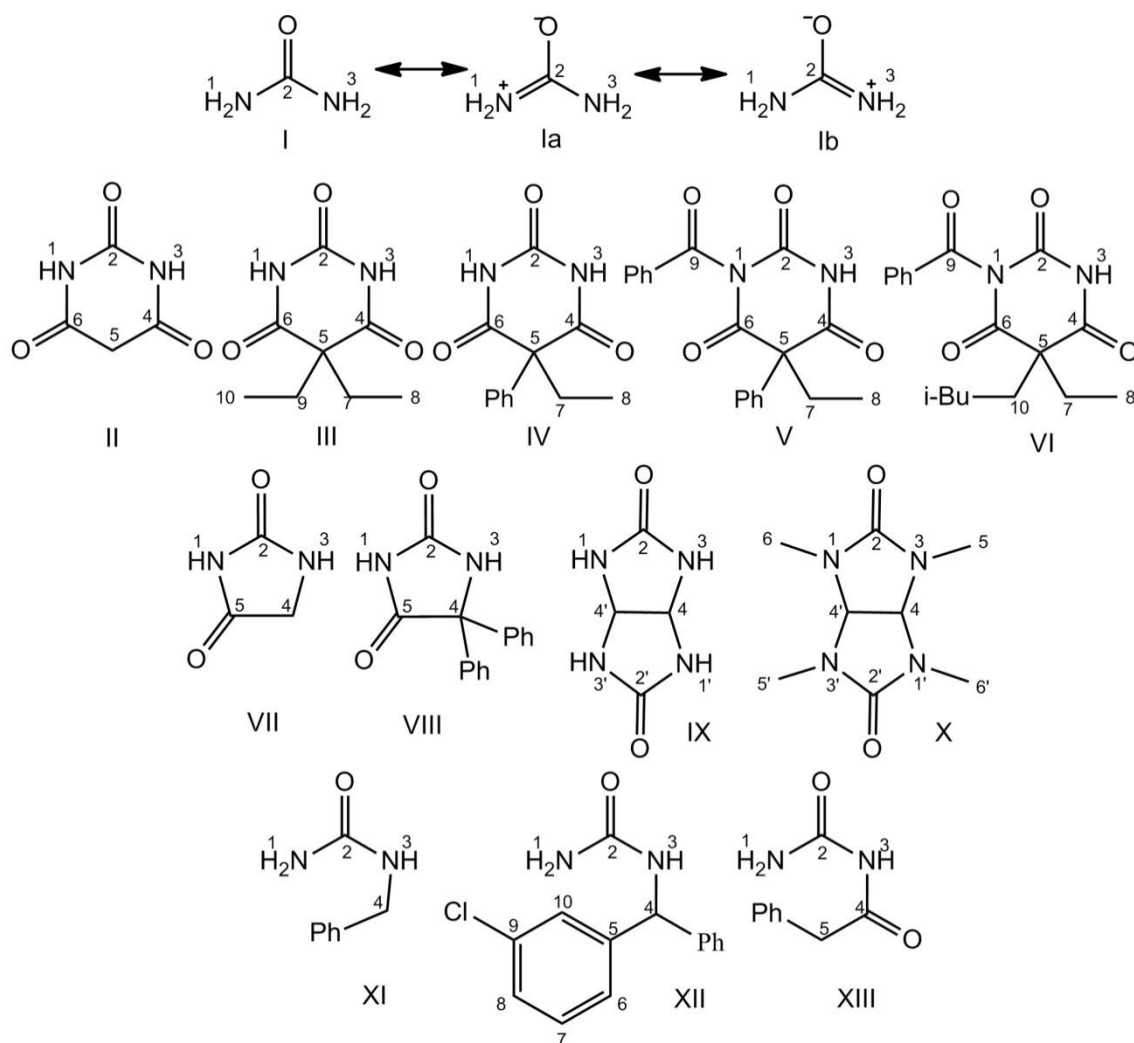
Keywords: urea, urea-containing compounds, barbiturates, glycoluril, imidazolidinone, NMR spectroscopy, hydrolysates, impurities.

Introduction

It is known that the urea (carbamide) **I** is a product of nitrogenous compounds' metabolism in mammals [1, 2]. In some sources there is an information about an independent biological role of the urea [3–5]. The urea **I** is presented in the form of resonance structures **Ia** and **Ib** (Fig. 1) to explain some of the physicochemical processes that occur with the participation of this compound. The studies carried out in the field of urea chemistry made it possible to create a variety of biologically active and other compounds of acyclic and heterocyclic structures containing the urea NH–CO–NH fragment [6–10].

Obviously, the substituting groups of urea directly affect its properties and characteristics which are reflected in the NMR spectral data, and this circumstance may be the basis for the identification of urea derivatives. In this study, the chemical shifts in the NMR spectra of various heterocyclic derivatives of ureas were studied and identified to assess the effect of the type of substituents on the NH–CO–NH fragment. There are heterocyclic urea derivatives of barbituric series (pyrimidine-2,4,6-trione **II**, 5,5-diethylpyrimidine-2,4,6-trione **III**, 5-ethyl-5-phenylpyrimidine-2,4,6-trione **IV**, 1-benzoyl-5-ethyl-5-phenylpyrimidine-2,4,6-trione **V**, 1-benzoyl-5-ethyl-5-isoamylpyrimidine-2,4,6-trione **VI**), of imidazolidinone series (imidazolidin-2,4-dione **VII**, 5,5-diphenylimidazolidin-2,4-dione **VIII**), bicyclic structure (2,4,6,8-tetraazabicyclo(3,3,0)-octanedione-3,7 (glycoluril) **IX**, 4,6,8-tetramethyl-2,4,6,8-tetraazabicyclo(3,3,0) octanedione-3,7 **X**), and of acyclic urea (N-(benzyl)urea **XI**, 1-[(3-chlorophenyl)(phenyl) methyl] urea **XII**, N-(phenylacetyl) urea **XIII**). The structures of these compounds are shown in Figure 1.

Substances **II–XIII** were previously known and identified by various analytical methods [11, 12]. However, a systematic analysis of the effect of different chemical environments on the position of signals in the NMR spectra of biologically active compounds **II–XIII** has not yet been carried out. Previous NMR spectroscopy studies did not provide sufficient explanations for the chemical shifts of compounds **II–XIII** relative to the carbamide fragment of NH–CO–NH in accordance with the shielding and deshielding effects of the substituents.

Figure 1. Structures of substances **I–XIII**

Therefore, the goal of our research was to identify and study the patterns of changes of chemical shifts in the 1D and 2D NMR spectra for a number of biologically active compounds **II–XIII**, urea **I** derivatives, and hydrolysates of these compounds **XIV–XXIV**.

Experimental

Samples of analyzed compounds **II–XIII** were provided by the Tomsk National Research Medical Center of the Russian Academy of Sciences (Scientific Research Institute of Mental Health). Samples of compounds **XIV–XVII** and **XVIII**, **XX** were synthesized according to the procedures [13, 14] and N-methylglycolurils **XXI–XXIV** were obtained by the method described Kurgachev et al. [15].

NMR spectra were recorded on a Bruker AVANCE III HD spectrometer (Bruker Corporation, Germany) with an operating frequency of 400 and 100 MHz for ^1H and ^{13}C nuclei, respectively, in DMSO-d_6 solution (0.001 mol : 0.5 ml of solvent). The internal standard was tetramethylsilane (TMS).

Results and Discussion

First of all, the analyzed compounds **II–XIII** are structurally intramolecular bisacetylated urea **II–VI** and mono-acetylated urea **VII**, **VIII**, bicyclic bisurea **IX**, **X**, arylmethylurea **XI**, **XII** and linear acetylurea **XIII**. Table 1 presents the chemical shifts of the key protons and carbonyl carbon atoms of the urea **I** (as a parent) and the carbamide-containing compounds **II–XIII**.

Table 1

Chemical shifts in the NMR spectra for substances I–XVIII

Substance	¹ H NMR spectrum, δ, ppm (<i>J</i> , Hz)					¹³ C NMR spectrum, δ, ppm (Hz)				
	1	3	4	5	Substituents	2	4	5	6	Substituents
I	5.93 (2H, s)	5.93 (2H, s)	–	–	–	161.5	–	–	–	–
II	11.12 (1H, s)	11.12 (1H, s)	–	3.46 (2H, s)	–	151.9	168.5	39.8	168.5	–
III	11.53 (1H, s)	11.53 (1H, s)	–	–	1.81 (4H, q, <i>J</i> =7.6, CH ₂), 0.74 (6H, t, <i>J</i> =7.6, CH ₃)	150.4	173.6	57.0	173.6	31.8 (C ⁷ , C ⁹), 9.7 (C ⁸ , C ¹⁰)
IV	11.74 (1H, s)	11.74 (1H, s)	–	–	7.31–7.40 (5H, m, Ph), 2.31 (2H, q, <i>J</i> =7.2, CH ₂), 0.87 (3H, t, <i>J</i> =7.6, CH ₃)	150.3	172.0	60.4	172.0	126.7, 128.7, 129.6, 138.9 (Ph), 29.0 (C ⁷), 10.2 (C ⁸)
V	–	12.41 (1H, s)	–	–	7.42–7.50 (5H, m, Ph), 7.98 (2H, d, <i>J</i> =7.6, Ph), 7.78 (2H, dd, Ph), 7.59 (1H, dd, Ph), 2,5 (2H, q, <i>J</i> =7.2, CH ₂), 0.99 (3H, t, <i>J</i> =7.2, CH ₃)	149.0	170.8	61.4	171.0	169.1 (C ⁹), 129.2, 130.1, 130.87, 137.7 (Ph), 131.5, 126.8, 129.8, 136.5 (Ph), 29.0 (C ⁷), 10.3 (C ⁸)
VI	–	11.76 (1H, s)	–	–	7.96 (2H, d, <i>J</i> =8.0, Ph), 7.81 (1H, dd, Ph), 7.63 (2H, dd, Ph), 1.97–1.91 (2H, m, CH ₂), 1.91–1.88 (2H, m, CH ₂), 1.48–1.41 (1H, m, CH), 1.14–1.09 (2H, m, CH ₂), 0.88 (3H, t, <i>J</i> =7.6, CH ₃ (Et)), 0.81 (6H, t, <i>J</i> =6.4, 2CH ₃ , (i-Bu))	149.4	172.8	57.5	173.1	169.5 (C ⁹), 130.5, 131.0, 131.7, 136.8 (Ph), 36.5 (C ¹⁰), 34.2 (C ⁷), 32.5 (CH ₂ , i-Bu), 28.3 (CH, i-Bu), 22.9 (CH ₃ , i-Bu), 22.9 (CH ₃ , i-Bu), 10.0 (C ⁸)
VII	10.66 (1H, s)	7.72 (1H, s)	3.84 (2H, s)	–	–	158.8	47.7	174.4	–	–
VIII	11.34 (1H, s)	9.55 (1H, s)	–	–	8.00 (5H, m, Ph), 7.32 (5H, m, Ph)	156.6	70.5	175.3	–	140.2, 129.7, 128.3, 126.8 (Ph)
IX	7.16 (1H, s)	–	5.24 (2H, s)	–	–	160.3	64.6	–	–	–
X	–	–	5.06 (2H, s)	–	2.82 (12H, s)	159.1	71.9	–	–	30.4 (C ^{5,6})
XI	5.72 (2H, s)	6.56 (1H, t, <i>J</i> =4.8)	4.23 (d, 2H, <i>J</i> =6.3)	–	7.29 (5H, m, Ph),	159.5	43.4	–	–	128.7, 127.5, 127.0, 141.3 (Ph),
XII	7.04 (1H, d, <i>J</i> =8.4)	5.60 (2H, s)	5.85 (1H, d, <i>J</i> =8.8)	–	7.22–7.38 (9H, m, (Ph, Ar).	158.0	56.6	–	–	126.2, 126.4, 127.6, 144.1 (Ph), 135.8, 128.1, 126.9, 140.8 (Cl-Ar)
XIII	7.74 (2H, s)	10.40 (2H, s)	–	3.61 (2H, s)	7.23–7.33 (5H, m, Ph)	154.9	173.7	43.3	–	127.7, 129.2, 130.1, 135.5 (Ph)

The following patterns can be identified based on the data in Table 1:

1. Significant shielding of C=O group compared to the urea I (C²-carbons, up to 12.5 ppm) occurs with intramolecular (compounds **II–VIII**) and linear acylation of the urea I (compound **IX**). While N-aryllalkylation (**XI, XII**) and bicyclization (**IX, X**) causes a slight change in the chemical shifts of C=O groups ($\Delta = 2$ ppm).

2. It is interesting to compare the chemical shifts of acyl carbonyl groups in the series of barbiturates (C²-carbon). Any type of N- and C-substitution in the pyrimidinone cycle (**III–VI** compounds) causes a higher-field C²-carbon shift compared to the chemical shifts of this carbon of the barbituric acid **II** itself (up to 2 ppm). This circumstance may be due to some changes in the geometry of the pyrimidinone cycle under the influence of substituents at C²-carbon.

3. The chemical shifts of C⁵-carbon in C,C-disubstituted derivatives of the barbituric acids **II–VI** are well distinguished in the ¹³C NMR spectra: in the dialkyl-substituted **III, VI** (57.0–57.5 ppm), and in the phenylalkyl-substituted compounds **IV, V** (60.4–61.4 ppm).

4. The data of the ¹H NMR spectra indicates that any type of N-substitution in the urea I leads to regular lower field shifts of NH-protons from 6.56 ppm (arylmethylation: acyclic compounds **XI–XIII**); up to 12.41 ppm (cyclic urea **VII, VIII**, barbituric derivative **V** and its analogues).

One of the main ways of transformation of the studied compounds **II–XIII** is the process of their hydrolysis or oxidative destruction in the biogenic medium. Initially, formation of the corresponding acylureas from compounds **II–VIII** or the corresponding amide from the urea **XII** and even from the urea itself can be

expected during the series of such type of reactions. In this regard, the ^1H and ^{13}C NMR spectra of a number of hydrolysates **XIV–XVII** of studied biologically active compounds **II–XIII** were taken and identified (Table 2).

Table 2

Chemical shifts in the NMR spectra of probable hydrolysates XI–XIV for compounds of urea derivatives II–X

Substance	^1H NMR spectrum, δ , ppm (J , Hz)				^{13}C NMR spectrum, δ , ppm (Hz)		
	1	3	4	Substituents	2	4	Substituents
XIV	10.77 (1H, s)	9.49 (1H, d)	6.27 (1H, d)	7.41–7.53 (5H, m, Ph), 2.25 (3H, s, CH_3)	153.2	57.2	173.7 (COR ₁), 142.5, 126.9, 128.9, 127.6 (Ph), 24.0 (CH_3)
XV	10.53 (1H, s)	9.02 (1H, d)	4.70 (2H, s)	7.45–7.50 (5H, m, Ph), 3.91 (1H, sep, CH), 1.17 (6H, d, CH_3 , <i>i</i> -Pr)	153.6	42.6	174.6 (COR), 139.4, 128.5, 127.3, 127.0 (Ph), 38.0 (CH), 23.6 (CH_3)
XVI	9.52 (1H, s)	8.47 (1H, d)	6.61 (1H, d)	7.41–7.62 (9H, m, Ph, Cl- C_6H_4)	160.4	54.2	141.6, 128.6, 127.3, 127.2 (Ph), 144.8, 126.0, 130.4, 128.1, 133.3, 126.3, (Cl- C_6H_4)
XVII	7.01 (1H, d)	7.01 (1H, d)	6.01 (2H, d)	7.49–7.54 (9H, m, Ph, Cl- C_6H_4)	156.57	56.57	142.6, 126.9, 128.5, 127.0 (Ph, 3-Cl- C_6H_4)

According to the result of the initial hydrolytic transformations of barbituric acid derivatives **II–VI** and imidazolidinone compound **VIII**, formation of the corresponding N-acetylureas is quite predictable. Therefore, N-alkyl (aryl)-N-acylurea **XIV–XV** was used as a model substance in the NMR spectra. Its data were also compared with the spectra of compounds **II–VI**, **VIII**. It was found that the chemical shifts of carbonyl group (NH–CO–NH) of barbiturates **II–VI** is located in a higher-field (149–151 ppm) than in N-acylureas **XIV–XV** (153 ppm). However, the chemical shifts of NH-protons of the barbituric acid and its derivatives **II–VI** are more strongly deshielded (11.20–12.41 ppm) than those of N-alkyl(aryl)-N-acylureas **XIV**, **XV** (9.02–10.77 ppm). Detailed analysis of the chemical shifts values (Table 1) of the compared compounds **II–VI**, **VIII** makes it possible to distinguish intramolecular acylated urea **II–VI**, **VIII** from their acyclic intermediates **XIV**, **XV**.

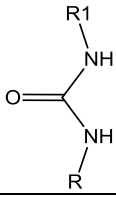
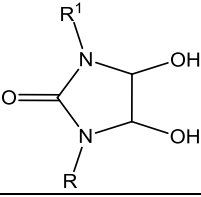
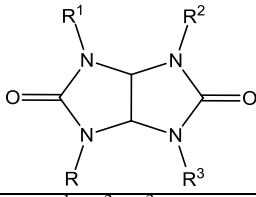
One of the most possible products of the hydrolysis of *m*-chlorobenzhydrylurea **XII** is *m*-chlorobenzhydrylformamide **XVI**. The chemical shifts of compounds **XVI** and *m*-chlorobenzhydrylurea **XII** were recorded and identified (Table 2). Comparison of the chemical shifts of these compounds makes it possible to reliably and distinguish them due to the perceptible difference in the chemical shifts of methine CH ($\Delta = 2.5$ ppm), CO-carbons ($\Delta = 2.39$ ppm), and NH-protons ($\Delta = 1.4$ ppm).

In our opinion, the NMR identification of di(*m*-chlorobenzhydryl)urea **XVII** is extremely important, since the synthesis of compound **XII** always results in its di-derivative **XVII**, which accompanies the substance of the preparation as a minor impurity. When NMR spectra of compounds **XII** and **XVII** were compared, a significant difference of the chemical shift of the carbonyl groups was observed (approximately 2 ppm). The observed difference in the chemical shift of the C=O groups makes it possible to establish the presence of an impurity of compound **XVII** in substance **XII** by NMR. Using ^{13}C , ^{15}N NMR spectroscopy and quantum chemical calculations, it was shown that the CS in the ^{13}C spectra of C=O groups of urea does not correlate well with the electron density on the carbon atom [16]. It was found that the shielding of the carbonyl carbon atom in the di(*m*-chlorobenzhydryl) derivative of **XVII** in comparison with **XII** in the N-substitution of urea **I** is due to the presence of «bulky» radicals. The reason is an increase in steric stresses (compression) in compound **XVII** due to the «bulkiness» of symmetric diarylmethyl radicals, and an increase in the order of the amide bond, as a result.

The possible products of the initial hydrolytic transformations of hydantoin **VII** and a bicyclic urea **IX** were examined (Table 3). Thus, the formation of 4,5-dihydroxyimidazolidin-2-one **XVIII** is possible in the reaction mixture as an intermediate of synthesis of component compounds **VII**, **IX**, and the product of their long hydrolysis, therefore, its identification as an impurity is important.

Table 3

Chemical shifts in the NMR spectra of the probable products XVIII–XXIV of hydrolytic transformations of substances VII, IX and X

					
R=R ¹ =H (I) R=R ¹ =Me (XIX)		R=R ¹ =H (XVIII) R=R ¹ =Me (XX)		R=R ¹ =R ² =R ³ =H (IX); R=R ³ =Me, R ¹ , R ² =H (XXI); R=R ² =Me, R ¹ , R ³ =H (XXII); R=R ¹ =Me, R ² =R ³ =H (XXIII); R=Me, R ¹ =R ² =R ³ =H (XXIV);	
Chemical shifts of ¹ H NMR spectrum, δ, ppm (J, Hz)					
Substance	CH ₃	CH	CH	NH	OH
I	–	–	–	5.93 (2H, s)	–
XVIII	–	4.48 (2H, d)	–	6.98 (2H, s)	5.76 (2H, d)
IX	–	5.24 (2H, s)	–	7.16 (2H, s)	–
XIX	2.51 (6H, s)	–	–	6.12 (2H, s)	–
XX	2.65 (6H, s)	4.50 (2H, s)	–	–	6.24 (2H, s)
X	2.81 (12H, s)	5.06 (2H, s)	–	–	–
XXI	2.78 (6H, s)	5.15 (1H, d)	5.18 (1H, d)	7.39 (2H, s)	–
XXII	2.60 (6H, s)	5.10 (2H, s)	–	7.57 (2H, s)	–
XXIII	2.64 (6H, s)	5.12 (2H, s)	–	7.54 (2H, s)	–
XXIV	2.60 (3H, s)	5.14 (1H, d)	5.19 (1H, d)	7.20 (1H, s)	7.30 (2H, s)
Chemical shifts of ¹³ C NMR spectrum, δ, ppm (Hz)					
Substance	CH ₃	CH	CH	C=O	
I	–	–	–	161.5	–
XVIII	–	84.3	–	160.9	–
IX	–	64.6	–	160.3	–
XIX	26.8	–	–	160.8	–
XX	27.2	86.1	–	158.3	–
X	30.4	71.9	–	159.1	–
XXI	29.7	60.6	75.6	159.5	160.2
XXII	27.4	67.4	–	159.7	–
XXIII	28.2	76.7	–	158.2	–
XXIV	27.6	62.5	69.9	159.8	161.8

A combined analysis of the chemical shifts of NH protons in the series of acyclic urea **I** (5.93 ppm), monocyclic urea **XVIII** (6.98 ppm) and bicyclic urea **IX** (7.16 ppm) allows them to be reliably distinguished in the NMR spectra. Probably, the cyclization (**XVIII**) of urea **I** affects the displacement of the chemical shift of the NH groups to 6.98 ppm, and the bicyclization deshielding this signal to 7.16 ppm. (**IX**). Methine protons in cycle **XVIII** are shifted by 0.76 ppm in a higher-field relative to CH–CH glycoluril (**IX**), and, due to the structural features, resonate with a doublet. However, when comparing the chemical shifts of methine carbons in the ¹³C NMR spectra, an antibathical shift of the peaks is observed: the CH–CH signals of urea **XVIII** are shifted to a weak field by 21.7 ppm relative to bicycle **IX**. The positions of the signals of the carbonyl C=O groups in the ¹³C NMR spectra for substances **I**, **XVIII**, **IX** are almost the same, but the signal C=O group in acyclic urea **I** is the most deshielded. It can be noted that for the identification of compounds **I**, **XVIII**, **IX** proton NMR spectra are more informative.

In study Kurgachev et al [15], we isolated and characterized by chromatography and mass spectrometry analytical methods all possible N-methyl derivatives of glycoluril **XXI–XXIV**, which can be present as probable products of mebicar **X** transformation in hydrolysis conditions. In this study we compare the values of chemical shifts in the NMR spectra of N-methylglycoluril (hereafter, MeGU) **X**, **XXI–XXIV** and N,N'-dimethylurea **XIX** (Table 3). However, it is also necessary to take into account the possible presence of

the monocyclic analogue of 1,3-dimethyl-4,5-dihydroxyimidazolidin-2-one **XX** as an intermediate in the synthesis of urea **X** and its half-life product, the NMR characteristics of which are described in Table 3.

^1H and ^{13}C NMR methods are highly informative for the identification of methyl derivatives of urea-containing compounds **XIX–XXIV**. The presence of CH_3 -groups in MeGU **X**, **XXI–XXIV** leads to shielding of CH protons (5.24–5.06 ppm) and to deshielding of NH protons (7.16–7.55 ppm) of these compounds relative to **IX** in ^1H NMR spectra. A similar antibate effect was found in the ^{13}C NMR spectra for chemical shifts of compounds **X**, **XXI–XXIV**. There is a general deshielding of CH-carbons and a higher-field shift of C=O groups relatively to bisurea **IX** (Table 3).

In MeGU **X**, **XXI–XXIV** the most sensitive fragments to changes in the structure of the bicyclic skeleton are CH–CH fragments (Table 3), where the shielding range for ^1H signals is 0.18 ppm, and the range of changes for ^{13}C signals is observed from –4.0 ppm up to +12.1 ppm and –14.2 ppm for **XX** relative to MeGU **X**. Symmetric MeGUs **X** and **XXII**, **XXII** regularly give singlet peaks of CH-protons in the regions of 5.10, 5.12, and 5.06 ppm and annelated carbon atoms in the region of 67.4, 76.7, 71.9 ppm (Table 3). In asymmetric MeGUs **XXI** and **XXIV**, due to their nonequivalence, protons and carbons resonate in pairs in the regions 5.14–5.19 ppm, 5.15–5.18 ppm (^1H NMR) and 62.5–70.0 ppm, 60.6–75.6 ppm (^{13}C NMR). It is seen, that CH_3 groups have a symbiotic effect of de-shielding of CH signal in the ^{13}C NMR spectra of monocycles **XVIII** (84.3 ppm) and **XX** (86.1 ppm).

When comparing the chemical shifts of unsubstituted urea (**I**, **XVIII**, **IX**) and N,N'-methylureas (**X**, **XX**, **XIX**) (Table 3), it can be noted that N-methyl substituents cause weak shielding of the carbonyl atom carbon N–CO–N in ^{13}C NMR spectra. It can be determined by the effects of steric inhibition of conjugation in the amide fragment with a corresponding decrease in the order of the amide bond [16].

Thus, variations of the chemical shifts in the NMR spectra of substances **X**, **XX–XXIV** can be additionally caused by an increase in the effect of steric compression from methyl groups in the CH–N–Me fragment. This effect is progressive with an increase in the number of methyl groups in nitrogen atoms, as indicated by spectral data in Table 3.

In our opinion, the characteristics of the NMR spectra of compounds **XIV–XXIV** are suitable for determining the possible products of hydrolytic or oxidative transformations of urea-containing biologically active compounds **II–XIII**.

The ^1H (Fig. 2) and ^{13}C (Fig. 3) NMR spectra of the model mixture consisting of urea **I**, barbituric acid **II**, phenobarbital **IV**, N,N'-dimethylurea **XIX** and N-methylglycoluril **X** in DMSO-d_6 were for visual investigation of the environmental effect on chemical signals of C=O in a carbonyl fragment.

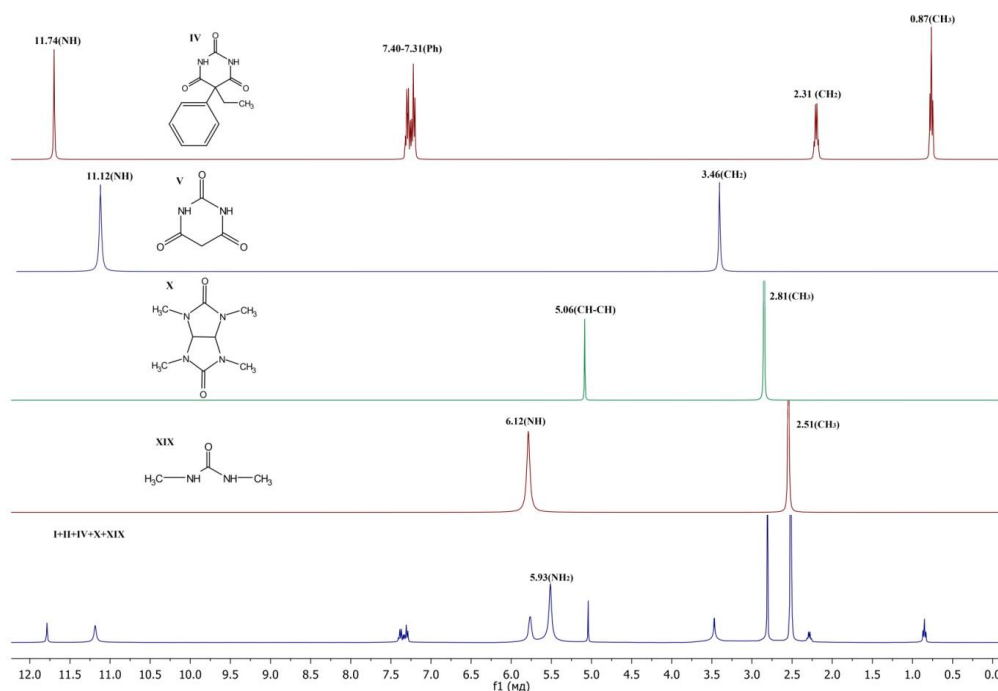


Figure 2. ^1H NMR spectrum of a model mixture of substances: urea **I**, barbituric acid **II**, phenobarbital **IV**, N,N'-dimethylurea **XIX** and N-methylglycoluril **X** in DMSO-d_6 (δ 2.50 ppm)

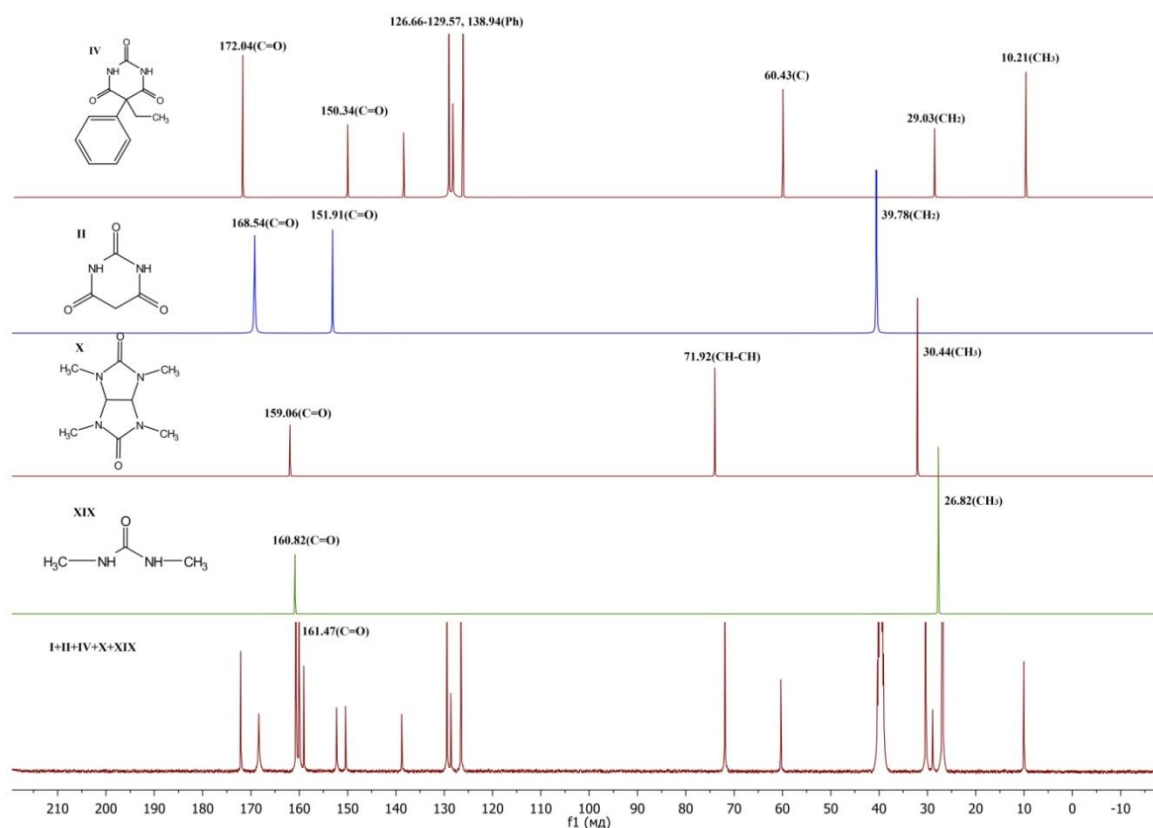


Figure 3. ^{13}C NMR spectrum of a model mixture of substances: urea **I**, barbituric acid **II**, phenobarbital **IV**, N,N'-dimethylurea **XIX** and N-methylglycoluril **X** in DMSO- d_6 (δ 39.5 ppm)

Resonance signals can overlap with solvent peaks when registering 1D spectra (Fig. 2 and 3) of mixtures of compounds **I**, **II**, **IV**, **XIX**, and **X** in DMSO- d_6 . But these substances are always distinguishable, since the same compound gives several signals in different regions of the NMR spectrum. In our example the difference in the chemical shifts of the urea NH-CO-NH fragment of compounds **I**, **II**, **IV**, **XIX**, and **X** is also noticeably. The position of the C=O signals depends on the substituent groups in NH-CO-NH.

Thus, the presented data of NMR spectra of the model mixture of substances **IV**, **X** and possible impurities **I**, **II**, **XIX** (Fig. 2 and 3) allows to reliably identify compounds and reliably distinguish them from each other. However, for this identification example (Fig. 2, 3), it is necessary to pre-record the spectra of the standards or to separate the components of the analyzed mixture.

In this paper, the possibility of using two-dimensional 2D NMR spectroscopy to simplify the identification procedure in the composition of complex mixtures was shown. Such widely recommended techniques [17–19] as ^1H - ^1H COSY homonuclear correlation spectroscopy (Fig. 4) and heteronuclear correlation methods (^1H - ^{13}C HSQC (Fig. 5) and ^1H - ^{15}N HSQC (Fig. 6)) were used. Determination of correlations in the spectra of COSY (Fig. 4) and HSQC (Fig. 5, 6) between the functional groups of compounds **I**, **II**, **IV**, **XIX**, and **X** in the mixture was shown.

It can be seen (Fig. 4) that the protons NH-CO-NH of phenobarbital **IV** have common cross peaks with the protons of their own molecule. The signal at 11.99 ppm correlates with the protons of the phenyl substituent 7.13 ppm, with a quartet at 2.25 ppm and triplet at 0.84 ppm of ethyl radical, which also have a peak of interaction (0.84 ppm; 2.24 ppm). Barbituric acid protons **II** (NH-CO-NH) have a common cross-peak with the signal of the CH_2 group (11.24 ppm, 3.46 ppm). Signal of the NH-group of N,N'-dimethylurea **XIX** at 5.82 ppm correlate with the doublet of the methyl radical at 2.53 ppm, and the methyl protons CH_3 of N-methylglycoluril **X** have a cross-peak with the methine group CH-CH (2.81 ppm; 5.04 ppm). Urea **I** NH protons at 5.32 ppm correlate with themselves due to equivalence and there is no cross-peak in the ^1H - ^1H COSY spectrum.

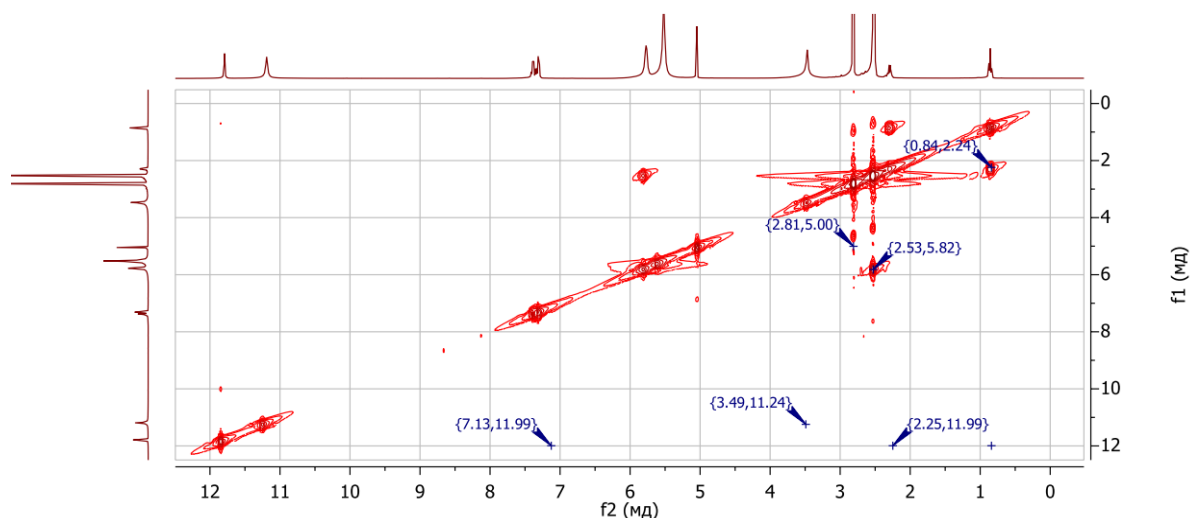


Figure 4. ^1H - ^1H COSY spectrum of a model mixture of substances: urea **I**, barbituric acid **II**, phenobarbital **IV**, N,N'-dimethylurea **XIX** and N-methylglycoluril **X** in DMSO- d_6 (δ 2.50 ppm)

After the correlation of the proton groups of individual substances was established, the data of the heteronuclear ^1H - ^{13}C HSQC spectrum were used (Fig. 5).

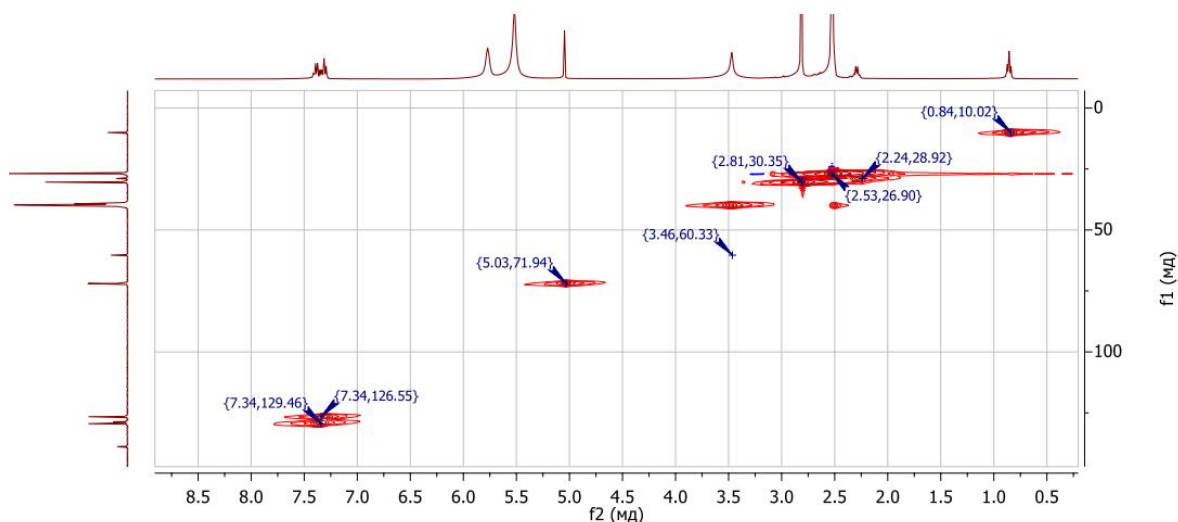


Figure 5. ^1H - ^{13}C HSQC spectrum of a model mixture of substances: urea **I**, barbituric acid **II**, phenobarbital **IV**, N,N'-dimethylurea **XIX** and N-methylglycoluril **X** in DMSO- d_6 (δ : 2.50 ppm; 39.5 ppm)

It is shown (Fig. 5) that previously established multiplet signals of Ph-protons of compound **IV** at 7.34 ppm have cross peaks with carbon signals at 126.6 ppm and 129.5 ppm, probably the carbon signal of the *para* position at 128.7 ppm is hidden. The proton signals of ethyl radical **IV** (0.84 ppm and 2.24 ppm) correlate with the signals of carbons (10.0 ppm and 28.9 ppm), respectively. Protons of the CH_2 group of barbituric acid **II** at 3.46 ppm directly bonded to carbon at 60.3 ppm. The signal of the methine $\text{CH}-\text{CH}$ group of the N-methylglycoluril **X** has a common peak in the regions: 5.04 ppm for ^1H and 71.9 ppm for ^{13}C , and methyl groups at 2.81 ppm correlate with a carbon signal of 30.4 ppm. Doublet of protons of the CH_3 group of N,N'-dimethylurea **XIX** at 2.53 ppm intersects with a carbon signal in the region of 26.9 ppm.

Chemical shifts of nitrogen atoms of ^{15}N amino groups of ureas **I**, **II**, **IV**, **XIX**, which have a direct N-H bond, can be determined in the ^1H - ^{15}N HSQC spectrum (Fig. 6).

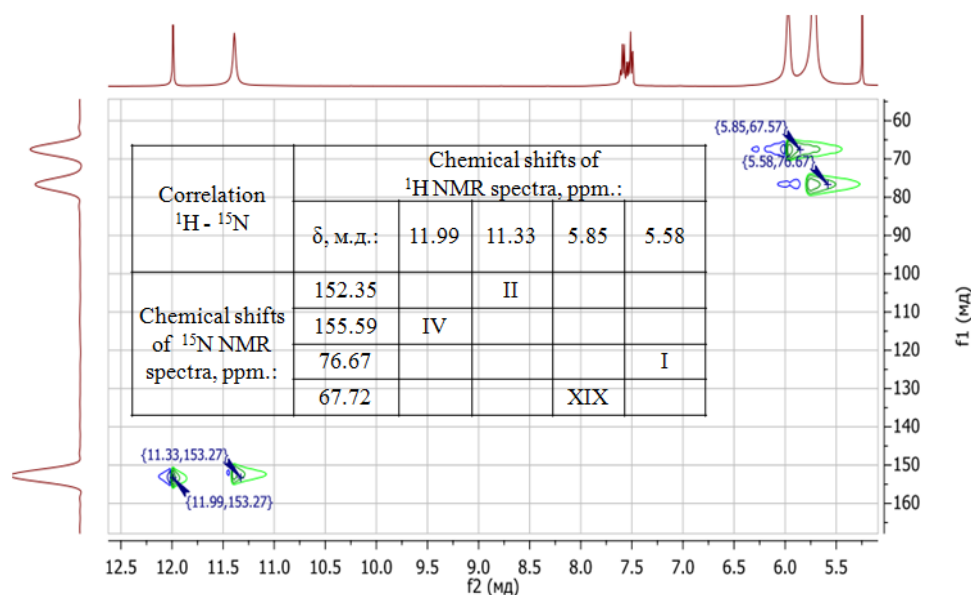


Figure 6. ^1H - ^{15}N HSQC spectrum of a model mixture of substances: urea **I**, barbituric acid **II**, phenobarbital **IV**, N,N'-dimethylurea **XIX** and N-methylglycoluril **X** in DMSO- d_6 (δ 2.50 ppm)

It can be seen (Fig. 6) that the chemical shift of the ^{15}N amino group of N,N'-dimethylurea **XIX** at 67.6 ppm is located in a stronger field relative to the signal ^{15}N of urea **I** (76.7 ppm) due to the electron-donating effect of methyl groups. A comparison of the ^{15}N chemical shifts of phenobarbital **IV** and barbituric acid **II** showed that the signals are in the same region (153.3 ppm), and this fact makes them indistinguishable. Almost twofold deshielding of the signals of the ^{15}N NH groups of compounds **II** and **IV** in comparison with the chemical shifts of urea **I** occurs due to intramolecular bisacetylation, causing an electron-withdrawing effect.

Conclusions

Thus, the data of chemical shifts of carbamide-containing biologically active compounds **I–XIII** (Table 1) make it possible to identify these substances, on the one hand, and, on the other, to reliably distinguish them in the ^1H and ^{13}C NMR spectra, including compounds of the same class of azaheterocycles (barbiturates **II–VI**, hydantoin **VII**, **VIII**, glycolurils **IX**, **X**, **XXI–XXIV**). It was shown on a model mixture of some urea-containing biologically active compounds **IV**, **X** and probable impurities **I**, **II**, **XIX** (Fig. 2, 3) that they can be easily identified by NMR spectra.

In addition, this study demonstrated the convenience of using two-dimensional 2D NMR spectroscopy to analyze a model mixture of **I**, **II**, **IV**, **XIX**, and **X** (Fig. 3–5), where the presence of standards and preliminary separation are not required to identify chemical shifts of compounds. The use of 2D methods of NMR spectroscopy can provide comprehensive information for the identification of all components of the analyzed sample.

In summary of the studies, it can be noted that the combined use of 1D and 2D NMR spectroscopy is convenient and informative to confirm the structure of biologically active compounds **I–XIII**. These methods make it possible to determine the presence and type of impurities **XIV–XXIV**, as well as to establish the destruction processes leading to the corresponding impurities **XIV–XXIV**.

References

- Haberle, J., Boddart, N., Burlina, A., Chakrapani, A., Dixon, M., & Huemer, M., et al. (2012). Suggested Guidelines for the Diagnosis and Management of Urea Cycle Disorders. *Orphanet journal of rare diseases*, 7, 1-30. <https://doi.org/10.1186/1750-1172-7-32>
- Meessen, J.H., & Petersen, H. (2010). Urea. *Ullmann's Encyclopedia of Industrial Chemistry: Electronic Release*. Weinheim: Wiley-VCH. https://doi.org/10.1002/14356007.a27_333.pub2
- Williams, A.C., Dragicevic, N., & Maibach, H. (2015). Urea. *Percutaneous Penetration Enhancers Chemical Methods in enetration Enhancement*. Berlin: Springer. <https://doi.org/10.1007/978-3-662-47039-8>

- 4 Bojic, J., Radovanovic, B., & Dimitrijevic, J. (2008). Spectrophotometric Determination of Urea in Dermatologic Formulations and Cosmetics. *Analytical science*, 24(6), 769-774. <https://doi.org/10.2116/analsci.24.769>
- 5 Decaux, G., Fabrice, C. A., Kengne, G., & Soupart, A. (2010). Treatment of euvoletic hyponatremia in the intensive care unit by urea. *Critical Care*, 14(5), R184. <https://doi.org/10.1186/cc9292>
- 6 Mamidi, R., Dallas, S., Sensenhauser, C., Lim, H. K., Scheers, E., & Verboven, P., et al. (2016). In vitro and physiologically-based pharmacokinetic assessment of drug-drug interaction potential of canagliflozin. *British Journal of Clinical Pharmacology*, 83(5), 1082–1096. <https://doi.org/10.1111/bcp.13186>
- 7 Citraro, R., Russo, E., Leo, A., Russo, R., Avagliano, C., & Navarra, M., et al. (2016). Pharmacokinetic-pharmacodynamic influence of N-palmitoylethanolamine, arachidonyl-2'-chloroethylamide and WIN 55,212-2 on the anticonvulsant activity of antiepileptic drugs against audiogenic seizures in DBA/2 mice. *European Journal of Pharmacology*, 791, 523–534. <https://doi.org/10.1016/j.ejphar.2016.09.029>
- 8 Williams, M., & Yokoyama N. (1986). Anxiolytics, Anticonvulsants and Sedative-Hypnotics. *Annual Reports in Medicinal Chemistry*, 21, 11–20. [https://doi.org/10.1016/S0065-7743\(08\)61112-4](https://doi.org/10.1016/S0065-7743(08)61112-4)
- 9 McElroy, N.R., Jurs, P.C., Morisseau, C., & Hammock, B.D. (2003). QSAR and classification of murine and human soluble epoxide hydrolase inhibition by urea-like compounds. *Journal of Medicinal Chemistry*, 46(6), 1066–1080. <https://doi.org/10.1021/jm020269o>
- 10 Librowski, T. Kubacka, M., Meusel, M., Scolari, S., Mueller, C.E., & Gütschow, M. (2007). Evaluation of anticonvulsant and analgesic effects of benzyl- and benzhydryl ureides. *European Journal of Pharmacology*, 559, 138–149. <https://doi.org/10.1016/j.ejphar.2006.12.002>
- 11 Bojarski, J.T., Mokrosz, J.L., Borton, H.J., & Paluchowska, M. H. (1985). Recent Progress in Barbituric Acid Chemistry *Advances in Heterocyclic Chemistry*, 38, 229–297. [https://doi.org/10.1016/S0065-2725\(08\)60921-6](https://doi.org/10.1016/S0065-2725(08)60921-6)
- 12 Lopez, C.A., & Trigo, G.G. (1985). The Chemistry of Hydantoins. *Advances in Heterocyclic Chemistry*, 38, 177–228. [https://doi.org/10.1016/S0065-2725\(08\)60920-4](https://doi.org/10.1016/S0065-2725(08)60920-4)
- 13 Bakibaev, A.A., Tignibidina, L.G., Filimonov, V.D., Gorshkova, V.K., Saratikov, A.S., & Pustovoitov, A.V., et al. (1991). Synthesis of arylmethylureas and effects of their structure on anticonvulsant activity. *Pharmaceutical chemistry journal*, 25, 31–35.
- 14 Gazieva, G.A., Kravchenko, A.N., Lebedev, O.V., Strelenko, Yu.A., & Chegaev, K.Yu. (1998). Reactions of sulfonamides with 4,5-dihydroxyimidazolidin-2-ones. *Russian Chemical Bulletin*, 47, 1561–1564. <https://doi.org/10.1007/BF02495610>
- 15 Kurgachev, D.A., Kotelnikov, O.A., Novikov, D.V., Kusherbaeva, V.R., Gorbin, S.I., & Tomilova, E.V., et al. (2018). Isolation, Identification, and Chromatographic Separation of N-Methyl Derivatives of Glycoluril. *Chromatographia*, 81, 1431–1437. <https://doi.org/10.1007/s10337-018-3599-9>
- 16 Reynolds, D.I., Webb, G.A., & Martin, M.L. (1982). Calculation of some ^{15}N and ^{13}C nuclear shielding parameters for some ureas and thioureas. *J. Mol. Struct.*, 90(3–4), P. 379–382. [https://doi.org/10.1016/0166-1280\(82\)80076-6](https://doi.org/10.1016/0166-1280(82)80076-6)
- 17 Hu, K., Westler, W.M., & Markley, J.L. (2011). Two-dimensional concurrent HMQC-COSY as an approach for small molecule chemical shift assignment and compound identification. *Journal of Biomolecular NMR*, 49, 291–296. <https://doi.org/10.1007/s10858-011-9494-4>
- 18 Jeannerat, D., & Furrer, J. (2012). NMR Experiments for the Analysis of Mixtures: Beyond 1D ^1H Spectra. *Combinatorial Chemistry & High Throughput Screening*, 15(1), 15–35. <https://doi.org/10.2174/138620712798280853>
- 19 Oman T., Tessem, M.B., Bathen, T.F., Bertilsson, H., Angelsen, A., & Hedenstrom, M., et al. (2014). Identification of metabolites from 2D ^1H - ^{13}C HSQC NMR using peak correlation plots. *BMC Bioinformatics*, 15, 413–420. <https://doi.org/10.1186/s12859-014-0413-z>

А.А. Бакибаев, С.Ю. Паньшина, О.В. Пономаренко,
В.С. Мальков, О.А. Котельников, А.К. Ташенов

Мочевина құрамындағы биологиялық белсенді қосылыстарды анықтауға арналған 1D және 2D NMR спектроскопиясы

Мочевина (карбамид) — сүтқоректілердегі азотты қосылыстардың алмасуының өнімі екені белгілі. Мочевина химияның саласындағы біртұтас зерттеулері көптеген биологиялық белсенді және басқа қосылыстар, құрамында мочевина NH–CO–NH фрагменті бар құрылымдарын жасауға мүмкіндік берді. Несепнәрді алмастыратын топтар оның қасиеттері мен сипаттамаларына тікелей әсер етеді, олар ЯМР спектрлік мәліметтерде көрініс табады және бұл жағдай мочевина туындыларын анықтауға негіз бола алады. Жұмыста мочевина мен оның туындыларының ЯМР спектрлеріндегі химиялық ауысулар зерттелді және анықталды: ациклдік құрылым, барбитуралық сериялар, имидазолидинондар сериясы және бициклдік құрылым. Орынбасар типінің s-ге NH–CO–NH фрагментінің NMR спектрлеріндегі позицияларының әсерін анықтау үшін жүйелік талдау жүргізілді. Сондай-ақ, кешенді қоспалар құрамындағы сәйкестендіру процедурасын жеңілдету үшін 2D NMR спектроскопиясын қолдану мүмкіндігі көрсетілген. 1D және 2D NMR спектроскопиясын бірге қолдану қосылыстар құрылымын құру үшін ыңғайлы және ақпараттылыққа ие. Бұл әдістер қоспалардың болуы мен түрін анықтауға және тиісті қоспаларға әкелетін жою процестерін орнатуға мүмкіндік береді.

Кілт сөздер: құрамында карбамид бар қосылыстар, барбитураттар, NMR спектроскопиясы, гидролизаттар, қоспалар.

А.А. Бакибаев, С.Ю. Паньшина, О.В. Пономаренко,
В.С. Мальков, О.А. Котельников, А.К. Ташенов

1D и 2D ЯМР-спектроскопия для идентификации карбамидсодержащих биологически активных соединений

Известно, что мочевина (карбамид) является продуктом метаболизма азотистых соединений у млекопитающих. Целенаправленные исследования в области химии мочевины позволили создать множество биологически активных и других соединений ациклической и гетероциклической структур, содержащих NH–CO–NH карбамидный фрагмент. Заместители в молекуле мочевины напрямую влияют на ее свойства и характеристики, которые отражаются в данных спектров ЯМР, и это обстоятельство может быть основанием для идентификации мочевины и ее производных. В статье изучены и идентифицированы химические сдвиги в спектрах ЯМР мочевины и ее производных: ациклического строения, барбитурового ряда, имидазолидинонового ряда и бициклического строения. Был проведен системный анализ для определения влияния типа заместителей на положения сигналов фрагмента NH–CO–NH в спектрах ЯМР. Авторами показана возможность использования 2D ЯМР-спектроскопии для упрощения процедуры идентификации сложных смесей, где совместное использование 1D и 2D ЯМР-спектроскопии достаточно удобно и информативно для установления структур биологически активных соединений. Данные методы позволяют нам определить наличие и тип примесей, а также процессы деструкции, приводящие к соответствующим примесям.

Ключевые слова: мочевина, карбамидсодержащие соединения, барбитураты, гликолурил, имидазолидинон, ЯМР-спектроскопия, гидролизаты, примеси.

Information about authors

Bakibaev, Abdigali Abdimanapvich — Doctor of Chemical Sciences, Professor, Leading Researcher of the Laboratory of Organic Synthesis, National Research Tomsk State University, Lenin str., 36, 634050, Tomsk, Russia; e-mail: bakibaev@mail.ru; <https://orcid.org/0000-0002-3335-3166>

Panshina, Svetlana Yur'evna (corresponding author) — Postgraduate of specialty chemistry, Analyst of the Laboratory of Organic Synthesis, National Research Tomsk Polytechnic University, Lenin str., 30, 634050, Tomsk, Russia, National Research Tomsk State University, Lenin str., 36, 634050, Tomsk, Russia; e-mail: janim_svetatusik@mail.ru; <https://orcid.org/0000-0001-6824-2645>

Ponomarenko, Oxana Vladimirovna — 3rd year PhD student of specialty chemistry, L.N. Gumilyov Eurasian National University, Satpaeva str., 2, 010000, Nur-Sultan, Kazakhstan; e-mail: oksana.ponomarenko.88@mail.ru, <https://orcid.org/0000-0002-8172-5139>

Malkov, Victor Sergeevich — Candidate of Chemical Sciences, Head of the Laboratory of Organic Synthesis, National Research Tomsk State University, Lenin str., 36, 634050, Tomsk, Russia; e-mail: malkov.vics@gmail.com; <https://orcid.org/0000-0003-4532-2882>

Kotelnikov, Oleg Alekseevich — Researcher of the Laboratory of Organic Synthesis, Spectroscopist, National Research Tomsk State University, Lenin str., 36, 634050, Tomsk, Russia; e-mail: kot_o_a@mail.ru; <https://orcid.org/0000-0002-1241-1312>

Tashenov, Auezkhan Karipkhanovich — Doctor of Chemical Sciences, Professor, Head of the Department of Chemistry, L.N. Gumilyov Eurasian National University, Satpaeva str., 2, 010000, Nur-Sultan, Kazakhstan; e-mail: tashenov_ak@enu.kz; <https://orcid.org/0000-0002-6880-2996>

CHEMICAL TECHNOLOGY

UDC 546.11:662.237.1

<https://doi.org/10.31489/2021Ch1/82-90>

D.E. Aitbekova^{1*}, D.K. Makenov¹, E.I. Andreikov², A.G. Tsauro³, Feng Yung Ma⁴,
G.G. Baikenova^{5,6}, A. Tusipkhan¹, A.A. Muratbekova¹, M.I. Baikenov¹

¹Karagandy University of the name of academician E.A. Buketov, Kazakhstan;

²Postovsky Institute of Organic Synthesis UB RAS, Ekaterinburg, Russia;

³Eastern Research Institute of Coal Chemistry, Ekaterinburg, Russia;

⁴Xinjiang University, Xinjiang Uyghur Autonomous Region, People's Republic of China;

⁵Karaganda Economic University of Kazpotreboysuz, Karaganda, Kazakhstan;

⁶South Ural State University, Chelyabinsk, Russia

(*Corresponding author's e-mail: darzhan91@mail.ru)

Hydrogen distribution in primary coke oven tar and its fractions

The aim of this work is to determine the hydrogen distribution in primary coke oven tar and its fractions. The hydrogen distribution in the primary coke oven tar of «ShubarkolKomir» JSC, its distillate fractions and distillation residue have been determined by the methods of elemental analysis, IR and PMR spectroscopy. The atomic ratio of C: H in the primary coke oven tar is 0.79. All fractions of the tar contain a large amount of alkyl-substituted aromatic compounds, phenols and other substances with alkyl groups. The initial tar characterized by a high content of hydrogen in the α - and β -positions to the aromatic ring, 29 % and 34 % respectively, which indicates a large number of alkyl substituents in the aromatic rings and near double bonds. The total amount of aliphatic and aromatic hydrogen in the tar is 79 % and 21 % respectively. Olefinic hydrogen is presented in the initial tar in an amount of 8 %. It is possible to make a choice of techniques for further processing (hydrogenation, coking, thermal cracking) to obtain products with high added value on the basis of determination of the elemental composition, quantitative distribution of hydrogen in the primary coke oven tar and its fractions by the using of above mentioned physical and chemical methods.

Keywords: primary coke oven tar, IR spectroscopy, PMR spectroscopy, elemental analysis, tar fractions, hydrogen distribution.

Introduction

Recently a decrease in reserves of low-viscosity, so-called «light» oils is observed. This requires the use of unconventional sources of hydrocarbon raw materials, new for oil refining, such as heavy oils and petroleum bitumens [1]. In addition, other types of alternative raw materials for oil refining and petrochemistry are coal products, which are not inferior in characteristics to their counterparts isolated from oil, and some have no analogues. This coal product is coke oven tar. Coke oven tars are obtained by the thermal processing of coal, which contain a significant amount of various organic compounds (hydrocarbons of all types and classes, heteroatomic, polyaromatic hydrocarbons, phenols and others). They can be used in oil refining, petrochemistry, ferrous and nonferrous metallurgy, nuclear industry. Coke-chemical tar is divided into two types: primary coke oven tar (PCOT) and high temperature coal tar [2–4]. It should be noted that high-temperature coke oven tar is used in industry, but primary coke oven tar doesn't find industrial application abroad and in our country, due to the high content of phenols (35–45 %) [5] and unstable low-boiling and resinous components [6]. The PCOT manufacturer in the Republic of Kazakhstan is «ShubarkolKomir» JSC [7]. All their products are sold in the near and far abroad as well as the entire produced volume of PCOT, which does not stimulate the development of innovative processes for obtaining multipurpose valuable low molecular weight hydrocarbons. Coke-chemical tar, consisting mainly of condensed aromatic hydrocarbons

and other high-molecular compounds, refers to a difficult-to-process raw material. Knowledge of the primary coke oven tar chemical composition and its fractions allows to determine the choice of methods for further processing (hydrogenation, coking, thermal cracking) to obtain products with high added value.

The aim of this work is to determine the hydrogen distribution in the initial tar and its fractions by the methods of elemental analysis, IR and PMR spectroscopy. The quantitative distribution of hydrogen in the initial coke oven tar and its fractions of «ShubarkolKomir» JSC was established using physicochemical methods for the first time.

Experimental

Physicochemical characteristics of the tar are determined according to the indicators listed in [8]. In addition, the fractional composition has been determined by the method described in [9, 10].

Due to the close values of the density of tar and water, dehydration of tar by sedimentation is practically impossible, which complicates the process of tar fractionation. Toluene was added in an amount of 10 % of the coal tar in order to separate water from the tar before distillation. After distillation of the azeotropic mixture of toluene with water, fractionation was carried out, and the temperature was measured both in the vapor and in the liquid phase. Fractionation has been stopped when the temperature in the liquid reached 390–405 °C, in order to avoid significant changes in the primary tar due to thermal reactions in the boiler. The fractions were selected as in the distillation of high-temperature coking tar. Fractions were selected in accordance with the range of their boiling points: up to 180 °C; 180–210 °C; 210–230 °C; 230–270 °C; above 270 °C and up to the end of distillation. A comparative analysis with the high-temperature coking tar of «ArcelorMittal Temirtau» JSC was carried out.

Determination of the carbon, and nitrogen content in the solid residue of pyrolysis has been carried out by «CHN PE 2400-II» an automatic analyzer of «PerkinElmerInstruments». The sulfur content has been determined by the method of barium titration.

IR spectra of pyrolysis solid residues were obtained by FTIR diffuse reflection spectroscopy on a spectrometer with a Fourier transducer «Perkin-ElmerSpectrumBX-II». The samples for the spectral recording were prepared by applying a thin layer of a carefully ground sample on a special holder plate. IR transmission spectra of liquid products were obtained by taking of layer.

The PMR spectra of the fractions obtained by distillation of the semi-coking tar were recorded by a Broker DRX 400 spectrometer with TMS, as an internal standard in a CDCl_3 solution, at room temperature.

The hydrogen distribution in the samples was determined by the PMR spectra according to the following signal assignments for chemical shifts:

0–1.0 ppm — corresponds to the protons of methyl groups that are not bound with aromatic rings or are in the γ -position to them, further (H_γ);

1.0–2.0 ppm — corresponds to the protons of methyl, methylene and methine groups located in β -position with regard to the aromatic ring and double bond, as well as methylene groups in saturated structures (H_β);

2.0–4.4 ppm — corresponds to the protons in all alkyl groups in the α -positions of aromatic rings and double bonds (H_α);

4.5–6.7 ppm — corresponds to the protons of olefinic structures (H_{olef});

6.7–9.0 ppm — corresponds to the protons of aromatic groups (H_{ar}).

Results and Discussion

Tar main characteristics

Provided by manufacturer two samples of tar with 12.5 % and 2.2 % of water content were studied (Table 1).

The main characteristics of «ShubarkolKomir» JSC tar in comparison with the high-temperature coking tar are shown in Table 2.

In comparison with the high-temperature coking tar, the studied tar is characterized by: low density (1.045–1.062 g/cm^3); low content of insoluble substances in toluene and the absence of insoluble substances in quinoline; a reduced yield of distillation residue (pitch); a high content of phenols and a low content of naphthalene.

Table 1

Technical analysis of «ShubarkolKomir» JSC tar samples

Description	1 st sample March 2019	2 nd sample April 2019
Tar density at 20 °C, g/cm ³	1.039	1.061
Tar density in terms of anhydrous at 20 °C, g/cm ³	1.045	1.062
Water content, %	12.5	2.2
Mass fraction of substances insoluble in toluene, %	1.3	1.4
Mass fraction of substances insoluble in quinoline, %	–	–
Ash content, %	0.12	–

Table 2

Comparison of the characteristics of tar from «ShubarkolKomir» JSC and «ArcelorMittal Temirtau» JSC

No.	Indicator	Tar types		Determination method
		«ShubarkolKomir» JSC tar	«ArcelorMittal Temirtau» JSC high-temperature coke oven tar	
1	Density at 20°C, g/cm ³	1.062	1.190	State Standard [11, 12]
2	Fractional composition, mass fraction (from anhydrous tar), %			Specification [9], [10]
	till 180 °C	5.1	0.5	
	180–210 °C	4.4	2.5	
	210–230 °C	4.8	10	
	230–270 °C	15.8	8	
	up to 270 °C by vapor			
	till 390 °C in a still	19.7	19	
	up to 270 °C by vapor			
	till 405°C in a still	26.1		
	Distillation residue (pitch) yield, %			
	at 390 °C in a still	49.8		
	at 405 °C in a still	40.0	60	
3	Mass fraction of substances insoluble in toluene (α -fraction), %	1.4	6–10	State Standard [13], specification [8]
4	Mass fraction of substances insoluble in quinoline (α 1-fraction), %	–	4–6	State Standard [14], specification [8]
5	Ash content, %	0.12	<0.3	Specification [8]
6	Phenol content, %	20.6	1–2	Calculated by the content of phenols in distillate fractions up to 390 °C in a still
7	Naphthalene content, %	1.6	7–12	According to GLC/MS data of distillate fractions

Elemental analysis of fractions

Data on the density of fractions and the elemental composition of fractions and pitch are shown in Table 3.

From the data in Table 3 it follows:

- the carbon content reaches 80.6–82.5 % in the fractions, and 83–84 % in pitch;
- the hydrogen content is 9.1–9.8 % in the fractions and it decreases to 7.4–7.8 % in the pitches;
- the atomic ratio of C: H is at the level of 0.71–0.79 in the fractions and it increases to 0.90–0.94 in pitch;
- fractions and pitch contain more than 9–10 % of the total oxygen and sulfur, while the sulfur content is less than 0.3 %, the oxygen content declines considerably in the distillation residues.

Density of fractions and results of elemental analysis

Name product	Density, g/cm ³	Content, % mass.				C/H atom
		C	H	N	S+O	
Dehydrated tar	1.039	81.45	8.57	0.69	9.29	0.79
180–210 °C fraction	0.954	80.60	9.11	1.07	10.29	0.74
210–230 °C fraction	0.965	80.64	9.41	1.06	8.89	0.71
230–270 °C fraction	0.970	80.89	9.23	0.93	8.95	0.73
up to 270 °C fraction by vapor till 405 °C in a still	0.993	82.46	8.73	0.91	7.98	0.79
up to 390 °C distillation residue in a still	–	83.11	7.40	0.87	8.62	0.94
up to 405 °C distillation residue in a still	–	84.10	7.78	0.68	7.44	0.90

Description of IR spectra

Figure 1 shows the IR spectrum of the initial tar.

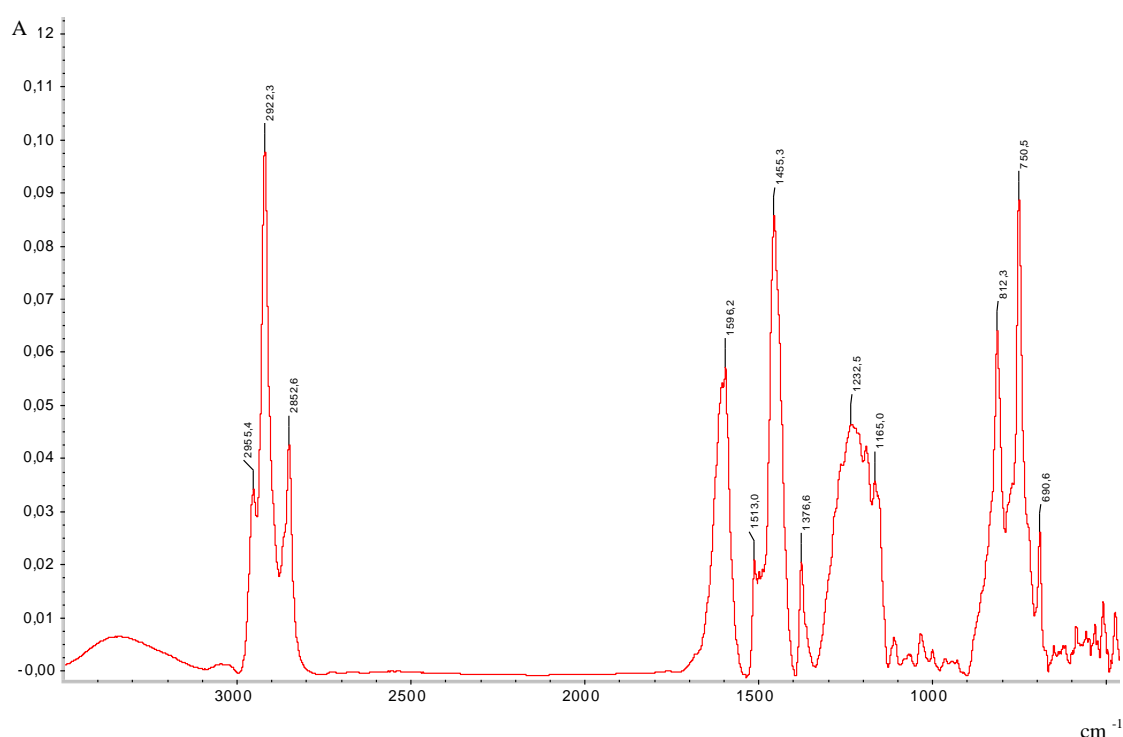


Figure 1. IR spectrum of dehydrated tar

The general view of the spectra for fractions and residues of tar distillations is similar, which indicates the presence of identical organic functional groups in all samples.

The most important information is the absorption in the region of 3.040–2.800 cm⁻¹. Strong absorption below 3.000 cm⁻¹ (C-H bonds of methyl and methylene groups) indicates a significant amount of alkyl groups. In addition, the vibrations of -CH₃ and -CH₂ groups correspond to absorption bands at about 1,450 and 1,375 cm⁻¹. At the same time, the absorption of aromatic hydrogen at 3.020 cm⁻¹ is weak.

The second feature is a wide band with a maximum at 3.380–3.370 cm⁻¹ which is related to phenolic hydroxyls.

The bands in the region of 900–700 cm⁻¹ correspond to the vibrations of the aromatic ring c-h bonds. The most pronounced bands are at 815 cm⁻¹ (1,4-substituted aromatic ring) and a peak at about 750 cm⁻¹ (1,2-substituted aromatic ring). Strong absorption around 1,600 cm⁻¹ belongs to the aromatic ring. The bands in the range of 1,280–1,050 cm⁻¹ refer to the Ar-O group in phenols.

The following small changes in the IR spectra for the coal tar and pitch fractions can be noted: the fractions (up to 230 °C and 230–270 °C) are characterized by stronger absorption at 1,514 cm⁻¹ (vibration of the benzene ring) and in the region of 900–700 cm⁻¹, which indicates a higher content of compounds with one benzene ring.

Description of PMR spectra

Figures 2, *a-c* show the PMR spectra of the initial tar, distillate fraction 230–270 °C and distillation residue. Quantitative data on the distribution of hydrogen types according to the PMR data in tar, distillate fractions and distillation residues are given in Table 4.

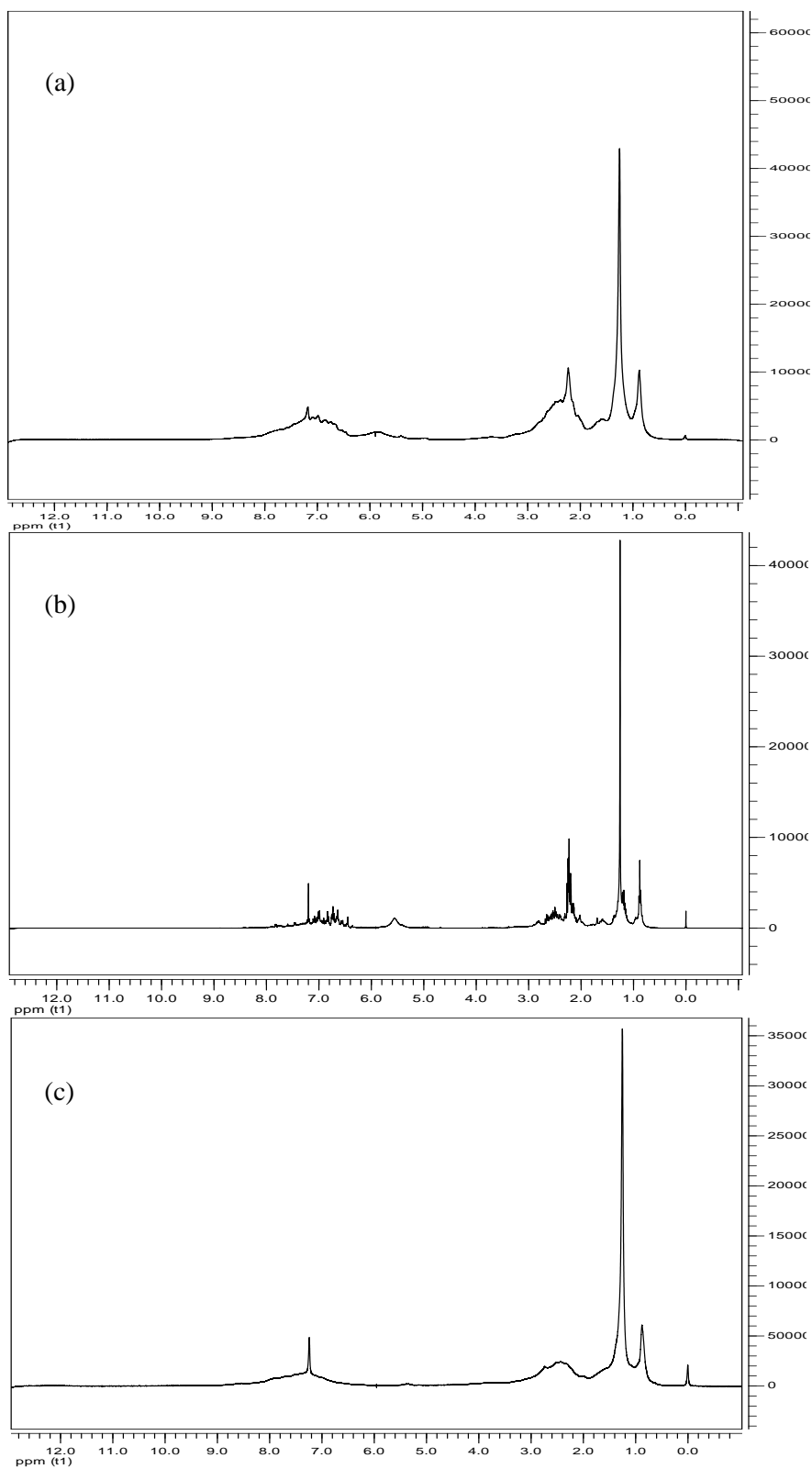


Figure 2. PMR spectra of dehydrated tar (*a*), 230–270 °C distillate fraction (*b*) and up to 405 °C distillation residue

Distribution of hydrogen types in tar, distillate fractions and distillation residues

Sample	Proton distribution, %				
	H _γ	H _β	H _α	H _{olef}	H _{ar}
Tar	8.42	33.84	29.38	7.74	20.62
180–210 °C fraction	8.57	28.79	28.36	10.03	24.25
210–230 °C fraction	8.95	32.59	29.36	10.29	18.81
230–270 °C fraction	8.55	32.65	31.28	10.51	17.01
up to 270 °C by vapor and till 405 °C in a still	8.46	39.93	28.54	7.70	15.40
up to 390 °C distillation residue in a still	11.66	40.56	26.57	–	21.21
up to 405 °C distillation residue in a still	9.79	43.29	25.17	–	21.75

All fractions and distillation residues are characterized by high content of hydrogen at the α - and β -positions to the aromatic ring. The number of alkyl groups with more than three carbon atoms in the chain is small, as $H_{\gamma} < H_{\alpha}$.

The total amount of aliphatic hydrogen is several times higher than that of aromatic hydrogen. The 180–210 °C fraction contains the largest amount of aromatic hydrogen.

Olefinic hydrogen (unsaturated compounds) is present in the initial primary coke oven tar and distillate fractions, its relative amount decreases for the heaviest fraction, and olefinic hydrogen is not found in the distillation residues.

Conclusions

Thus the results of IR spectral studies show that all fractions of the coke oven tar and the pitch obtained from it contain a large amount of alkyl-substituted aromatic compounds, phenols and other substances with alkyl groups. Aromatic compounds generally contain substituents at the ortho- and para- positions. The IR spectrum of the pitch does not fundamentally differ from the IR spectra of the fractions, i.e. it also contains hydrogen mainly in alkyl groups and contains phenolic groups.

According to the results of the elemental analysis the atomic ratio of C: H in the primary coke oven tar is 0.79.

Primary coke oven tar has a high content of hydrogen in the α - and β -positions to the aromatic ring, 29 % and 34 % respectively, which indicates a large number of alkyl substituents in the aromatic rings and near double bonds. The total amount of aliphatic hydrogen is 79 %. It is several times more than the amount of aromatic hydrogen, which is 21 %. The high content of alkyl substituents in aromatic rings allows using 180–230 °C distillate fractions of the tar to increase the octane and cetane number in the production of motor fuel.

Fractions with a boiling point above 270 °C can be used to obtain boiler fuel, carbon black, coke and needle coke.

The products manufactured by oil refinery or coal chemical enterprises can be diversified through knowledge of the hydrogen distribution and the use of the compounding method.

Thus the results obtained in this study can be the basis for choosing the most preferable direction for further processing of raw materials.

References

- 1 Dmitriev D.E. Transformations of resins and asphaltenes during the thermal treatment of heavy oils / D.E. Dmitriev, A.K. Golovko // *Petroleum Chemistry*. — 2010. — Vol. 50, No. 2. — P. 106–113. <https://doi.org/10.1134/S0965544110020040>
- 2 Бейлина Н.Ю. Совершенствование технологии переработки каменноугольной смолы / Н.Ю. Бейлина, В.В. Заманов, А.А. Кричко, А.А. Озеренко, Е.А. Озеренко, С.Б. Фросин // *Кокс и химия*. — 2006. — № 7. — С. 35, 36.
- 3 Кричко А.А. Получение и применение псевдогомогенных катализаторов для гидрогенизации и крекинга углеводородного сырья. Сообщение 2. Применение псевдогомогенных катализаторов для глубокой переработки нефтяного и коксохимического сырья / А.А. Кричко, А.А. Озеренко, Е.А. Озеренко, С.Б. Фросин, Л.А. Зекель, А.С. Малолетнев, М.Я. Шпирт, В.В. Заманов // *Катализ в промышленности*. — 2007. — № 3. — С. 23–32.
- 4 Lapidus A.L. Characterization of pitch and coke obtained from the semicoking tar of high-sulfur oil shale from the Volga basin / A.L. Lapidus, D.S. Khudyakov, F.G. Zhagfarov, N.Y. Beilina // *Solid Fuel Chemistry*. — 2020. — Vol. 54, No. 1. — P. 21–24. <https://doi.org/10.3103/S0361521920010048>

5 Baikenov M.I. Cavitation extraction of phenols from coal tar / M.I. Baikenov, S.K. Amerkhanova, G.G. Baikenova, R.M. Shlyapov, A.E. Tuktybaeva // Solid Fuel Chemistry. — 2013. — Vol. 47, No. 1. — P. 27–33. <https://doi.org/10.3103/S0361521912060031>

6 Burkeev M.Zh. Thermal destruction of copolymers of polypropylene glycol maleate with acrylic acid / M.Zh. Burkeev, A.Zh. Sarsenbekova, E.M. Tazhbaev, I.V. Figurinene // Russian Journal of Physical Chemistry A. — 2015. — Vol. 89, No. 12. — P. 2183–2189. <https://doi.org/10.1134/S0036024415120067>

7 Tateyeva A.B. Researching of physicochemical properties of the special coke of «ShubarkolKomir» JSC / A.B. Tateyeva, M.I. Baikenov, V.I. Parafilov, Ye.N. Martynova, S.K. Mukhametzhanova, D.Ye. Aitbekova // Bulletin of the Karaganda University. — 2018. — Vol. 91, No. 3. — P. 120–125.

8 Смола каменноугольная для переработки. Технические условия: ТУ 2453–203–00190437–2005 [Введен в действие от 2005–03–09]. — Регистр Роспотребнадзора санитарно-эпидемиологических заключений на проектную документацию.

9 Глузман Л.Д. Лабораторный контроль коксохимического производства / Л.Д. Глузман, И.И. Эдельман. — М.: Металлургия, 1968. — 472 с.

10 Патент № 0002512620 РФ. Способ определения группового фракционного состава каменноугольных смол / Косарева М.А., Загайнов В.С., Кондратов В.К., Онищук Н.И. Опубл. 10.04.2014.

11 Нефтепродукты. Методы анализа. Часть 1: Сборник национальных стандартов: ГОСТ 3900–85 Нефть и нефтепродукты. Методы определения плотности (с Изменением N 1, с Поправкой) [Введен в действие от 1987–01–01]. — М.: Стандартинформ, 2006. — (Госстандарт СССР).

12 Сырье коксохимическое для производства технического углерода. Технические условия: ГОСТ 11126–2019. [Введен в действие от 2020–03–01]. — М.: Стандартинформ, 2019. — (Росстандарт).

13 Пек каменноугольный. Метод определения массовой доли веществ, нерастворимых в толуоле (с Изменениями N 1, 2, 3, 4): ГОСТ 7847–73. [Введен в действие от 1975–01–01]. — М.: ИПК Издательство стандартов, 1997. — (Госстандарт СССР).

14 Пек каменноугольный электродный. Технические условия: ГОСТ 10200–2017. [Введен в действие от 2019–03–01]. — М.: Стандартинформ, 2018. — (Росстандарт).

Д.Е. Айтбекова, Д.К. Макенов, Е.И. Андрейков, А.Г. Цаур, Фен Юн Ма,
Г.Г. Байкенова, А. Түсіпхан, А.А. Муратбекова, М.И. Байкенов

Біріншілік таскөмір шайыры мен оның фракцияларында сутегінің таралуы

Элементтік талдау, ИК- және ПМР-спектроскопия әдістерімен «Шұбаркөл Көмір» АҚ бастапқы таскөмір шайырында, оның дистилляттық фракцияларында және дистилляция қалдығында сутектің таралуы анықталды. Біріншілік көмір шайырындағы С : Н атомдық қатынасы 0.79 құрайды. Шайырдың барлық фракцияларында алкилорынбасылған ароматты қосылыстар, фенолдар және алкил топтары бар басқа қосылыстар көп. Бастапқы шайыр ароматты сақинаға α - және β -жағдайларда орналасқан сутектің жоғары құрамымен сипатталады, сәйкесінше 29 % және 34 %, бұл ароматты сақиналарда және қос байланыстардың жанында алкилді орынбасушылардың көп мөлшерін көрсетеді. Біріншілік таскөмір шайырындағы алифатты және ароматты сутектің жалпы мөлшері сәйкесінше 79 % және 21 % құрайды. Біріншілік шайырда олефинді сутегі 8 % құрайды. Жоғарыда аталған физика-химиялық әдістердің көмегімен біріншілік таскөмір шайырындағы және оның фракцияларындағы сутектің элементтік құрамын, сандық таралуын анықтау жоғары құнды өнімдерді алу үшін одан әрі қайта өңдеу (гидрогенизация, кокстеу, термиялық крекинг) әдістерін таңдауды айқындауға мүмкіндік береді.

Кілт сөздер: біріншілік таскөмір шайыры, ИК-спектроскопия, ПМР-спектроскопия, элементтік талдау, шайыр фракциялары, сутегінің таралуы.

Д.Е. Айтбекова, Д.К. Макенов, Е.И. Андрейков, А.Г. Цаур, Фен Юн Ма,
Г.Г. Байкенова, А. Түсіпхан, А.А. Муратбекова, М.И. Байкенов

Распределение водорода в первичной каменноугольной смоле и ее фракциях

Методами элементного анализа, ИК- и ПМР-спектроскопии установлено распределение водорода в первичной каменноугольной смоле АО «Шубарколь Комир», ее дистиллятных фракциях и непереогневаемом остатке дистилляции. Атомное соотношение С : Н в первичной каменноугольной смоле составляет 0,79. Все фракции смолы содержат большое количество алкилзамещенных ароматических соединений, фенолов и других соединений с алкильными группировками. Исходная смола характеризуется высоким содержанием водорода, находящегося в α - и β -положениях к ароматическому кольцу, 29 и 34 % соответственно, что свидетельствует о большом количестве алкильных заместителей в ароматических кольцах и рядом с двойными связями. Общее количество алифатического и ароматического водорода в смоле составляет 79 и 21 % соответственно. В исходной смоле олефиновый водород

присутствует в количестве 8 %. Установление элементного состава, количественного распределения водорода в первичной каменноугольной смоле и ее фракциях с помощью названных выше физико-химических методов позволяет определиться в выборе методов дальнейшей переработки (гидрогенизация, коксование, термический крекинг) для получения продуктов, имеющих высокую добавленную стоимость.

Ключевые слова: первичная каменноугольная смола, ИК-спектроскопия, ПМР-спектроскопия, элементный анализ, фракции смолы, распределение водорода.

References

- 1 Dmitriev, D.E., Golovko, A.K. (2010) Transformations of resins and asphaltenes during the thermal treatment of heavy oils. *Petroleum Chemistry*, 50(2), 106–113. <https://doi.org/10.1134/S0965544110020040>
- 2 Beilina, N.Yu., Zamanov, V.V., Krichko, A.A., & Frosin, S.B. (2006). Sovershenstvovanie tekhnologii pererabotki kamennouholnoi smoly [Improvement of coal tar processing technology]. *Koks i khimiia — Coke and Chemistry*, 7, 35–36 [in Russian].
- 3 Krichko, A.A., Ozerenko, A.A., Ozerenko, E.A., & Zamanov, V.V. (2007). Poluchenie i primeneniye psevdohomohennykh katalizatorov dlia hidrogenizatsii i krekinha uhlevodorodnogo syria. Soobshchenie 2. Primeneniye psevdohomohennykh katalizatorov dlia hlubokoi pererabotki neftianoho i koksokhimicheskoho syria [Preparation and application of pseudo-homogeneous catalysts for hydrogenation and cracking of hydrocarbon raw materials. Message 2. Application pseudo-homogeneous catalysts for deep processing of oil and coke-chemical raw materials]. *Kataliz v promyshlennosti — Catalysis in Industry*, 3, 23–32 [in Russian].
- 4 Lapidus, A.L., Khudyakov, D.S., Zhagfarov, F.G., & Beilina, N.Y. (2020). Characterization of pitch and coke obtained from the semicoking tar of high-sulfur oil shale from the Volga basin. *Solid Fuel Chemistry*, 54(1), 21–24. <https://doi.org/10.3103/S0361521920010048>
- 5 Baikenov, M.I., Amerkhanova, S.K., Baikenova, G.G., Shlyapov, R.M., & Tuktybaeva, A.E. (2013). Cavitation extraction of phenols form coal tar. *Solid Fuel Chemistry*, 47(1), 27–33. <https://doi.org/10.3103/S0361521912060031>
- 6 Burkeev, M.Zh., Sarsenbekova, A.Zh., Tazhbaev, E.M., & Figurinene, I.V. (2015). Thermal destruction of copolymers of polypropylene glycol maleate with acrylic acid. *Russian Journal of Physical Chemistry A*, 89(12), 2183–2189. <https://doi.org/10.1134/S0036024415120067>
- 7 Tateyeva, A.B., Baikenov, M.I., Parafilov, V.I., Martynova, Ye.N., Mukhametzhanova, S.K., & Aitbekova, D.Ye. (2018). Researching of physicochemical properties of the special coke of «ShubarkolKomir» JSC. *Bulletin of the Karaganda University*, 91(3), 120–125.
- 8 Smola kamennouholnaia dlia pererabotki. Tekhnicheskie usloviia: TU 2453–203–00190437–2005 (Vveden v deistvie ot 2005-03-09) [Coal tar for processing. Specifications: TU 2453–203–00190437–2005 from 9th March 2005]. (2005). *Reestr Rospotrebnadzora sanitarno-epidemiologicheskikh zakliucheni na proektnuiu dokumentatsiiu — Rospotrebnadzor Register of Sanitary and Epidemiological Conclusions for Design Documentation* [in Russian].
- 9 Hluzman, L.D., & Edelman, I.I. (1968). *Laboratornyi kontrol koksokhimicheskoho proizvodstva [Laboratory control of coke-chemical production]*. Moscow: Metallurhiia [in Russian].
- 10 Kosareva, M.A., & Onishchuk, N.I. (2014). Sposob opredeleniia hruppovoho fraktsionnogo sostava kamennouholnykh smol [Method for determining the group fractional composition of coal tar]. *Patent No. 0002512620 RF* [in Russian].
- 11 Nefteprodukty. Metody analiza. Chast 1: Sbornik natsionalnykh standartov [Petroleum products. Method of analysis. Part 1: Collection of national standards]. (2006). *HOST 3900–85 Neft i nefteprodukty. Metody opredeleniia plotnosti (s Izmeneniami N 1, s Popravkoi) [Oil and petroleum products. Methods for determining density (with Change N 1, with Correction)] from 1st January 1987*. Moscow: Standartinform [in Russian].
- 12 Syre koksokhimicheskoe dliia proizvodstva tekhnicheskoho uhlevodoroda. Tekhnicheskie usloviia [Coke chemical raw materials for production of industrial carbon. Specifications]. (2019). *HOST 11126–2019 from 1st March 2020*. Moscow: Standartinform [in Russian].
- 13 Pek kamennouholnyi. Metod opredeleniia massovoi doli veshchestv, nerastvorimyykh v toluole (s Izmeneniami N 1, 2, 3, 4) [Coal-tar pitch. Method for determination of mass fraction of substances insoluble in toluene]. (1997). *HOST 7847–73 from 1st January 1975*. Moscow: IPK Izdatelstvo standartov [in Russian].
- 14 Pek kamennouholnyi elektrodnyi. Tekhnicheskie usloviia [Electrode coal-tar pitch. Specifications]. (2018). *HOST 10200–2017 from 1st March 2019*. Moscow: Standartinform [in Russian].

Information about authors

Aitbekova, Darzhan Ergalievna (*corresponding author*) — doctoral student, Karagandy University of the name of academician E.A. Buketov, Universitetskaya street, 28, 100028, Karaganda, Kazakhstan; e-mail: darzhan91@mail.ru; <https://orcid.org/0000-0002-6839-9711>

Makenov, Daulet Kairzhanovich — doctoral student, Karagandy University of the name of academician E.A. Buketov, Universitetskaya street, 28, 100028, Karaganda, Kazakhstan; e-mail: mckenov.daulet@gmail.com; <https://orcid.org/0000-0002-1011-7662>

Andreikov, Eugeny Iosifovich — doctor of chemical sciences, Postovsky Institute of organic synthesis UB RAS, Sofia Kovalevskaya, 22, 620108, Ekaterinburg, Russia; e-mail: cc@ios.uran.ru; <https://orcid.org/0000-0002-9285-9036>

Tsaur, Anatoly Grigorevich — senior researcher, JSC «Eastern research Institute of coal chemistry», 8-Marta, 14, 620990, Ekaterinburg, Russia; e-mail: tsaur@rosfirm.ru

Ma, Feng Yung — PhD doctor, professor, Xinjiang University, Urumqi, People's Republic of China, ma_fy@126.com

Baikenova, Gulzhan Causilevna — doctor of chemical sciences, professor, Karaganda Economic University of Kazpotrebsoyuz, Karaganda, Kazakhstan; South Ural State University, Chelyabinsk, Russia; e-mail: murzabek_b@mail.ru; <https://orcid.org/0000-0002-2816-3341>

Tusipkhan, Almas — PhD doctor, senior lecturer, Karagandy University of the name of academician E.A. Buketov, Universitetskaya street, 28, 100028, Karaganda, Kazakhstan; e-mail: almas_kz_22@mail.ru; <https://orcid.org/0000-0002-6452-4925>

Muratbekova, Aigul Akizhanovna — candidate of chemistry sciences, docent, Karagandy University of the name of academician E.A. Buketov, Universitetskaya street, 28, 100028, Karaganda, Kazakhstan; e-mail: aigulmuratbekova@mail.ru; <https://orcid.org/0000-0002-2156-9306>

Baikenov, Murzabek Ispolovich — doctor of chemical sciences, professor, Karagandy University of the name of academician E.A. Buketov, Universitetskaya street, 28, 100028, Karaganda, Kazakhstan; e-mail: murzabek_b@mail.ru; <https://orcid.org/0000-0002-8703-0397>

K.K. Pirniyazov^{1*}, V.E. Tikhonov², S.Sh. Rashidova¹

¹*Institute of Chemistry and Physics of Polymers of the Academy of Sciences of the Republic of Uzbekistan, Tashkent, Uzbekistan;*

²*Institute of Organoelement Compounds, Russian Academy of Sciences A.N. Nesmeyanov, Moscow, Russia*

(*Corresponding author's e-mail: qudrat.pirniyazov@mail.ru)

Synthesis and properties of oligochitosan ascorbate from *Bombyx mori*

Oligochitosan samples were obtained by acid hydrolysis of high molecular weight chitosan isolated from *Bombyx mori* (B.M.). Carrying out acid hydrolysis for 6 hours, it was found that after 4 hours and further with increasing duration, the molecular weight of chitosan decreases to a value corresponding to the ranges of molecular weights of oligochitosan 2–16 kDa. It has been seen that the optimal duration of hydrolysis, leading to the production of oligochitosan with a molecular weight of less than 16 kDa, should be considered 4–5 hours. Depolymerization of chitosan with a molecular weight of 177 kDa was carried out using sodium nitrite in solution to obtain oligochitosan with a molecular weight of 6 kDa. On the basis of oligochitosan samples obtained by two methods, their ascorbates were received. Under constant conditions with varying the ratio of the components (ChS:AA) and the pH of the solution, the reaction of chitosan ascorbate formation was carried out on the basis of the suspension method. The composition, structure, and molecular weight characteristics of oligochitosan ascorbate and oligochitosan *Bombyx mori* samples were confirmed by physicochemical methods. It has been seen that the obtained samples have antimicrobial properties against *Fuzarium oxysporum*.

Keywords: *Bombyx mori* chitosan ascorbate, *Bombyx mori* oligochitosan, ascorbic acid, donor-acceptor bond, degree of binding, degrees of acetylation, depolymerization.

Introduction

One of the most promising and relevant areas of modern chemistry and technology is the production of water-soluble natural polymers, the study of the structure, properties, physical and chemical modifications, their application in various fields. The production of water-soluble chitosan derivatives expands the range of applications of this natural aminopolysaccharide in agriculture and biomedical sphere. The solubility of chitosan in water depends on a number of factors including the molecular weight and deacetylation degree (DD) of the polymer, the degree of protonation of amino groups in the macromolecule (pH of the solution) [1, 2]. Chitosan macromolecules are characterized by different molecular weights (degree of polymerization), degree of deacetylation, degree of protonation (pKa value), viscosity of solutions, arrangement of acetylated and deacetylated residues in the polymer chain and molecular weight distribution. Most of the mentioned characteristics affect the solubility of chitosan in water, while the manifestation of biologically active properties by chitosan largely depends on the solubility [3–4]. In [5, 6], the antibacterial activity of narrowly dispersed samples of oligochitosans, varying in molecular weight, at different pH values was studied. It was shown that under acidic conditions a stronger inhibitory effect is characteristic of samples with a higher molecular weight, while under slightly alkaline conditions, chitosan forms close to oligomeric are more active. It is assumed that the antibacterial activity of chitosan is determined by the protonation degree of its amino groups, which is variable and depends on both the molecular weight of the substance and the pH of the medium.

The analysis of numerous studies shows that the water solubility of low molecular weight chitosan (oligochitosan) increases with biological activity, especially antiviral and antibacterial activity, as well as biocompatibility with a decrease in molecular weight compared to the high molecular weight chitosan [6–8].

Chitosan derivatives are of great interest in the world, including chitosan ascorbate, which has bactericidal, growth-stimulating and antifungal properties. It should be noted that water-soluble forms of oligochitosan with organic acids have the most pronounced antimicrobial properties against the following bacteria: *Streptococcus mutans*, *Lactobacilli brevis* using in vitro and in vivo methods compared to similar forms of high molecular weight chitosans [9]. Chitosan ascorbate also has antioxidant properties against a number of bacteria, such as *E. coli*, *P. aeruginosa*, *S. typhimurium*, *L. monocytogenes*, and *S. aureus* at low concentrations [9–11]. In order to obtain biologically active, water-soluble derivatives of oligochitosans with ascorbic acid, the synthesis was carried out by the suspension method with varying the pH of the solution.

Experimental part

Two samples of high molecular chitosan which were achieved from pupae of the silkworm *Bombyx mori* with a molecular weight of 123 kDa (ChS-1) and 177 kDa (ChS-2) have been used in this experiment. The molecular weights of the samples were determined by viscometry, and the degree of deacetylation was measured by conductometric titration, where the value was 94 % and 80 %, respectively. The degree of deacetylation was also confirmed by PMR spectroscopy. The molecular weight of the initial chitosan was determined by the viscometric method using an Ubellode viscometer based on the Mark-Kuhn-Houwink equation, and the kinematic viscosities of the starting chitosans and oligochitosan were measured at constant temperature. The average weight (Aw) and average number (An) molecular weights of oligochitosan and oligochitosan ascorbate, and the value of the polydispersity index (pI) were determined by gel-penetrating chromatography. In this case, we used 0.3 M CH₃COOH / 0.225 M CH₃COONH₄ (pH 4.5) buffer solutions and hydrophilic polyvinylidene membranes for preliminary filtration of the analyzing solutions. Next, IR spectroscopic studies were carried out using an IR spectrometer from Bruker (Germany). The process of acid hydrolysis of chitosan ChS-1 in a solution of hydrochloric acid at 75 °C for 6 hours was studied, while 6 samples were taken (variants were encrypted depending on the duration of the reaction, for example, ChS-1/1 was taken from the reaction mixture for 1 hour) every 60 minutes. Oligochitosan ascorbate *Bombyx mori* (ChA-1 B.M.) was obtained on the basis of the formed oligochitosan by the acid hydrolysis method. The reaction of chitosan ascorbate formation was carried out on the basis of the suspension method under constant conditions with varying the ratio of the components (ChS:AA) and the pH of the solution [12]. The depolymerization of chitosan ChS-2 was carried out using an inorganic sodium nitrite salt in solution to obtain oligochitosan ChS-2/1 with a molecular weight of 6 kDa. The reaction was carried out at room temperature during 60 minutes. A chitosan derivative — oligochitosan ascorbate *Bombyx mori* (ChA-2 B.M.) was formed on the basis of the oligochitosan.

Results and Discussion

The results show that with an increase in the duration of the chitosan hydrolysis reaction, a significant decrease in the average number and weight mass of the obtained samples is observed up to 6 kDa Mn and 11 kDa Mw. The degree of acetylation of the samples was determined by the PMR method. For this, oligochitosan samples were dissolved in D₂O, and chitosan samples — in D₂O + DCl. The results obtained are presented in Table 1. The molecular weight and the degree of acetylation (DA) of the initial chitosan ChS-1 are 123 kDa and 20 % according to the GPC and PMR data, respectively.

Table 1

The chromatography results of oligochitosan and oligochitosan ascorbate samples

The samples	Synthesis time, min	Mn *10 ³	Mw *10 ³	Mz *10 ³	Mp *10 ³	pI (Mw/Mn)	CA±1, %
ChS-1/1	60	15.9	28.3	41.5	28.5	1.77	16.7
ChS-1/2	120	11.8	22.1	34.3	19.0	1.88	15.3
ChS-1/3	180	13.0	21.7	31.7	21.8	1.67	14.0
ChS-1/4	240	8.56	15.6	24.7	9.28	1.82	13.8
ChS-1/5	300	8.16	14.1	22.0	9.15	1.73	9.1
ChS-1/6	360	6.06	10.8	18.2	5.60	1.75	9.0
ChSA-1 B.M.	60	7.68	14.8	26.3	7.63	1.93	9.0

As can be seen from the data obtained, with an increase in the duration of the reactions, a strong cleavage of the glycosidic and acetamide bonds of chitosan macromolecules occurs, therefore, due to depolymerization, a noticeable recession in the molecular weight and the degree of acetylation is observed. Carrying out acid hydrolysis for 6 hours, it was found that after 4 hours and further the molecular weight of chitosan falls to the value corresponding to the molecular weights of oligochitosan 2–16 kDa [6]. The yield of the final product comparing with the original chitosan is approximately 40 % after 6 hours of hydrolysis. The optimal duration of hydrolysis under these conditions should be 4–5 hours. After the completion of the hydrolysis the product was isolated by sedimentation with an aqueous ammonia solution, followed by washing with distilled water. The oligochitosan ascorbate ChSA-1 B.M. was formed on the basis of obtained product. In order to compare the properties of the oligochitosan and its ascorbate, the oxidative

depolymerization of chitosan ChS-2 was carried out using a 0.2 % NaNO₂ solution. The results show that the nitrite method causes deep depolymerization even at room temperature in a short time. The obtained oligochitosan ChS-2/1 was used to prepare oligochitosan ascorbate ChSA-2 B.M. The results are shown in Table 2.

Table 2

The results of chromatography of oligochitosan and oligochitosan ascorbate samples

The samples	Synthesis time, min	Mn *10 ³	Mw *10 ³	Mz *10 ³	Mp *10 ³	pI (M _w /Mn)	CA±1, %
ChS-2/1	60	4.13	5.93	8.23	4.0	1.46	9.6
ChSA-2 B.M.	60	3.73	6.20	9.93	3.48	1.66	6.1

The data given in the table above inform that the average number and average weight masses of the oligochitosan and oligochitosan ascorbate samples practically coincide. Also, during hydrolysis with sodium nitrite, in comparison with the acid hydrolysis method, the molecular weight characteristics of the samples decrease. Despite this, the literature data show that redistribution of functional groups is observed in the structure of oligochitosan, and aldehyde groups are also formed [11].

In addition to the GPC (gel-penetrating chromatography) data, the kinematic viscosity of the samples of the initial chitosan and its ascorbate was determined. For measurements, 1 % aqueous solutions of the samples were prepared. Viscometers of the VPJ-2 type were used for measurements (the radius of the capillary is 0.34 or 1.31 mm). Kinetic viscosity (V , mm²/s) was calculated by the formula:

$$V = (g / 9.807) \times K \times T,$$

where: K is the constant of the viscometer, 0.0045632 or 0.30215 mm²/s², respectively; T is the liquid flow time (s); g — acceleration due to gravity (m/s²). The obtained results are shown in the Table 3.

Table 3

Kinematic viscosity of samples of initial chitosans and oligochitosan ascorbates

The samples	Capillary radius, mm	Solution flow time, s	Kinetic viscosity, mPas	Molecular weight of samples, kDa	N, %	C%, AK
ChS-1	1.31	39.0	13.0	Δ M 123	8.36	—
ChS-2	1.31	59.0	19.6	Δ M 177	8.56	—
ChSA-1 B.M.	0.34	265.0	1.33	M ₀ 14.8	6.18	26
ChSA-2 B.M.	0.34	233.0	1.17	M ₀ 6.2	4.10	52

The results show that the kinetic viscosity of oligochitosan ascorbate ChSA-1 B.M. in comparison with the initial chitosan, ChS-1 decreases almost 10 times, and the kinetic viscosity of the obtained sample by the nitrite method decreases 16.7 times. The results indicate that oxidative depolymerization degrades the chitosan macromolecule more actively in comparison with acid hydrolysis. The ratio of oligochitosan was defined: ascorbic acid in the product was determined by elemental analysis for nitrogen content. The results show that with the growing of ascorbic acid content, a decrease in the amount of total nitrogen and kinetic viscosity of the samples is observed.

The structure of the samples was confirmed using IR and PMR spectroscopy. In order to compare the structural characteristics the IR spectra of the initial chitosans, oligochitosans, and their ascorbates have been obtained.

The results are shown in Figure 1. In the IR spectrum of chitosan (Fig. 1 b), characteristic absorption bands at 1645 and 1574 cm⁻¹ were found corresponding to the functional groups of acetamide (amide I) and amine. In the range of 1310–1420 cm⁻¹ and at 2900 cm⁻¹, absorption bands of methylene groups were revealed. In the range 3200–3350 cm⁻¹, absorption bands of the hydroxyl group were found.

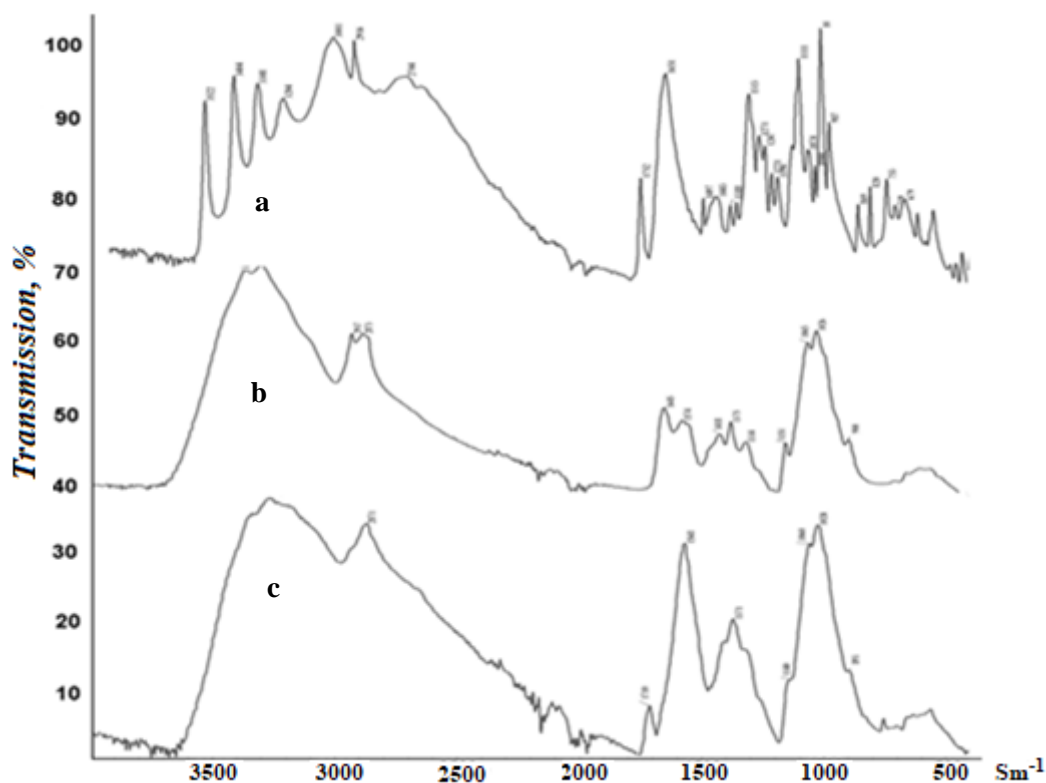


Figure 1. IR-spectra of ascorbic acid (a), chitosan-1 (b) and oligochitosan ascorbate *Bombyx mori* (c)

There are absorptions of stretching vibrations of C2 and C3 hydroxyl groups in the IR spectrum of ascorbic acid in the range of 3200–2900 cm^{-1} . The absorption bands for the methylene group in the range of 2915–2900 cm^{-1} also have been found (Fig. 1). At 1750 cm^{-1} , an absorption band is observed for the carbonyl group included in the lactone ring of ascorbic acid; at 1650 cm^{-1} — absorption band characteristic of C=C groups. Along with this, at 1320, 1270, 1140 cm^{-1} , absorption bands of C3-, C2-, C5- hydroxyl groups are found.

In the IR spectrum of the obtained oligochitosan ascorbate, a mixing of absorption bands appears, compared to the absorption bands of chitosan and ascorbic acid. Slight difference was observed due to the mixing of absorption bands towards lower wave numbers from 1645 and 1568 cm^{-1} , which means the formation of oligochitosan ascorbate in the presence of amino groups. In the range of 1400–900 cm^{-1} absorption bands appear which are characteristic of chitosan with low intensity which indicate a decrease of the hydrogen bonds. The change in the intensity and shift of the characteristic absorption bands in the IR spectrum of oligochitosan ascorbate in comparison with the IR spectra of the initial components — ascorbic acid and chitosan — indicate the formation of a water-soluble derivative of chitosan — oligochitosan ascorbate.

NMR spectroscopic studies were also carried out. NMR spectra were recorded on a VARIAN-400 spectrophotometer (USA). In all experiments, the D_2O solvents were used with the addition of DCl. It is known that the NMR spectra of chitosan are characterized by resonances in the range of 4.6–4.9 ppm, which coincide for the proton at C-1, which indicates glucosidic bonds. Further, chemical shifts of the C-2, C-3, C-6 protons are observed in the range of 3.7–4.0 ppm. There are also resonances in the 3.2 ppm and — 2.1 ppm region, which correspond to the protons of the amino group and the acetamide group of this polysaccharide (Fig. 2) [12]. The obtained NMR spectra of the initial chitosan and oligochitosan are shown in Figures 3, 4.

The degrees of acetylation (DA) of the samples were also calculated. Based on the equation of $\text{CA} = n/(n-100) = (0.1/3) / (1/6) = 0.199$ then $1.199 n = 19.9$, and $n = 0.167$ or $\text{CA} (\%) = 16.7 \%$. The results show a gradual decrease in the content of acetamide groups can be seen in the spectrum of the achieved oligochitosans, for example in the spectrum of samples ChS-1/6 (Fig. 3).

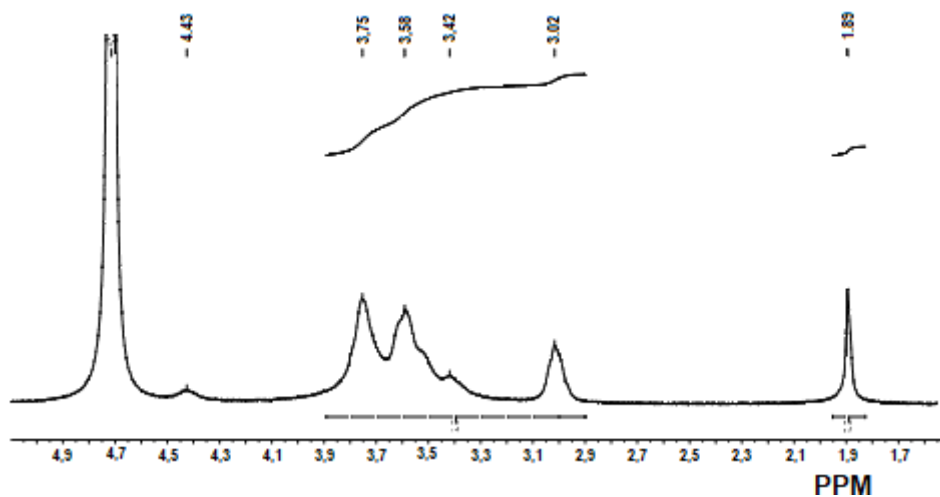


Figure 2. H^1 -NMR spectra of the initial chitosan ChS-1

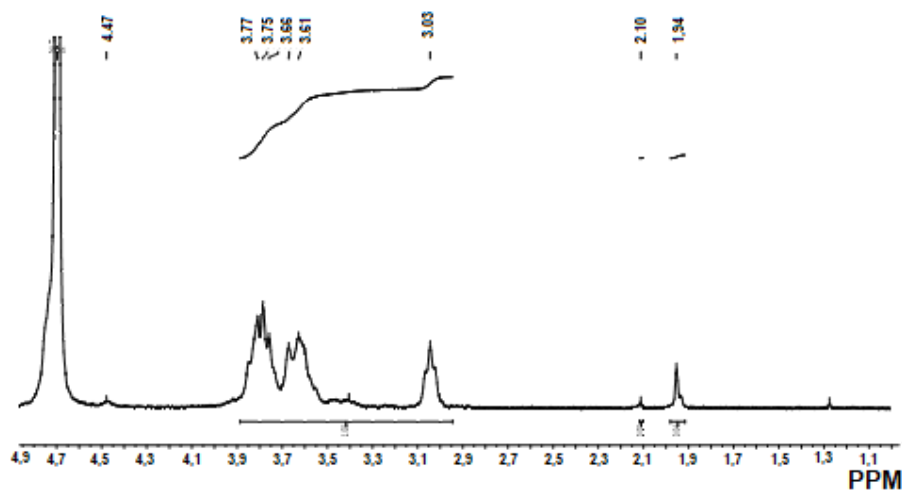


Figure 3. H^1 -NMR spectra of oligochitosan ChS-1/6

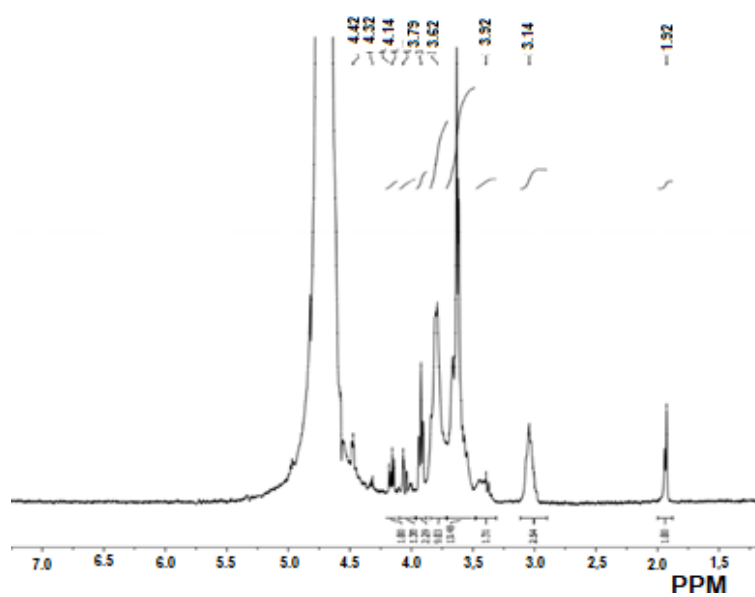


Figure 4. H^1 -NMR spectra of chitosan oligoascorbate ChSA-2

As can be seen from the spectrum (Fig. 3), the degree of acetylation (DA) based on the equation $DA = n/(n-100) = (0.05/3) / (1/6) = 0.099$ then $1.099 n = 9.9$ and the value of the $n = 0.09$ or $CA = 9\%$. Thus, it can be concluded that as a result of acid hydrolysis up to 6 hours, the degree of acetylation decreases from 16.7% to 9%.

In the NMR spectrum of oligochitosan ascorbate, a shift of signals compared to the signals of the initial oligochitosan from 2.8 ppm to 3.1 ppm was found, which can be explained by the interaction of the amino groups of oligochitosan with ascorbic acid [12, 13]. An increase in the intensity of signals in the range of 3.5–4.1 ppm is also observed, which indicates the surge in the polydispersity of the sample and proton signals at C-6, C-5, C-4 due to the formation of oligochitosan ascorbate (Fig. 4).

In the spectrum of ascorbic acid, characteristic signals are observed at 3.6 ppm, which correspond to the C-6 carbon protons and two protons in the CH_2OH group of ascorbic acid molecules. Peaks 3.8, 3.9 ppm. refer to the protons associated with the C-4, C-5 and C-3 atoms of the lactone ring of ascorbic acid, respectively. The detected signals in the range of 4.9 ppm correspond to protons at C-4 in the furanose ring of ascorbic acid, which corresponds to the literature data [13].

0.5% solutions of oligochitosan ascorbate were prepared in order to realize these studies. Experiments were carried out on the basis of the obtained solutions 4 times. Certain biologically active properties of oligochitosan ascorbate showed that the obtained samples have antimicrobial properties against *Fuzarium oxysporum* in comparison with the reference and control. It was revealed that oligochitosan and oligochitosan ascorbate have antimicrobial properties, the zone of suppression of which is 22 mm on average, and no zone of suppression was found in the control (water).

Conclusions

Thus, the process of acid hydrolysis of chitosan ChS-1 in a solution of 1 M hydrochloric acid at 75 °C for 6 hours has been studied. It has been shown that the optimal duration of hydrolysis, leading to the production of oligochitosan with a molecular weight of less than 16 kDa, should be considered as 4–5 hours. Depolymerization of chitosan ChS-2 was carried out using sodium nitrite in solution to obtain oligochitosan with a molecular weight of 6 kDa. On the basis of the achieved oligochitosan samples by two methods, their ascorbates were prepared. The composition, structure, and molecular weight characteristics of oligochitosan ascorbate samples were confirmed by physicochemical methods. Certain biologically active properties of oligochitosan ascorbate showed that the obtained samples have antimicrobial properties against *Fuzarium oxysporum* in comparison with the reference and control.

This work was carried out with the financial support of the «El-Yurt Umidi» Foundation of the Republic of Uzbekistan. There is no conflict of interest. K.K. Pirniyazov with the leadership of S.Sh. Rashidova and V.E. Tikhonova carried out synthesis and calculations. All authors participated in data processing and in the discussion of the results.

References

- 1 Шиповская А.Б. Биологическая активность олигомеров хитозана / А.Б. Шиповская, В.И. Фомина, М.Н. Киреев, Е.С. Казакова, И.А. Касьян // Изв. Сарат. ун-та. Нов. сер. Химия. Биология. Экология. — 2008. — Т. 8, № 2. — С. 46–49.
- 2 Хитозан / под ред. К.Г. Скрыбина, С.Н. Михайлова, В.П. Варламова. — М.: Центр «Биоинженерия» РАН, 2013. — 591 с.
- 3 Куликов С.Н. Определения антибактериальной активности хитозана / С.Н. Куликов, Л.Т. Баязитова, О.Ф. Тюпкина, П.В. Зеленихин, М.М. Сальникова, Е.А. Безродных, В.Е. Тихонов // Прикладная биохимия и микробиология. — 2016. — Т. 52, № 5. — С. 1–7.
- 4 Куликов С.Н. Сравнительная оценка антибактериальных свойств олигохитозанов в отношении *Klebsiella pneumoniae* / С.Н. Куликов, В.Е. Тихонов, Е.А. Безродных, С.А. Лопатин, В.П. Варламов // Биоорганическая химия. — 2015. — Т. 41, № 1. — С. 67–73.
- 5 Blagodatskikh I.V. N-Reacetylated Oligochitosan: pH Dependence of Self-Assembly Properties and Antibacterial Activity / I.V. Blagodatskikh, S.N. Kulikov, O.V. Vyshivannaya, E.A. Bezrodnykh, V.E. Tikhonov // Biomacromolecules. — 2017. — Vol. 18, No. 5. — P. 1491–1498. <https://doi.org/10.1021/acs.biomac.7b00039>
- 6 Tikhonov V.E. Bactericidal and antifungal activities of a low molecular weight chitosan and its N-2/(3)-(dodec-2-enyl)-succinoyl-derivatives / V.E. Tikhonov, E.A. Stepnova, V.G. Babak, I.A. Yamskov, et al. // Carbohydrate polymers. — 2006. — Vol. 64. — P. 66–72. <https://doi.org/10.1016/j.carbpol.2005.10.021>
- 7 Kulikov S. Molecular weight and pH aspects of the efficacy of oligochitosan against methicillin-resistant *Staphylococcus aureus* (MRSA) / S. Kulikov, V. Tikhonov, I. Blagodatskikh, E. Bezrodnykh, S. Lopatin et al. // Carbohydrate Polymers. — 2012. — Vol. 87. — P. 545–550. <https://doi.org/10.1016/j.carbpol.2011.08.017>

- 8 Chih-Yu Chen. Antibacterial effect of water-soluble chitosan on representative dental pathogens *Streptococcus mutans* and *Lactobacilli brevis* / Chen Chih-Yu, Chung Ying-Chien // *Journal Appl. Oral Sci.* — 2012. — Vol. 20, No. 6. — P. 620–627. <https://doi.org/10.1590/S1678-77572012000600006>
- 9 Shipovskaya A.B. Novel antimicrobial drugs based on complex chitosan salts with chiral organic ligands / A.B. Shipovskaya, I.V. Zudina, V.I. Fomina, O.N. Malinkina // *Butlerov Communications.* — 2015. — Vol. 41, No. 3. — P. 82. <http://foundation.butlerov.com/bh-2015>.
- 10 Tommeraas K. Preparation and characterization of oligosaccharides produced by nitrous acid depolymerization of chitosans / K. Tommeraas, K.M. Varum, B.E. Christensen, O. Smidsrod // *Carbohydrate Research.* — 2001. — Vol. 333. — P. 137–144.
- 11 Pirniyazov K.K. Synthesis and structural characteristics of the ascorbate chitosan *Bombyx mori* / K.K. Pirniyazov, S.Sh. Rashidova // *American journal of research.* — USA, Michigan, 2019. — No. 7–8. — P. 114–119. DOI: <http://dx.doi.org/10.26739/2573-5616-2019-8-10>
- 12 Tian X.L. Synthesis and evaluation of chitosan-vitamin C complex / X.L. Tian, D.F. Tian, et al. / *Indian J. Pharm Sci.* — 2009. — Vol. 71(4). — P. 371–376. <https://doi.org/10.4103/0250-474X.57284>
- 13 Шиповская А.Б. Новые антимикробные препараты на основе комплексной соли хитозана с хиральным органическим лигандом / А.Б. Шиповская, И.В. Зудина, В.И. Фомина, О.Н. Малинкина // *Бутлеровские сообщения.* — 2015. — Т. 41, № 3. — С. 82–94. <http://foundation.butlerov.com/bh-2015>.

К.К. Пирниязов, В.Е. Тихонов, С.Ш. Рашидова

***Bombyx mori*-ден алынған олигохитозан аскорбатының синтезі және қасиеттері**

Олигохитозан сынамалары *Bombyx mori*-ден оқшауланған жоғары молекулалық хитозанның қышқылдық гидролизі арқылы алынды. 6 сағат ішінде қышқыл гидролизін жүргізгенде, 4 сағаттан кейін және одан әрі ұзақтығы артқан сайын хитозанның молекулалық салмағы олигохитозанның 2–16 кДа молекулалық салмақтарының диапазонына сәйкес мәнге дейін азаятындығы анықталды. Молекулалық салмағы 16 кДа-дан аз олигохитозан өндірісіне әкелетін гидролиздің оңтайлы ұзақтығын 4–5 сағат деп санау керек екендігі көрсетілген. Молекулалық салмағы 177 кДа хитозанды деполимерлеу натрий нитритін пайдаланып, молекулалық массасы 6 кДа олигохитозан алу үшін жүргізілді. Екі әдіспен алынған олигохитозан сынамалары негізінде олардың аскорбаттары синтезделді. Хитозан аскорбатының түзілу реакциясы суспензия әдісі негізінде компоненттердің (ХЗ:АА) және ерітіндінің рН қатынасының өзгеруімен тұрақты жағдайда жүргізілді. Олигохитозан аскорбат пен олигохитозан *Bombyx mori* сынамаларының құрамы, құрылымы және молекулалық сипаттамалары физикалық-химиялық әдістермен расталды. Алынған үлгілердің микробқақарсы әсері, яғни *Fuzarium oxysporum*-ға қарсы әсері бар екендігі дәлелденген.

Кілт сөздер: хитозан аскорбат *Bombyx mori*, олигохитозан *Bombyx mori*, аскорбин қышқылы, донор-акцепторлық байланыс, байланыс дәрежесі, ацетилдену дәрежесі, деполимеризация.

К.К. Пирниязов, В.Е. Тихонов, С.Ш. Рашидова

Синтез и свойства аскорбат олигохитозана из *Bombyx mori*

Получены образцы олигохитозана кислотным гидролизом высокомолекулярного хитозана, выделенного из *Bombyx mori*. В ходе проведения кислотного гидролиза в течение 6 ч было обнаружено, что через 4 ч и далее с увеличением продолжительности молекулярная масса хитозана снижается до значения, соответствующего интервалам молекулярных масс олигохитозана 2–16 кДа. Показано, что оптимальной продолжительностью гидролиза, приводящего к получению олигохитозана с молекулярной массой менее 16 кДа, следует считать 4–5 ч. Осуществлена деполимеризация хитозана с молекулярной массой 177 кДа с помощью нитрита натрия в растворе с получением олигохитозана с молекулярной массой 6 кДа. На основе полученных двумя методами образцов олигохитозана синтезированы их аскорбаты. Реакция образования аскорбат хитозана проводили на основе суспензионном методом при постоянных условиях с варьированием соотношений компонентов (ХЗ:АК) и рН раствора. Состав, структура и молекулярно-массовые характеристики образцов аскорбата олигохитозана и олигохитозана *Bombyx mori* подтверждены физико-химическими методами. Показано, что полученные образцы обладают антимикробным действием против *Fuzarium oxysporum*.

Ключевые слова: аскорбат хитозана *Bombyx mori*, олигохитозан *Bombyx mori*, аскорбиновая кислота, донорно-акцепторная связь, степень связывания, степень ацетилирования, деполимеризация.

References

- 1 Shipovskaya, A.B., Fomina, V.I., Kireyev, M.N., Kazakova, Ye.S., & Kas'yan, I.A. (2008). Biologicheskaya aktivnost olihomerov khitozana [Biological Activity of Chitosan Oligomers] *Izvestiia Saratovskoho universiteta. Novaia seriia. Khimiia. Biologiya. Ekologiya* — *News of the Saratov University. Ser. Chemistry. Biology. Ecology*, 8, 2, 46–49 [in Russian].
- 2 Skryabin, K.G., Mikhaylov, S.N., & Varlamov, V.P. (2013). *Khitozan [Chitosan]*. Moscow: Tsentr «Bioinzheneriia» RAN [in Russian].
- 3 Kulikov, S.N., Bayazitova, L.T., Tyupkina, O.F., Zelenikhin, P.V., Sal'nikova M.M., Bezrodnykh, Ye. A., & Tikhonov, V.Ye. (2016). Opredeleniia antibakterialnoi aktivnosti khitozana [Determination of the antibacterial activity of chitosan]. *Prikladnaia biokhimiia i mikrobiologiya* — *Applied Biochemistry and Microbiology*, 52, 5, 1–7 [in Russian].
- 4 Kulikov, S.N., Tikhonov, V.Ye., Bezrodnykh, Ye.A., Lopatin, S.A., & Varlamov, V.P. (2015). Sravnitel'naya otsenka antibakterialnykh svoystv olihokhitozanov v otnoshenii *Klebsiella pneumoniae* [Comparative evaluation of the antibacterial properties of oligochitosans against *Klebsiella pneumoniae*]. *Bioorganicheskaya khimiia* — *Bioorganic chemistry*, 41, 1, 67–73 [in Russian].
- 5 Blagodatskikh, I.V., Kulikov, S.N., Vyshivannaya, O.V., Bezrodnykh, E.A., & Tikhonov, V.E. (2017). N-Reacetylated Oligochitosan: pH Dependence of Self-Assembly Properties and Antibacterial Activity. *Biomacromolecules*, 18, 5, 1491–1498. <https://doi.org/10.1021/acs.biomac.7b00039>
- 6 Tikhonov, V.E., Stepnova, E.A., Babak, V.G., & Yamskov, I.A. et al. (2006). Bactericidal and antifungal activities of a low molecular weight chitosan and it is N-2/(3)-(dodec-2-enyl)-succinoyl/-derivatives. *Carbohydrate polymers*, 64, 66–72. <https://doi.org/10.1016/j.carbpol.2005.10.021>
- 7 Kulikov, S., Tikhonov, V., Blagodatskikh, I., Bezrodnykh, E., & Lopatin, S. et al. (2012). Molecular weight and pH aspects of the efficacy of oligochitosan against methicillin-resistant *Staphylococcus aureus* (MRSA). *Carbohydrate Polymers*, 87, 545–550. <https://doi.org/10.1016/j.carbpol.2011.08.017>
- 8 Chen Chih-Yu., & Chung Ying-Chien (2012). Antibacterial effect of water-soluble chitosan on representative dental pathogens *Streptococcus mutans* and *Lactobacilli brevis*. *Journal Appl. Oral Sci.*, 20, 6, 620–627. <https://doi.org/10.1590/S1678-77572012000600006>
- 9 Shipovskaia, A.B., Zudina, I.V., Fomina, V.I. & Malinkina, O.N. (2015). Novel antimicrobial drugs based on complex chitosan salts with chiral organic ligands. *Butlerov Communications*, 41, 3, 82. <http://foundation.butlerov.com/bh-2015>.
- 10 Tommeraas, K., Varum, K.M., Christensen, B.E., & Smidsrod, O. (2001). Preparation and characterization of oligosaccharides produced by nitrous acid depolymerization of chitosans. *Carbohydrate Research*, 333, 137–144.
- 11 Pirniyazov, K.K., & Rashidova, S.Sh. (2019). Synthesis and structural characteristics of the ascorbate chitosan *Bombyx mori*. *American journal of research*, 7–8, 114–119. DOI: <http://dx.doi.org/10.26739/2573-5616-2019-8-10>
- 12 Tian, X.L., & Tian, D.F. et al. (2009). Synthesis and evaluation of chitosan-vitamin C complex. *Indian J. Pharm Sci.*, 71 (4), 371–376. <https://doi.org/10.4103/0250-474X.57284>
- 13 Shipovskaya, A.B., Zudina, I.V., Fomina, V.I., & Malinkina, O.N. (2015). Novye antimikrobynye preparaty na osnove kompleksnoi soli khitozana s khiralnym organicheskim lihandom [New antimicrobial drugs based on a complex chitosan salt with a chiral organic ligand]. *Butlerovskie soobshcheniia* — *Butlerov communications*, 41, 3, 82–94 [in Russian]. <http://foundation.butlerov.com/bh-2015>.

Information about authors

Pirniyazov, Kudrat Kadambayevich — Junior Researcher, Institute of Chemistry and Physics of Polymers of the Academy of Sciences of the Republic of Uzbekistan, 100128, Tashkent, A. Kadyri st, 7 b, Uzbekistan e-mail: quadrat.pirniyazov@mail.ru <https://orcid.org/0000-0002-3549-6363>

Tikhanov, Vladimir Evgenevich — Candidate of chemical sciences, Leading researcher, Institute of Organoelement Compounds, Russian Academy of Sciences A.N. Nesmeyanova, 119991, Moscow, GSP-1, V-334, Vavilova st., 28, Russia. e-mail: tikhon@ineos.ac.ru

Rashidova, Sayyora Sharafovna — Doctor of chemical Sciences, Professor, Academician, Director of the Institute of Chemistry and Physics of Polymers of the Academy of Sciences of the Republic of Uzbekistan, 100128, Tashkent, A. Kadyri st, 7 b, Uzbekistan e-mail: polymer@academy.uz <https://orcid.org/0000-0003-3104-6004>

I.V. Korolkov^{1, 2*}, K. Ludzik^{3, 4}, L.I. Lisovskaya¹,
A.V. Zibert², A.B. Yeszhanov^{1, 2}, M.V. Zdorovets^{1, 2}

¹*Institute of Nuclear Physics of the Republic of Kazakhstan, Almaty, Kazakhstan;*

²*L.N. Gumilyov Eurasian National University, Nur-Sultan, Kazakhstan;*

³*Department of Physical Chemistry, University of Lodz, Poland;*

⁴*Frank Laboratory of Neutron Physics, Joint Institute for Nuclear Research, Dubna, Russia*

(*Corresponding author's e-mail: i.korolkov@inp.kz)

Modification of magnetic Fe₃O₄ nanoparticles for targeted delivery of payloads

The development of methods for targeted delivery of payload is a rapidly developing area of research. For this reason, iron oxide nanoparticles have potential to be used in delivery of substances by using external magnetic field. However it is necessary to develop methods of their modification, which will lead to the possibility of immobilization of payloads with the required concentration for therapeutic use. In this article, supermagnetic iron oxide nanoparticles (Fe₃O₄) were modified with silanes such as (3-chloropropyl)trimethoxysilane, (3-mercaptopropyl)trimethoxysilane, (3-aminopropyl)trimethoxysilane and (3-glycidylpropyl)trimethoxysilane by reaction of polycondensation. Then carborane compound (payload) was successfully attached on the modified nanoparticles via covalent bonding. Structure, size and element composition were studied by Fourier-transform infrared spectroscopy (FTIR), scanning electron microscopy (SEM) and Energy-dispersive X-ray spectroscopy (EDA). It was found that resulting nanoparticles contain 16.6 % of boron (according to EDA), and their average size is 32±9 nm (according to SEM). In vitro test using HeLa (cervical cancer cell) and PC-3 (prostate cancer cell) shows low cytotoxicity in concentration range of 1–200 µg/ml.

Keywords: Fe₃O₄ nanoparticles, silane, surface modification, targeted delivery of payload, BNCT, carborane, biological test, cytotoxicity.

Introduction

The science and engineering of nanometer-sized materials is currently being used to develop numerous scientific, industrial, environmental, and technological fields. Biology, medicine, chemistry, pharmaceuticals, agriculture, food industry and materials science are the main areas that have benefited from the technological progress achieved in the field of nanoscience. In recent years, significant growth has been observed in the biomedical application of nanostructured materials [1–4]. Nanostructures of different composition and shapes form the basis for a huge variety of pharmaceutical and medical applications, including diagnosis and drug delivery, and they have particular potential in cancer therapy. According to the International Agency for Research on Cancer [5], 18.1 million new cancer cases and 9.6 million cancer deaths were reported in 2018. Kazakhstan mortality index is 140.2 while average of worldwide is 102.4 and it is predicted that this index will grow. Despite all the preventive measures and therapeutic efforts of the last decades, the upward trend in incidence continues [6]. Typical chemotherapy drugs cannot be sufficiently concentrated in the area of the tumor and have a negative effect on the entire body. Thus, one of the problems is the development of methods of targeted therapy, which selectively affects the tumor, while maintaining healthy tissue and increasing the effectiveness of the drugs used. Biomimetic properties as well as an unusual surface-to-volume ratio make nanoparticles promising tools for the treatment of diseases [1].

Nanoparticles have unique physical and chemical properties due to their size, which can be comparable with the sizes of antibodies, receptors, nucleic acids, proteins, and other biological macromolecules. In addition, the use of nanostructures may allow the use of compounds that have poor solubility in water or low chemical and biological stability, metabolic barriers and etc. For these purposes, various nanostructures are used: liposomes, polymer and protein nanocapsules, micelles, gold and silicon nanoparticles [7]. Moreover, magnetic iron oxide nanoparticles have wide potential applications in biomedicine [8–12], including magnetic resonance imaging, magnetic hyperthermia, cancer therapy, and targeted drug delivery; in catalysis [13–15] and magnetic separation [16, 17]. Despite these promising results, their successful transition into clinical conditions depends strongly on their physicochemical properties, toxicity, and functionalization possibilities. Iron oxide nanoparticles are low stable, have a tendency to agglomerate in solutions, they have lack of bio-

compatibility. Various materials, such as silanes, metals, polymers, fatty acids and amino acids, are used to functionalize the surface and to stabilize magnetic nanoparticles [18–20]. Among other materials, silane based compounds are the most promising because they have high biocompatibility, stability, low toxicity, low cost, and high capacity for functionalization [21–23]. Moreover, the modification of magnetic nanoparticles with silanes with various functional groups will allow immobilization of drugs with different chemical nature. One of such drugs can be carborane derivatives for potential use in neutron capture cancer therapy (NCT) and chemotherapeutic drugs.

In this article, we present the results of synthesis and modification of iron oxide nanoparticles with various silanes and immobilization of carborane compound (payload) on their surface. Moreover, the biocompatibility was evaluated in vitro using human cancer cell lines: HeLa (cervical cancer cell) and PC-3 (prostate cancer cell).

Experimental

Synthesis and modification of iron oxide nanoparticles

Fe₃O₄ nanoparticles were obtained by co-precipitation of a mixture of iron chloride (II) and iron chloride (III) with the addition of ammonium hydroxide according to the method described in the our previous published article [24].

Modification of the surface of iron oxide nanoparticles with silanes such as (3-chloropropyl)trimethoxysilane (Si-Cl), (3-mercaptopropyl)trimethoxysilane (Si-SH), (3-aminopropyl)trimethoxysilane (Si-NH₂) and (3-glycidylpropyl)trimethoxysilane (Si-epoxy) was performed by reaction of polycondensation. With this aim, 0.5 g of Fe₃O₄ was dispersed in 100 ml of o-xylene, 3 ml of silane was added, the reaction mixture was purged with argon. The reaction was carried out at 90 °C for 5 hours. After that, the obtained nanoparticles were separated with a magnet, washed in o-xylene, acetone, and dried.

Immobilization of carboranes to functionalized Fe₃O₄ nanoparticles

Commercial available isopropyl-o-carborane (0.016 M) was dissolved in 30 ml anhydrous benzene. The solution was bubbled with argon, then freshly prepared butyl lithium solution (0.016 M) was added, isopropyl-o-carboranyl lithium was precipitated after 1 hour of stirring. Diethyl ether was added to the reaction mixture to dissolve the precipitate. After that, suspension of Fe₃O₄-Si-epoxy in benzene was added. The reaction was carried out at room temperature during 6 hours. The resulting suspension was magnetically separated, washed with benzene and diethyl ether several times, dried at 50 °C.

Methods of characterization

FTIR spectra were recorded on InfraLum FT-08 FTIR Spectrometer (Lumex, Russia) with Single Reflection Diamond ATR accessory (GladiATR, PIKE) to study chemical group shifts before and after nanoparticles modification. Measurements were taken in the range of 400 to 4000 cm⁻¹. All spectra (25 scans at 2 cm⁻¹ resolution) were recorded at 21–25 °C.

JEOL JSM-7500F scanning electron microscope (SEM) was used for characterization of nanoparticle morphology and size during functionalization. Nanoparticle distribution were evaluated by analyzing SEM images using ImageJ. EDX analysis was done using Hitachi TM 3030 with microanalysis system Bruker XFlash MIN SVE at 15 kV. Before the analysis, the samples were glued to carbon tape and sputtered with gold on magnetron JFC-1600. The analysis of the elemental composition was carried out evaluating the spectra from various points of the sample, the average values of the element content were calculated based on the 10 spectra.

Cytotoxicity Assay

In order to monitor the cytotoxic effect of functionalised magnetic nanoparticles different human cancer cell lines were used: HeLa (cervical cancer cell), PC-3 (prostate cancer cell). As recommended, fibroblasts like cells of L929 obtained from subcutaneous adipose tissue of mouse were used as normal cells (PN-EN ISO 10993–5:2009 norm). The cell culture for HeLa and PC-3 was described previously [25].

Cytotoxicity of nanoparticles was evaluated using in vitro model and day 3-(4,5-dimethylthiazol-2-yl)-2,5-diphenyltetrazolium bromide [26, 27]. All cancer cell lines were plated into 96-well plates in volume of 8–10·10³/100 µl/well. After 24 hours incubation, the samples were added in a concentration range of 1–200 µg/ml and a volume of 100 µl/well into wells with suspensions of particular cell lines. Subsequently, cells were incubated for next 24 hours and 72 hours under standard conditions (37 °C and 5 % CO₂). In experiments two types of cell culture medium were used: with fetal bovine serum (FBS+) and without (FBS–). After that time, fresh prepared MTT solution (5 mg/1 ml PBS) was added in volume of 20 µl to each well

and cells were incubated for the next 3 hours under the same conditions. Then, the wells contents were removed and lasting crystals were dissolved by the addition of 100 μ l DMSO to each well. Absorbance was measured using BioTek Power Wave XS spectrophotometer at the wavelength of $\lambda=570$ nm. Prior to investigation the nanoparticles solution in PBS probes were sonicated in order to disintegrate particles with ultrasounds. Control values were absorbance measurements received for the wells with cells incubated without the addition of the studied compounds. For each concentration of the nanoparticles 6 absorbance measurements were carried out, for which average values \pm SEM were calculated. Obtained MTT results were processed using GraphPad Prism 7 Program, into graphs, which depict inhibition of cell viability in relation to compound concentration.

Results and Discussion

At the first stage of the study, methods of coating magnetic iron oxide nanoparticles with a silane shell were studied. Silanes can serve as an intermediate link between inorganic nanoparticles and organic/organo-element payloads. Trimethoxysilanes with different reactive groups such as chlorine-, amino-, epoxy- and mercapto- were chosen to be able to attach different payloads at next stage. To create the shell, the polycondensation reaction of silanes was used, which occurs both with silane molecules and with hydroxyl groups that are on the surface of iron oxide nanoparticles. Thus (3-chloropropyl)trimethoxysilane, (3-mercaptopropyl)trimethoxysilane, (3-aminopropyl)trimethoxysilane and (3-glycidylpropyl)trimethoxysilane were chosen. The reaction was carried out in *o*-xylene under argon. Magnetic separation made it possible to well purify magnetically modified nanoparticles from non-magnetic silane nanoparticles, which were a by-product. Figure 1 shows the results of Fe₃O₄ modification with (3-chloropropyl) trimethoxysilane. It was found out that size of nanoparticles increased from 21 ± 4 nm (initial Fe₃O₄) to 29 ± 5 nm according to SEM analysis. At the same time, the weight gain was 2.8 %. Elemental composition according to EDA analysis is as follows (Fig. 1c): Fe — 13 %, O — 43.6 %, C — 40.2 %, Cl — 0.6 %, Si — 0.5 %, Au — 1.1 %, Cu — 1 %. It should be noted that gold and copper appeared as a result of magnetron sputtering before SEM analysis to avoid surface charge. The FTIR spectrum (Fig. 1d) of the initial Fe₃O₄ nanoparticles is characterized by absorption at $3500\text{--}3000$ cm⁻¹ (OH), 1614 cm⁻¹ associated with O–H vibrations in combination with Fe atoms, as well as at 544 and 399 cm⁻¹ (Fe–O). The coating of nanoparticles led to the appearance of new peaks at 1040 and 1146 cm⁻¹ (Si–O–Si) and 628 cm⁻¹ (C–Cl). The absence of peak at 913 and 940 cm⁻¹ allow us to conclude that the reaction of polycondensation completed.

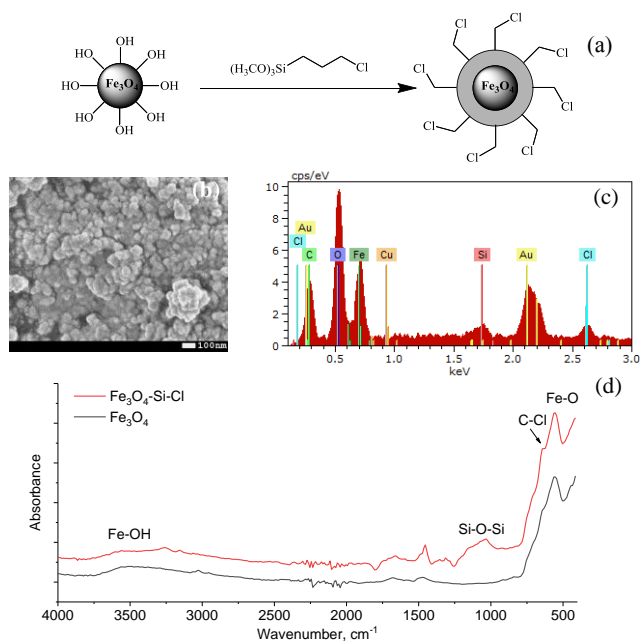


Figure 1. Scheme of modification of Fe₃O₄ by (3-chloropropyl)trimethoxysilane (a), SEM image (b), EDA (c) and FTIR spectra (d)

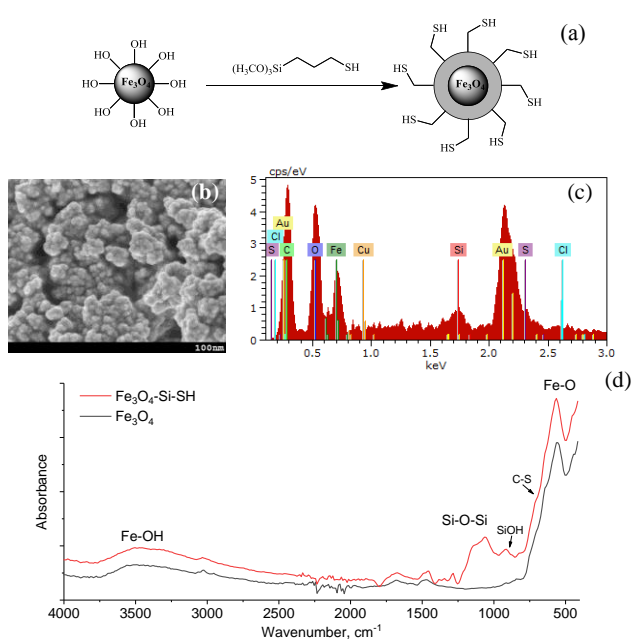


Figure 2. Scheme of modification of Fe₃O₄ by (3-mercaptopropyl)trimethoxysilane (a), SEM image (b), EDA (c) and FTIR spectra (d)

Modification with (3-mercaptopropyl)-trimethoxysilane led to formation of nanoparticles with size of 26 ± 6 nm (Fig. 2b). The FTIR spectra (Fig. 2d) show the appearance of new peaks at 706 cm^{-1} (S-C), 1059 and 1144 cm^{-1} (Si-O-Si). At the time the broad peak at 913 cm^{-1} were detected which is related to Si-OH group. This indicates the incompleteness of the reaction. EDA (Fig. 2c) registered 1.3 % of sulfur and 1.5 % of silicon.

Modification with (3-aminopropyl) trimethoxysilane was carried out according to the same procedure in *o*-xylene at 90°C . The average size of obtained nanoparticles was 30 ± 8 nm. Aminated nanoparticles are characterized by the appearance of new peaks at 1677 cm^{-1} (NH_2), at 1163 and 1064 cm^{-1} (Si-O-Si), and at 1265 cm^{-1} (C-N) (Fig. 3). It was also found out appearance the peak related to Si-OH bonds, but with a lower concentration than in the case of (3-mercaptopropyl)trimethoxysilane. Nitrogen in the amount of 7.6 % was observed in EDA. Modification of Fe_3O_4 by (3-glycidylpropyl)trimethoxysilane allowed to create chemical active epoxy groups for further isopropyl-*o*-carborane attachment (payload). Epoxy ring were detected in FTIR spectra at around $900\text{--}920 \text{ cm}^{-1}$. In the same region, the peak related to Si-OH can be appeared. The presence of the epoxy group will also be confirmed by further chemical transformations. SEM analysis (Fig. 4b) shows an average nanoparticles size of 39 ± 8 nm.

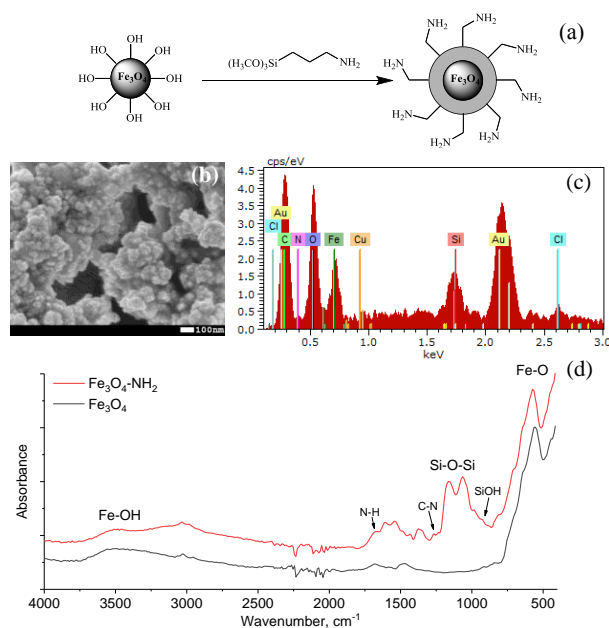


Figure 3. Scheme of modification of Fe_3O_4 by (3-aminopropyl)trimethoxysilane (a), SEM image (b), EDA (c) and FTIR spectra (d)

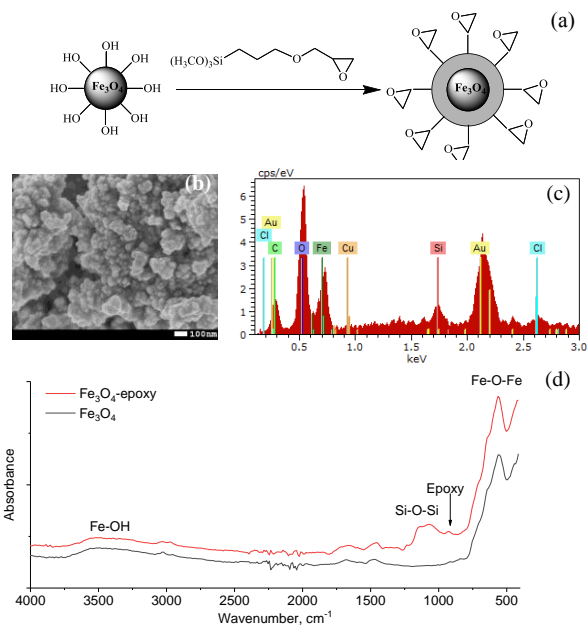


Figure 4. Scheme of modification of Fe_3O_4 by (3-glycidylpropyl)trimethoxysilane (a), SEM image (b), EDA (c) and FTIR spectra (d)

Commercial available isopropyl-*o*-carborane was immobilized to Fe_3O_4 -Si-epoxy nanoparticles via covalent bonding using butyl lithium as shown in Figure 5a. New peaks in FTIR spectra (Fig. 5d) appeared at 3353 , 2924 , 2572 , 1496 , 1433 and 860 cm^{-1} are related to OH, C-H, B-H, $\delta_{\text{as}} \text{CH}_3$ and carborane skeleton vibrations respectively [29], with increase in average nanoparticles size according to SEM analysis to 32 ± 9 nm (Fig. 5b-c).

EDA analysis was performed to study element content on Fe_3O_4 nanoparticles surface before and after modification. The data extracted from the EDA spectra are collected in Table 1. Initial Fe_3O_4 consist of 43.1 % Fe and 56.9 % O. Isopropyl-*o*-carborane attachment led to the appearance of boron in an amount of 16.5 %.

Table 1

Data from EDA spectra

Sample	Atomic content, %				
	Fe	O	Si	B	C
Initial Fe_3O_4	43.1 \pm 2.1	56.9 \pm 3.6	–	–	–
Fe_3O_4 /GPTMS	20.7 \pm 2.1	52.9 \pm 2.1	6.4 \pm 1.3	–	20.0 \pm 1.5
Fe_3O_4 /GPTMS/Carborane	22.2 \pm 1.5	38.9 \pm 3.1	2.4 \pm 0.3	16.5 \pm 2.3	20.0 \pm 1.4

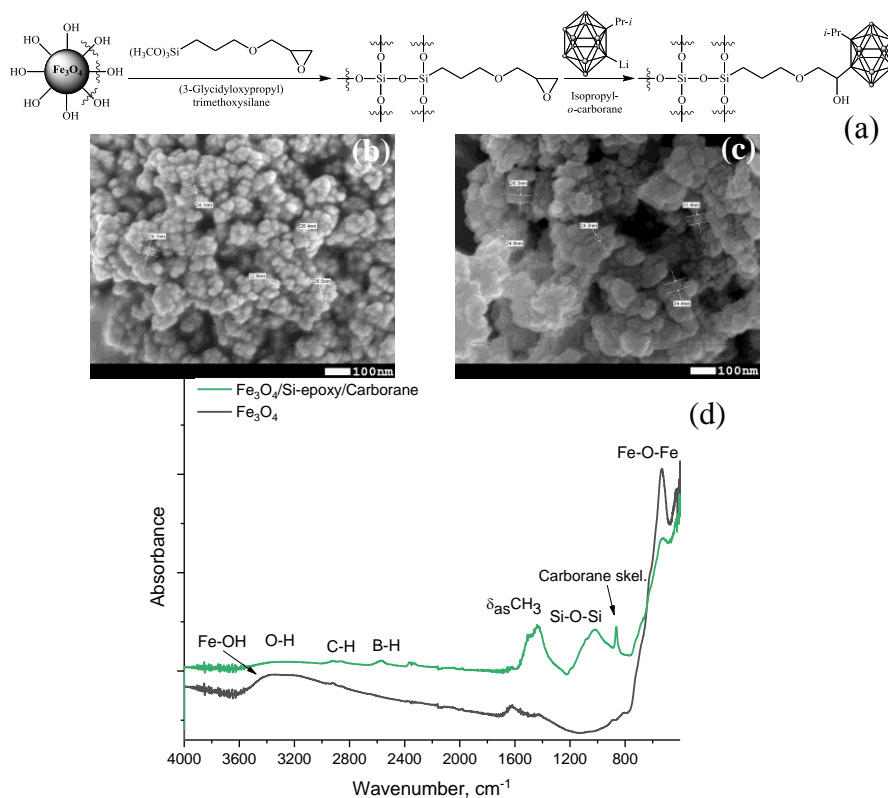


Figure 5. Scheme of Fe₃O₄ modification and carborane immobilization (a), SEM image of initial Fe₃O₄ nanoparticles (b), SEM image of Fe₃O₄-Si-epoxy-carborane nanoparticles (c) and FTIR spectra of Fe₃O₄ before and after modification (d)

Results of XRD analysis of the studied nanoparticles before and after modification are presented in Figure 6. The general view of X-ray diffraction patterns evidence to the polycrystalline type of nanoparticles with a low degree of structural ordering and crystallinity. Table 2 shows the results of changes in structural parameters calculated based on the analysis of X-ray diffraction patterns, which were made according to [30–31].

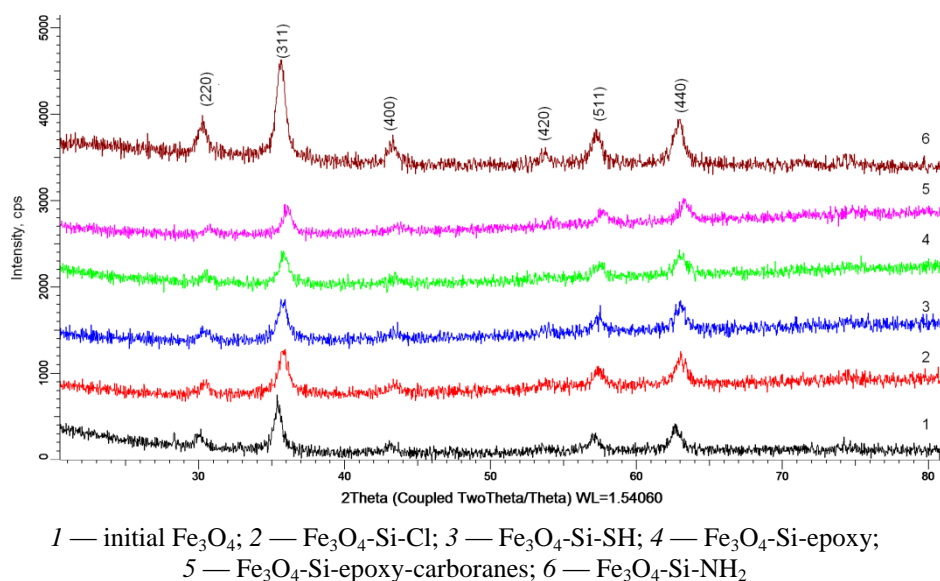


Figure 6. XRD patterns

Data of XRD analysis

Sample	Initial Fe ₃ O ₄	Fe ₃ O ₄ -Si-Cl	Fe ₃ O ₄ -Si-SH	Fe ₃ O ₄ -Si-NH ₂	Fe ₃ O ₄ -Si-epoxy	Fe ₃ O ₄ -Si-epoxy-carboranes
Structure type	Cubic Fd-3m(227) PDF-00-065-0731					
Lattice parameter, Å	<i>a</i> = 8.4226	<i>a</i> = 8.3384	<i>a</i> = 8.3139	<i>a</i> = 8.3429	<i>a</i> = 8.3039	<i>a</i> = 8.2603
δ	0.009	0.02	0.193	0.091	0.206	0.234
Structure	Fe _{2.99} O ₄	Fe _{2.98} O ₄	Fe _{2.81} O ₄	Fe _{2.91} O ₄	Fe _{2.80} O ₄	Fe _{2.77} O ₄
Crystalline size, nm	18.92±1.86	14.89±1.54	21.33±1.78	18.03±1.69	17.82±1.49	17.41±1.39

It was found that with a high degree of probability (more than 85 %), the diffraction pattern of the obtained nanoparticles corresponds to the cubic phase of magnetite, with the spatial system Fd-3m (227). Comparison analysis was carried out using the PDF-2 database. In this case, the parameters of the crystal lattice differ from the reference values selected from the PDF-00-065-0731 database. The differences can be caused both by the processes of disordering of the structure arising as a result of synthesis, as well as by subsequent oxidation processes associated with the processes of modification. In this case, the modification leads both to a change in the stoichiometric ratio and in the crystallite size.

The cytotoxicity of Fe₃O₄-Si-epoxy-Carborane nanoparticles was characterized by determination of cell vitality. The percentages of active cells — cell viability ± SEM values after 24h and 72 hours incubation are shown in Figure 7.

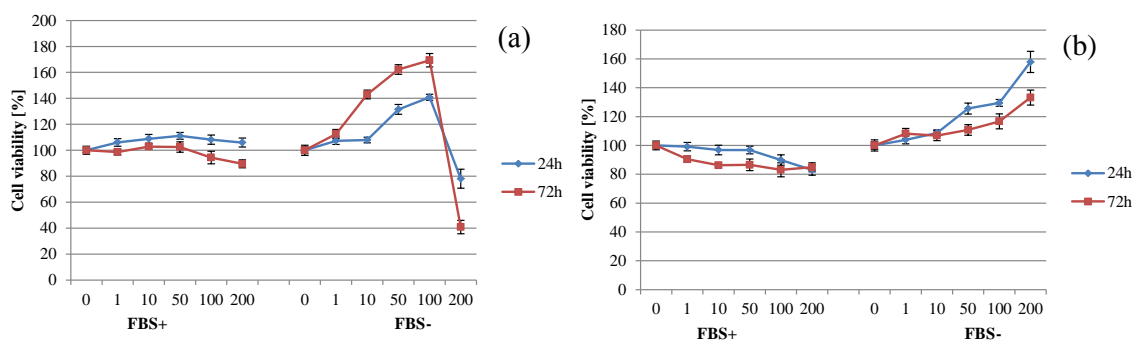


Figure 7. Cell viability after 24 and 72 hours incubation with FBS and without FBS as a function of nanoparticles concentrations for HeLa (a) and PC-3 (b) cell lines

Visual inspection of cells along with the viability and cytotoxicity after 24 hours as well as 72 hours incubation results indicated a low cytotoxicity of investigated particles for concentrations < 200 μg/ml in case all investigated cell lines. For that reason, the value of IC₅₀ (half maximal inhibitory concentration) has not been established. The dose-dependent decrease in viability is well visible for HeLa and PC-3 cells. The experiments indicate that mitochondrial and overall cell viability is maintained. Unexpected increase in viability visible especially for medium without (FBS-) may be due to increased mitochondrial activity associated with cell phagocytosis of nanoparticles.

Conclusions

Functionalization of Fe₃O₄ nanoparticles with epoxy, amino, mercapto, chloro group using silanes was carried out. The features of the reactions were studied; the optimal conditions for the process were established. The formation of functional groups has been proven by FTIR spectroscopy, SEM, and EDA. Further, the obtained modified nanoparticles with chemically active groups can be used to immobilize payload. For this propose, carborane compound was successfully attached to the modified nanoparticles via formation of covalent bond for potential application in boron neutron capture therapy of cancer. It was found that resulting nanoparticles contain 16.6 % of boron (according to EDA), and their average size is 32±9 nm (according to SEM). In vitro test using HeLa (cervical cancer cell) and PC-3 (prostate cancer cell) shows low cytotoxicity in concentration range of 1–200 μg/ml.

This study was funded by the Ministry of Education and Science of the Republic of Kazakhstan (grant No AP08051954) and Joint Institute for Nuclear Research-Republic of Kazakhstan cooperation program (Order No. 391, 20.07.2020).

References

- 1 Anselmo A.C. Nanoparticles in the clinic / A.C. Anselmo, S. Mitragotri // *Bioeng. Transl. Med.* — 2016. — Vol. 1, No. 1. — P. 10–29. <https://doi.org/10.1002/btm2.10003>
- 2 Cruz M.M. Nanoparticles for magnetic hyperthermia / M.M. Cruz, L.P. Ferreira, A.F. Alves, S.G. Mendo, P. Ferreira, M. Godinho, M.D. Carvalho // *Nanostructures Cancer Ther.* — 2017. — P. 485–511. <https://doi.org/10.1016/B978-0-323-46144-3.00019-2>
- 3 Meola A. Magnetic Particle Imaging in Neurosurgery / A. Meola, J. Rao, N. Chaudhary, G. Song, X. Zheng, S.D. Chang // *World Neurosurg.* — 2019. — Vol. 125. — P. 261–270. <https://doi.org/10.1016/j.wneu.2019.01.180>
- 4 Doswald S. Biochemical functionality of magnetic particles as nanosensors: how far away are we to implement them into clinical practice? / S. Doswald, W.J. Stark, B. Beck-Schimmer // *J. Nanobiotechnology.* — 2019. — Vol. 17, No.1. — P. 1–11. <https://doi.org/10.1186/s12951-019-0506-y>
- 5 Bray F. Global cancer statistics 2018: GLOBOCAN estimates of incidence and mortality worldwide for 36 cancers in 185 countries / F. Bray, J. Ferlay, I. Soerjomataram, R.L. Siegel, L.A. Torre, A. Jemal // *CA. Cancer J. Clin.* — 2018. — Vol. 68. — P. 394–424. <https://doi.org/10.3322/caac.21492>
- 6 Tietze R. Magnetic nanoparticle-based drug delivery for cancer therapy / R. Tietze, J. Zaloga, H. Unterweger, S. Lyer, R.P. Friedrich, C. Janko, M. Pöttler, S. Dürr // *Biochem. Biophys. Res. Commun.* — 2015. — Vol. 468. — P. 463–470. <https://doi.org/10.1016/J.BBRC.2015.08.022>
- 7 Wolfram J. Clinical cancer nanomedicine / J. Wolfram, M. Ferrari // *Nano Today.* — 2019. — Vol. 25. — P. 85–98. <https://doi.org/10.1016/j.nantod.2019.02.005>
- 8 Remya N. Toxicity, toxicokinetics and biodistribution of dextran stabilized Iron oxide Nanoparticles for biomedical applications / N.S. Remya, S. Syama, A. Sabareeswaran, P.V. Mohanan // *Int. J. Pharm.* — 2016. — Vol. 511. — P. 586–598. <https://doi.org/10.1016/J.IJPHARM.2016.06.119>
- 9 Chandra S. PEGylated Iron Oxide Nanoparticles for pH Responsive Drug Delivery Application / S. Chandra Mohanta, A. Saha, P. Sujatha Devi // *Mater. Today Proc.* — 2018. — Vol. 5. — P. 9715–9125.
- 10 Hauser A.K. Targeted iron oxide nanoparticles for the enhancement of radiation therapy / A.K. Hauser, M.I. Mitov, E.F. Daley, R.C. McGarry, K.W. Anderson, J.Z. Hilt // *Biomaterials.* — 2016. — Vol. 105. — P. 127–135. <https://doi.org/10.1016/J.BIOMATERIALS.2016.07.032>
- 11 Shelat R. Detailed toxicity evaluation of β -cyclodextrin coated iron oxide nanoparticles for biomedical applications / R. Shelat, S. Chandra, A. Khanna // *Int. J. Biol. Macromol.* — 2018. — Vol. 110. — P. 357–365. <https://doi.org/10.1016/J.IJBIOMAC.2017.09.067>
- 12 Dadfar S.M. Iron oxide nanoparticles: Diagnostic, therapeutic and theranostic applications / S.M. Dadfar, K. Roemhild, N.I. Drude, S. von Stillfried, R. Knüchel, F. Kiessling, T. Lammers // *Adv. Drug Deliv. Rev.* — 2019. — Vol. 138. — P. 302–325. <https://doi.org/10.1016/J.ADDR.2019.01.005>
- 13 Rajabi F. Oxidative esterification of alcohols and aldehydes using supported iron oxide nanoparticle catalysts / F. Rajabi, R.A.D. Arancon, R. Luque // *Catal. Commun.* — 2015. — Vol. 59. — P. 101–103. <https://doi.org/10.1016/J.CATCOM.2014.09.022>
- 14 Pizzolato E. Water oxidation electrocatalysis with iron oxide nanoparticles prepared via laser ablation / E. Pizzolato, S. Scaramuzza, F. Carraro, A. Sartori, S. Agnoli, V. Amendola, M. Bonchio, A. Sartorel // *J. Energy Chem.* — 2016. — Vol. 25. — P. 246–250. <https://doi.org/10.1016/J.JECHEM.2015.12.004>
- 15 Devi H.S. Singh, Iron oxide nanoparticles synthesis through a benign approach and its catalytic application / H.S. Devi, T.D. Singh // *Perspect. Sci.* — 2016. — Vol. 8. — P. 287–289.
- 16 Nebu J. Fluorescence turn-on detection of fenitrothion using gold nanoparticle quenched fluorescein and its separation using superparamagnetic iron oxide nanoparticle / J. Nebu, J.S. Anjali Devi, R.S. Aparna, B. Aswathy, G.M. Lekha, G. Sony // *Actuators B Chem.* — 2018. — Vol. 277. — P. 271–280. <https://doi.org/10.1016/J.SNB.2018.08.153>
- 17 van de Loosdrecht M.M. Separation of excitation and detection coils for in vivo detection of superparamagnetic iron oxide nanoparticles / M.M. van de Loosdrecht, S. Waanders, H.J.G. Krooshoop, B. ten Haken // *J. Magn. Magn. Mater.* — 2019. — Vol. 475. — P. 563–569. <https://doi.org/10.1016/J.JMMM.2018.12.012>
- 18 Ozel F. Characterization of tartaric acid and ascorbic acid coated iron oxide nanoparticles and their biocompatibility studies / F. Ozel, E. Tokay, F. Köçkar, H. Köçkar // *J. Magn. Magn. Mater.* — 2018. — Vol. 474. — P. 654–660. <https://doi.org/10.1016/J.JMMM.2018.11.025>
- 19 Yathindranath V. Thliveris, One-Pot Synthesis of Iron Oxide Nanoparticles with Functional Silane Shells: A Versatile General Precursor for Conjugations and Biomedical Applications / V. Yathindranath, Z. Sun, M. Worden, L.J. Donald, J.A., J.A. Thliveris // *Langmuir.* — 2013. — Vol. 29. — P. 10850–10858.
- 20 Özgür M. The Toxicity Assessment of Iron Oxide (Fe₃O₄) Nanoparticles on Physical and Biochemical Quality of Rainbow Trout Spermatozoon / M. Özgür, A. Ulu, S. Balcioglu, İ. Özcan, S. Köytepe, B. Ateş // *Toxics.* — 2018. — Vol. 6. — P. 62. <https://doi.org/10.3390/toxics6040062>
- 21 Fernández-Bertólez N. Toxicological assessment of silica-coated iron oxide nanoparticles in human astrocytes / N. Fernández-Bertólez, C. Costa, F. Brandão, G. Kiliç, J.A. Duarte, J.P. Teixeira, E. Pávaro, V. Valdiglesias, B. Laffon // *Food Chem. Toxicol.* — 2018. — Vol. 118. — P. 13–23. <https://doi.org/10.1016/J.FCT.2018.04.058>

- 22 Janko C. Strategies to optimize the biocompatibility of iron oxide nanoparticles — «SPIONs safe by design / C. Janko, J. Zaloga, M. Pöttler, S. Dürr, D. Eberbeck, R. Tietze, S. Lyer, C. Alexiou // J. Magn. Magn. Mater. — 2017. — Vol. 431. — P. 281–284. <https://doi.org/10.1016/J.JMMM.2016.09.034>
- 23 Kurczewska J. Preparation of multifunctional cascade iron oxide nanoparticles for drug delivery / J. Kurczewska, M. Ceglowski, G. Schroeder // Mater. Chem. Phys. — 2018. — Vol. 211. — P. 34–41. <https://doi.org/10.1016/J.MATCHEMPHYS.2018.01.064>
- 24 Tishkevich D.I. Immobilization of boron-rich compound on Fe₃O₄ nanoparticles: Stability and cytotoxicity / D.I. Tishkevich, I.V. Korolkov, A.L. Kozlovskiy, M. Anisovich, D.A. Vinnik, A.E. Ermekova, A.I. Vorobjova, E.E. Shumskaya, T.I. Zubar, S.V. Trukhanov, M.V. Zdorovets // J. Alloys Compd. — 2019. — Vol. 794. — P. 573–581. <https://doi.org/10.1016/j.jallcom.2019.05.075>
- 25 Kozlovskiy A.L. Study of phase transformations, structural, corrosion properties and cytotoxicity of magnetite-based nanoparticles / A.L. Kozlovskiy, A.E. Ermekova, I.V. Korolkov, D. Chudoba, M. Jazdzewska, K. Ludzik, A. Nazarova, B. Marciniak, R. Kontek, A.E. Shumskaya, M.V. Zdorovets // Vacuum. — 2019. — Vol. 163. — P. 236–247. <https://doi.org/10.1016/J.VACUUM.2019.02.029>
- 26 Stockert J.C. Tetrazolium salts and formazan products in Cell Biology: Viability assessment, fluorescence imaging, and labeling perspectives / J.C. Stockert, R.W. Horobin, L.L. Colombo, A. Blázquez-Castro // Acta Histochem. — 2018. — Vol. 120. — P. 159–167. <https://doi.org/10.1016/j.acthis.2018.02.005>
- 27 Abe K. Measurement of cellular 3-(4,5-dimethylthiazol-2-yl)-2,5-diphenyltetrazolium bromide (MTT) reduction activity and lactate dehydrogenase release using MTT / K. Abe, N. Matsuki // Neurosci. Res. — 2000. — Vol. 38. — P. 325–329. [https://doi.org/10.1016/S0168-0102\(00\)00188-7](https://doi.org/10.1016/S0168-0102(00)00188-7)
- 28 Rubio F. A FT-IR study of the hydrolysis of Tetraethylorthosilicate (TEOS) / F. Rubio, J. Rubio, J.L. Oteo // Spectrosc. Lett. — 1998. — Vol. 31. — P. 199–219. <https://doi.org/10.1080/00387019808006772>
- 29 Leites L.A. Vibrational Spectroscopy of Carboranes and Parent Boranes and Its Capabilities in Carborane Chemistry / L.A. Leites // Chem. Rev. — 1992. — Vol. 92. — P. 279–323.
- 30 Bondarenko L.S. Effects of Modified Magnetite Nanoparticles on Bacterial Cells and Enzyme Reactions/ L.S. Bondarenko, E.S. Kovel, K.A. Kydraliev, G.I. Dzhardimalieva, E. Illés, E. Tombácz, A.G. Kicheeva, N.S. Kudryasheva // Polymers. — 2020. — Vol. 10. — P. 1499. <https://doi.org/10.3390/nano10081499>
- 31 Bondarenko L.S. Effects of Humic Acids on the Ecotoxicity of Fe₃O₄ Nanoparticles and Fe-Ions: Impact of Oxidation and Aging/ L.S. Bondarenko, A. Kahru, V. Terekhova, G. Dzhardimalieva, P. Uchanov, K. Kydraliev // Nanomaterials. — 2020. — Vol. 10. — P. 1–18. <https://doi.org/10.3390/nano10102011>

И.В. Корольков, К. Луджик, Л.И. Лисовская,
А.В. Зиберт, А.Б. Есжанов, М.В. Здоровец

Пайдалы жүктемені жеткізу үшін магнитті Fe₃O₄ нанобөлшектерін модификациялау

Пайдалы жүктемені мақсатты жеткізу әдістерін жасау — бұл жедел дамып келе жатқан зерттеу бағыты. Осыған байланысты темір оксидінің нанобөлшектері сыртқы магнит өрісін пайдаланып заттарды жеткізу үшін пайдаланылуы мүмкін. Алайда терапиялық қолдану үшін қажетті концентрациядағы дәрілік заттарды иммобилизациялау мүмкіндігіне әкелетін оларды модификациялау әдістерін әзірлеу қажет. Мақалада (3-хлоропропил)триметоксисилан, (3-меркаптопропил)триметоксисилан, (3-аминопропил)триметоксисилан және (3-глицидилпропил)триметоксисилан сияқты силандармен супермагниттік (Fe₃O₄) темір оксиді нанобөлшектері модификацияланды. Содан кейін карборанды қосылыс модификацияланған нанобөлшектерде ковалентті байланыс түзу арқылы сәтті иммобилизденді. Құрылымы, мөлшері және элементтік құрамы ИҚ-Фурье трансформациялық инфрақызыл спектроскопиясы (ИҚ), сканерлейтін электронды микроскопия (СЭМ) және энергодисперсиялық рентген спектроскопиясы (ЭДС) көмегімен зерттелді. Алынған нанобөлшектерде (ЭДС деректері бойынша) 16,6 % бор бар екендігі анықталды, ал олардың орташа мөлшері (СЭМ деректері бойынша) 34±9 нм. *In vitro* тест HeLa (жатыр мойны обыры жасушалары) және РС-3 (қуық асты безінің қатерлі ісігі жасушалары) үшін 1–200 мкг/мл концентрация ауқымында төмен цитотоксикалықты көрсетеді.

Кілт сөздер: Fe₃O₄ нанобөлшектері, силан, беттік модификациялау, пайдалы жүктемені мақсатты жеткізу, БНҰТ, карборан, биологиялық сынақ, цитотоксикалық.

И.В. Корольков, К. Луджик, Л.И. Лисовская,
А.В. Зиберт, А.Б. Есжанов, М.В. Здоровец

Модификация магнитных наночастиц Fe₃O₄ для адресной доставки полезного груза

Разработка методов адресной доставки полезного груза — быстро развивающееся направление исследований. В связи с этим наночастицы оксида железа потенциально могут быть использованы для доставки веществ с помощью внешнего магнитного поля. Однако необходимо разработать методы их модификации, которые приведут к возможности иммобилизации лекарственных веществ необходимой концентрации для терапевтического использования. В статье супермагнитные наночастицы оксида железа (Fe₃O₄) были модифицированы силанами, такими как (3-хлорпропил)триметоксисилан, (3-меркаптопропил)триметоксисилан, (3-аминопропил)триметоксисилан и (3-глицидилпропил)триметоксисилан. Затем карборановое соединение было успешно иммобилизовано на модифицированные наночастицы посредством образования ковалентной связи. Структура, размер и элементный состав изучены с помощью инфракрасной спектроскопии с преобразованием Фурье (ИК), сканирующей электронной микроскопии (СЭМ) и энергодисперсионной рентгеновской спектроскопии (ЭДА). Было обнаружено, что полученные наночастицы содержат 16,6 % бора (по данным ЭДА), а их средний размер составляет 34±9 нм (по данным СЭМ). Тест *in vitro* показывает низкую цитотоксичность в диапазоне концентраций 1–200 мкг/мл для HeLa (клетки рака шейки матки) и РС-3 (клетки рака простаты).

Ключевые слова: наночастицы Fe₃O₄, силан, модификация поверхности, адресная доставка полезного груза, БНЗТ, карборан, биологический тест, цитотоксичность.

References

- 1 Anselmo, A.C., & Mitragotri, S. (2016). Nanoparticles in the clinic. *Bioeng. Transl. Med.*, 1(1), 10–29. <https://doi.org/10.1002/btm2.10003>
- 2 Cruz, M.M., Ferreira, L.P., Alves, A.F., Mendo, S.G., Ferreira, P., & M. Godinho et al. (2017). Nanoparticles for magnetic hyperthermia. *Nanostructures Cancer Ther.*, 2017, 485–511. <https://doi.org/10.1016/B978-0-323-46144-3.00019-2>
- 3 Meola, A., Rao, J., Chaudhary, N., Song, G., Zheng, X., & Chang, S.D. (2019). Magnetic Particle Imaging in Neurosurgery. *World Neurosurg*, 125, 261–270. <https://doi.org/10.1016/j.wneu.2019.01.180>
- 4 Doswald, S., Stark, W.J., & Beck-Schimmer, B. (2019). Biochemical functionality of magnetic particles as nanosensors: how far away are we to implement them into clinical practice? *J. Nanobiotechnology*, 17, 1–11. <https://doi.org/10.1186/s12951-019-0506-y>
- 5 Bray, F., Ferlay, J., Soerjomataram, I., Siegel, R.L., Torre, L.A., & Jemal, A. (2018). Global cancer statistics 2018: GLOBOCAN estimates of incidence and mortality worldwide for 36 cancers in 185 countries. *CA. Cancer J. Clin.*, 68, 394–424. <https://doi.org/10.3322/caac.21492>
- 6 Tietze, R., Zaloga, J., Unterweger, H., Lyer, S., Friedrich, R.P., & Janko, C. (2016). Magnetic nanoparticle-based drug delivery for cancer therapy. *Biochem. Biophys. Res. Commun.*, 468, 463–470. <https://doi.org/10.1016/J.BBRC.2015.08.022>
- 7 Wolfram, J., & Ferrari M. (2019). Clinical cancer nanomedicine. *Nano Today.*, 25, 85–98. <https://doi.org/10.1016/j.nantod.2019.02.005>
- 8 Remya, N.S., Syama, S., Sabareeswaran, A., & Mohanan, P.V. (2016). Toxicity, toxicokinetics and biodistribution of dextran stabilized Iron oxide Nanoparticles for biomedical applications. *Int. J. Pharm.*, 511, 586–598. <https://doi.org/10.1016/J.IJPHARM.2016.06.119>
- 9 Chandra Mohanta, S., Saha, A., & Sujatha Devi P. (2018). PEGylated Iron Oxide Nanoparticles for pH Responsive Drug Delivery Application. *Mater. Today Proc.*, 5, 9715–9125.
- 10 Hauser, A.K., Mitov, M.I., Daley, E.F., McGarry, R.C., Anderson K.W., & Hilt, J.Z. (2016). Targeted iron oxide nanoparticles for the enhancement of radiation therapy. *Biomaterials*, 105, 127–135. <https://doi.org/10.1016/J.BIOMATERIALS.2016.07.032>
- 11 Shelat, R., Chandra, S., & Khanna, A. (2018). Detailed toxicity evaluation of β-cyclodextrin coated iron oxide nanoparticles for biomedical applications. *Int. J. Biol. Macromol.*, 110, 357–365. <https://doi.org/10.1016/J.IJBIOMAC.2017.09.067>
- 12 Dadfar, S.M., Roemhild, K., Drude, N.I., von Stillfried, S., Knüchel, R., & Kiessling F., et al. (2019). Iron oxide nanoparticles: Diagnostic, therapeutic and theranostic applications. *Adv. Drug Deliv. Rev.*, 138, 302–325. <https://doi.org/10.1016/J.ADDR.2019.01.005>
- 13 Rajabi, F., Arancon, R.A.D., & Luque, R. (2015). Oxidative esterification of alcohols and aldehydes using supported iron oxide nanoparticle catalysts. *Catal. Commun.*, 59, 101–103. <https://doi.org/10.1016/J.CATCOM.2014.09.022>
- 14 Pizzolato, E., Scaramuzza, S., Carraro, F., Sartori, A., Agnoli, S., & Amendola, V. et al. (2016). Water oxidation electrocatalysis with iron oxide nanoparticles prepared via laser ablation. *J. Energy Chem.*, 25, 246–250. <https://doi.org/10.1016/J.JECHEM.2015.12.004>
- 15 Devi, H.S., & Singh, T.D. (2016). Iron oxide nanoparticles synthesis through a benign approach and its catalytic application. *Perspect. Sci.*, 8, 287–289.

- 16 Nebu, J., Anjali Devi, J.S., Aparna, R.S., Aswathy, B., Lekha, G.M., & Sony, G. (2018). Fluorescence turn-on detection of fenitrothion using gold nanoparticle quenched fluorescein and its separation using superparamagnetic iron oxide nanoparticle. *Actuators B Chem.*, 277, 271–280. <https://doi.org/10.1016/J.SNB.2018.08.153>
- 17 van de Loosdrecht, M.M., Waanders, S., Krooshoop, H.J.G., & ten Haken, B. (2019). Separation of excitation and detection coils for in vivo detection of superparamagnetic iron oxide nanoparticles. *J. Magn. Magn. Mater.*, 475, 563–569. <https://doi.org/10.1016/J.JMMM.2018.12.012>
- 18 Ozel, F., Tokay, E., Köçkar, F., & Köçkar, H. (2018). Characterization of tartaric acid and ascorbic acid coated iron oxide nanoparticles and their biocompatibility studies. *J. Magn. Magn. Mater.*, 474, 654–660. <https://doi.org/10.1016/J.JMMM.2018.12.012>
- 19 Yathindranath, V., Sun, Z., Worden, M., Donald, L.J., & Thliveris, J.A. (2013). One-Pot Synthesis of Iron Oxide Nanoparticles with Functional Silane Shells: A Versatile General Precursor for Conjugations and Biomedical Applications. *Langmuir*, 29, 10850–10858.
- 20 Özgür, M., Ulu, A., Balcıoğlu, S., Özcan, İ., Köytepe, S., & Ateş, B. (2018). The Toxicity Assessment of Iron Oxide (Fe₃O₄) Nanoparticles on Physical and Biochemical Quality of Rainbow Trout Spermatozoon. *Toxics*, 6, 62. <https://doi.org/10.3390/toxics6040062>
- 21 Fernández-Bertólez, N., Costa, C., Brandão, F., Kiliç, G., Duarte, J.A., & Teixeira, J.P. et al. (2018). Toxicological assessment of silica-coated iron oxide nanoparticles in human astrocytes. *Food Chem. Toxicol.*, 118, 13–23. <https://doi.org/10.1016/J.FCT.2018.04.058>
- 22 Janko, C., Zaloga, J., Pöttler, M., Dürr, S., Eberbeck, D., & Tietze, R. et al. (2017). Strategies to optimize the biocompatibility of iron oxide nanoparticles — «SPIONs safe by design». *J. Magn. Magn. Mater.*, 431, 281–284. <https://doi.org/10.1016/J.JMMM.2016.09.034>
- 23 Kurczewska, J., Ceglowski, M., & Schroeder, G. (2018). Preparation of multifunctional cascade iron oxide nanoparticles for drug delivery. *Mater. Chem. Phys.*, 211, 34–41. <https://doi.org/10.1016/J.MATCHEMPHYS.2018.01.064>
- 24 Tishkevich, D.I., Korolkov, I. V., Kozlovskiy, A.L., Anisovich, M., Vinnik, D.A., & Ermekova, A.E. et al. (2019). Immobilization of boron-rich compound on Fe₃O₄ nanoparticles: Stability and cytotoxicity. *J. Alloys Compd.*, 794, 573–581. <https://doi.org/10.1016/j.jallcom.2019.05.075>
- 25 Kozlovskiy, A.L., Ermekova, A.E., Korolkov, I.V., Chudoba, D., Jazdzewska, M., & Ludzik, K. et al. (2019). Study of phase transformations, structural, corrosion properties and cytotoxicity of magnetite-based nanoparticles. *Vacuum*, 163, 236–247. <https://doi.org/10.1016/J.VACUUM.2019.02.029>
- 26 Stockert, J.C., Horobin, R.W., Colombo, L.L., & Blázquez-Castro, A. (2018). Tetrazolium salts and formazan products in Cell Biology: Viability assessment, fluorescence imaging, and labeling perspectives. *Acta Histochem.*, 120, 159–167. <https://doi.org/10.1016/j.acthis.2018.02.005>
- 27 Abe, K., & Matsuki, N. (2000). Measurement of cellular 3-(4,5-dimethylthiazol-2-yl)-2,5-diphenyltetrazolium bromide (MTT) reduction activity and lactate dehydrogenase release using MTT. *Neurosci. Res.*, 38, 325–329. [https://doi.org/10.1016/S0168-0102\(00\)00188-7](https://doi.org/10.1016/S0168-0102(00)00188-7)
- 28 Rubio, F., Rubio, J., & Oteo, J.L. (1998). A FT-IR study of the hydrolysis of Tetraethylorthosilicate (TEOS). *Spectrosc. Lett.*, 31, 199–219. <https://doi.org/10.1080/00387019808006772>
- 29 Leites, L.A. (1992). Vibrational Spectroscopy of Carboranes and Parent Boranes and Its Capabilities in Carborane Chemistry. *Chem. Rev.*, 92, 279–323.
- 30 Bondarenko, L.S., Kovel, E.S., Kydraliev, K.A., Dzhardimalieva, G.I., Illés, E., & Tombác E. et al. (2020). Effects of Modified Magnetite Nanoparticles on Bacterial Cells and Enzyme Reactions. *Polymers*, 10, 1499. <https://doi.org/10.3390/nano10081499>
- 31 Bondarenko, L.S., Kahru, A., Terekhova, V., Dzhardimalieva, G., Uchanov, P., & Kydraliev, K. (2020). Effects of Humic Acids on the Ecotoxicity of Fe₃O₄ Nanoparticles and Fe-Ions: Impact of Oxidation and Aging. *Nanomaterials*, 10, 1–18. <https://doi.org/10.3390/nano10102011>

Information about authors

Korolkov, Ilya Vladimirovich (*corresponding author*) — PhD, senior researcher of the Institute of Nuclear Physics, Abylay khana 2/1, 010000, Nur-Sultan, Kazakhstan; e-mail: i.korolkov@inp.kz, <https://orcid.org/0000-0002-0766-2803>

Katarzyna, Ludzik — researcher of the University of Lodz, ul. Uniwersytecka 3, 90–137 Łódź, Poland; e-mail: katarzynaludzik82@gmail.com, <https://orcid.org/0000-0003-1749-808X>

Lisovskaya, Lana Igorevna — engineer of the Institute of Nuclear Physics, Abylay khana 2/1, 010000, Nur-Sultan, Kazakhstan; e-mail: ms.defrance@mail.ru.

Zibert, Aleksandr Vitalevich — student of L.N. Gumilyov Eurasian National University, Satbayev str., 2, 010000, Nur-Sultan, Kazakhstan; e-mail: alexandr.zibert@bk.ru.

Yeszhanov, Arman Bachitzhanovich — junior researcher of the Institute of Nuclear Physics, Abylay khana 2/1, 010000, Nur-Sultan, Kazakhstan; e-mail: arman_e7@mail.ru, <https://orcid.org/0000-0002-1328-8678>

Zdorovets, Maxim Vladimirovich — Director of the Institute of Nuclear Physics, Abylay khana 2/1, 010000, Nur-Sultan, Kazakhstan; e-mail: mzdorovets@inp.kz, <https://orcid.org/0000-0003-2992-1375>